Global Risk Assessment of Natural Disasters: new perspectives

by

Mona Khaleghy Rad

A thesis

Presented to the University of Waterloo

in fulfillment of the

thesis requirement for the degree of

Doctor of Philosophy

in

Earth Sciences

Waterloo, Ontario, Canada, 2014

Author's Declaration

I hereby declare that I am the sole author of this thesis. This is a true copy of the thesis, including any required final revisions, as accepted by my examiners.

I understand that my thesis may be made electronically available to the public.

Abstract

Natural disasters such as earthquakes, tsunamis, landslides and volcanic activities has had devastating effects on human life. Risk is the probability of harmful consequences from the interaction of hazards and vulnerable conditions. With increasing numbers of people living in crowded cities and other vulnerable areas, it is more important than ever to advance our understanding of natural disasters and the ways in which humans respond to them. My interdisciplinary study reflected in my thesis includes integrated research on the risk assessment methods for natural hazards with focus on earthquake disasters.

This thesis address firstly the development of a scaled risk assessment framework, comparative assessment of natural hazard losses, including respective case studies and global overview of natural hazard risk, and secondly a comparative risk assessment of geological disasters to elaborate the major disastrous hazards for global population. Furthermore, I evaluate the effect of past events in form of the number of losses with respect to the exposed population on the proneness of people to the disaster. I summarize acceptable risk criteria and the necessity of having a normalized framework for societal risk assessment. I evaluate the natural hazard risk assessment and acceptable risk criteria of 32 European countries. I also introduce the concept of resistance in both risk equation and in FN-curves. Resistance is the societal resilience of a society to the occurrence of a natural disaster. Moreover, using components of FN-curves (slopes and intercepts) for risk assessment of geological disasters based on real data, I showed that the world has been more at risk of earthquakes than tsunamis, volcanic activities and landslides since 1600. Also. based on the earthquake disasters data (1973-2010), I evaluated the temporal trend of hazard, risk, exposure and resistance of the world towards earthquake disasters. Our results does not provide any evidence of increase or decrease in the temporal trend of fatality rate and earthquake resistance while there is a significant decrease in the crude death rate. Finally, we evaluated the reliability of earthquake disaster system during 1950-2012 using probability of more than 1000 fatalities as probability of failure. Our yearly estimate of reliability at the beginning of each mission year shows that the avreage reliability of earthquake disaster system is very low (~0.3) and it is decreasing over time, too.

Acknowledgements

I would like to thank all the people who made this possible. I would like to thank and acknowledge inspirational instruction and guidance from Prof. Stephen G. Evans, my supervisor, for the initial impetus to read the "Mathematics of Natural Catastrophes" (by Gordon Woo) and "How Nature Works" (by Per Bak) and his continuous discussions, guidance and support throughout my study.

I would like to thank and acknowledge members of the International Center for Geohazards at the Norwegian Geotechnical Institute (NGI) for their support during my five months visit in 2009. One of the major parts of my thesis was developed at NGI with the useful discussions and insightful advice of Prof. Farrokh Nadim and Dr. Suzanne Lacasse. They supported me even after I left, in the form of letters of reference for the Ontario Graduate Scholarship in both 2010 and 2011. I also thank Prof. Nadim, Prof. Breedveld and Prof. Gottschalk for their great lectures during an environmental hazard and risk analysis course at Oslo University. I gained good knowledge on various environmental hazards from their course.

I would like to thank and acknowledge Prof. Alexander Brenning for his useful course on spatial statistics during which I was inspired to extend my project using R statistical software and RSAGA to examine the effective parameters of life loss in the Middle East. Due to the interdisciplinarity of his course, I was also inspired to organize the first Waterloo conference on Characteristics, Risk and Management of Natural Hazards (ChaRisMa) in December 2010. I am especially thankful for Prof. Brenning's availability, patience and precious time through email or in person.

I also thank Scott MacFarlane for his useful ArcGIS expertise and his unsparing helps. Scott helped me with a Python code and in data modification and visualization for use in spatial analysis of earthquake death tolls in the Middle East.

I would like to thank Prof. Mahesh Pandey for his course on engineering risk and reliability, during which I learned risk and reliability assessment, their application and the underlying mathematics. This course inspired me to apply engineering reliability assessment to natural hazard risk assessment for my thesis. In particular, I thank Prof. Pandey for welcoming my questions and discussions, in spite of his busy schedule. I also

thank Prof. Pandey for introducing me to Tianjin Cheng, his PhD student, with whom I had useful discussions on assessing the reliability of natural hazard systems.

I would like to acknowledge and thank my committee members, Prof. Andre Unger, Prof. Alexander Brenning and Prof. Francis Poulin for their useful insights, comments, and precious time.

I would like to thank the my colleagues, Keith Delaney and Negar Ghahramani for creating an intellectual environment in which discussions and questions were welcomed.

I also thank Mary McPherson of the Graduate Writing Center for her availability and encouraging remarks. Mary helped me with the English correction of my thesis.

I especially thank the Ontario Graduate Scholarship committee for their support of my research for two years (2010 and 2011). Receiving this scholarship gave me confidence that my research is valuable.

Dedication

I dedicate my dissertation to my family and friends. A special feeling of gratitude to my loving parents, Hossein and Shokofeh, who have always supported me and encouraged me to seek the science in everything. Thanks also to my sister, Zoha and my brother, Majid, who have never left my side.

I also dedicate my dissertation to my friends who have supported me throughout the process. I will always appreciate their support.

I especially dedicate this work to my best friend, a wonderful husband, and the love of my life, Farzad, whose charming supports, inspiring advices and intellectual discussions have always been lights in the dark and kept me going throughout the entire doctorate program.

Table of Content

List of Figures

List of Tables

Chapter 1 Introduction to the new perspectives of the global risk assessment of natural disasters

Due to increasing numbers of people living in crowded cities (Bilham, 2009), it is more important than ever to advance our understanding of natural hazards and the ways in which humans respond to them. Recent typhoon in the Philippines (2013) (aka Haiyan and Filipino disaster) has been an example of an extreme natural hazard that occurred in a region which was 1) highly populated, 2) vulnerable to atmospheric hazards, and 3) poorly responsive to disasters. An extreme typhoon such as the recent one could cause more than 6,000 fatalities (CNN, http://www.cnn.com/2013/12/13/world/asia/philippines-typhoon-haiyan/) and make many homeless.

Natural disasters are rare events that have been sources of devastation for human populations and economies. Woo (1999) introduced and analyzed different aspects of natural catastrophes/disasters, their underlying mathematics, corresponding risk and the available decision-making processes. Natural disasters/catastrophes are thought to be rare events either based on their long return intervals, or on their unpredictability. These events are called black swans (Taleb, 2007) if they have long return periods, or dragon kings (Sornette, 2009) if they are unpredictable. Black swans are high magnitude events that occur with very low frequencies which makes them indistinguishable from smaller events in a power-law distribution (a power-law distribution forms a straight line with a negative slope on a log-log plot, $y=ax^{-b}$), therefore, since they share the same properties (except their sizes). On the other hand, dragon kings are the outliers of a power-law distribution which makes them distinguishable from the smaller events. Sornette (2009) suggests that these outliers can be predictable by applying *small* changes to their distribution function.

In this thesis, I consider natural disasters as rare events in all my assessments which include both black swans (very low frequency events which locate at the tail of the power-law distribution) and dragon kings (outliers/peaks in the tail of the power-law distribution). Looking at the frequency-size distribution of various natural hazards, Sachs et al. (2012) showed that the global frequency-magnitude of earthquakes and volcanic eruptions exhibit power-law behavior for small sizes but have roll over for large events.

However, in the data for landslides neither roll over nor dragon-king behavior is observed. Considering these facts, I analyze the risk of both types of events and provide a unified framework for risk assessment of natural disasters.

To explain the terms black swans and dragon kings on a frequency-magnitude curve generated from a set of data that is best fitted to a (fat-tailed) power-law distribution, black swans are the rare (high magnitude and low frequency) events located at the tail of the curve and dragon kings, are the events that are the outliers located in the high magnitude area of the curve while holding frequencies that are much different from the frequency that the power-law curve suggests. Sornette (2009) well illustrated the existence of dragon-kings in six different examples one of which is the distribution of earthquake energies. Fig. 1.1 which is reproduced from Fig. 22 of Sornette (2009) shows the magnitude frequency distribution of the ruptures in San Andreas fault in California where dragon-kings are associated with the clusters located above the extrapolation of the Gutenberg-Richter distribution from smaller events.

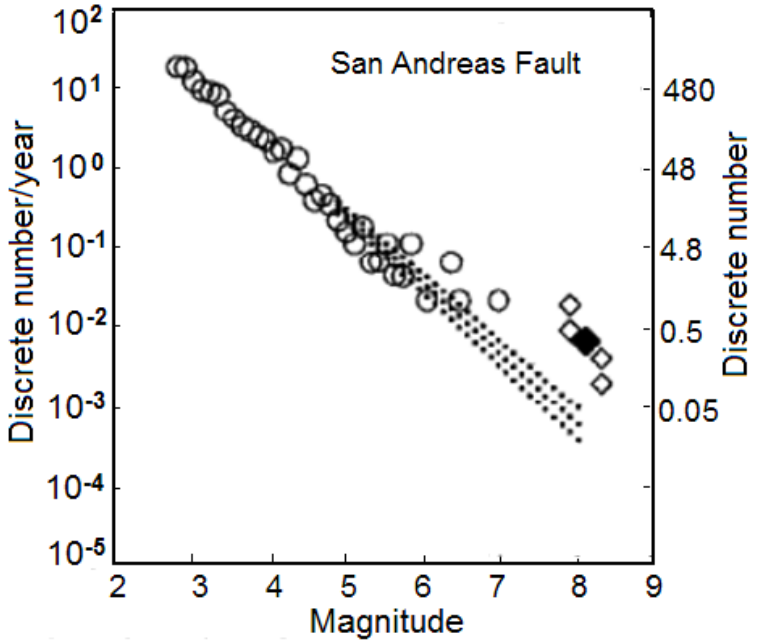

Figure 1.1: frequency-magnitude of earthquakes in San Andreas fault. Clustered events above from the power-law fit (Gutenberg-Richter distribution) are called dragon kings (reproduced from Sornette (2009), Fig. 22).

In regards to the predictability of rare events, Cavalcante et al. (2013) used two coupled chaotic oscillators in an electric circuit in a synchronized state which then leads to the desynchronized state through a bubbling phase (aka the burst mechanism), where a

bubble corresponds to a large temporary digression from the state of the system away from a nominal value. The behavior of this system reveals an approximate power-law distribution for small and intermediate size events but a noticeable peak for large events (dragon-kings). The peaks are associated with the bubbling phenomenon.

Cavalcante et al. (2013) proposed that the dragon-king events can be controlled and suppressed through the bubbling phase. The mechanism is through applying small feedback perturbations to the large bubblings of the system while small bubblings are allowed to proceed, therefore, large bubblings are suppressed. Thus, this way, by understanding the burst mechanism of certain disasters, large dragon-king events may be able to be avoided by producing small, wise system perturbations.

We believe that while considering the lack of knowledge in black swans is essential for analyzing the risk of natural disasters, looking at characteristics and trends in the behavior of natural disaster data helps prediction and reducing of risk. Thus, we support the dragon-king approach for natural disasters, their risk assessment and risk reduction which considers them as events that can be predicted and controlled, rather than uncontrolled "acts of God".

Risk has various definitions one of which is the probability of harmful consequences from the interaction of hazards and associated vulnerability conditions (UNDP, 2004; HSE, 2001). The definition of risk can be summarized in an equation, *Risk=Hazard×Vulnerability*(×*Exposure*) (Birkmann, 2006), in which hazard is defined as a risk source event where consequences relate to harm (Aven, 2011) and *Vulnerability* and *Exposure* are defined as the effect of uncertainty on objectives at the occurrence of an event, and the presence of an object being subject to an event or risk source, respectively (Aven, 2011). The effect of hazard on risk has been studied in depth in the literature (e.g., Marfai and Njagih (2004) on floods, McCall et al. (1992) on earthquakes and Woo (1999) on most of natural hazards). On the effect of exposure on risk, Bilham (2009) compared the number of fatalities due to earthquakes to the global population. However, the effect of vulnerability on risk has been a source of debate.

There are various definitions in the literature for vulnerability (Cutter, 1996). One unifying definition based on Watts and Bohle (1993) indicates that vulnerability is a multidimensional variable integrating the environmental, social, economic and political

situations of people in a society in the case of potential harm. In case of natural hazards, vulnerability is defined as the degree of loss resulting from the occurrence of a natural disaster (Marfai and Njagih, 2004). One can conclude that vulnerability provides a measure of the resistance of the elements at risk to the impact of a natural hazard (Blong, 2009). Some current natural hazard vulnerability indicators include development measures, such as buildings' resistance to earthquake ground-shaking (Blong, 2009).

In terms of current vulnerability analyses, Mustafa et al. (2011) claim that vulnerability analysis has deepened our understanding of the behavior and origin of damage due to extreme events. However, policy makers and researchers do not agree on their vulnerability frameworks and mainly seek different goals. The reasons for the discrepancies between academic and policy-makers vulnerability analyses have been summarized by Mustafa et al. (2011), one of which is the different concerns of vulnerability analysts (e.g., a fundamental approach) and policy makers (e.g., a practical approach). Another underlying difference, according to Mustafa et al. (2011), is that policy makers are seeking a quantitative input for their policy processes, while vulnerability analysts want mainly qualitative data (e.g., vulnerability assessment of hunger and famine by Watts and Bohle (1993)). However, in the field of engineering, there are in-depth quantitative measures of vulnerability (e.g., Li et al., 2012). These measures, however, are mainly based on detailed specifications of the related system, and therefore, are only applicable in special conditions. Furthermore, most of vulnerability assessments are locally valid. We are looking for a global assessment since our concern is vulnerability to natural disasters.

"Earthquakes don't kill, buildings do" (Musson, 2012). Musson (2012) argues that there is no fully resistant building. However, in the best-case scenario, the damage is minimal and no fatality occurs. This argument can also be applicable to the effect of natural disasters on the countries, cities, or societies. There is no perfect resistance towards natural disasters, but the damage can become minimal by building well-equipped structures and well-prepared societies. Using this terminology (resistance), instead of vulnerability, can bring a positive notion to the aspect of risk assessment, when the question is how societies can withstand an occurrence of natural disasters, i.e., how does the structure of the region resists. As part of this thesis, I illustrate the concept of

resistance towards natural disasters from various perspectives (Chapter 3). I also investigate the trend of global resistance towards earthquake disasters (Chapter 5).

Why are we looking at global assessment of resistance and risk of natural disasters, when most events are local? Local events sometimes have non-local strong effects on each other (e.g., a correlation between hydrocarbon reservoir properties and induced seismicity in the Netherlands (Eijs et al., 2006)). Furthermore, the actions taken for risk reduction on a local scale (e.g., development of building codes to improve earthquake resistance) do not guarantee the reduction of risk on a global scale. Therefore, we need to have a figure of merit in order to be able to evaluate our developments in the world. A quantitative, integrative and frame-independent measure is vital for such a unified approach.

FN-curves have been a major tool of societal risk assessment in health studies, human-caused (industrial) accidents and natural hazard events for many years. In this approach, F is the frequency of death cumulatively plotted versus the number of fatalities (N) due to an event. Associated best-fit to the data plotted on an FN-curve is a power-law distribution. We believe that FN-curves can provide a frame-independent scheme for risk assessment from integrated historical data of natural disaster losses. The data integration brings together social and physical science information in ways useful for decision-making and the definition of acceptable risk criteria based on historical background losses for a region.

As debates exist about all aspects of vulnerability and risk, any quantification can help policy makers and authorities take action towards natural hazard global risk reduction. The main goal of this thesis is to advance one step forward in quantification of global vulnerability and risk assessment measures.

This study addresses five main objectives. The first objective is to pursue an integrated research that combines social and physical dimensions of hazards and provides linkages to decision-making policies. The second objective of my thesis is to better understand and quantify the concept of resistance in risk assessment of natural disasters. The third objective is to quantitatively analyze geological disasters and their risk to provide better understanding of the contributions of hazard, vulnerability (1/Resistance) and exposure to risk. The fourth objective is to investigate the behavior of the global

societal resistance to earthquake disasters. The fifth objective of this thesis is to improve acceptable risk criteria for natural disaster risk assessment by investigating the deficiencies and misinterpretations in other approaches and by using effective tools borrowed from engineering (e.g., reliability assessment) to define a better criteria for a global risk assessment of natural hazards.

1.1 Chapter objectives

Each chapter is written as a stand-alone paper that covers a specific aspect of the thesis objectives. The format means that a chapter may be read on its own and that each chapter can contain new science with its own results and conclusions. However, the format also necessarily results in repetition of some fundamental concepts and descriptions of data, definitions or study areas. To this end, the reader's indulgence is requested. Each chapter is outlined below.

1.1.1 Review of FN-curves and their implications for natural hazard risk assessment

This chapter, reviews the background of FN-curves draw from works in the literature such as Farmer (1967), Cox and Baybutt (1982), Hirst (1998), Skjong and Eknes (2002), and Horn et al. (2008) and their usage in risk assessment in literature such as Hagon (1984), Vrijling et al. (1995), and Jonkman et al. (2003). It also reviews the challenges of risk neutral, aversion and proneness. The mathematics of and the arguments that Griffiths (1981) and Evans and Verlander (1998) pose on the functionality of FN-curves are also studied. Societal risk assessment is compared with individual risk assessment, and the acceptable risk criteria based on FN-curves, used in some countries (Trbojevic, 2005), is summarized and analyzed. We evaluate the application of FN-curves to natural disaster risk assessment particularly the usage of industrial risk criteria. We also introduce the need for normalization of FN-curves and the normalization methods suggested by others (Prugh, 1992; Nishenko and Barton, 1995; Hungr and Wong, 2007; Horn et al., 2008). We compare the risk of natural hazards in Europe with the industrial risk assessment criteria in some European countries as a case study.

1.1.2 Concept of resistance in natural disaster risk assessment with an earthquake example (Haiti 2010)

We introduce the concept of resistance in this chapter from two perspectives: 1) from modification of risk equation (*Risk*=*Hazard*×(1/*Resistance*)×*Exp.Pop*) and 2) from the slope of the FN-curves. We introduce two types of resistance, R_c and R_e, country-specific and event-specific resistance, respectively in order to be able to compare the resistance that countries would have in case of occurrence of a geological hazard to prevent a geological disaster. We compare the resistance of Haiti, Iran, and Japan both at the country level and at the events of Haiti (2010), Bam (2003), and Kobe (1995). We also use seismic hazard assessment as well as destruction image processing to evaluate the resistance of the commune of Port au Prince to the 2010 Haiti earthquake at the gridded level.

1.1.4 Magnitude and Frequency of Geological disasters

In this chapter, we review and summarize the magnitude scales for geological hazards (earthquakes, tsunamis, volcanic activities and landslides) proposed in the literature (e.g., Gutenberg and Richter, 1942 and 1956; Scheidegger, 1975; Abe, 1989; Woo, 1999; Bardet et al., 2003; Kanamori and Brodsky, 2004; Self, 2006; McGuire, 2006). We introduce a new unified scale for magnitude of geological hazards based on their energy release (J). We modify some methodologies introduced in the literature to estimate the source energy of some of the geological hazards which caused 1,000 fatalities (disaster) and greater for which enough technical information recorded during (1600-2012). Then, we calculate the energy efficiency of the geological hazards for causing disasters (death/energy, D/J). We also compare the global risk of geological disasters with each other using FN-curve framework. We use the slope and intercept of FN-curves as indicators (one expressing resistance and one expressing the annual frequency of 1,000 fatalities and more, respectively) of risk and introduce a new risk factor.

1.1.5 Has global societal earthquake resistance improved since 1973?

In this chapter, based on a simple risk-based conceptual model, we introduce the concept of “global societal earthquake resistance". In our proposed approach, there are three main

determinants of global societal earthquake resistance: the hazard (energy release of earthquakes with M≥5.5), the number of fatalities and the exposed population. Furthermore, we compare the annual ratio of earthquake casualties to exposed population (at 5-year pentade level), with the total number of deaths per year per 1000 people (crude death rate), excluding earthquake (and other) natural disaster) deaths. We further estimate the trend of log(resistance) during the period of 1973-2010.

1.1.6 Risk and reliability in a natural disaster system

This chapter compares the risk assessment methods in natural and industrial events. We examine the application of industrial risk assessment criteria to introduce a unified framework for risk assessment of natural hazards. We estimate the probability of failure of earthquake disaster system P_f(more than 1000 fatalities is considered as failure in a natural disaster system), to compare the P_f–N curve of earthquake disasters with industrial accidents. Furthermore, we introduce the concept of reliability to natural disaster risk assessment based on failure rate of the system. We also investigate the yearly trend of reliability in the global earthquake disaster system (1950-2012) at the beginning of each yea

Chapter 2 FN-Curves and their implications for natural hazard risk assessment

2.1 Introduction

As stated by Woo (1999) (Pg. 1), “a natural catastrophe is a tragedy played on the Earth’s stage, brought about by events which are today called as the acts of God”. These acts of God are (in fact) natural hazards, defined as natural events that potentially can cause harmful consequences to human life. Natural hazards become natural catastrophes when large numbers of people or economic assets are damaged or destroyed during a natural event. Catastrophes have two sets of causes. The first set is the characteristics of the natural hazards themselves, including floods, droughts, hurricanes, cyclones, volcanic eruptions, earthquakes, landslides, snow storms and meteorites. The second set comprises the vulnerabilities of elements at risk; populations, infrastructure, and economic activities, that make them more (or less) susceptible to being harmed or damaged by a hazard event (Wisner and Luce, 1993). “Man may be powerless to stop catastrophic events” (Woo (1999), Pg.1), but creative ways have been adopted to reduce the losses. First step is to understand the extent of the risk that natural hazards impose to the human society based on past events.

Risk can be defined (among many definitions) as the probability of harmful consequences or expected losses (deaths, injuries, loss of property and livelihood, economic activity disruption, or environment damage) resulting from interactions between natural or human-induced hazards and vulnerable conditions (United Nations International Strategy for Disaster Reduction, UNISDR (2009)). Conventionally, risk is expressed by the notation $Risk=Hazard\times Vulnerability(\times Exposure)$ (Birkmann, 2006). Risk assessment/analysis is defined as "A process to determine the nature and extent of risk by analyzing potential hazards and evaluating existing conditions of vulnerability that could pose a potential threat or harm to people, property, livelihoods, and the environment on which they depend" (UNISDR, 2009). Therefore, natural hazard risk assessment is a tool that provides information on the effect of natural hazards on the life or environments of human beings.

Here, our main goal is to investigate about one of the quantitative societal risk assessment measures, the *FN*-curve. *FN*-curves are log-log plots that illustrate frequency of exceedance of

losses versus magnitude of losses. These curves are commonly used for societal risk assessment (e.g., nuclear power plant risk (Rasmussen, 1975), landslide risk (Fell et al., 2005), flood risk (Jonkman, 2007), (comparative) risk assessment in Germany (Mendes-Victor et al., 2009)) and to develop acceptable risk criteria (e.g., societal acceptable risk calculations by Skjong, 2003). However, there are debates on their applicability (e.g., Evans and Verlander, 1998), mathematics (e.g., Hungr and Wong, 2007) and importance (e.g., Abrahamsson and Johnsson, 2006).

One of the major applications of these curves is for decision-making based on quantitative risk limits. Acceptable probability (or frequency[1]) of an event with certain consequences can be examined by means of a limit line on the *FN*-curve (Ball and Floyd, 1998; Jonkman, 2007). *FN*-criteria (based on fatalities) can provide a valid basis for the evaluation of societal risks (Ball and Floyd, 1998). However, we show that (in section 2.4.3) the limit lines proposed for practice are far below the *FN*-curves of natural disaster data. *FN*-curves and their application are discussed in various literature (e.g., Jonkman (2007); CCPS (2009)); however, there are common mis-understandings and misinterpretations about these curves and their application for natural hazards. We explore methods and notations used for *FN*-curves, address misunderstandings about their application and clarify their underlying concepts in order to be able to use them for natural hazard risk assessment purposes.

In this chapter, we introduce *FN*-curves, summarize their history, and their mathematics. We also illustrate the normalization of *FN*-curves in general and for natural hazard risk assessment in particular. We use European natural disaster data for our illustrations.

2.2 History of FN-curves

FN-curves are introduced in literature as one of the quantitative measures of societal risk. Societal risk itself is not well-defined (Ball and Floyd, 1998), however, from its name, it is a measure of the sustainability of a number of people at a specific level of harm in case of certain hazards (Ball and Floyd, 1998). When quantitative risk assessment (QRA) and consequence analysis developed based on the probabilistic analysis of major hazards in 1960s and 1970s (Ball and Floyd, 1998), *FN*-curves started to be used for societal risk criteria. Lees (1996) (Chapter 9)

[1] Since the occurrence in time is commonly used for generating FN-curves, frequency is a better word to use.

claims that, using *FN*-curves as a quantitative risk assessment (QRA) method is an element that cannot be ignored in societal risk assessment and decision making processes.

Individual risk, on the other hand, is a measure of risk that defines the expected tolerance of an individual at a certain level of harm in case of certain hazards. The relationship between individual and societal risk levels varies with circumstances, however, a commonly-used guide is that, if the societal risk of more than 10 fatalities is x, the maximum individual risk is in order of $10x$ (Ball and Floyd, 1998). In section 2.4.1 we compare the relationship between individual and societal risk from various literature.

Frequency-number (*FN*) curves are generated from a set of loss data gathered over a period of time. In these plots, frequency of exceedance of the loss is on the y-axis, and the magnitude of the loss is on the x-axis. However, the other way to construct frequency-number (*FN*) curves is based on regulations and judgment of authorities. These curves have been used for design requirements and estimation of predicted values (Lees (1996), Chapter 9) since they were first developed in 1960s. The general procedure of generating *FN*-curves based on estimated fatalities of incidents is given in CCPS (2000) (P. 419) based on Marshall (1987).

The history of design requirement use of *FN*-curves goes back to Farmer (1976), who used these plots to illustrate the consequences of reactor years in the form of radiation of I^{131} in Curies (Ci) and limit the acceptability of risk of I^{131} with a straight line in a log-log area (Fig. 2.1). Fig. 2.1 illustrates the dosage of I^{133} in Curies on the x-axis and the reactor years of the dosage production on the y-axis (Farmer, 1967). Fig. 2.2 illustrates the probability of accidents versus the equivalent I^{133} release in Curies which is the closest version of Farmer-type graphs to the current P_f–N curves, which are extensively used in engineering practice (e.g., Baecher, 1982).

Although the acceptable risk defined by Farmer (1967) according to $(Consequence)\times(Frequency)=1 Ci/yr$ proposes the slope of -1 on Fig. 2.1, the acceptable limit line that Farmer (1967) proposed considering the risk aversion towards higher releases of I^{133}, in Fig. 2.1 has a slope of -1.5. This way, Farmer tries to impose a criterion for risk assessment using slope of the frequency-consequence curves.

After Farmer (Farmer, 1967), certain people (e.g., Beattie (1967)) interpreted Farmer's curve in another way with the limit line in terms of the number of casualties instead of Curies. *fN*-curves were generated for the first time by Beattie (1967), in which *f* is the frequency of casualties per year and *N* is the number of deaths per year. Note that the *f* is not cumulative. Table 2.1 shows the suggested conversion of the Curie released by I^{131} to the death rate (from thyroid cancer).

Table 2.1 Suggested acceptable estimated casualty rates for various Iodine releases (reproduced from Beattie (1967), Table 3)

Iodine released, curies	Casualty rate, persons per 10^3 reactor-years
10	0.3
10^2	2
10^3	3
10^4	2
10^5	0.7
10^6	0.2

However, the Farmer-type limit lines cannot estimate the overall risk of a system as they are based on single accidents with multiple fatalities. In other words, if the number of fatalities in an event has a frequency of *f(N)* and *N* is in the range of N_1 to N_2 , where N_2=10N_1, and the range is in a logarithmic unit, if *f* times *N* equals to a constant, $f(N)=k/N$, the line has the slope of -1 on the log-log scale. In this example, if the total maximum and minimum average death is calculated, only two numbers with a 10 factor difference will remain because of the width of interval in the definition of our criterion (Griffiths (1981), P.64). Farmer (1981) introduced the cumulative frequency of *N* or more losses versus the value of losses (*FN*-diagram) for the purpose of quantitative (comparative) risk assessment of natural and man-caused events (Fig. 2.3). Using *FN*-diagrams, Farmer proposed an acceptable limit line for risk assessment. As stated by Ballard (1993), Farmer suggested a slope of greater than -1 in order to reduce the effect of average fatalities/year from larger accidents because at slope of -1, all accidents make an equal contribution to the average fatality level.

Baecher (1982) later plotted the accepted risks for various civil facilities as a graph with annual probability on the *y*-axis and lives/cost on the *x*-axis at log-log scale. This graph was used later in a book by Baecher and Christian (2003) (Fig.507, P. 106) with the misspelling "*F–N*

chart", and by Christian (2004) when compared *fN* and *FN* diagrams. Ball and Floyd (1998) analyzed and compared the acceptable criteria based on *fN* and *FN* diagrams in more detail.

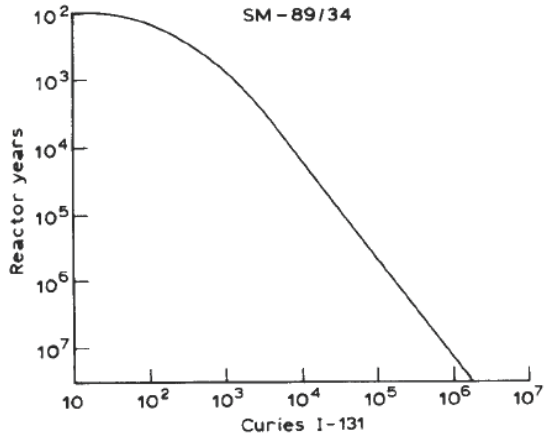

Figure 2.1: The Farmer limit line (reproduced from Farmer (1967))

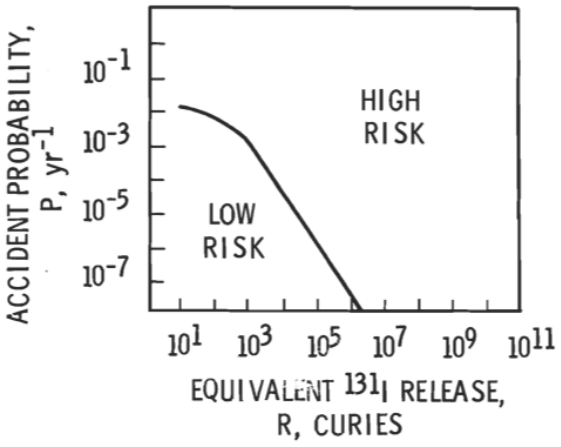

Figure 2.2: Farmer's risk averse (slope of -1.5) limit line (reproduced from Farmer (1967)).

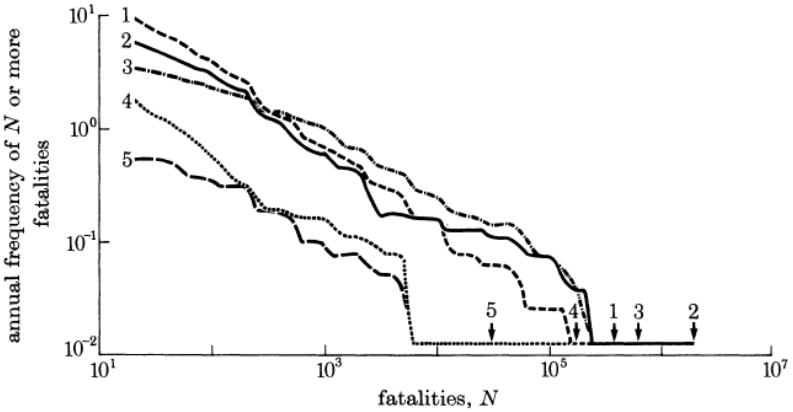

a) Frequency of global multiple-fatality accidents from natural causes. The numbered arrows are 1, Storms; 2, floods; 3, earthquakes; 4, avalanches and landslides; 5, volcanic eruptions (reproduced from Farmer (1981), Fig. 1)

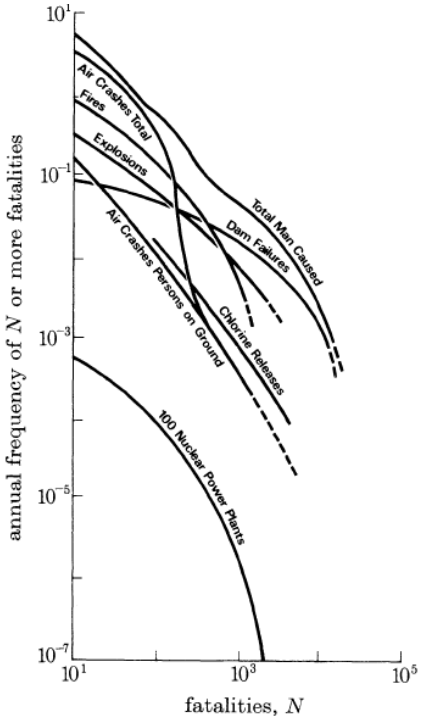

b) Frequency of man-caused events (reproduced from Farmer (1981), Fig. 3) (as stated by Farmer (1981), "fatalities due to car accidents are not shown because data were not available; car accidents cause about 5×10^4 fatalities per year").

Figure 2.3: *FN*-curves of natural (a) and man-caused (b) events (based on real data) for comparative risk assessment reproduced from Farmer (1981).

In order to be able to visually compare the frequencies of occurrences on a log-log graph, a cumulated frequency, F, is a better measure than a non-cumulative one, f (Griffiths (1981), P.64). The cumulative approach has also been interpreted through mathematical formulations (Kaplan

and Garrick (1981); Cox and Baybutt (1982); and Hagon (1984)). These two approaches, *fN* and *FN*, are simply transferable through a certain formulation that will be explained in detail in section 2.3.

In some industrial reports on risk, e.g., the Rasmussen Report-USA (1975), the Canvey Report-UK (Health and Safety Executive (HSE) (1978) and the Rijnmond Report-the Netherlands (1982), *FN*-diagrams were plotted for comparative risk assessment of industrial accidents and natural events, introducing the curves to derive acceptable levels of risk. In other words, these empirical *FN*-curves are used to obtain a frequency for the annual fatalities that makes comparisons of risk of different activities possible (Lees (1996), Chapter 9).

The other usage of *FN*-curves that has been introduced by Farmer and others was to impose acceptable levels of risk for risk assessment practices and for decision-making. Fig. 2.4 is a schematic graph of *FN*-curves which shows the anatomy of the curve on a log-log plot. Although the equation of the curve is not linear, but since the *FN*-curves are mostly plotted on a log-log scale, the curve is depicted as a straight line. The illustrated steepness (slope) of the schematic *FN*-curve in Fig. 2.4 is -1. If an *FN*-curve is steeper (e.g., slope of -1.5), it means that higher fatalities are less frequent. On the other hand, a less steep *FN*-curve (e.g., slope of -0.5) shows higher fatalities with more frequency.

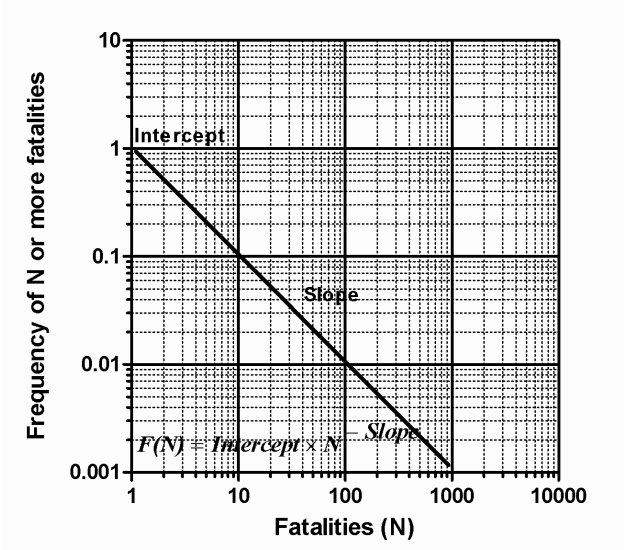

Figure 2.4: Schematic FN-curve on a log-log scale. The slope and the intercept creates an equation for the curve, $F(N)=Intercept \times N^{Slope}$.

To define acceptable criteria for risk assessment based on *FN*-diagrams (not based on real-data), following facts and rules introduced in literature must first be understood:

- (Fact) *FN*-curves hold a shape of $F \times N^{\alpha}=k$ (power-law) in which α is the slope of the *FN*-diagram and *k* is a constant (Porske, 2008). Although, other fits also can be considered in some cases, the power-law is considered as a universal fit to these type of data.
- (Rule) The slope of the *FN*-diagram is a measure of aversion to risk (Griffiths and Fryer (1979); Hagon (1984); Cox and Baybutt (1982); Slovic et al. (1984); Hirst (1998)), which is being imposed as a risk assessment criteria.
- (Rule) The minimum and maximum criteria are proposed in the form of intercepts at various *N*s on *FN*-curves by local authorities based on discretion (Skjong and Eknes, 2002).

There are several approaches to selecting the slope and intercept of *FN*-curves for risk assessment purposes. The acceptable levels of risk adopted by industrial concerns, and more generally by countries differ according to their desire for risk reduction (the slope of the curve). Some studies review the use of these criteria by countries that accept this method of risk assessment (such as Ball and Floyd (1998); Jonkman et al. (2003); Trbojevic (2005); Jonkman (2007); Porske (2008); Trbojevic (2009)). We analyze some of these criteria in section 2.3 and 2.4.1.

2.3 Mathematics of FN-curves

FN-curves that are plotted based on real data (of natural or man-caused events) are generated according to the frequency of *N* or more losses versus the value of these losses; here, our focus is on life-loss. More simply, the process of generating an *FN*-curve (based on real data) is to make an ascending sort of the number of fatalities due to an event, rank them accordingly and divide them all by the considered time period. This simple process produces a cumulative frequency of fatalities during a series of events over a specific period of time. If the result of this process is plotted versus the number of fatalities in a log-log scale, the graph would be several points that in

most cases to which a straight line can be fitted on a log-log plot with certain slope and intercept[2] which together represents the nature of that dataset. The unit of the *x*-axis and the *y*-axis on the generated graph would be number of losses and frequency (1/time) respectively. The fitted trendline is used for comparative risk assessment (e.g., Mendes-Victor et al., 2009).

Furthermore, *FN*-curves are plotted to define a reference curve for risk assessment purposes. For this purpose, one has to plot a line with a certain slope and an intercept on a log-log scale. This way, the generated line is not based on real data; it is based on the authority judgments and discretion. The imposed line is used for decision-making and setting acceptable risk criteria for risk reduction purposes (e.g., Skjong and Eknes (2002)). These criteria are extremely subjective.

Porske (2008) calls the lines that limit the acceptable risk in countries (or industrial activities) as proof line. To introduce the different depicted levels of risk on FN-curves, we borrow the diagrams that Porske (2008) used in his book for summarizing the work by Ball and Floyd (1998) in Fig. 2.5. The dark gray area limits the acceptable level of risk, the lightest gray area limits the As Low As Reasonably Practicable (ALARP) levels of risk and the white area limits the unacceptable level of risk. Fig. 2.5 from top left, respectively, shows the Groningen curve (1978), the Farmer curve (1967), Hong Kong for hazardous material (1997), Hong Kong for transport of chlorine, the revised Kinchin curve (1982), Hong Kong (1988), Netherlands (1980s), Netherlands (1996), Netherlands for transport of dangerous goods (1996), Great Britain ACDS (1991), safety of off-shore installations in UK (1991), Hong Kong (1993), and Switzerland for the transportation of hazardous material (1991-92) [Porske, 2008, pp, 305]. Variation among the limit lines in Fig. 2.5 suggests that acceptability of risk depends on the purpose of the authorities and their judgment for risk reduction. The concept of ALARP introduced by Health and Safety Executive of United Kingdom (1989) for cost-benefit analysis and risk reduction purposes.

[2] The fit is a power-law formula but when it is plotted on a log-log scale, it visualized as a straight line with a certain slope and intercept.

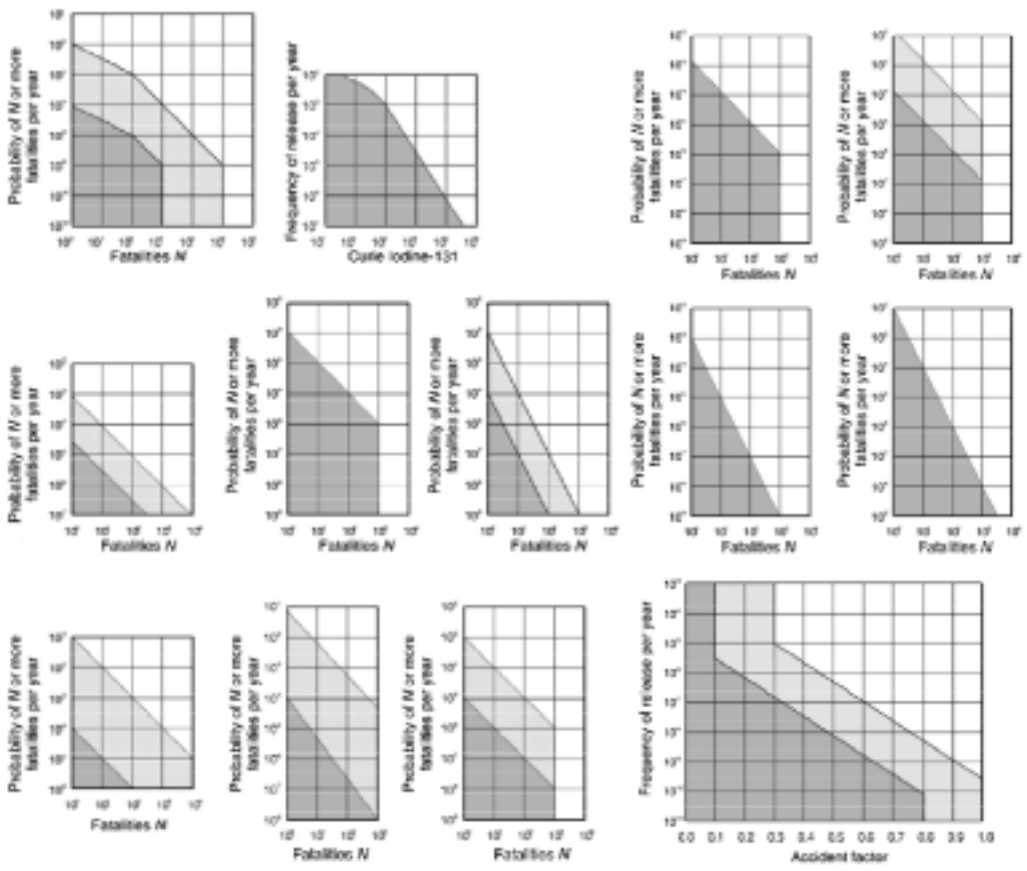

Figure 2.5: Proof lines for *FN*-diagrams (reproduced from Porske (2008), Fig. 3-24, based on Ball and Floyd (1998))

Cox and Baybutt (1982) introduce the mathematical basis of *FN*-curves (in general) as a complementary cumulative distribution function (CCDF). In Cox and Baybutt's (1982) notation, $\overline{F}(N)$ is the annual probability of consequences exceeding *N*, where the F(N) is the cumulative distribution function of N, and the over bar is defining the complementary of the function. This function can be expressed both in a discrete, Eq. 2.1 (Cox and Baybutt (1982), Eq. A.1), and a continuous, Eq. 2.2 (Cox and Baybutt, 1982, Eq. A.5) format, depending on the underlying source of and purpose for its generation, i.e., if it is generated from a dataset[3] or from a decision-making model[4].

[3] The real data from natural or man-caused events are mainly plotted in a discrete format.

[4] based on a slope and an intercept of the *FN*-curve as an acceptable limit line for risk assessment. The line is mainly plotted in a continuous format.

$$\overline{F}(N) = \text{Prob(consequences exceeding } N\text{)} \quad (1)$$

$$= \overline{\sum_{N_i \geq N} P_i}$$

$$= \int_{N}^{\infty} f(x)dx \quad (2.2)$$

where P_i s are annual probabilities of N_i consequences; $\overline{\sum_{i=1}^{n} P_i = 1}$, $P_i \geq 0$ in the case of a discrete function, and $f(x)dx$ is the annual probability of having consequences between N and $N+dN$, $0 \leq N < \infty$. The transformation of a probability density function from CCDF is simply as the minus derivative of the cumulative distribution function of N, Eq. 2.3, in continues cases (Cox and Baybutt, 1982, Eq. A.5).

$$f(N) = -\frac{d}{dN}\overline{F}(N) \quad (2.3)$$

In the industries and countries where *FN*-diagrams are used for risk assessment purposes (among other risk assessment approaches), the measure of societal risk can be estimated. This measure is defined as the expected value of the number of deaths per year, $E(N)$, and mathematically is the total number of deaths per year, Eq. 2.4 (derived from Jonkman et al., 2003).

$$E(N) = \int_{0}^{\infty} x f_N(x)dx \quad (2.4)$$

Limiting conditions that can be imposed for determining acceptable risk in a national level (considering aversion factors) through the calculation of $E(N)$ were proposed by Vrijling et al. (1995), Eq. 2.5 (Eq. 7 from Vrijling et al., 1995).

$$E(N)+k\times\sigma(N) < \beta.100 \quad (2.5)$$

where k is the risk aversion index, a constant, and β is the policy factor that varies with the degree of voluntariness which changes from 10 in the case of complete freedom of choice to 0.01

in case of an imposed acceptable risk. On the other hand, at a local level, the acceptable levels of risk are based on the *FN* criteria[5], Eq. 2.6 (Eq. 8 in Vrijling et al., 1995).

$$1-F_N(x) \quad \leq \quad \frac{C}{x^n} \; forall \; x \geq 10 \qquad (2.6)$$

where $1\text{-}F_N(x)$ is the frequency of exceedance of x fatalities, n is the slope of the limit line[6] and C is a constant that determines the position of the limit line . In order to relate and apply the acceptable levels of risk in a national level to a local level, some assumptions are considered: 1) the number of casualties obey a Bernoulli distribution function, 2) the probability distribution function of the annual number of deaths can be driven from the *FN*-curve[7] and 3) the probability distribution function of casualties should fulfill the same requirement as the associated *FN*-curve. Considering these assumptions, in a single location, we would come up with the $f(N) \leq \frac{C}{N^2}$ requirement. If the expected value of the number of fatalities is much smaller than its standard deviation, which is often the case of disasters, in a national level with N_A independent locations, Eq. 2.5 and Eq.2.4, would lead us to Eq. 2.7 (Eq. 12 in Vrijling et al., 1995).

$$C \quad = \quad \left[\frac{\beta.100}{k\sqrt{N_A}} \right]^2 \qquad (2.7)$$

where β is the policy factor and k is the risk aversion index. From the general criteria formulized in Eq. 2.5 and using Eq. 2.7 which is derived based on the conversion of the national societal acceptable risk criterion to a local acceptable risk criterion, one can derive the criteria proposed by the Dutch Ministry of Housing, Spatial Planning and the Environment (Ministerie van Volkshuisvesting, Ruimtelijke Ordening en Milieubeheer, VROM) by replacing β, k and N_A, by 0.03, 3 and 1,000, respectively (VROM-type criteria; Vrijling et al., 1995).

The ways various countries define their acceptable risk criteria are explored in more detail in the paper by Vrijling and Glender (1997). Table 2.2 is a summary of the criteria for *FN*-diagram

[5] Vrijling et al. (1995) call this as VROM-type criteria

[6] limit line in Vrijling et al. (1995) is the same as proof line in Porske (2008)(Fig. 2.5)

[7] using Eq. 2.3 to convert probability distribution function to *FN*-curve

parameters undertaken by selected countries based on different C and n values. These criteria are gathered from Jonkman et al. (2003) and complemented by the acceptable levels of risk in European Countries from Trbojevic (2005) and with the Hong Kong criteria (based on Hong-Kong (1994)). Fig. 2.6 illustrates a complete version of these criteria along with the Health and Safety Executive of the UK criterion, *Reducing Risk, Protecting People (R2P2)* (HSE, 2001).

Table 2.2 Summary of societal risk criteria used for decision-making of industrial activities in selected countries (reproduced from Jonkman et al. (2003))

Country	n	C
UK (HSE)	1	10^{-2}
Hong Kong (truncated)	1	10^{-3}
The Netherlands (VROM)	2	10^{-3}
Denmark	2	10^{-2}
Czech Republic	2	10^{-4}
France	0	10^{-7}

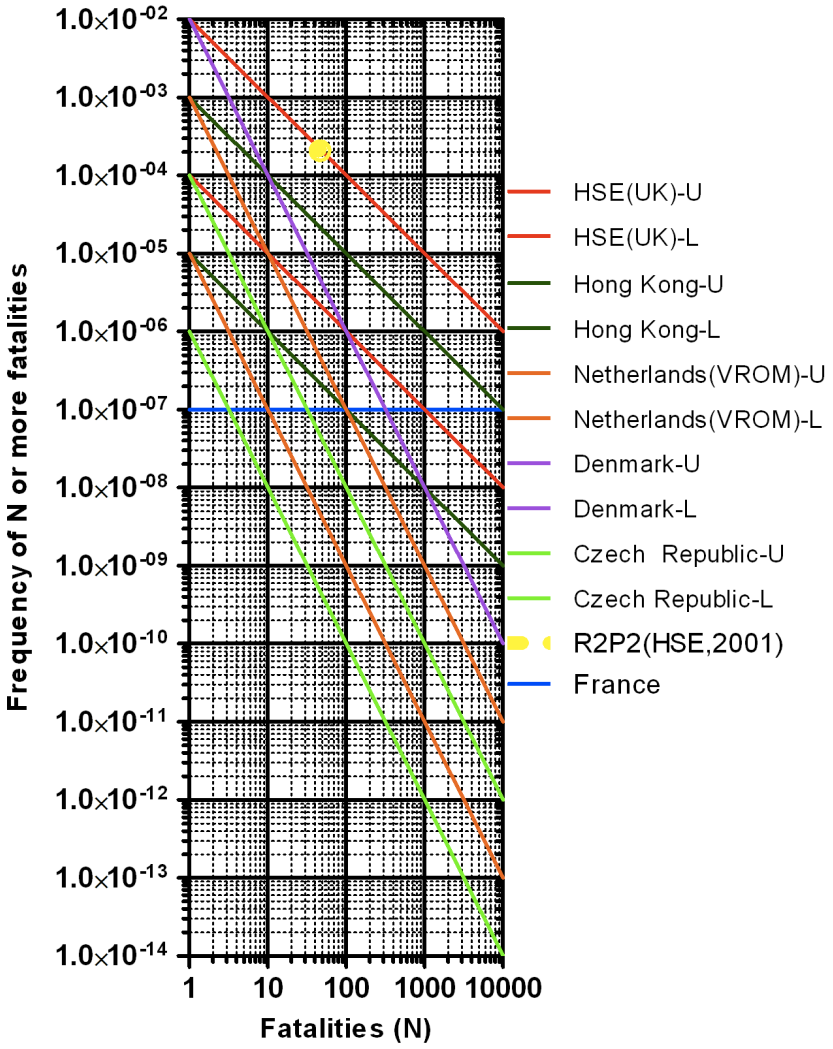

Figure 2.6: Acceptable level of risk in some countries based on HSE (2001) (R2P2), Trbojevic (2005) and Jonkman et al. (2003) (Netherlands, Denmark, UK and France), and Hong Kong Report (1994).

Since Eq. 2.5 is used for the total risk and it includes risk aversion index, k, and the standard deviation, σ, the term "risk averse" is used when the criteria is imposed. On *FN*-curves, the concept of risk averse, neutral and prone is contained in the slope (steepness) of the curve, n in Eq.2.6. Slope of -1 represents risk neutrality, slope of smaller than -1 represents risk aversion and slope of greater than -1 represents risk proneness (Pikaar and Seaman, 1995). Jonkman et al. (2003) compare the aversion indices used in various acceptable risk level calculations in literature in more detail. Vrijling and van Gelder (1997) showed that the area under *FN*-curve (which is a measure for societal risk (Ale et al., 1996)) equals the expected number of fatalities per year. Later, Jonkman et al. (2003) derived a mathematical relationship between the individual

risk and societal risk based on the individual risk contours. More details on individual risk contours can be found in section 2.4.1.

Hagon (1984), uses slightly different notation and approach in using *FN*-curves as a risk analysis tool based on a graph that compares different aversion indices, α, on a diagram of $S(N,\alpha) = \sum 1/N^{\alpha}$ on the *y*-axis and the maximum number of fatalities, *N*, on the *x*-axis, Fig. 2.7. S(N, α) is a function that is based on summation of the $1/N^{\alpha}$ values, which is borrowed from a simple power-law formula of $fN^{\alpha}=r$, where *f* is the frequency (per year) and *r* is a constant. Calculation of the cumulative frequency (for *FN*-diagrams) is introduced as a discrete and continuous summation of *f* s, Eq. 2.8 (Eq. 2 in Hagon-1984). This transformation brings a new function, *S*(*N*,α), of number of fatalities, *N*, and aversion index, α , to the mathematics of *FN*-diagrams. In Eq. 2.8, the frequencies are summed and generate the cumulative frequency of N=1 to N=K. Replacing *f* by the inverse of the power-law formula, $fN^{\alpha}=r$, and considering the new *S*(*N*,α) function, Eq. 2.9 (Eq. 3 in Hagon, 1984) is evident. Eqs. 2.8 and 2.9 show the relationship between *FN*-curve and the new function. Results of the cumulative frequencies and the total deaths per year for different aversion factors, α, are shown in Table 2.3.

$$(F)_1^K = \sum_{N=1}^{N=K} f \qquad (2.8)$$

$$= \sum_{N=1}^{N=K} \frac{r}{N^{\alpha}}$$

$$= rS(N,\alpha) \qquad (2.9)$$

Table 2.3: Integrals based on $fN^{\alpha}=r$, reproduced from Hagon (1984)

Table 1. Integrals Based on $fN^{\alpha} = r$

Aversion Index	Cumulative Frequency $(F)_{N_1}^{N_2}$	$F_N = (F)_N^{\infty}$	Total Deaths/Year $(D)_{N_1}^{N_2}$
$\alpha = 1$	$r \ln \frac{N_2}{N_1}$	∞	$r(N_2 - N_1)$
$1 < \alpha < 2$	$\frac{r}{\alpha - 1}\left(\frac{1}{N_1^{\alpha-1}} - \frac{1}{N_2^{\alpha-1}}\right)$	$\frac{r}{\alpha - 1}\left(\frac{1}{N^{\alpha-1}}\right)$	$\frac{r}{2-\alpha}(N_2^{2-\alpha} - N_1^{2-d})$
$\alpha = 2$	$r\left(\frac{1}{N_1} - \frac{1}{N_2}\right)$	$\frac{r}{N}$	$r \ln \frac{N_2}{N_1}$
$\alpha > 2$	$\frac{r}{\alpha - 1}\left(\frac{1}{N_1^{\alpha-1}} - \frac{1}{N_2^{\alpha-1}}\right)$	$\frac{r}{\alpha - 1}\left(\frac{1}{N^{\alpha-1}}\right)$	$\frac{r}{\alpha - 2}\left(\frac{1}{N_1^{\alpha-2}} - \frac{1}{N_2^{\alpha-2}}\right)$
			$= \frac{r}{\alpha - 2}$ for $N_2 = \infty$, $N_1 = 1$

Note: The above relations approximate to the exact equations (3), (4), (5) and (6) if $N > 30$ and limits are taken to be $N_2 + 0.5$, $N_1 - 0.5$.

Hagon's (1984) approach for the estimation of the total number of fatalities per year is shown in Eq. 2.10 (Eq. 8 in Hagon, 1984) which is a similar approach to that of Vrijling et al. (1995) in Eq. 2.4, but with slight changes. The domain in which the summation is calculated is between 1 and the maximum number of fatalities that can occur (i.e., maximum exposure) whereas in Eq. 2.4 the domain starts from the minimum number of fatalities, which can be zero or one, and goes to the infinity. The relationship between the estimated total number of fatalities and the new function is shown in Eq. 2.11 (Eq. 6 in Hagon, 1984).

$$(D)_1^K = \sum_{N=1}^{N=K} fN \qquad (2.10)$$

$$= \sum_{N=1}^{N=K} \frac{r}{N^{\alpha-1}}$$

$$= rS(N,\alpha-1) \qquad (2.11)$$

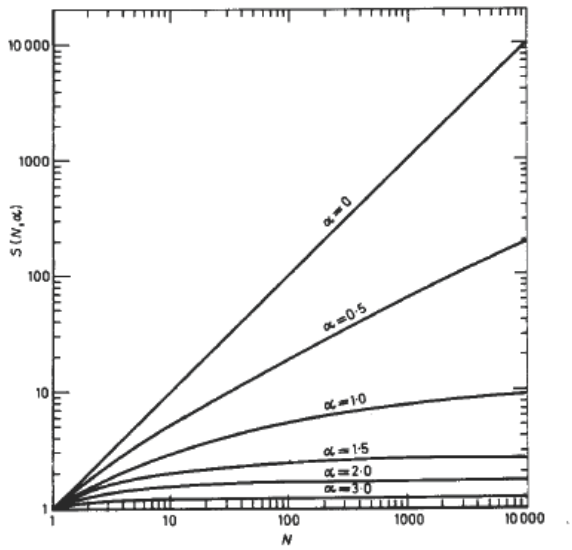

Figure 2.7: Different aversion indices, α, on $S(N,\alpha)$ versus maximum number of fatalities, N (reproduced from Hagon (1984))

Wilson (1975) proposed that the risk involving N people simultaneously is N^2 times as important as an accident involving one person. This proposal indicates a slope of -1 for less than one fatality and -2 for more than one fatality on *FN*-diagrams; these slopes used as nuclear reactor risk assessment criteria (Fig. 2.8). This is similar to the Risk Integral, *RI*, approach proposed by Carter (1995) and Cassidy (1996), Eq. 2.12, and interpreted by Vrijling and van Gelder (1997) in terms of the area of the *FN*-curve, Eq. 2.13 (Eq. 10 in Vrijling and van Gelder (1997)). In Eq. 2.12 and Eq. 2.13, the unit is $(death^2/year)$[8]. The *RI* method is justified by Hirst (1998) as it is compatible with the expected (dis)utility function. This justification is in reply to the published arguments in which *FN*-curves are alleged to be unsatisfactory (Evans and Verlander, 1998). In section 2.3.1 and Appendix I, we go into the detail of the comparison of *FN*-curves with disutility functions with focus on justification of *FN*-curves. Hirst (1998) uses a term called "weighted risk indication" which emphasizes the number of fatalities in an event by applying a power greater than one to *N*, similar to the approach that Wilson (1975) suggested. Hirst (1998) proved that the *RI* can be expressed as an equation in the form of an expected

[8] since in the Eq. 2.12, x has the unit of *death*, and the frequency, $\overline{F}(x)$, has the unit of $1/year$, an integration over x will have the unit of $death^2/year$.

disutility function, $ENFY = \sum f(N).N = \sum F(N)$, where ENFY is an abbreviation for the expected number of fatalities per year. By applying some mathematical transformation between $f(N)$ and $F(N)$, using Eq. 2.3, we can derive Eq. 2.14 (Eq. R.1 in Hirst (1998)). The term in the square brackets in Eq. 2.14 is the aversion multiplier and it includes the slope of an *FN*-curve, a. Later, Horn et al. (2008) introduced the general form of ENFY equation as a measure for societal risk, $Wf_a = \sum_{n=1}^{M} \boldsymbol{f(N).N^a}$, where a is an aversion factor for large incidents ($1 \leq a \leq 2$) and M is an upper limit on the number of fatalities per incident.

$$RI_{Cassidy/Carter} = \int_0^{\infty} \boldsymbol{x.\overline{F}(x)dx} \quad (2.12)$$

$$RI_{Vrijling} = \frac{1}{2}(E^2(N)+\sigma^2(N)) \quad (2.13)$$

$$RI_{Hirst} = \int_N^{\infty} \overline{\boldsymbol{F}}(\boldsymbol{x}).\left[\frac{(\boldsymbol{x}+\boldsymbol{1})^{\boldsymbol{a}}}{(\boldsymbol{x}+\boldsymbol{1})^{\boldsymbol{a}} - (\boldsymbol{x})^{\boldsymbol{a}}}\right]\boldsymbol{dx} \quad (2.14)$$

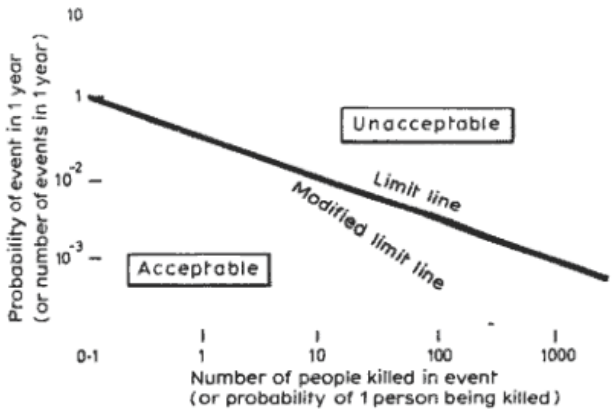

Figure 2.8: Wilson Criteria for multiple fatality, reproduced from Wilson (1975)

Horn et al. (2008) also proposed a more generalized formulation that summarizes the risk integral approaches of above-mentioned authors, based on the fact that the risk value at a composite region S is equal to the sum of the values of its parts ($z(S) = \sum_{s \in S} z(s)$). Eq. 2.15 (Eq. 12 in Horn et al. (2008)) shows the steps that one can follow from the definitions of risk measures in

terms of *f(n)* introduced by Hirst (1998) to find the relationship between the scalar measure of societal risk, Wf_a with respect to its parts in a composite region *S*.

$$Wf_a(S) = \sum_{n=1}^{M(S)} f(n,s).n^a$$

$$= \sum_{s \in S} \sum_{n=1}^{M(S)} f(n,s).n^a$$

$$= \sum_{s \in S} Wf_a(s) \qquad (2.15)$$

Skjong and Eknes (2002) suggested a method to calculate the acceptable risk criteria in terms of the intercept of *FN*-diagrams in a general format. Their method is based on the Potential Loss of Life (*PLL*), which is the expected loss of life due to an event. The *PLL* is calculated by averaging the fatality rate per Gross National Product (GNP), *q*, and economic value, *EV*, of the activity, Eq. 2.16 (Eq. 1 in Skjong and Eknes (2002)). This value is equal to the summation of the number of fatalities that may occur in the event times the frequency of occurrence of an accident involving *N* fatalities, Eq. 2.17 (Eq. 2 in Skjong and Eknes (2002)).

$$PLL = q.EV \qquad (2.16)$$

$$= \sum_{N=1}^{N_u - 1} N f_N \qquad (2.17)$$

$$= F_1 \left(\frac{1}{N_u^{b-1}} + \sum_{N=1}^{N_u - 1} \frac{(N+1)^b - N^b}{N^{b-1}(N+1)^b} \right) \qquad (2.18)$$

where *N* is number of fatalities, N_u is the upper limit for fatalities, F_1 is frequency of events with one or more fatalities, and *b* is the slope of *FN*-curve. Using Eq. 2.18, and setting the slope to $b = -1$, F_1, frequency of events involving one or more fatalities, can be calculated. According to Skjong and Eknes (2002), the ALARP area would be limited by $\frac{F_1}{10}$ and $F_1 \times 10$ on the *y*-axis, shown on Fig. 2.9 (reproduced from Fig. 1 in Skjong and Eknes (2002)).

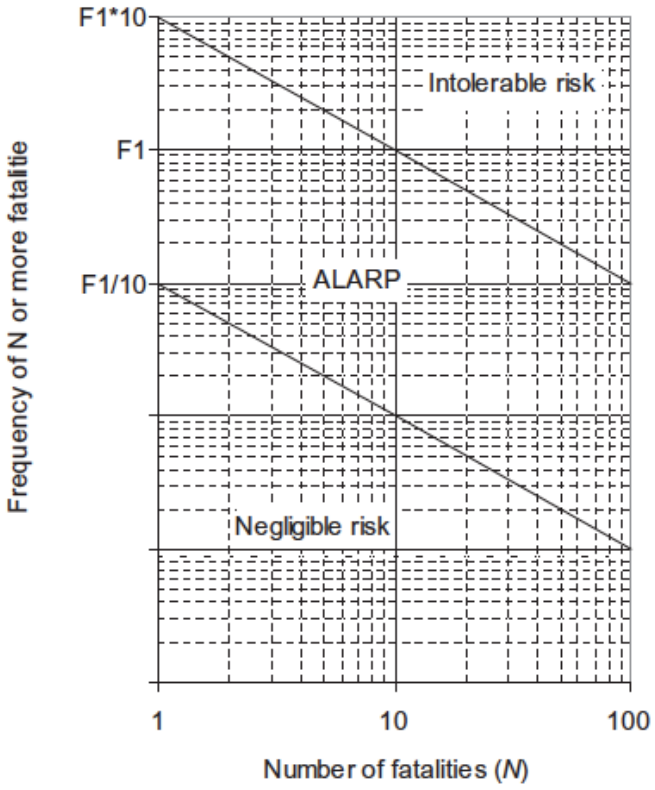

Figure 2.9: General format of societal acceptance criteria, FN-curves (reproduced from Fig. 1 in Skjong and Eknes (2002))

All of the approaches mentioned above are different perspectives of various authors from the integrated societal risk used as acceptable risk criteria mostly in industry. However, containing similar realization of the frequency-based measures of risk; $f(N)$ and $F(N)$ are the bases of the calculations and methods. All above measures can also be derived from the combination of the individual risk (IR) and the societal risk (SR) formulations and criteria. In section 2.4.1 we further compare the bases and the mathematics of IR and SR.

2.3.1 Is the mathematics of *FN*-criterion adequate?

Evans and Verlander (1998) criticize the mathematical formalism of the *FN*-criterion in comparison with (dis)utility criterion. The disutility function is based on the expected utility of multiple fatality accidents. In this comparison, Evans and Verlander (1998) use an example of two systems with disutility of $u(n)$, where n is the size of accidents, and tolerability thresholds of U_1 and U_2. The *FN*-criteria for the two systems are given as $C_1(n)$ and $C_2(n)$. In this example, these two systems are combined into a single system, without any changes in the risks. In Evans

and Verlander's approach, disutility functions and *FN*-criteria are both considered as linear functions, therefore, in a combined system, they are linearly additive. However, in *FN*-curves, the relationship between the intercept (*FN*-criterion, $C(n)$) and size of the accident, n, is not linear. From Eq. 2.6, Eq. 2.9, Eq. 2.11 and Eq. 2.32 (from Evans and Verlander, 1998) this nonlinearity is obvious.

In a combined system using *FN*-criterion framework, if the criteria are added non-linearly $\frac{1}{C(n)}=\frac{1}{C_1(n)}+\frac{1}{C_2(n)}$, instead of the linear summation used by Evans and Verlander (1998), $C(n)=C_1(n)+C_2(n)$, the result of the combined intolerability measure, in both disutility and *FN* approach will be the same. Details of this derivation is given in Appendix I.

Horn et al. (2008) used another strategy based on the same examples used in Evans and Verlander (1998) to criticize their conclusion regarding the usefulness of *FN*-curves. Horn et.al (2008) in reply to the following paragraph by Evans and Verlander (1998):

"This is a situation where the judgment about tolerability [i.e., acceptability] changes for reasons that have nothing to do with safety. It follows that the criterion based on FN curves does not always come up with the same judgment for the same safety situation. It thus fails an essential logical test for a prescriptive criterion." (Evans and Verlander, 1998, P.165),

suggest that:

"... this interpretation ignores the critical element of organizational context. In terms of ENFY or F(n), the system as a whole (i.e., the two airlines combined) is identical in the two scenarios, as one would expect. The difference between the scenarios is due to differences in the types of risk assumed by each airline, taking into account both the frequency and severity of accidents. In particular, the exchange of aircraft has produced imbalances in each airline's "risk portfolio" such that Airline 1 is overexposed to high-frequency incidents, and Airline 2 to high-loss incidents. The F(n)/C(n) criterion thus has potential value in detecting such imbalances within individual enterprises, with potential ramifications in fields such as the insurance industry." (Horn et al., 2008, P.1717)

From Horn et al.'s (2008) reasoning, beside our mathematical argument on the non-linearity of the *FN*-criteria, we can conclude that *FN*-curves are still (mathematically and rationally) good tools for decision-making purposes.

2.3.2 FN-curve or Power-law distrubution

Power law (PL) distributions, also known as Pareto distribution, Yule-Simon distribution, and Zipf's law, have been largely reported in the modeling of distinct real phenomena. Nevertheless, this is still a controversial issue on PLs being simply spurious facts or they are about how well or how poorly these distributions fit the data (Pinto et al., 2012). When we have a non-negative random variable, x, that follows a PL distribution, the complementary cumulative distribution function of x is: $$F(x) = P(X \geq x) = \frac{C}{(a-1)} x^{-(a-1)} \qquad (2.19)$$

where **a** > 0 and C > 0. A random variable that follows a Pareto distribution, the rank-frequency plot, in log–log scales, is asymptotically a straight line. This is exactly similar to what we introduced for FN-curves, Fig. 2.4.

PL distributions are detected in various real-data random variables, such as size of the cities, income (wealth) in various countries or local regions (Nitsch, 2005), size of the fire (Weiguo et al., 2006), online sales (Newman, 2005), wars and terrorist attacks (Richardson, 1948, 1960), occurrence of earthquakes (Gutenberg and Richter 1944), epidemics (Stroud, 2006) and size of craters (Pinto et al., 2012).

Clauset et al. (2009) tested and reported the parameters of PL distribution among 24 datasets drawn from physics, earth sciences, biology, ecology, paleontology, computer and information sciences, engineering, and the social sciences.

As shown by many authors, PL distribution is very common in nature and around us. Using the term "FN-curve" in the context of risk assessment is only because of its distinction otherwise, FN-curves are not curves that have not been introduced or assessed before; they are simple PL distributions that are applicable for loss data.

Distributions of many natural processes, such as earthquake energy, and casualties from natural disasters, are often modeled by power-like laws, such as the Pareto distribution. Pisarenko and Rodskin (2014) show that in heavy-tailed distributions (such as power-law) the expected maximum event is not a stable measure for estimation of risk. Instead, the high-level quintile of generalized Pareto distribution (GPD) in a certain time is a more stable measure of risk.

Now, why does PLs give a good description of data from seemingly completely unrelated phenomena? Baek et al. (2011) argue that because they can all be described as outcomes of a ubiquitous random group division in a Random Group Formation (RGF), i.e., there is a systematic change in the PL-index (the slope of the log-log plot) with system size. One consequence of this theory is that, the PL index is determined by the size of the largest group. This will be helpful when we aim to analyze the slope of a real-data FN-curves.

2.4 Risk and Risk Assessment

Bernstein (1998) (pg. 8) states that the word "*risk*" is derived from an Italian word, "*risican*", which means "*to dare*", i.e., risk is "*the action we dare to take, which depends on how free we are to make choices, are what the story of risk is all about*" (Bernstein (1998), pg. 8). The definition of risk includes two main components: 1) in-determination and 2) consequences (Porske, 2008). The conceptual, mathematical and engineering definitions of risk (to life) always carry these two components. As Aven (2011a) mentioned, the quality, consistency, and meaning of the definitions are important for a unified framework for risk assessment and management. The conceptual definition of risk, Eq. 2.19, is based on the common knowledge of risk, which includes hazard and consequences.

$$Risk = Hazard \times Consequenses \qquad (2.19)$$

Here, *Hazard* from *al zahr* (the Arabic word for dice) indicates probabilistic nature of risk with the unit of 1/time or , and *Consequences* is the total value of elements at-risk which is expressed as financial or life loss with the unit of the value of consequences (e.g., number of fatalities, or amount of money loss). *"Risk analysis is a process that determines risk by analyzing potential hazards and evaluating the conditions that could pose a potential harm to people, property, livelihoods, and the environment"* (Dilley et al., 2005). Risk assessment involves defining an acceptable criterion for risk at which the consequences are affordable (CCPS, 2009). Acceptable risk criteria are mainly developed locally based on the opinion of the decision-makers. However, there are certain theoretical (and mathematical) bases for decision-making process. We introduce a number of approaches in this section.

2.4.1 Individual Risk (IR) vs Societal Risk (SR)

Individual Risk (IR) is a measure that explains the possibility of harm to individuals in an at-risk location. The (mathematical and conceptual) definition of IR however, varies in literature and practice. IoCE (1985) nomenclature defines IR as "the frequency at which an individual may be expected to sustain a given level of harm". According to Bottelberghs (2000), IR is defined as the probability that an average unprotected person, permanently located at a certain location, would die due to a hazard. Eq. 2.20 (from Jonkman et al. (2003)) is the mathematical formulation for IR that Jonkman et al. (2003) use based on the understanding of the definition of individual risk and the realization of dependent failure from Bedford and Cooke (2001) (Chapter 8).

$$IR = P_f P_{d|f} \tag{2.20}$$

where P_f is the probability of failure (unit of 1/time) and $P_{d|f}$ is the probability of the death of an individual in the case of failure (no unit); this definition was used by the Dutch Ministry of Housing, Spatial Planning and Environment (VROM) (Jonkman et al., 2003). From this definition, IR is a property of a place since it assumes permanent location for the individual. That is why Stallen et al. (1996) and later Bottelberghs (2000) and Jonkman et al. (2003) use risk contours for presentation of (individual) risk. Common graphical illustration of individual risk contours is shown in Fig. 2.10 (reproduced from Fig. 4.2 in CCPS (2000)) and in Fig. 2.11 (reproduced from Fig. 1 in Jonkman et al. (2003)). The procedure of generating risk contours for chemical installations is vastly discussed in CCPS (2000) (P. 411 and P. 413).

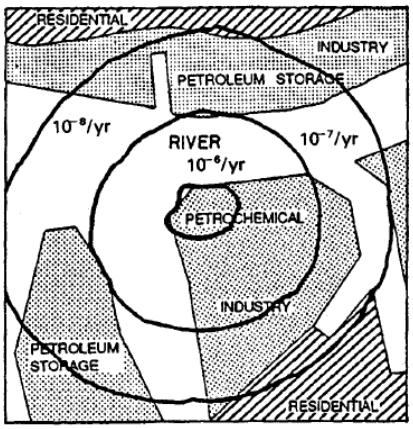

Figure 2.10: Example of an individual risk contour (circles that connect points of equal individual risk of fatality, per year). (reproduced from Fig. 4.2 of CCPS (2000))

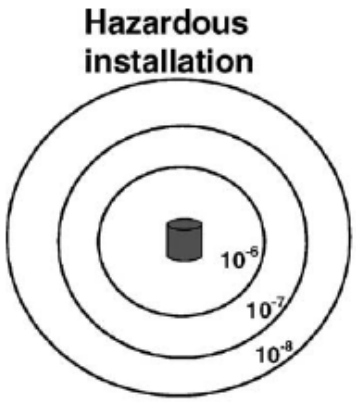

Figure 2.11: Individual risk contours for hazardous installations (point source). (Reproduced from Fig. 1 of Jonkman et al. (2003))

Societal risk (SR) is defined by IoCE (1985) as the relationship between frequency and the number of people who suffer from a specific level of harm in a given population. SR is the risk of multiple-fatality events that affects the whole society. Individual risk contours are also used for the realization of societal risk (SR) by Stallen et al. (1996) and later by Jonkman et al. (2003). The relationship between IR and SR is shown in Fig. 2.12 using individual risk contours. Both situations (A and B) have equal contours with individual risk levels (shown by IR and IR'), however, the SR in situation B is greater than SR in situation A since the population density in situation B is larger.

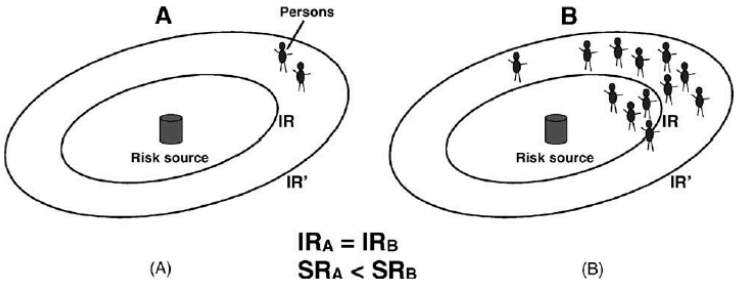

Figure 2.12: The difference between individual and societal risk proposed by Jonkman et al. (2003). Both situations have equal contours with two individual risk levels (shown by IR and IR'). Situation B has a larger societal risk because of a larger population density (reproduced from Jonkman et al. (2003), Fig. 4).

Trbojevic (2005) also relates the IR to SR by using the approach that Schofield (1993) developed for societal risk criteria. Trbojevic (2005) applies this method to compare the IR and SR of

European countries. In this approach, potential loss of life, *PLL*, is defined as Eq. 2.21[9](from Trbojevic (2005)), which relates the individual risk to the frequency of *N* fatalities.

$$PLL=N_{max}\times IR \quad = \quad \sum f(N)\times N \qquad (2.21)$$

where $f(N)$ is the frequency of exactly *N* fatalities ($f(N)=F_N-F_{N+1}$ (Schofield, 1993)), *N* is the number of fatalities, *IR* is the maximum tolerable individual risk and N_{max} is the number of exposed population. Table 2.4 (based on Table 4, Trbojevic (2005)) is a list of the old (previously used criteria) and new (updated criteria over time) values of $F(1)$ (frequency of exceedance of 1 fatality, intercept on *FN*-curve), aversion factor (slope of *FN*-curve[10]), acceptable *IR* (based on policy factor of countries) and N_{max} (number of exposed population), calculated from Eq. 2.21 at the given values of cumulative frequency F(1), risk aversion factor and the maximum individual risk corresponding to the *FN*-criteria imposed by United Kingdom, the Netherlands and Czech Republic.

It must be pointed out that the acceptable criteria used in Table 2.4, F(1) and IR, are based on the acceptable criteria proposed by the authorities of the selected European countries.

Table 2.4 Comparison of the frequency of 1 fatality based on *FN*-criteria, F(1), aversion factor, individual risk, IR, and calculated exposed population (N_{max}) (from Eq. 2.21) of selected countries (reproduced from Trbojevic (2005

Criterion	F(1)	Aversion Factor	IR	N_{max}
UK (R2P2)	1.00E-02	1	1.00E-05	9,763
UK (Old LUP)	1.00E-03	2	1.00E-05	163
UK (New LUP)	1.00E-03	1.5	3.00E-06	847
Netherlands (Old)	1.00E-03	2	1.00E-05	163
Netherlands (New)	1.00E-03	2	1.00E-06	1,644
Czech Republic (New)	1.00E-04	2	1.00E-06	163

[9] The definition of *PLL* in Eq. 2.17, defined by Skjong and Eknes (2002), is similar in the $\sum f(N)\times N$ part, which is the route of *FN*-curves. However, the Trbojevic's(2005) approach includes an IR-related definition, therefore, connects the IR to the FN-curves.

[10] for calculation of $f(N)$ based on $f(N)=F_N-F_{N+1}$, where $F_N=F(1)\times N^{-b}$

There is a further concept called the annual probability of loss of life (*PLL* or P_{LOL}), which has a notation similar to *PLL*, in Eq. 2.21 but an aspect similar to Eq. 2.20. For example, the probability of loss of life in case of a landslide is calculated from Eq. 2.22 (Eq. 4 of Fell et al. (2005)).

$$P_{(LOL)}=P_{(L)}\times P_{(T:L)}\times P_{(S:T)}\times V_{(D:T)} \qquad (2.22)$$

where $P_{(L)}$ is the frequency of the landslide, $P_{(T:L)}$ is the probability of the landslide reaching the element at risk, $P_{(S:T)}$ is the temporal spatial probability of the element at risk and $V_{(D:T)}$ is the vulnerability of the person to the landslide event (Fell et al. (2005)).

Horn et al., (2008) use a definition for the IR that HSE (1992) proposed, the probability of death per person per year, and interpreted this definition as the total number of deaths per year, F_A, divided by the number of persons at risk, *P*, Eq. 2.23 (Eq. 1 in Horn et al. (2008)).

$$IR=\frac{F_A}{P} \qquad (2.23)$$

Since IR and SR are mainly defined separately and independent from each other [11], an installation (or a development) might be acceptable in terms of IR but unacceptable in terms of SR. This can occur if authorities do not define risk standards with respect to the differences of the two; e.g., SR per capita can be expressed as IR, but the opposite is not true (Horn et al., 2008). This suggests that the collective behavior in societal risk is not the result of the risk that a certain individual might have; therefore, one cannot just sum up the individual risk over a certain population for calculation of the societal risk. Horn et al. (2008) also propose scaling for the SR with respect to the exposed population [12] which will be discussed in section 2.4.2 in more detail.

[11] They are mostly defined as acceptable levels of risk used for practice.

[12] For example, Horn et al. (2008) suggest that, a common unit for comparing risks to travellers at different-sized airports (from an IR perspective) which is "fatalities per traveler per annum" can be modified as "fatalities per incident per traveler per annum" when considering estimates of SR.

2.4.2 Normalization of *FN*-diagrams

Efforts have been made to normalize *FN*-curves before, such as Nishenko and Barton (1995), and Hungr and Wong (2007). However, which axis on the diagram has to be normalized? Ferreira and Slesin (1976) introduced a parameter called severity function, $S(N)$, which is defined as the "total number of fatalities in incidents in which at least N persons die" divided by the "total number of incidents during a specific period of time in which at least N persons die" (Ferreira and Slesin, 1976). This function is used in a diagram called an $F-S$ diagram which shows the cumulative frequency of fatalities, $F(N)$, on its y-axis and $S(N)$ on its x-axis, a plot similar to *FN*-diagrams but scaled with respect to the number of incidents. An acceptable risk criteria based on Ferreira and Slesin (1976) model implies a reverse cubic $F-S$ relation, $F \approx S^{-2}$, according to empirical data, (Ferreira and Slesin (1976), Figure 1, P. 8).

Nishenko and Barton (1995), applied normalization of *FN*-curves to real earthquake fatality data of several countries. Fig. 2.13 illustrates the earthquake fatality-frequency distribution of 8 countries normalized by the population of the country at the time of the earthquake. Using this method, Nishenko and Barton (1995) compared the risk of earthquake in the eight countries. Nishenko and Barton (1995) also proposed that the breaks in the slopes of some of these curves are associated with the selection and reporting criteria of fatalities in different countries. We believe that this was the first time that (normalized) *FN*-curves used for the risk assessment of a natural hazard based on the characteristics of the curves[13]. We use this approach in section 2.4.3 for the European countries. A similar method has been suggested by Horn et al. (2008) in which fatalities are normalized by exposed population for societal risk assessment. Using an example of application of societal risk assessment (based on *FN*-curves) in civil aviation, Horn-et.al-2008 conclude that, using un-scaled[14] frequency data will tend to be uninformative. Fig. 2.14 (Fig. 6 in Horn et al. (2008)) illustrates the method that Horn et al. (2008) suggests for normalization of *FN*-curves for a multi-level system, S, with components $\{s_1, s_2, s_3\}$. The deviations of the frequency of each component, $F(n,s_k)$, from the mean, $F(n,S)$, are shaded, and the upper

[13] This method is 1) based on real data and 2) normalized by the exposed population.

[14] scaling according to the population exposed to events

edge, $F(n,s_k)_{max}$, (i.e., worst-case risk) can be used for decision-making purposes. From Fig 2.14, we could also see the importance and the application of normalization on FN-curves. Neither the work of Horn et al. (2008) nor Nishenko and Barton's(1995) effort have been taken seriously in the literature or in practice. We suggest that this method will strengthen the basis of *FN*-diagrams as the confusions about these curves have resulted in less interest in them.

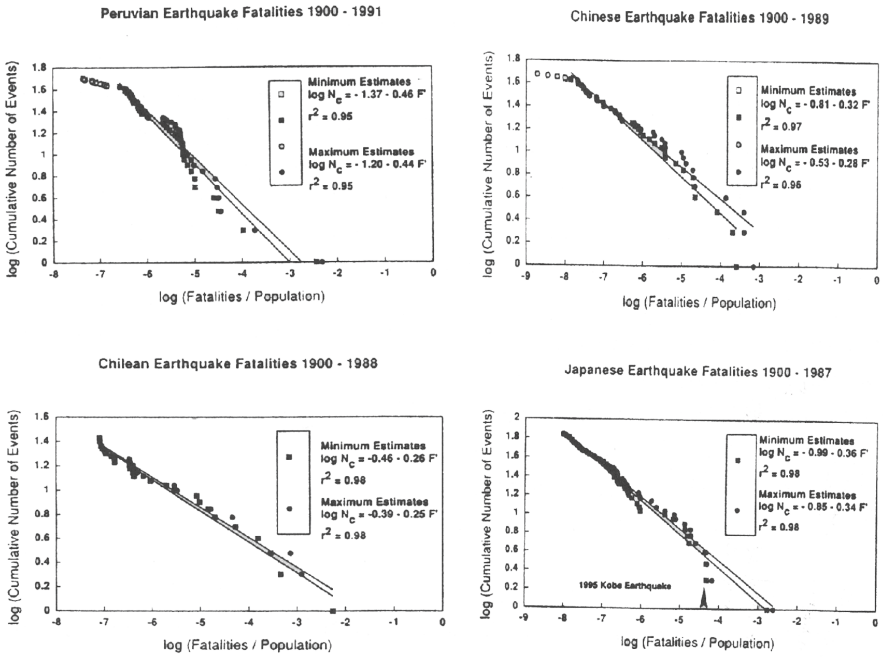

Figure 2.13: Normalized *FN*-curve for earthquake fatalities in 8 countries in log-log scale. The fatality data is based on minimum and maximum estimates of past events in the countries: Peruvian, Chinese, Chilean, and Japanese earthquake fatalities (reproduced from Nishenko and Barton (1995)).

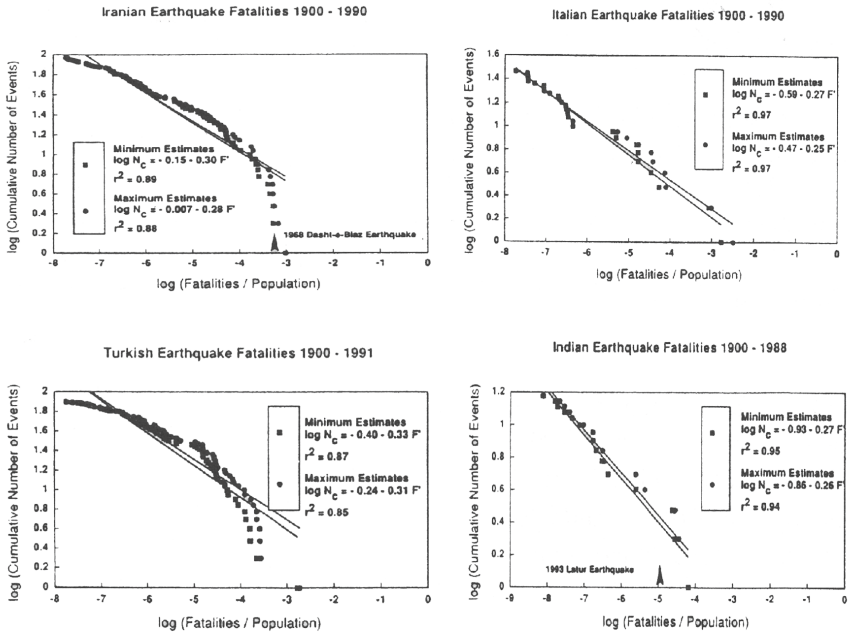

Figure 2.13(continued): Normalized *FN*-curve for earthquake fatalities in 8 countries in log-log scale. The fatality data is based on minimum and maximum estimates of past events in the countries: Iranian, Italian, Turkish, and Indian earthquake fatalities (reproduced from Nishenko and Barton (1995)).

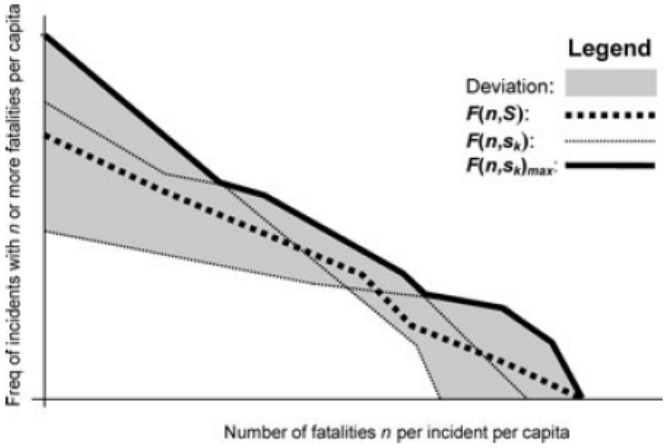

Figure 2.14: Scaled *FN*-curve (fatality per capita) proposed by Horn-et.al-2008 which shows $F(n)$ curves for a multi-level system, S with components $\{s_1, s_2, s_3\}$. The deviations of each component $F(n,s_k)$ from the mean $F(n,S)$ are shaded, and the upper edge (i.e., worst-case risk) is of particular interest for decision-making purposes. (reproduced from Fig. 6 of Horn et al. (2008))

There has been other methods introduced in literature to normalize of FN-curves that include exposed populations. To compare the background risks to the risks of a given project, Hungr and Wong (2007) proposed that the *FN*-line associated with the background risks must be normalized

to the size of the group exposed to a specific project [15]. Therefore, Hungr and Wong (2007), by considering the total *FN*-curve of human-caused accidents as background risk, proposed a scaling to the cumulative frequency, *F*(*N*), for landslide risk assessment in which the plotted data on the *y*-axis is normalized by the exposed population, in their example, the population of the USA, Fig. 2.15. As shown in Fig. 2.15, the original Rasmussen (1975) data of the total human-caused accidents (air crashes, dam failures, explosions and chlorine releases) [solid black line on top] is normalized to 1 by dividing the Rasmussen data by the population of USA, 1×10^7 [solid black line at the bottom]. Since the cumulative frequency of accidents per year with the unit of (1/time) is being divided by the population of the USA with the unit of (number), this approach is not mathematically and logically justifiable, although it acknowledges the difference between the acceptable risk criteria of natural hazards (here, landslides) and the industrial accidents. In section 2.4.3 we further introduce the use of *FN*-curves for natural hazard risk assessment.

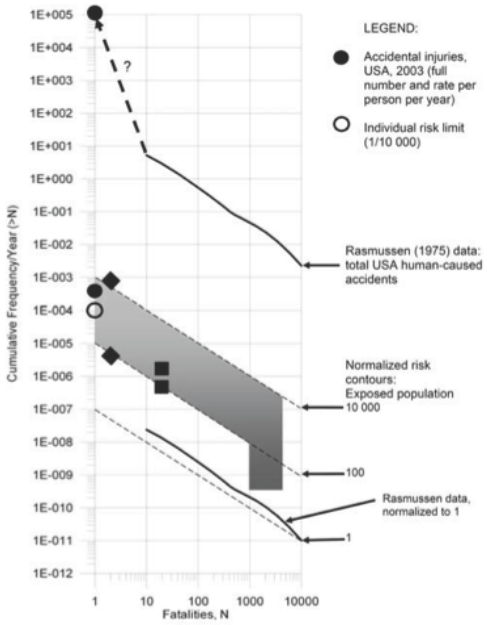

Figure 2.15: Scaling method proposed by Hungr-and-Wong-2007 for normalization of the *FN*-curve of USA human-caused accidents to 1 [solid black line at the bottom, near a dashed line] , by dividing the cumulative frequency/year of the Rasmussen (1975) data of total human-caused events [solid black line on top] by the population of the USA (1×10^7) on the *y*-axis. (reproduced from Hungr-and-Wong-2007, Fig.2)

[15] Because, 1) "the line represents a summation of many types of hazards that constitute the background risk." and "it is questionable as to whether it is a suitable 'yardstick' for evaluation of risk tolerability of only a single hazard, i.e. landslides."(Hungr and Wong (2007), P. 5)

2.4.3 *FN*-curves and Natural Hazard Risk Assessment

FN-diagrams, both with acceptable criteria lines and with real-data curves, have been used for non-natural risk assessment more than natural hazard risk assessment has. Rasmussen (1975) and some other pioneers used natural hazard *FN*-curves to define the acceptable criteria for industrial and human-caused accidents.

The *FN*-based criteria are imposed on and compared with both industrial activities and natural events without differentiation, although natural events have fewer controllable factors, i.e., nature is not controllable. Fig. 2.16 illustrates the difference between the acceptable risk criteria of some European countries and the *FN*-curves of the European countries' natural hazards (earthquakes, landslides, volcanic activities, floods, wind storms, wild fires, extreme temperatures, drought and epidemics[16]) real data. In Fig. 2.16, we use the EM-DAT database for natural disasters that killed more than 1 person[17] between 1950 and 2012 in 32 European countries (shown by blue dots). Table 2.5 shows the list of European countries and number of fatalities due to each natural hazard. These data are compared to acceptable risk criteria defined by some of the European countries including the United Kingdom Health and Safety Executive (HSE, 2001) R2P2 (Reducing Risk, Protecting People, which limits 50 or more fatalities with a frequency of 1 in 5000 per annum and imposes a slope of -1, risk neutral) shown by a red dot on Fig. 2.16; France (with a slope of zero, no criterion on aversion, neutrality or proneness), the green line on Fig. 2.16; Denmark, the Netherlands and Czech Republic (with slopes of -2, risk averse) (Jonkman et al. (2003), Ale (2005), and Trbojevic (2005)) shown by orange, purple and light blue lines on Fig.2.16, respectively; and As Low As Reasonably Practicable (ALARP) criteria (HSE, 1989) that limit the minimum and maximum fatalities between 10^{-3} to 10^{-5} per year with two lines of slope -1 (risk neutral) shown by black lines on Fig. 2.16. The average slope for the *FN*-curve of natural hazards in European countries (the blue zone on Fig. 2.16) is -0.5 (risk prone), which is not even risk neutral. As can be seen from Fig. 2.16, the acceptable criteria imposed for risk assessment are far below the real *FN*-curve trend of natural hazards.

[16] EM-DAT database considers epidemic as a natural disaster. In this research, we don't consider epidemics as a natural disaster. Although EM-DAT is not a complete database, but since it is the only integrated database for losses in natural disasters, we use it for comparison purposes.

[17] due to small number of over 1,000-fatality events, we use over 1-fatality events

This suggests that the criteria being used in some countries are too conservative for natural hazard risk assessment.

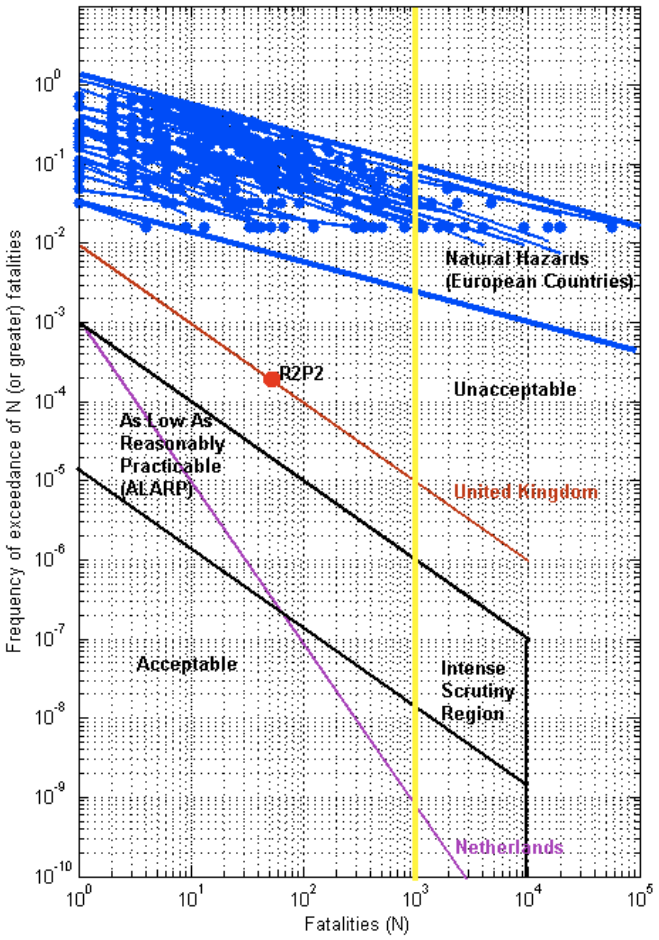

Figure 2.16: FN-curve of fatality (greater than 1) caused by natural hazards (earthquakes, landslides, volcanic activities, floods, wind storms, wild fires, extreme temperatures, drought and epidemics) in 32 European countries (thick blue lines) with respect to acceptable risk criteria in some of them. Red dot is the Health and Safety Executive criteria (HSE, 2001) and colored lines are dark red line, United Kingdom; green, France; orange, Denmark; purple, Netherlands and light blue, Czech Republic criteria (Jonkman et al. (2003); Trbojevic (2005); Ale (2005)). Thin black lines are based on the ALARP criteria (HSE, 1989). The European fatality data is obtained from EM_DAT database.

Fig. 2.17 compares the normalized *FN*−curve for natural disasters in European countries. We used the population of countries in the year that the events occurred in order to normalize the *FN*-curves generated from the data of fatalities due to natural disasters in the European countries. Population data was obtained from the World Bank (2008-2012) record

(*http://data.worldbank.org/indicator/SP.POP.TOTL*). We also put the normalized R2P2 (by the current population of United Kingdom) as a reference on Fig. 2.1. As can be seen, the R2P2 is around 3 orders of magnitude lower that the average of normalized FN-curve of European countries. Furthermore, in most of the countries, there is a break-point (aka saturation) observed on the normalized FN-curve.

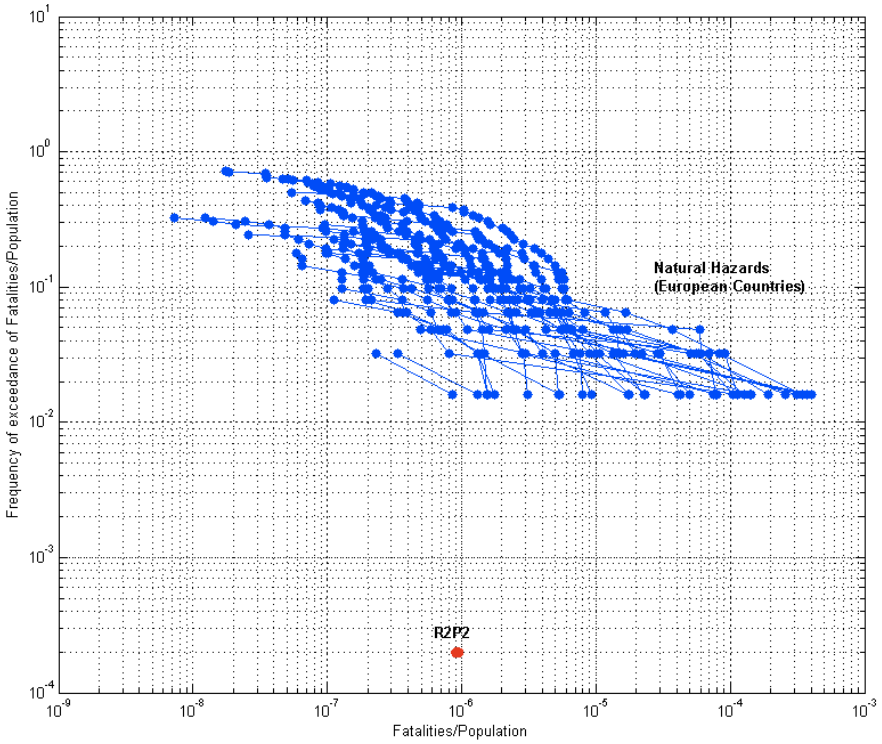

Figure 2.17: Normalized *FN*-curve of fatality (greater than 1) caused by natural hazards (earthquakes, landslides, volcanic activities, floods, wind storms, wild fires, extreme temperatures, drought and epidemics) in 32 European countries (thick blue lines) with respect to the R2P2 acceptable point

Break Points on FN-curves

From the comparison of Fig. 2.16 and Fig. 2.17, most of the normalized plots hold distinct curvatures[18] or as Nishenko and Barton (1995) stated, they have break points. The breakpoints are actually representing transitions between lines of different slopes. The reason behind these breaks can be because of the selection and reporting criteria of fatalities in different countries (as

[18] We show some examples of these curvatures using black fitted lines on Fig. 2.18

reasoned by Nishenko and Barton (1995)). From a statistical point of view, these break-points are effects of saturation and inhomogeneity in the sequence of the data.

We use another societal analogy to explain this effect on FN-curves. The fact that, for example, F(10) on an *FN*-curve is associated with 10 fatalities, however, F(0.0001), on a normalized *FN*-curve can be associated with both $\frac{10}{100000}$ and $\frac{1}{10000}$, suggests that the normalized FN-curves include some sort of superposition of data which may help to analyze the underlying societal factors of risk in the countries. In other words, (normalized) *FN*-curves bring unification to the comparison of risk (e.g., 1 fatality in a community of 10,000 population implies as high risk as 10 fatalities in a community of 100,000 population). The breaking points on Fig. 2.17 change the slope of the fitted lines (shown in black on Fig. 2.17) of the two parts of the curve from a shallow to a steeper slope. Using risk-prone, risk neutral and risk-averse expressions here, we could say that at the breaking points of a normalized *FN*-curve, a certain society transform from a risk-prone situation[19], to a risk-averse situation[20] at the breaking points of the curve.

In Fig. 2.18 we compare four countries' natural hazard data to compare their normalized FN-curves. We chose Greece, Italy, Ukraine and UK as our examples. The best power-law fits to the lower part of the FN-curves of these countries, and their confidence intervals are listed in Table 2.6.

Although, the best fit to the countries' normalized FN-curve shows similar slopes in the steeper part of the curves, between -0.47 (Ukraine) to -0.63 (Greece) with 95% confidence intervals that overlap, we argue that even the small differences on the fit reveal information on the feedback of the countries to natural hazards.

Fig. 2.18a (Greece) and Fig. 2.18b (Italy) are examples of countries which hold breaking points. In Greece, the slope is changing from -0.15 to -0.63, and for Italy, from -0.19 to -0.49. This means that Greece and Italy are less responsive (risk prone) to the low fatality/population-rate events, while for high rates of consequences, they are both risk averse (more responsive).

If no breaking point exists on the curve may imply that the response of the society to both situations of high and low consequence events are almost the same. This can be because of a

[19] more likely to cause much smaller fatalities than the exposed population

[20] less likely to cause number of fatalities closer to the number of the exposed population

constructive strategy for risk reduction in the country, e.g., Fig. 2.18c (UK), or because of the low hazard characteristics of the area, e.g., Fig. 2.18d (Ukraine). Response-analysis of these two countries (UK and Ukraine) need more information on the frequency of hazard in the countries, i.e., if the country is in a hazardous region, no-break-point is due to its preparedness and responsive actions to disasters, while when it is not in a hazardous area, lack of break-point on its normalized FN-curve is due to the nature of the region.

This information (the place of the breaking point of a normalized *FN*-curve and the different slopes of the curve before and after the breaking point) can be useful in comparative societal risk assessment of societies from the respond perspective of the countries.

Table 2.5: List of European countries and fatalities due to natural hazards (1900-2012) based on EM_DAT natural hazard database

	Drought	Earthquake (seismic activity)	Epidemic	Extreme temperature	Flood	Mass movement dry	Mass movement wet	Storm	Volcano	Wildfire	Total
Albania	0	47	7	71	19	0	0	8	0	0	152
Armenia	0	0	0	0	5	0	0	0	0	0	5
Austria	0	0	0	357	39	0	358	22	0	0	776
Azerbaijan	0	33	0	5	19	0	11	0	0	0	68
Belgium	0	2	0	2133	21	0	0	37	0	0	2193
Bulgaria	0	24	0	73	57	0	11	2	0	10	177
Cyprus	0	42	0	61	0	0	0	3	0	0	106
Czech Rep	0	0	0	470	85	0	0	10	0	0	565
Denmark	0	0	0	0	0	0	0	24	0	0	24
France	0	11	21	20956	253	64	114	414	0	32	21865
Georgia	0	15	0	0	16	0	0	0	0	0	31
Germany	0	1	0	9418	50	0	5	196	0	0	9670
Greece	0	848	0	1129	84	0	0	99	48	108	2316
Hungary	0	0	0	662	310	0	0	60	0	0	1032
Iceland	0	1	0	0	0	0	50	0	0	0	51
Ireland	0	0	2	0	5	0	0	36	0	0	43
Italy	0	6258	3	20169	1053	0	2463	190	9	21	30166
Latvia	0	0	0	86	0	0	0	6	0	0	92
Lithuania	0	0	0	81	4	0	0	8	0	0	93
Netherlands	0	0	13	1966	2001	0	0	34	0	0	4014
Norway	0	0	0	0	1	0	0	4	0	0	5
Poland	0	0	0	1684	113	0	0	42	0	35	1874
Portugal	0	0	0	2737	596	0	0	47	0	60	3440
Romania	0	1650	0	516	694	0	0	44	0	0	2904
Russia	0	2019	33	57744	566	60	414	212	0	137	61185
Slovakia	0	0	0	128	64	0	0	2	0	6	200
Slovenia	0	1	0	289	0	0	0	6	0	0	296
Spain	0	21	2	15616	1287	0	84	151	0	66	17227
Sweden	0	0	0	0	11	0	13	11	0	0	35
Switzerland	0	0	0	1039	10	0	295	22	0	0	1366
Ukraine	0	0	275	968	82	0	0	21	0	0	1346
United Kingdom	0	0	71	319	83	0	140	4338	0	0	4951
Total	0	10973	427	138677	7528	124	3958	6049	57	475	168268

Created on: Jun-8-2012. - Data version: v12.07
Source: "EM-DAT: The OFDA/CRED International Disaster Database
www.emdat.be - Université Catholique de Louvain - Brussels - Belgium"

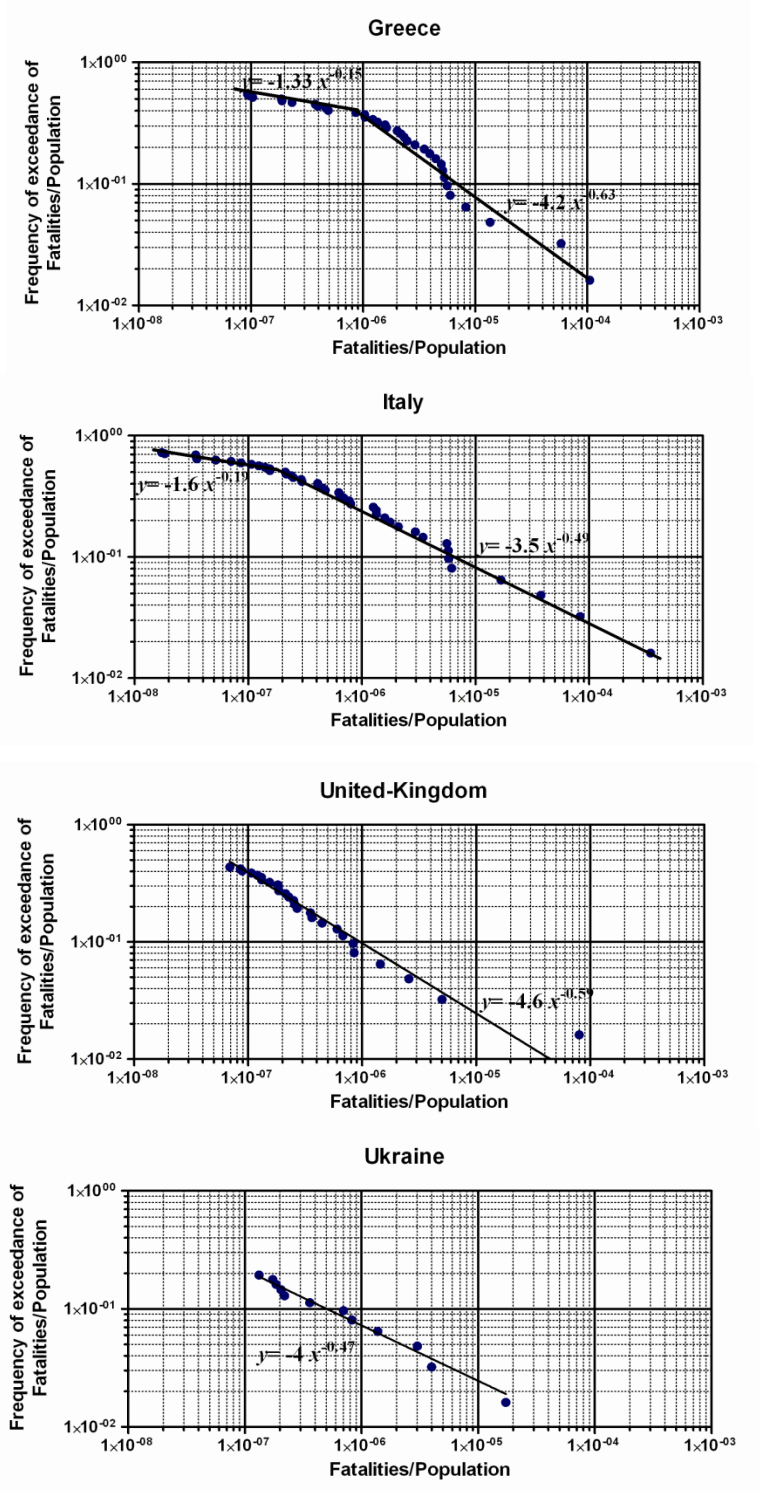

Figure 2.18: Normalized *FN*-curve of fatality in Greece (a) and Italy (b) as examples of countries that have break points on the curve, and in United Kingdom (c) and Ukraine (d) as examples of countries with no breaking point in the curve.

Table 2.6: List of the best power-law fits to the lower part of the FN-data of Greece, Italy, Ukraine, and United Kingdom shown in Fig. 2.18 (after the breaking points).

	Power-Law fit	R2	95% confidence interval of slope
Greece	*Log(Y)=-4.2-0.63x*	0.96 (n=24)	-0.69 to -0.56
Italy	*Log(Y)=-3.5-0.49x*	0.98 (n=21)	-0.53 to -0.45
United Kingdom	*Log(Y)=-4.61-0.59x*	0.98 (n=27)	-0.65 to -0.55
Ukraine	*Log(Y)=-3.95-0.47x*	0.97 (n=12)	-0.54 to -0.4

2.5 Summary and discussion

Summary:

In this chapter, we summarized the history, mathematics and application of *FN*-curves. We showed that *FN*-curves are useful tools for (comparative) risk assessment of natural hazards. Furthermore, we proved that these curves are mathematically adequate, and therefore, can be used for the analysis of loss data, for decision making purposes and defining acceptable criteria for risk. However, to improve these curves for risk assessment of natural hazards, we propose normalizing the number of fatalities used in the FN-curves by the number of exposed population.

We also compared the acceptable criteria in certain European countries with *FN*-curves and concluded that the acceptable criteria used for industrial activities and engineering practice are far too conservative for natural hazard risk assessment practice. We compared the *FN*-curve of natural hazards in Europe with the normalized *FN*-curves. We introduced a new analogy for explaining the break points on the normalized *FN*-curves, which indicates that they are due to the difference between the response of the countries to low and high consequence events. If normalization does not cause any break point it might mean that the response of the society to both high and low consequence events are almost the same. The locations of the breaking points and the slopes before and after these points are the new characteristics that can be used for comparative risk assessment of natural hazards using *FN*-curves.

Discussion:

Normalization by exposed population is a rational idea when we want to compare two events with the same impacts but different exposures, e.g. 10 fatalities in a flooded village indicates different situation from 10 fatalities in a tsunami that affects more than 1 country. Now, how

does normalization on FN-curves help in terms of risk analysis? If normalization is done based on the population of the country as an index of exposed population to the event, which is what we have done to normalize the FN-curves of Italy, Greece, Ukraine, and UK, and we do not consider the precise number of exposure in an event, one might argue that the result only shifts the trend of the non-normalized curve on y-axis. However, since the normalization is done based on the yearly population of the country and in case that we have access to the detailed number of population exposed to each event, we will be able to distinguish differences in the trend of the curves and more information will be revealed. The more precise approach is something that can be pursued in following studies.

Appendix I. Comparison of disutility criterion with FN-criterion

Disutlity Criterion

Based on Evans and Verlander (1998) it is assumed that fatal accidents occur as a Poisson process with mean frequency, f, per unit time and once it happened, the probability of n fatalities would be $p(n)$, where n is a range of integer numbers between 1 and n_{max}. The mean frequency of exact n fatalities is defined as $f(n)=f.p(n)$, therefore, $p(n)$ is:

$$p(n) = \frac{f(n)}{f} \qquad (2.24)$$

According to the theory of decision making under uncertainty, if tolerability decisions must be made , they are on the basis of so-called *expected disutility* (Evans and Verlander, 1998). The first step in the decision making process is to associate a number, $u(n)$ with an accident having n fatalities, as a measure of its harm, Eq. 2.25 (Eq. 6 in Evans and Verlander (1998)).

$$u(n) = n^{\beta} \qquad (2.25)$$

where β is a parameter for weighting the large and small accidents or "aversion to high consequence accidents" which must be greater than 1 if $u(n)$ is greater than n. Disutility of an accident, u_a, of uncertain size in the engineering system is given in Eq. 2.26 (Eq. 7 in Evans and Verlander (1998)).

$$u_a = \sum_n u(n)p(n) \qquad (2.26)$$

The disutility of k accidents each with disutility of u_a in a given period, t, is ku_a. Using the expected disutility theorem, disutility per unit time, u, is $\sum_k ku_a p(k)=u_a \sum_k kp(k)=ftu_a$, where $p(k)$ is the probability of exactly k events in a Poisson distribution with mean ft (Evans and Verlander, 1998). Therefore, the disutility per unit time, u, of such a process is fu_a. Eq. 2.26 will then become as Eq. 2.27 (Eq. 8 in Evans and Verlander (1998)).

$$u = f\sum_n u(n)p(n)= \sum_n u(n)f(n) \qquad (2.27)$$

Combining Eq. 2.25 with Eq. 2.27, we get Eq. 2.28 (Eq. 9 in Evans and Verlander (1998)) .

$$u = \sum_{n} n^{\beta} f(n) \qquad (2.28)$$

For decision makers, if u exceeds some threshold, U, the risk is intolerable and if u is less than or equal to U, the risks are tolerable.

FN-Criterion

According to Evans and Verlander (1998), $F(n)$ is the mean absolute frequency of accidents with n or more fatalities. In an *FN*-curve plot, $F(n)$ is plotted against n, in log-log scale. $f(n)$ is the mean frequency of accidents with exactly n fatalities. The relationship between $F(n)$ and $f(n)$ is given in Eq. 2.29 (Eq. 1 in Evans and Verlander (1998)).

$$F(n) = \sum_{i=1}^{n_{max}} f(i) \qquad (2.29)$$

where n_{max} is the largest possible number of fatalities in a single accident and $f(n)=F(n)-F(n+1)$ (Eq. 2 in Evans and Verlander (1998)). f is the frequency of fatal accidents of all sizes, therefore, $f=\sum_{i=1}^{n_{max}} f(i)=F(1)$ (Eq. 3 in Evans and Verlander (1998)). Tolerable criterion defined here is $F=F(n)$ and intolerable criterion is $F=C(n)$. The tolerability if a system is judged by comparing $F(n)$ and $C(n)$, therefore, a tolerable system has to satisfy tolerable condition of $log[F(n)]-log[C(n)]\leq 0$ for all n values. This condition suggests $nmax\{log[F(n)]-log[C(n)]\}\leq 0$. The system is just tolerable of equality holds, Eq. 2.30 (Eq. 4 in Evans and Verlander (1998)).

$$nmax\{log(\frac{F(n)}{C(n)})\}=0$$

$$nmax\{\frac{F(n)}{C(n)}\}=1 \qquad (2.30)$$

In a general case of $F=\nu C(n)$, where ν is a positive number from 0 to ∞ (defined as the intolerability measure of the system , Evans and Verlander (1998)), Eq. 2.30 can be generalized to Eq. 2.31 (Eq. 5 in Evans and Verlander (1998)).

$$\nu = nmax\{\frac{F(n)}{C(n)}\} \quad (2.31)$$

If the criterion function is a line with slope of $-\beta$ in a double-logarithmic scale, Eq. 2.32 is applicable for $C(n)$. This changes Eq. 2.31 to Eq. 2.33.

$$C(n) = \frac{\alpha}{n^{\beta}} \quad (2.32)$$

$$v = nmax\{\frac{F(n)n^{\beta}}{\alpha}\} \quad (2.33)$$

Consistency check of disutility criterion and FN*-criterion*

Based on what we introduced according to Evans and Verlander (1998)) about disutility and *FN* criteria in the last two sections, if we consider two systems combined into a single system without any changes in the risks (assuming the disutility of accidents of size n is $u(n)$, tolerability thresholds are U_1 and U_2, and the *FN*-criterion for two systems are $C_1(n)$ and $C_2(n)$) then, based on Eq. 2.26, we can find the disutility function of the combined system from summation of $f(n)$s, $f(n)=f_1(n)+f_2(n)$ (Eq. 11 in Evans and Verlander (1998)).

The tolerability threshold based on the disutility function, U, for the combined system using Eq. 2.27, is $U=f(n)u(n)=[f_1(n)+f_2(n)]u(n)=U_1+U_2$ (Eq. 13 in Evans and Verlander (1998)). The overall criterion based on *FN*-intolerability, $C(n)$, and *FN*-tolerability, $F(n)$, in Evans and Verlander (1998), are assumed similar to disutility function (linear), therefore, $C_1(n)+C_2(n)$ (Eq. 14 in Evans and Verlander (1998)) and $F_1(n)+F_2(n)$ (Eq. 12 in Evans and Verlander (1998)), respectively. We argue that the linear summation is not rational when the functions of $C(n)$ and $F(n)$ are non-linear with respect to n, Eq. 2.32. Our suggestion for the overall intolerable criterion, $C(n)$, is based on a non-linear summation of $C(n)$, Eq. 2.35. For the tolerable criterion, $F(n)$, Eq. 2.36 is derived based on the non-linear summation of $F(n)$. Here, for the sake of simplicity $\beta=1$ is assumed.

$$\frac{1}{C(n)} = \frac{1}{C_1(n)} + \frac{1}{C_2(n)} \quad (2.34)$$

$$C(n) = \frac{C_1(n)C_2(n)}{C_1(n)+C_2(n)} \qquad (2.35)$$

$$F(n) = \frac{F_1(n)F_2(n)}{F_1(n)+F_2(n)} \qquad (2.36)$$

To check the general consistency condition, its is assumed that systems 1 and 2 are just tolerable, therefore, the combined system should also be tolerable. The logical criteria that have to be satisfied by each approach are:

- for the disutility function: if $u_1=U_1$ and $u_2=U_2$,then u must be U_1+U_2 . (Eq. 15 in Evans and Verlander (1998)) (Condition 1)
- for FN-criterion intolerability measure, Eq. 2.31, if $\nu_1=1$ and $\nu_2=1$,then ν must be 1, where $\nu_i=nmax\{\frac{F_i(n)}{C_i(n)}\}$ and ν is the combination of ν_is. (Eq. 16 in Evans and Verlander (1998)) (Condition 2)

From Evans and Verlander (1998), the first condition is logically proved using Eq. 2.27. However, in a defined example by Evans and Verlander (1998), the second causal sentence fails, since in a linear approach the FN-criterion does not satisfy the Condition 2. Here, using the same examples (from Evans and Verlander (1998)), we show that with the non-linear summation, Eq. 2.35, this condition will be satisfied and their conclusion about the misfunctionality of *FN*-curves based on this approach will be falsified.

Example (modified from Evans and Verlander (1998)):

Suppose that system 1 has a mean frequency of 0.1 accidents per year, in which there are exactly 10 fatalities, and $C_1(n)=\frac{1}{n}$ (slope of *FN*-line is -1), then $\nu_1=nmax\{\frac{F_1(n)}{C_1(n)}\}=nmax\{nF_1(n)\}=0.1\times10=1$, therefore, risk of this system is just tolerable. The mean frequency of system 2 is supposedly 0.01 accidents per year with exactly 100 fatalities and

$C_2(n)=\frac{1}{n}$, then $\nu_2=nmax\{\frac{F_2(n)}{C_2(n)}\}=nmax\{nF_2(n)\}=0.01\times100=1$ which is also just tolerable and meet the condition 2. Combining system 1 and system 2 using Eq. 2.35 and Eq. 2.36 in Eq. 2.31, we get $\nu=nmax\{\frac{[\frac{F_1(n)F_2(2)}{F_1(n)+F_2(n)}]}{[\frac{C_1(n)C_2(n)}{C_1(n)+C_2(n)}]}\}=\frac{\frac{0.1\times0.1}{0.1+0.1}}{\frac{\frac{1}{10}\times\frac{1}{100}}{\frac{1}{10}+\frac{1}{100}}}=1$ which is again tolerable and meet the condition 2. This means that if we include the non-linearity of the FN function in calculating the tolerability and intolerability of an overall system, combination of two tolerable systems is also tolerable which is the conclusion that comes out of disutility criterion.

Appendix Conclusion

Considering non-linear relationship between frequency and the size of events in *FN*-curves, *FN*-criterion does not fail any mathematical conditions and suggests that these curves can also be used for decision making beside disutility functions.

Chapter 3 Resistance in natural disaster systems: the case of earthquakes and the 2010 Haiti event

3.1 Introduction

3.1.1 Background

Natural disasters in the last decade (2004-2012) have resulted in the deaths of over 1.2 Million people (Swiss Re Sigma reports 2005-2013, http://www.swissre.com/sigma/). These events have included the 2004 Great Sumatra, 2008 Cyclone Nargis and the 2010 Haiti earthquake all of which have reportedly caused over 100,000 deaths. The asymmetrical distribution of the number of disasters as well as the magnitude of associated losses in developing countries (e.g., Kahn, 2005; Keefer et al., 2011) has given rise to a renewed interest in the role of resilience and vulnerability in natural disaster losses (Adger et al., 2006; Zhou et al., 2010). Further, in the face of increased global urbanization, a focus has emerged on the characteristics of urban disaster risk (Bilham, 2009); In the same time period major developments have taken place in concepts and quantitative analysis of risk with application mainly to technological risks (e.g., Aven, 2009, 2011; Jonkman et al., 2010; Zio and Aven, 2013). Meanwhile, the discussion around the concept of Black Swan events (Aven, 2009; Paté-Cornell, 2012; Stein et al., 2012), following the publication of Taleb (2007, 2010) illustrate the need to re-examine the nature of the occurrence and loss behavior of natural hazard systems, particularly as they relate to natural disasters.

Here, we examine life loss in natural disasters. Whilst there has been much recent discussion of economic losses in natural disasters (e.g, Noy 2009; Cavallo et al., 2010; Neumayer and Barthel, 2011; and Schumacher and Strobl 2011) there have been fewer attempts at rigorous analysis of the factors that lead to life loss in natural disasters. Exceptions are Kahn (2005) and Vranes and Pielke (2009) and more recent work by Holzer and Savage (2013), Keefer et al., (2011), and Doocy et al. (2013). This is despite the occurrence of hyper-life-loss in recent natural disasters as noted above and that the frequency of natural disasters appears to be increasing (Swisse Re, Sigma No. 2/2013, http://www.swissre.com/sigma/). Geospatial life-loss analysis reached its nadir in the aftermath of the Haiti earthquake when the inability of the world is illustrated by the wide range of estimates of the Haiti death toll vary from 65,000 to 350,000 is unprecedented.

At the outset, it is worth noting that the investigation of life loss in natural disasters became a significant scientific and societal issue in the 1960s in the context of industrial safety and nuclear power development where industrial risk was compared to the natural disasters' risk on graphs called FN-curves by Farmer (1967), Beattie (1967), Rasmussen (1975), and Farmer (1980).

3.1.2 Definition of disaster

A disaster is defined in the Oxford English Dictionary as "*a sudden accident or a natural catastrophe that causes great damage or loss of life*". In more detail, a disaster happens when *"an extreme event occurs in the context of societal vulnerability"* (Pielke, 2006, p. 138) that disrupts the functioning of a society (UNISDR, 2009) and results in losses that exceed a threshold determined by the characteristics and behavior of the loss system of the society affected. This definition is an example of a disaster occurrence conditioned by vulnerability. A disaster can also occur when a natural hazard event of extreme magnitude overwhelms any resistance in the society affected and causes losses above the same threshold. In this case the disaster occurrence is conditioned by hazard. Disasters imply a sudden-onset impact, a disruption of immediate effect, with or without warning.

For the purposes of this paper, losses are life loss and the disaster threshold of loss is defined as 1,000 fatalities, which is considered as the minimum number of fatalities that has been called disastrous; it is at this threshold that the natural disaster system is activated.

This threshold (and the magnitude of losses above it) is determined by the manner/mechanism in which the societal system resists the impact of the natural hazard. We term this natural disaster resistance.

3.1.3 Natural disaster systems

A natural disaster system can be viewed as a complex system, i.e., a system consisting of many elements that interact in a disordered way, but result in a robust response pattern, that possesses memory (Ladyman et al., 2013). In a natural disaster scenario, it consists of an interaction between a natural hazard, which itself is a complex dynamic of nature, and a society, which also involves a highly dynamic behavior of engineering infrastructure (buildings and lifelines) and an exposed population. The nature of this interaction defines a destructive outcome, which is conditioned by such factors as the nature of the building stock, population density, building

construction quality, buildings, preparedness, warning. In addition, the geophysical characteristics of the impacted area may amplify or dampen the hazard (as in the case of seismic amplification resulting from foundation conditions); both hazard and its impact may also be amplified by cascade (domino) effects which can be initiated by the occurrence of a natural hazard.

Thus the losses in a natural disaster is a complex consequence of the occurrence of a forcing natural hazard event and its interaction with the society impacted; they are thus not a simple function of event magnitude or necessarily the result of an "extreme natural hazard" (cf. McGuire et al. , 2006). Fig. 3.1 illustrates a disaster system in a schematic loss model.

Figure 3.1: Schematic loss model of elements involved in a natural disaster system

3.1.4 Objectives

Our objectives here are i) to outline a simple conceptual model of a natural disaster system in which a natural hazard as input, an immediate preventative reaction by the affected society or region (which we call resistance) and a destructive consequence as output (which in this context is life loss), ii) to explore the possibilities of quantifying resistance as defined in i), in an analysis of global and international earthquake fatality data, iii) to explore the mathematical linkage between power-law historical frequency-fatality relations and the conventional risk equation, iv) to apply these results to an after-event international analysis of loss data from the 2010 Haiti earthquake (event-specific resistance), and v) to evaluate global resistance to earthquake disasters (comparison with Bam and Kobe).

FN-curves are power-law graphs that hold the history of losses in the areas. We examine the slopes of these curves as measures of resistance towards earthquakes in these areas.

3.2 Resistance in the Natural Disaster System

3.2.1 Resistance and the risk equation (Resilience, robustness)

We attempt to place resistance in the natural disaster system within the current definitions of risk. As Aven (2009) has noted there are many conceptual and quantitative definitions of risk. All involve (or imply) some combination or product of the probability of an event and its negative consequences (e.g., HSE, 2001; UNDP, 2004; Baecher and Christian, 2003; Porske 2008; and UNISDR, 2009).

According to ISO 31000-2009 risk is the "effect of uncertainty on objectives" (Aven, 2011a) which is often quantified as probability of occurrence of a dangerous event, times its negative impact (loss or damage) (Helbing, 2013).

The conventional risk equation, as stated by Birkman (2006), for example, summarizes the definition of risk as multiplication of hazard, vulnerability and exposure (Eq. 3.1).

Risk (R) =Hazard (H) × Vulnerability (V) × Exposure (E) **(3.1)**

Where Hazard (H) is the likelihood of a dangerous event occurrence (Aven, 2011), most frequently expressed as an annual probability of occurrence, vulnerability (V) is the state of susceptibility to harm due to the stresses of an environmental and social change or due to incapability to adapt with it (Adger, 2006), and exposure (E) is the number of elements at risk (Aven, 2011). Hazard has the unit of 1/time (1/year), Vulnerability may have a value between 0 and 1 (if the vulnerability is zero no risk exists) with no unit, and exposure has a counting unit of numbers. Thus the unit of risk in Eq. 3.1 is numbers/year, which indicates loss/year and so risk in this type of equation is expressed as a loss rate.

Vulnerability (V) is defined in many ways (Cutter, 1996, 2003), Watts and Bohle (1993) define vulnerability as a multidimensional variable integrating the environmental, social, economic and political situations of people in a society in the case of potential harm. Generally, vulnerability is used in a ***passive*** sense.

Related to the concept of vulnerability is the concept of resilience. One of the many formulations of vulnerability is linked to the socio-ecological term, "resilience" (Adger, 2006). Scholz et al. (2012) argued that vulnerability and resilience are "highly similar, and in many respects, identical concepts". We would like to capture this similarity in the quantification of resistance.

In the context of natural hazards our concern is loss of life due to natural disasters; hence, our definition for vulnerability includes the extent of losses in occurrence of natural disasters. Since we also use resistance as an equivalent to resilience, our definition of vulnerability provides a measure of resistance to the impact of natural disasters. Pelling (2003) uses the terms resistance and resilience besides the term exposure as components of a vulnerability of the cities in a social perspective for environmental risk/disaster events model.

Resistance, is used here in an ***active*** sense, is an equivalent to the definition of "resilience"[21] in civil engineering i.e., the risk-absorption level of a system (Aven (2011b), p. 26). As we define it here, resistance is an immediate reaction to a natural hazard event. In this sense it contrasts to the use of resilience as used in engineering and the social sciences which implies a longer-term/delayed process of coping and recovery in the aftermath of a hazard impact. It is thus more in the original meaning of Holling (1973, p. 17) in ecology.

With this redefinition, we consider a natural hazard as posing potential societal harm to a population, harm that can be resisted by human effort (e.g., engineering measures, warning systems, disaster mitigation and preparedness). Furthermore, in civil engineering, the definition and measurement of resistance is based on the capability of a structure to withstand possible sources of destruction represented by natural hazards such as earthquakes (e.g., Coburn and Spence, 1992; Dowrick, 2009).

By indicating the new definition of vulnerability in the loss model, Fig. 3.1, and risk equation (Eq. 3.1), vulnerability can be replaced by 1/Resistance (1/R), Eq. 3.2. We justify this replacement by the argument of a highly vulnerable society is less resistant towards a disaster.

$$\textit{Risk} = \textit{Hazard} \times 1/\textit{Resistance} \times \textit{Exposure} \qquad (3.2)$$

The value of 1/*Resistance*, as in the case of vulnerability, integrates various properties of the affected region. For example, the economic capability of the region for developing and adopting technology for damage prevention is one of the main factors influencing resistance. Using the natural disaster system loss model in Fig. 3.1 and Eq. 3.2 we are able to quantify the resistance of an affected area after a disaster event by back-calculation to detect the most vulnerable areas. In this way, without going into details of socioeconomic factors of a society, we can estimate the disaster response of a society. We apply this strategy to the 2010 Haiti earthquake to estimate the

[21] Not to be confused with resilience in social sciences

resistance at an urban scale of grid cell level of 100 m^2 based on the destruction imagery of the satellite GeoEye-1 and population density according to the United states Census Bureau data (USCB, 2003, http://www.census.gov/did/www/saipe/data/statecounty/maps/2003.html) for the city of Port au Prince in the section 3.3.

3.2.2 Characterizing loss behavior - Resistance based on FN-curves

We introduced FN-curves in Chapter 2. FN-curves are power-law graphs on a log-log scale used for the quantitative societal risk assessment of natural and industrial disasters. Societal risk assessment is the risk assessment method that considers multiple-fatality events and therefore, the overall risk to a society. In FN-curves, F, which is the frequency of exceedance of losses (in this case loss of life), is plotted against the value of losses, N. These curves may be summarized by an inverse power-law equation, $y=ax^{-b}$, relating the frequency of loss, y, to the value of loss, x. For actual data this equation is calculated by regression to determine the slope, $-b$, and a intercept, a, on a log-log graph. Slope and intercept of real-data plots are naturally determined by the characteristics of the data, i.e., risk aversion, slope of >1, proneness, slope of <1, and neutral, slope of 1, are not common terms used for real-data FN-curves.

The slope of FN-curves generated based on real-data, i.e, that it represents the resistance of the affected area to losses generated by a hazard. A schematic plot in Fig. 3.2, shows that as the slope of the FN-curve decreases, the resistance also decreases while we keep the intercept the same. A shallower slope, -0.5, implies a higher number of fatalities at the same event frequency as the line with a steeper slope, -1, i.e., the hazard encountered with a less resistant environment or society in the shallower slope case.

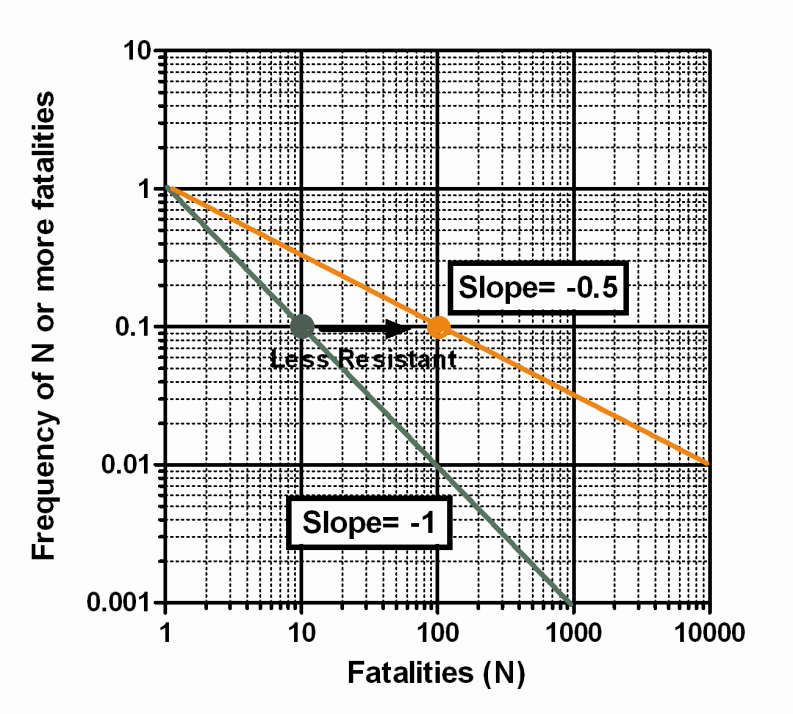

Figure 3.2: Schematic effect of the slope of the FN-curve on the societal resistance. As the slope decreases from -1 to -0.5, the resistance also decreases.

3.2.3 Why slope of FN is a measure of resistance:

Although, the risk-proneness is not used for FN-curves produced based on real data, this concept can be borrowed from the industrial criteria to analyze the behavior of the real-data curves. Thus, for example, if the slope of a real-data curve is <1, the data suggests a risk-prone background of the region under consideration, i.e., the area suffers from a low resistance. This means that steeper curves are generated in higher resistance environments/regions. Since the loss behavior of the curve is controlled by the frequency of the larger events (Kagan, 1997), we could conclude that the slope of FN-curve is a measure of resistance towards large events.

3.3 Global comparison on FN-curve - the case of earthquakes

3.3.1 Global earthquake disasters 1950-2010

For the remainder of the paper we focus on natural disasters caused by earthquakes in an attempt to quantify resistance in earthquake disaster systems at global, national, and international scales.

As noted above, we define a disaster as a natural hazard event resulting in 1,000 or more fatalities. We assembled a database of earthquake disasters for the period 1950-2012, a period of 62 years. The selection of the time period was arbitrary but determined by the data availability.

Data sources consisted of i) the USGS table of earthquakes with 1,000 or more deaths since 1900, http://earthquake.usgs.gov/earthquakes/world/world_deaths.php, ii) the list of deadly earthquakes in the world: 1500-2000 compiled by Utsu (2002), and iii) significant earthquakes database, NGDC-NOAA, http://www.ngdc.noaa.gov/nndc/struts/form?t=101650&s=1&d=1. The accuracy of data is very important in risk assessment of past events. Inconsistency in the number of losses reported in various databases brings difficulty for judgment. Extra care and investigation is needed for these types of data. For example, for the case of Haiti earthquake in 2010, the number of casualties reported varies between 65,000 to 330,000. We also note that precise numbers of life loss in mass casualty events has always been subject to significant debate. Some of these debates come from the fact that deaths in earthquakes are mostly result of collapsed buildings and identifying the number of people in the buildings and the type of building that was collapsed are not trivial, specially, in case of lack of documentation in a region.

According to our disaster criteria of 1,000 fatalities and more, there were 75 earthquake disasters between 1950 and 2012 in which there were an approximate total of 1,240,000 fatalities (see data in Supplementary information).

We plotted cumulative annual frequency of N deaths or more (Y axis) versus number of deaths (N) in the earthquake disaster event (X axis) for the 75 events in the period 1950-2012 following the method of Clauset et al. (2009). We modified the method by expressing the frequency on the y axis as frequency of N (or more) per year, i.e., an annual frequency).

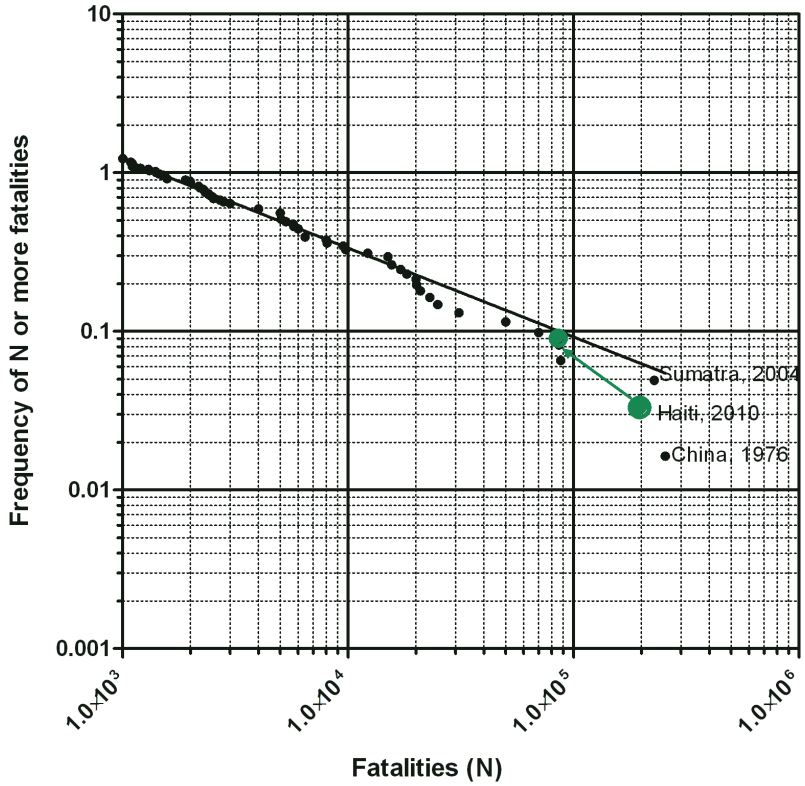

Figure 3.3: Historical fatality frequency (FN) plot for global earthquake disasters (n=75) where N≥ 1,000 fatalities, 1950-2012. Green dots are two scenarios of fatalities for Haiti, 2010 as discussed in text. The fitted line is a power law curve which represents the trend of Frequency-Fatality in 62 years and the slope (-0.56) shows the resistance of the global earthquake disaster system. Data sources are given in the supplementary information.

As in plots of similar data of death tolls in natural disasters, e.g. Knopoff and Sornette (1995), Nishenko and Barton (1995), Guzzetti et al. (2002), Evans (2006); Petley, (2012) the plot yields a robust power law. The power law in Fig. 3.3 is expressed as $Y= 1.77X^{-0.56}$ (R^2=0.99) (n= 75) with the 95% confidence interval of (-0.54, -0.57) for the slope of the fitted line. Saturation at high magnitudes is evident at N~250,000. Fig. 3.3 also indicates that earthquake disasters as defined here are a yearly occurrence. Disasters involving 10,000 and 100,000 fatalities or more occur with an annual frequency of approximately 3 years and 10 years respectively.

It is of interest to compare the slope of the FN plot in Fig. 3.3 to FN plots in industrial safety and risk analysis. In industrial accidents (e.g., road tunnels (Meng et al, 2011)) real-data FN-curves generate slopes that are much steeper (e.g., ~2 for road tunnels) than these curves. Only based on the difference between slopes of these two types of disasters, we could conclude that the resistance towards road tunnel accidents is much higher than earthquake disasters.

3.3.2 Earthquake disaster resistance - an inter-national comparison

To explore further the earthquake disaster resistance in different countries, as an example, we compare the FN-curve of earthquake fatalities of 1 and greater in three countries of Japan, Iran, and Haiti in Fig. 3.4. We compare the best power-law fit to the data of each country and the 95% confidence interval of the slopes in Table 3.1. Although, in the assessment of global earthquake disasters, fatalities of more than 1,000 is considered as minimum threshold, here by choosing 1 fatalities as the minimum fatalities in these three countries, the statistical comparison become possible, since Haiti holds very few earthquake fatality data.

As Fig. 3.4 and Table 3.1 illustrate, Haiti holds the smallest slope among Japan, Iran, and Haiti which means the lowest resistance. On the other hand, Haiti is located lower on the FN-curve which means that frequency of earthquake disasters in Haiti is smaller than Japan and Iran. This suggests that lower frequency disasters do not necessarily cause less losses in the world.

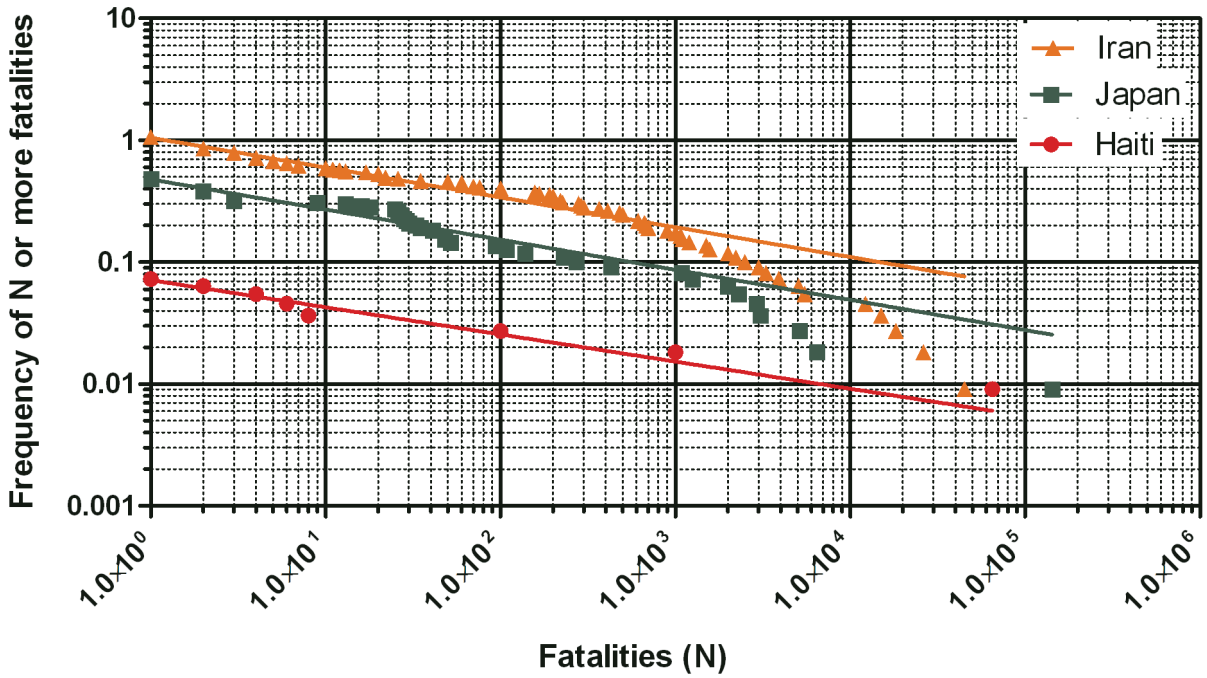

Figure 3.4: FN-curves of earthquake fatalities (greater than 1) in Iran (orange triangles, n=117), Japan (green squares, n=53), and Haiti (red dots, n=8) during the period of 1900-2010. Data are obtained from the USGS Pager catalogue (*http://earthquake.usgs.gov/research/data/pager/*), EM_DAT (http://www.emdat.be/), and Utsu (2002); data listed in Supplementary Information.

Table 3.1 Equations of the power-law fit to the real-data FN-curve (N≥1) of Iran, Japan, and Haiti, shown on Fig. 3.3 (a), with R^2 values and 95% confidence intervals of the slopes.

	Power-Law fit	**R^2**	**Slope Confidence Interval**
Iran	*Log(Y)* =0.02-0.24*x*	0.98 (n=117)	-0.25 to -0.24
Japan	*Log(Y)* =-0.32-0.25*x*	0.97 (n=53)	-0.26 to -0.23
Haiti	*Log(Y)* =-1.15-0.22*x*	0.96 (n=8)	-0.28 to -0.16

The slopes of the power-law fits to the countries' plots on Fig. 3.4 only vary between -0.16 to -0.28 (Table 3.1). Small variations of slopes in these curves suggest that the resistances of these countries are not significantly different from each other while they all are indicating very shallow curves (slope <1). However, this result is counter-intuitive, since earthquake events in Haiti have consequences that are hugely different from Japan or Iran. Why do they carry the same societal resistance on FN-curves, then? This result is rooted in the variation of fatalities with respect to the frequency of fatal events in these countries. For example, if the frequencies of large events were significantly smaller that small events on the FN-curve (or the scaled FN-curve), the slope of the curve would become steeper since the ratio of the range of frequencies to the range of fatalities would be a larger number, and consequently, the resistance would be greater. In the case of Iran, Japan, and Haiti this is not the case, i.e., the ratio of the range of frequencies to the range of fatalities for each country is almost constant, and therefore, the resistance is the same.

3.4 Resistance in terms of Power-law equation

Risk in Eq. 3.2 is the expected loss due to the hazard. If we replace Hazard by P(H), Resistance by R, and Exposure by Exp.Pop, Eq. 3.2' would be

$$\text{Loss}=P(H)\times 1/R\times \text{Exp.Pop} \quad (3.2')$$

P(H) is the probability of hazard that can be estimated based on the probability of occurrence of exceeding a certain magnitude of hazard, e.g., a certain magnitude of earthquake or a peak ground acceleration.

On the other hand, from Jonkman et al. (2003), it is derived that the expected loss of life (Loss) can be estimated from the area underneath the power-law fit of the frequency-fatality curve of natural disasters (FN-curve), e.g., Fig. 3.3. (Eq. 3.3), between certain values of x (loss), d_1 and d_2 are the minimum and maximum number of fatalities reported in the data, respectively.

$$Area\ under\ power-law\ fit = Loss = |\int_{d_1}^{d_2} ax^{-b}\,dx| = |\frac{a}{-b+1}\left(d_2{}^{-b+1} - d_1{}^{-b+1}\right)|\,, (b \neq 1)$$

(3.3)

We use absolute value because Loss cannot be negative, and in case of b>1, the integral would become negative.

Since the left side of Eq. 3.2' and Eq. 3.3 are the same, we equate the right sides of Eq. 3.2' and Eq. 3.3 in Eq. 3.4.

$$\frac{a}{-b+1}\left(d_2{}^{-b+1} - d_1{}^{-b+1}\right) = \frac{1}{R}\times P(H)\times Exp.Pop \qquad (3.4)$$

Eq. 3.4 is an equation that is a function of *a*, *b*, d_1, d_2, *R*, *P(H)*, and *Exp.Pop*. Rearranging Eq. 3.4., we could express resistance in terms of parameters of the power-law fit to the frequency-fatality curve and the equation of loss for certain countries in Eq. 3.5. R_c is called the ***country-specific resistance***.

$$\mathrm{R}_c = \frac{C(a,b)}{D(b)} \times P(H) \times Exp.Pop \qquad (3.5)$$

Where *D(b)*= $d_2{}^{-b+1} - d_1{}^{-b+1}$, and $C(a,b) = \frac{1-b}{a}$

Eq.3.5 shows the relationship between resistance and the slope of power-law fit. From Eq. 3.5, R_c is a function of *D(b)* which varies by different values of d_1, d_2, and *b*; therefore, the precision in data collection of fatalities affect the values of d_1 and d_2 and consequently R_c. As the slope increases (become steeper), the resistance also increases while the slope is b≠1. In case of b=1, the integral of Eq.3.3 would lead to $Loss=a\,(ln|d_2|-ln|d_1|)$, which results in $R = \frac{P(H)\times Exp.Pop}{a\,(\ln|d_2|-\ln|d_1|)}$.

b=1 is the slope that is considered as risk neutral in FN-diagrams. It is compared to b>1 (risk averse) and b<1 (risk prone). In many cases of natural hazards, b<1 is observed, however, in industrial hazards, such as railroad accidents, b>1 is observed. For risk assessment purposes, imposed slope criteria are mainly b=1 (UK) and b=2 (Netherlands).

Fig. 3.5 shows the relationship between Log(R) and different slopes for the example of Haiti, with *P(H)=0.04*, *Exp.Pop=10,173,775*, *a=0.07*, and a death interval of d_2*=65,000,* d_1*=1* where *P(H)* is calculated based on the probability of occurrence of magnitudes greater than 5.5 in Haiti, *Exp.Pop*. is the population of Haiti in 2010, *a* is the intercept of the FN-curve of Haiti from Table 3.1, d_2 is one of the scenarios of the number of fatalities in Haiti 2010 earthquake that we believe is closer to reality, and d_1 is the minimum number of reported death due to earthquakes in Haiti.

The actual *b* value of the fit to FN-curve of Haiti from Table 3.1 is 0.22 which leads to Log(R)=2.9. However, in Fig. 3.5 we assume different slope values in order to examine the effect of the value of *b* (slope) on the value of resistance.

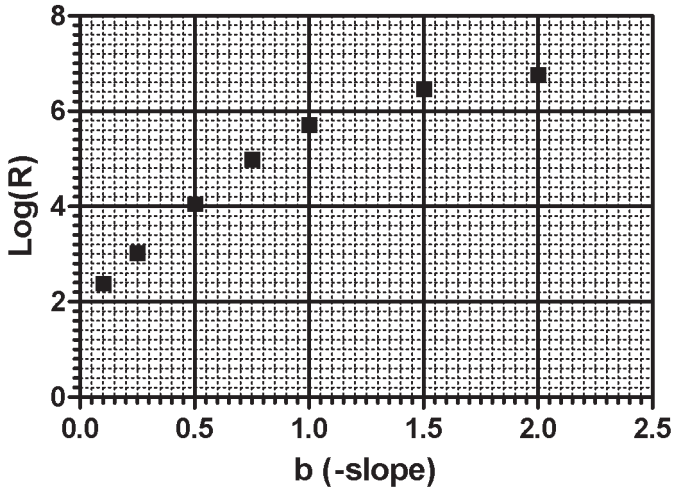

Figure 3.5: Log of resistance values with respect to different *b* values in Eq. 3.5 for Haiti with *P(H)=0.04, Exp.Pop=10,173,775, a=0.07*, and a death interval of d_2=65,000, d_1=1. The actual *b*-value of the fit to FN-curve of Haiti is 0.22.

As shown in Fig. 3.5, as the slope gets steeper (greater b), the resistance increases. Thus, our comparison of power-law fit to real-data FN-curves with the concepts of risk-avers, risk-prone, and risk neutral is valid, i.e., steeper slope means a risk-averse situation, it means a more resistant situation in a country.

3.4.1 Country-specific resistance comparison

We compared Haiti with Japan, and Iran in Fig. 3.4 and Table 3.1 in terms of their FN-curves. Now, after introducing the country-specific resistance in Eq. 3.5, we are going to compare their resistance based on some assumptions. Our first assumption is that the exposed population of the country is an index of exposure to earthquake disasters, *Exp.Pop*. The second assumption, here, is that moment magnitude can be considered as the earthquake hazard in these countries; therefore, we choose magnitude of 5.5 as the minimum threshold for causing earthquake disasters, since, based on our data of 75 disastrous earthquakes since 1950, the lowest moment magnitude that caused 1,000 fatalities is 5.5. Our final assumption is that probability of occurrence of magnitude

5.5 based on the Poisson probability distribution function is a good estimate for probability of hazard, *P(H)*, since the occurrence of earthquakes can be considered as Poisson process (Scheidegger, 1975).

However, for estimation of the ***event-specific resistance*** that we introduce later, the *P(H)* is the probability of exceeding a peak ground acceleration, *PGA*, threshold that is meaningful for that event, considering the distance to the epicenter. We will see an example of this method for the Kobe 1995, Bam 2003, and Haiti 2010, in section 3.7.

For now, to calculate the *P(H)* of Haiti, Iran, and Japan, we gathered the total number of earthquakes with any magnitude greater than 5.5 in the earthquake catalogue (NEIC) over the period of 1973-2013, and estimated the parameter of Poisson probability distribution function, λ, for each year in order to calculate the yearly value of P(H). The average value of the yearly P(H)s is our estimate for the probability of hazard of the country.

The resistance of Haiti, Iran, and Japan, based on the values of P(M≥5.5) of the countries, the exposed population of the country, and parameters of their FN-curves are calculated according to Eq. 3.5 (Table 3.2). We used NEIC catalogue (http://earthquake.usgs.gov/earthquakes/search/) for the period of 1900-2013, start_time=1900/01/01,00:00:00, end_time=2013/01/01,00:00:00 at the latitudes and longitudes in which these countries are surrounded. Table 3.2 lists the parameters used to calculate R_c from Eq. 3.5.

Table 3.2 List of number of events with magnitude M≥5.5, probability of occurrence of magnitude 5.5 in the period of 1900-2013 (based on Poisson probability distribution function), current exposed population of the countries, intercept, a, and slope, b, of the power-law fit to the FN-curve of the countries of Iran, Japan, and Haiti, in order to calculate the resistance from Eq. 3.5, and log(R). Population data is based on World Bank (2008-2012) record *(http://data.worldbank.org/indicator/SP.POP.TOTL)*

	Lat.	Long.	P(M≥5.5)	Exp.pop (2008-2012)	a	b	d_1	d_2	Rc	log(Rc)
Iran	18-42 N	42-63 E	0.347	76,424,443	1.05	0.24	1	45000	5598.35	3.75
Japan	40-50 N	130-150 E	0.695	127,561,489	0.48	0.25	1	142807	127868.2	5.11
Haiti	18-20 N	71.5-75 W	0.011	10,173,775	0.07	0.22	1	65000	32.13	1.51

From Table 3.2, log(R_c) of Haiti is the lowest value among the others. The very low probability of earthquakes with magnitudes greater than 5.5 in this area seems to play an important role in the case of Haiti. This suggests that, since the country doesn't experience earthquakes so often, the resistance of the country towards earthquakes has not strengthened accordingly.

3.4.2 Resistance of the global earthquake system

Here, we would like to investigate the resistance of the global earthquake disaster system as one country based on Eq. 3.5 and Fig. 3.3. In order to find the P(H) for the global earthquake system, we need to find the probability of occurrence of earthquakes with certain magnitudes, during 1900-2013. From NEIC catalogue (http://earthquake.usgs.gov/earthquakes/search/), we gathered the global number of earthquakes with magnitude equal or greater than 5.5, which is the threshold of magnitude that can cause 1,000 fatalities in the period of 1900-2013, start_time=1900/01/01,00:00:00, end_time=2013/01/01,00:00:00. The number of recorded earthquake in this period is 24,276 earthquakes. The average probability of hazard, based on the Poisson probability distribution function, is around 0.99. Hence, the resistance of the global earthquake system, using Eq. 3.5 with a=58.88, b=0.56, $Exp.Pop$ =7,046,368,812, d_1=1 and d_2=255,000 would be 218773.4, therefore, $Log(R)$=5.34. This value is an average of global resistance towards earthquakes with magnitude 5.5 and greater per year. This suggests that the background resistance of the world, based on 113 years of data, is quite high with respect to specific countries such as Iran, and Haiti. However, Japan's Log(R_c) is very close to the global societal resistance towards earthquake disasters. This means that the advancements of technologies in Japan in order to reduce the effects of earthquake disasters have been so successful that they have reached to the norm of global resistance towards earthquake disasters.

3.5 Structure of a Natural Disaster System (with resistance) - the 2010 Haiti Earthquake

3.5.1 Haiti - Overview

The Haiti earthquake on January 12, 2010 with Mw= 7.0 (Hayes et al., 2010), is reportedly among the most destructive earthquakes in recorded history and it is considered as a natural disaster system in this study, i.e., it caused more than 1,000 fatalities.

The death toll announced by the Government of Haiti exceeds 230,000 (http://news.bbc.co.uk/2/hi/americas/8507531.stm). More than 5 million people live in the area directly affected by the earthquake (Eberhard et al., 2010). The Republic of Haiti covers 27,750 km^2 of the island of Hispaniola, and has a total population of approximately 9 million. Port-au-Prince is the largest city in Haiti that has an estimated population of between 2.5 and 3 million

people within the metropolitan area and is located 25 km east- northeast of the epicenter with an area of 36.04 km² (Eberhard et al., 2010). Haiti is the poorest country in the Western Hemisphere, with an estimated 80 percent of its people living under the poverty line (CIA, 2010, https://www.cia.gov/library/publications/the-world-factbook/geos/ha.html).

3.5.2 Historical Earthquakes

Haiti has also been impacted by other earthquakes with magnitude of 7.0 and greater before, we have defined a rectangle polygon of Greater Antilles region (15°-19°N, 77°-68°W) in which Haiti is located. We analyzed historical seismic activities in this region between 1500-2010. We found that there have been earthquakes in 1564, 1692, 1751, 1770, 1842, 1860, 1887, 1899, 1916, 1946, and 1948 (Ghahramani, 2011). Table 3.3 summarize these earthquakes with their latitude, longitude of the epicenters, moment magnitude of the earthquakes and the refernce that the information gathered from. Fig. 3.6 is the map of Hispaniola and some of the historical earthquakes in the region. The magnitude-frequency of these earthquakes are plotted in Fig. 3.7. The equation of the fitted log-linear line is $y=10^{-0.9x+4.9}$ (n=9, R^2=0.97) with 95% confidence interval slope of (-1.1,-0.7), and intercept of (3.8,6.2).

Table 3.3 List of 12 largest earthquakes from 1500 to 2010 in Haiti

Date	latitude	longitude	Mw	Reference
1564	19.38141	-70.5913	7	Scherer (2012) and Utsu[1]
1692	17.8	-76.7	7.5	Utsu
1751	18.45966	-72.2439	7.5	Scherer (2012) and Utsu
1770	18.34708	-72.8683	7.3	Scherer (2012) and Utsu
1842	19.84992	-72.837	8	Scherer (2012) and Utsu
1860	18.38	-73	7	Scherer (2012) and Utsu
1887	19.7	-73.1	7	Scherer (2012) and Utsu
1899	18	-77	7.5	Utsu
1916	18.5	-68	7.8	PAGER[2]
1946	19.25	-69	7.9	PAGER
1948	19.25	-69.25	7.1	PAGER
2010	18.447	-72.55	7	USGS[3]

1.UTSU online searchable catalog: (http://iisee.kenken.go.jp/utsu/index_eng.html).

2. Pager catalog. Available at (*http://earthquake.usgs.gov/research/data/*pager*/*).

3. U.S. Geological Survey, 2010, U.S. Geological Survey, significant earthquakes; magnitude 7.0 Haiti region, 2010 January 12, 21:53:10 UTC [*http://earthquake.usgs.gov/earthquakes/eqinthenews/2010/us2010rja6/* accessed on March 2, 2010].

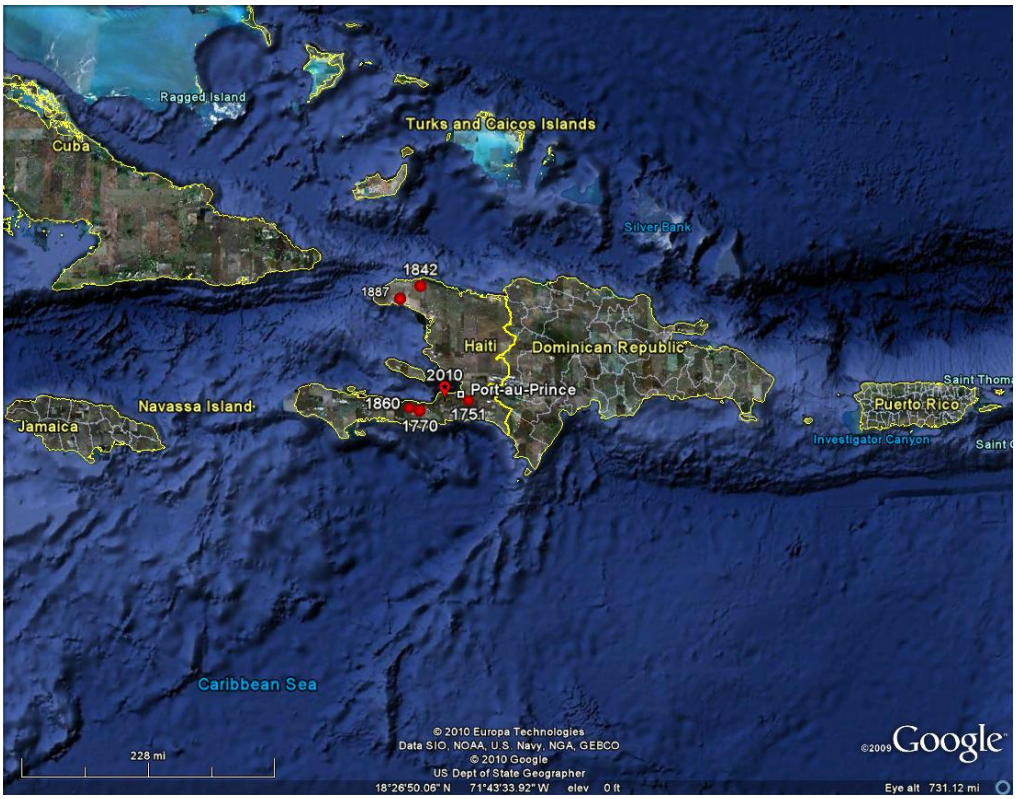

Figure 3.6: Location map of Hispaniola and Some historical Earthquakes within Haiti as well as the location of 2010 Earthquake.

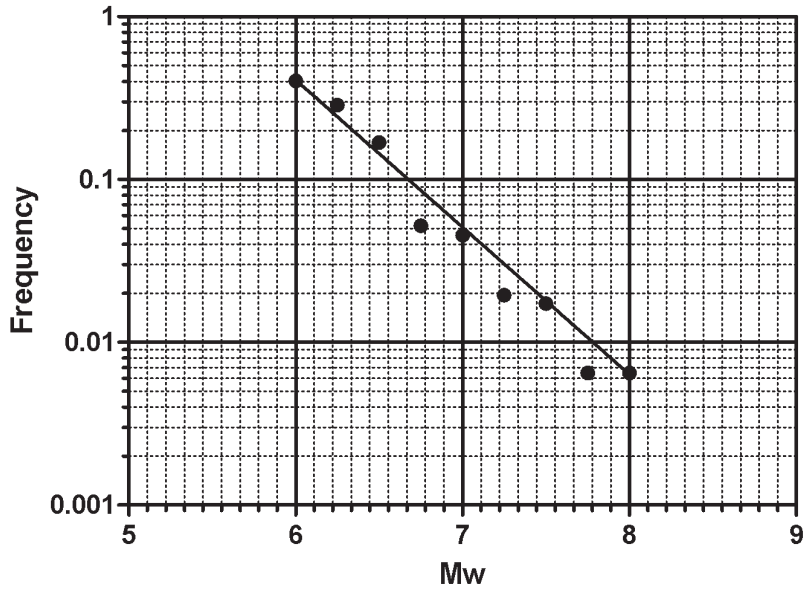

Figure 3.7: Annual magnitude Frequency plot of the earthquakes with M≥5 within the rectangle polygon of Greater Antilles region (15°-19°N, 77°-68°W) from 1500 to 2010. Equation of the log-linear fitted line is $y=10^{-0.9x+4.9}$ (n=9, $R^2=0.97$).

Other natural hazards for Haiti are hurricane, severe storms from June to October, occasional flooding, and periodic droughts. For instance, in 2008, more than 800 people were killed by a series of four hurricanes and tropical storms that struck Haiti during a two-month period (CIA, 2010, https://www.cia.gov/library/publications/the-world-factbook/geos/ha.html).

3.5.3 Seismic hazard of Port-au-Prince

Based on our conceptual loss model summarised in Fig. 3.1 and Eq. 3.2, the assessment of losses in an earthquake disaster system requires the determination of hazard (in this case ground acceleration), the resistance of the area to the ground motion, and the number of people exposed to the hazard..

Based on the analysis of historical earthquakes in the Port au Prince region (Fig. 3.7) we found that that the return period of the 2010 Haiti M7.0 earthquake is almost 250 years. In order to estimate the peak ground acceleration (PGA) for Port-au-Prince (Presidential Palace at 18.543261N, 72.338861W) (Fig.3.8) Since there no attenuation relation for the city of Port-Au-Prince has been published, we used the Boore and Atkinson (2008) attenuation equation to estimate PGA. Fig. 3.9 shows the frequency-attenuation curve of historical earthquakes listed in Table 3.3 at the Presidential Palace of Port au Prince (Ghahramani, 2011) which holds the attenuation relation of $y=0.0134e^{-6.63x}$.

Figure 3.8: Map of Port au Prince with respect to the Haiti 2010 earthqake epicenter at the 18.44◦ N, 72.57◦ W (orange icon), the location of Port au Prince is estimated at the Presidential Palace at the 18.543261N, 72.338861W (red and purple icon, A) [Google Earth].

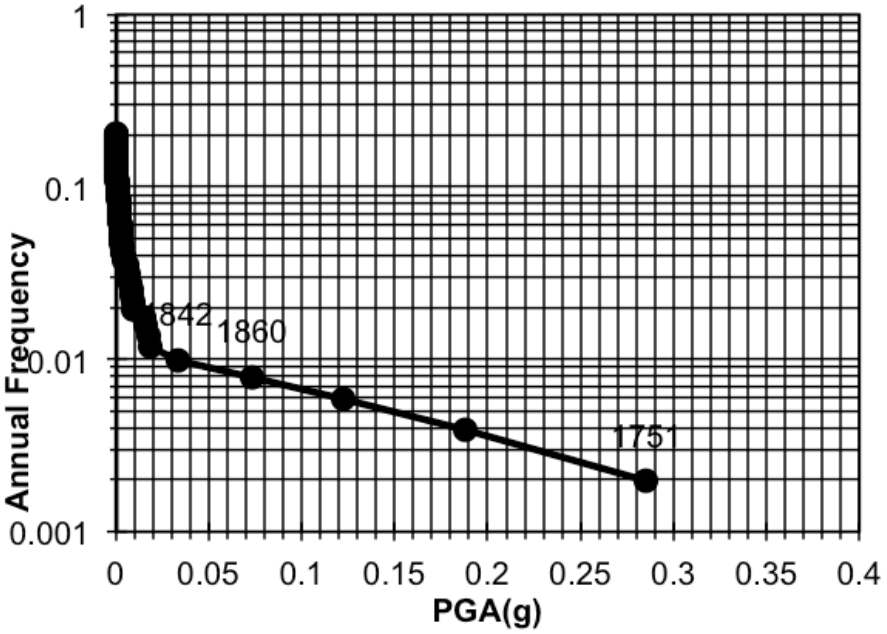

Figure 3.9: Annual frequency of exceedance versus PGA for the city of Port-au-Prince based on Boore and Atkinson (2008) attenuation relation is $y=0.0134e^{-6.63x}$ (Reproduced from Ghahramani (2011)).

Since the PGA of 2010 Haiti is 0.18 g, we choose the PGA threshold of damage as 0.18g (Ghahramani, 2011) (Fig. 3.9). Furthermore, among all historical events, earthquake in 1860 has been considered to cause the lowest damage on Port au Prince; as a result, the PGA for threshold of damage is approximately 7.3 % of g, with the return period of 125 years.

One result that we obtained from the frequency-PGA analysisi of the region of Port au Prince was that based on Fig. 3.9, it seems to be an underestimation of PGA values in the global seismic hazard map with the return period of 475 years (Ghahramani, 2011).

3.5.5 Population characterisitics, building damage, and life loss in affected area

The pre-earthquake population of Haiti can be estimated from two sources: the 2003 Haitian Census conducted by the United States Census Bureau (USCB, 2003, http://www.census.gov/did/www/saipe/data/statecounty/maps/2003.html) and the 2009 census (IHSI, 2009). The 2009 population of Haiti was estimated at 9.923 M (IHSI, 2009). This population has lived on an area of 27,751 km², which yield a population density of around 360 p/km^2; p stands for people. Damage mapping by the European Union-World Bank-UN consortium, summarized by Kemper et al. (2010) and Corbane et al. (2011) indicates that 11 communes were heavily damaged by the earthquake. The total population of these communes in

2009 was estimated at 3.091 M, 31% of Haiti's total population (IHSI, 2009). This number constitutes the exposed population for the 2010 Haiti earthquake disaster. The affected communes covered an area of 1,992.8 km^2, about 7% of Haiti's total area. The highest population density was in Port-au-Prince commune where it reached 24,913 p/km^2.

3.5.6 Occupants per building

Loss of life in earthquakes is largely a result of building damage and collapse. We aim to estimate the total number of fatalities due to building collapse in the 2010 Haiti earthquake. The number of residential buildings and family units in each commune is provided by the 2003 Haitian Census data. However, a pre numeration of households (menages) of the affected area was carried out as part of the 2003 Census.

From Census data we could calculate the number of persons per building in each of the affected communes in 2003. It should be pointed out that the number of buildings and occupants might have changed since 2003; however, the data is not available. If we assume that this number is the same in 2009, by dividing the number of persons per building into the estimated 2009 population of these communes, we are able to obtain the number of buildings present in 2009. This estimate is thus the number of exposed buildings in the Haiti Earthquake. For the commune of Port au Prince, the number of buildings is reported as 129,183 and Census (2003) recorded the total number of families in this commune as 158,790, while the total exposed population is 736,618 (USCB, 2003, http://www.census.gov/did/www/saipe/data/statecounty/maps/2003.html). From these numbers, we could estimate the average person per building as 5.7 (p/bldg); bldg. stands for building.

The detailed damage survey work of Kemper et al., 2010 and Corbane et al. (2011) indicates that in the 11 affected communes, 58,562 buildings were classified as destroyed or badly damaged according to the EMS-98 building damage scale (i.e., damage grade 4 and 5). This number constitutes 9.4% of the estimated exposed building stock in 2009.

UNOSAT, http://www.unitar.org/unosat/maps/hti, estimates the number of damaged buildings in all districts of Haiti. 27,694 out of 92,740 buildings in Port au Prince were damaged as follows; totally damaged (11,663), heavily damaged (10,801), and substantially damaged (5,230).

Thus the following question emerges; what proportion of the occupants of these destroyed or badly damaged buildings were killed as a result of the 2010 earthquake-generated housing damage?

Schwartz et al. (2011) in a controversial report, have estimated the 2010 Haiti death toll to be between 46,190 and 84,961, much lower than official estimates. In a more recent paper, Doocy et al. (2013) reported the results of a stratified cluster survey in metropolitan Port-Au-Prince. They concluded that the number of fatalities was defined by the range 49,033 and 86,555, a range almost precisely the same as reported by Schwartz et al. (2011) and corresponds roughly to 2% of the exposed population in the Haiti event.

Schwartz et al. (2011) estimate is equivalent to 0.79 to 1.45 deaths per destroyed building (fatality rate 17-32%) whereas the Doocy et al. (2013) estimate is equivalent to 0.84 to 1.48 deaths per destroyed building (fatality rate 18-32%). Taking the mean of these numbers we obtain a mean deaths per building 1.5 per destroyed building, which is equivalent to a (fatality rate 25%).

Now, we use a sequence of steps shown in Table 3.4 to estimate the number of fatalities due to building collapse. By having the number of occupancy per building, we are able to estimate the total number of buildings per grid cell (BPG) by dividing the population at the grid cell by the occupancy estimate. The total number of destructed buildings would be the result of multiplication of BPG by the percentage of destruction in the buildings. Having the ratio of the number of deaths at buildings to the number of destroyed buildings, the total number of deaths at all building destroyed due to earthquakes would be that ratio times the number of destructed buildings. This ratio is assumed to be 1.5. We apply this method to estimate the total number of deaths due to building collapse in the commune of Port au Prince due to the Haiti 2010 earthquake.

Table 3.4 List of components, equations, and calculations needed to calculate number of deaths at buildings destructed at Haiti 2010 earthquake.

Occupancy per building in Haiti=	5.7 person (based on Census, 2003)
Total number of buildings per grid cell (BPG)=	population of the grid cell/5.7
Number of destructed buildings in a grid cell=	BPG× percentage of destruction in buildings
number of deaths at buildings/number of buildings destroyed =	1.5
Number of deaths at buildings=	1.5 × number of destructed buildings

Numbers of deaths and destructed buildings in the total grid cells of 3585 (Port au Prince Commune) at all three estimations of the population from gridded population (2003), census 2003 (USCB, 2003), and census 2009 (IHSI, 2009) are listed in Table 3.5. In Table 3.5 calculation of fatalities is based on 1.5 numbers of deaths in the buildings per number of buildings destroyed at both lower and upper limits of destruction map of Haiti which are estimated in section 3.5.5.

Table 3.5 Three scenarios of the exposed population (Ex.Pop) gathered from gridded population data (*http://www.census.gov/population/international/data/mapping/demobase.html*), 2003 census, and 2009 census data. The total number of destructed buildings (upper and lower limits) are calculated based on Table 3.4, and the number of deaths at destructed buildings of Haiti 2010 event is calculated by considering 1.5 number of deaths per building destroyed.

	Exp.Pop	**Number of destructed buildings - Upper limit**	**Number of destructed buildings- Lower limit**	**Number of deaths based on upper limit destruction and 1.5 death/building**	**Number of deaths based on lower limit destruction and 1.5 death/building**
gridded population 2003	**598,811**	29286.6	17851.9	43929.9	26777.9
Census 2003	**736,618**	36022.5	21957.9	54033.7	32936.8
Census 2009	**897,859**	43900.6	26760.0	65850.9	40140.1

From the range of total destructed buildings in the commune of Port au Prince, between 17,852 and 43,901, we can see that our results is very compatible with the UNOSAT report of destructed buildings (27,694). The total damaged buildings based on Kemper et al (2010) and Corbane et al. (2011) is 58,562 in the 11 communes. Thus, based on the range of damaged buildings in Port au Prince (Table 3.5), we could conclude that between 31%-75% of the whole earthquake damage occurred in the commune of Port au Prince.

The total lower and upper estimates of deaths in the three scenarios of exposed population in the 2010 Haiti earthquake indicate that the range of fatalities in the commune of Port au Prince is between 26,778 and 65,851. This estimate range, is much closer to the range of total deaths that Schwartz et al. (2011) and Doocy et al (2013) suggested which we think are more reasonable estimates.

3.6 Fatalities and Gridded Resistance in Port-Au-Prince Commune

3.6.1 Damage mapping in Port-au-Prince

In order to quantify the earthquake-generated urban damage that occurred in Port au Prince, we conducted a damage assessment using high resolution satellite imagery provided by GeoEye-1. The GeoEye-1 satellite produces images showing 225 km^2 at a resolution of <0.2 m. A 100 m^2 grid was overlain on the satellite imagery of Port-au-Prince and damage was assessed on a square by square basis (Delaney, 2011). Each grid square was assigned a value from 0 to 6 corresponding to the level of damage. Values of 0 (no building present) and 1 (unaffected buildings) expressed areas of no damage. The values of 2 through 6 denoted grid squares which contained damage and collapsed structures. Table 3.6 summarizes the list of the number of grid cells based on the percentage of building damage categories. The damage was determined through visual inspection with each class representing 20% intervals (Delaney, 2011). The destruction map of Port au Prince is shown in Fig. 3.10.

Table 3.6 Damage categories used for destruction assessment of the commune of Port au Prince based on the GeoEye-1 satellite images (total of 3585 grid cells with the area of 100m×100m).

Damage code	**0**	**1**	**2**	**3**	**4**	**5**	**6**
Definition of the damage code	No building and no damage	Buildings but no damage	<20% Damage	20%-40% Damage	40%-60% Damage	60%-80% Damage	>80% Damage
Number of grid cells	1098	972	1032	202	138	71	72
Total area (m^2) [1]	10,980,000	9,720,000	10,320,000	2,020,000	1,380,000	710,000	720,000
Percentage to the total area (%)[2]	30.6	27.1	28.8	5.6	3.9	2.0	2.0

1 Total area of damage coded square(s) = (number of grid cells) × (10,000m^2)
2 Percentage to the total area= (Area of squares) / 35,850,000m^2

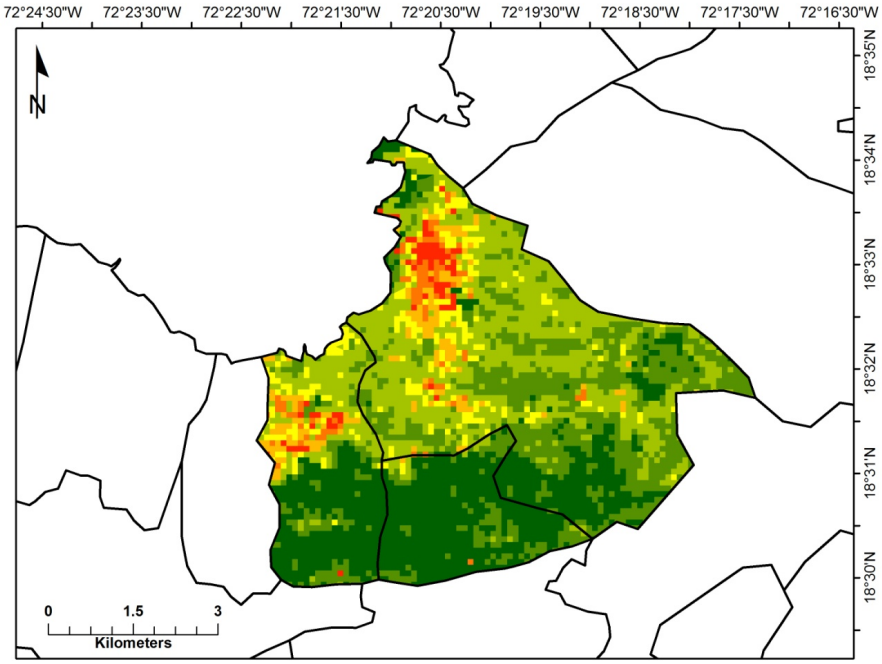

Figure 3.10: Destruction map of the commune of Port au Prince. The range of damage is between green (0), and red (6) based on the codes in Table 3.6

3.6.2 Number of deaths in gridded Port-au-Prince map

After preparing the damage percentage of each grid cell, in order to estimate the number of deaths in each grid cell, we follow the steps explained in the previous section, Table 3.4. The assumption, here, again is 5.7 person occupancy in each building and 1.5 fatalities per buildings destroyed. Estimated values of fatalities in each grid cells are used for two purposes in this study. The first use was to calculate the lower and upper estimates of total number of fatalities in Port au Prince which showed in Table 3.5, and the second use is to estimate the resistance of each grid-cell using the steps that we will explain in the section 3.6.3.

3.6.3 Resistance of Port au Prince grid-cells to the 2010 Haiti earthquake

The loss equation that we introduced in Eq. 3.2' provides a relationship between the number of fatalities, *Loss*, probability of exceeding a certain peak ground acceleration, *P(H)*, population exposed to the PGA, *Exp.Pop*, and resistance, *R*. If there is only one unknown parameter in this equation, by solving the equation we could estimate the value of the unknown. Here, the values of resistance of the grid cells of Port au Prince are our unknown parameters. Eq. 3.6 is derived from re-arranging Eq. 3.2', where resistance is written with respect to probability of hazard, P(H), exposed population, Exp.Pop, and life-loss, Loss.

$$R = \frac{P(H) \times Exp.Pop}{Loss} \qquad (3.6)$$

To estimate the resistance of each grid cell (total of 5272 grid cells for four main districts of Port au Prince) to the impact of the M7.0 2010 Haiti earthquake, we defined the values in Eq. 3.6 as follows;

Loss - the estimated destruction level in each gridded cell based on the methodology explained in section 3.5.5 (Delaney, 2011):

P(H), the exceedance probability of the peak ground acceleration that strike the grid cell. The PGA is calculated from Boore and Atkinson (2008) and the exceeding probability is estimated based on the annual frequency-PGA curve of the region, Fig. 3.9 (Ghahramani, 2011).

Exp. Pop - the population of the gridded cell based on the population density of the gridded cells obtained from the Census (2003).

Gridded resistance estimates calculated by Eq. 3.6 are depicted on Fig. 3.11 in which red cells show the lowest resistance areas and green cells show the highest resistance areas.

Comparing the number of losses with respect to the resistance of the grids, we observe that less losses occur at more resistant areas, Fig. 3.12. Furthermore, Fig. 3.12 shows that the number of grid cells that have very large number of deaths and have very low resistance are much smaller than the number of grid cells that have small number of deaths and occur in high resistant areas. This reflects the characteristics of the population distribution and the urbanization of the city of Port au Prince.

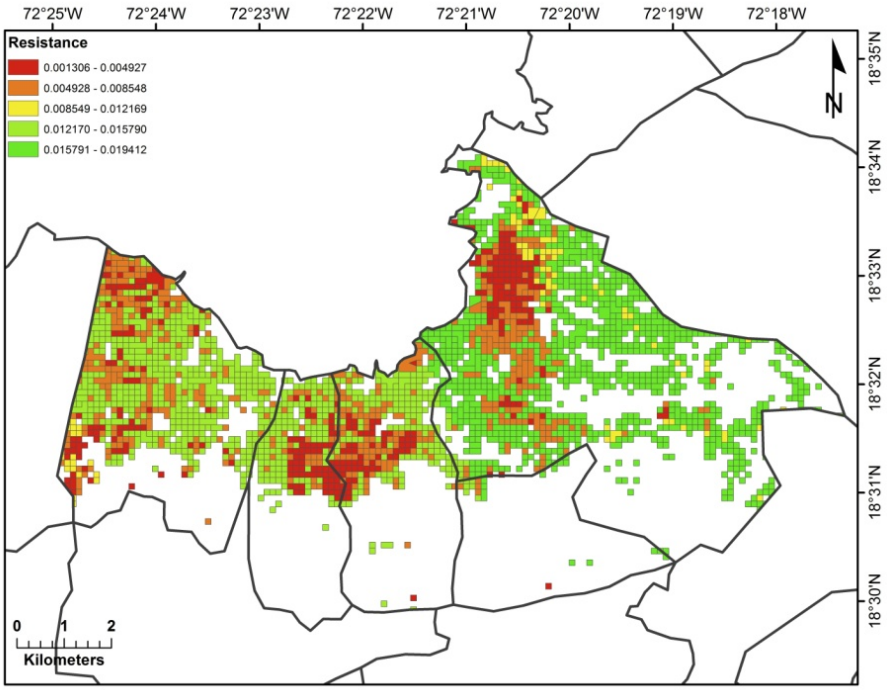

Figure 3.11: Resistance of gridded cells of the city of Port au Prince, Haiti calculated from Eq. 3.6. Here, red shows grid cells with low resistance and green shows high resistance grid cells.

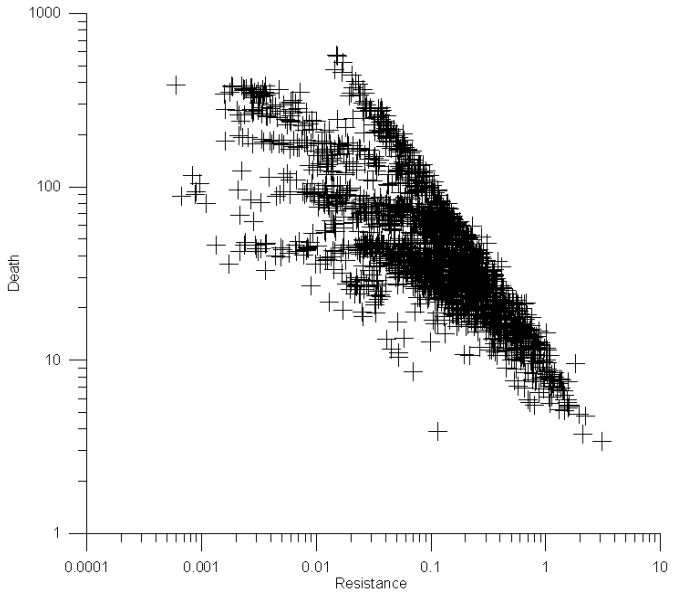

Figure 3.12: Estimated number of deaths in each grid cell with respect to the resistance of the grid (calculated from Eq. 3.6).

3.7 Comparison of resistance of earthquake disasters (event-specific resistance)

According to the disaster risk index table of countries (UNDP, 2004), every year, there are an average of 93.14 people are killed on streets of Haiti. This suggests that we need to eliminate the number of fatalities due to other causes by considering daily death rate of the country in our country-based comparisons. We compare resistance of different earthquake events in different countries by modifying Eq. 3.6 using the daily death rate, *DDR*, number of deaths per year per 1,000 people, in the equation, Eq. 3.7. Daily death rate is the rate of death due to normal, non-disastrous effects (crude death rate) (UNdata, http://data.un.org/Glossary.aspx?q=Crude+death+rate+%28CDR%29, 2010). We use a modified resistance equation in Eq. 3.7, where the sub-index of e stands for event-specific.

$$R_e = \frac{P(H) \times Exp.Pop}{Loss \times D.D.R} \qquad (3.7)$$

In Eq. 3.6, $P(H)$ is the probability of hazard, i.e., the probability of exceeding a certain PGA based on the attenuation of the earthquake at the center of the nearest city affected by the event, *Exp.Pop* is the population of the country affected by the event at the time of the event, *Loss* is the number of fatalities in the event and *DDR* is the daily death rate of the country (UNData, http://data.un.org/Data.aspx?q=Crude&d=SOWC&f=inID%3a91, 2010).

In section 3.2, we introduced the concept of resistance represented by the slope of the FN-curves and in Fig. 3.4 we compared the slope of the FN-curves of earthquake fatalities in the three countries of Haiti, Iran, and Japan. We also compared the country-specific resistance of these countries in Table 3.2. Here, we estimate the resistance of three specific events in these three countries and compare the results with the results of the country-specific resistance in Table 3.7.

Eq. 3.5 is used for calculation of the event-specific resistance, R_e. We use Eq. 3.5 to back-calculate the life-loss resistance of Haiti in case of both scenarios of 65,000 and 230,000 fatalities. We compare these estimates with Bam (2003) and Kobe (1997) in Table 3.7. Table 3.7 lists the components required to calculate event specific resistance, R_e and $\log(R_e)$.

One of the components listed in Table 3.7 is the PGA and P(PGA) of the events. The peak ground attenuations of the events are calculated at the nearest city to the epicenters of the earthquakes; Haiti at the National Palace (Lat: 18.5, Long: -72.39), Bam at the center of the city (Lat: 29.00, Long: 58.34), and Kobe at the city center (Lat: 34.683, Long: 135.183) based on Boore and

Atkinson (2008). To calculate P(PGA), we use hazard curves (frequency-PGA) of these cities. These curves are plotted based on the previous record of earthquakes in the area at the given latitude and longitudes. Earthquake data, i.e., magnitude, depth, and location (to calculate the distance) are gathered from Utsu (2002). Fig. 3.13 shows the hazard curves of Haiti, Bam, and Kobe which are plotted to estimate the P(PGA) of the three events listed in Table 3.7.

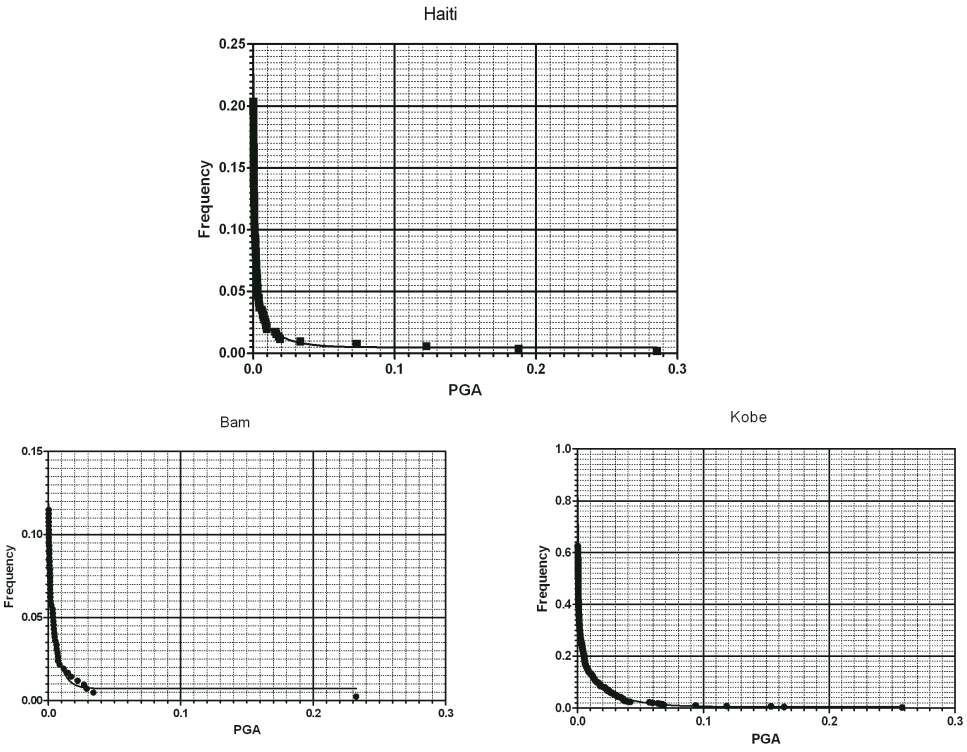

Figure 3.13: Hazard curves (Frequency-PGA) of Haiti, Bam, and Kobe based on Boore and Atkinson (2008) attenuation relation. Earthquake data is gathered from Utsu (2002).

Table 3.7 Components of the event-specific resistance, R_e, equation: P(PGA), life-loss, daily death rate (DDR), and calculated values of R_e and log (R_e) for Haiti 2010, Bam 2003, and Kobe 1995 earthquake events.

Event	PGA	P(PGA)	life loss	Source (life loss)	DDR	Exp.Pop	Source (Population)	R_e	log(R_e)
Haiti 2010	0.18	0.0035	65,000	Schwartz (2011)	0.009	3,091,000	IHIS, 2009	18.49	1.27
			230,000	Bilham (2010)				5.23	0.72
Bam 2003	0.23	0.0024	31,383	Ghafory-Ashtiany & Hosseini (2008)	0.0058	90,000	Kuwata et al. (2005)	1.19	0.07
Kobe 1995	0.16	0.004	4,571	Kobe City Statistics	0.0075	1,529,365	Kobe City Statistics	178.44	2.25

Table 3.7 illustrate that even with the scenario of 230,000 fatalities, the resistance of Bam is much lower than Haiti. This result is very interesting since in Table 3.2, Haiti has the lowest country-specific resistance. This means that Haiti 2010 event was not an extraordinary event with respect to the resistance of the country that it occurred in. The comparison between event specific resistance and the country-specific resistance of Haiti, Iran, and Japan is shown in Table 3.8

Table 3.8 Comparison between event specific resistance, $\log(R_e)$, calculated from Eq. 3.7 and country-based resistance, $\log(R_c)$, calculated from Eq,. 3.5 of Haiti, Iran, and Japan.

Country	**$\log(R_e)$**	**$\log(R_c)$**
Haiti	1.27 (Haiti 2010, 65,000 fatalities)	1.51
	0.72 (Haiti 2010, 230,000 fatalities)	
Iran	0.07 (Bam 2003, 31,383 fatalities)	3.75
Japan	2.25 (Kobe 1995, 4,571 fatalities)	5.11

From Table 3.8 we can see that, resistances of events are lower than resistance of the countries they occurred in. For both cases of Bam 2003 and Kobe 1995, the event's resistances are almost 3 orders of magnitude less resistant to earthquakes than Iran and Japan, in general. Haiti 2010 event has two scenarios of resistance, 1.27 for 65,000 fatalities and 0.72 for 230,000 fatalities. Both are smaller than the value for Haiti, in general. It worth mentioning that the $\text{Log}(R_e)$ for 65,000-fatality scenario is much closer to the $\text{Log}(R_c)$ of Haiti, which suggests that, this scenario is more reasonable and acceptable. Moreover, it can be interpreted that, the resistance of the country towards earthquake disasters like Haiti 2010 is almost as low as what is expected from this country, based on its background disaster experiences.

3.8 Summary and discussion

In this chapter, we mainly focused on the transformer component, resistance, of a natural disaster system in our conceptual loss model of Hazard, Resistance, and Loss. We reviewed the two methods that define resistance, one based on the slope of FN-curves, and another based on back-calculation of losses in great disasters. It was shown that the results of these two methodologies are consistent with each other. However, each of these methods are useful for different purposes. For example, the FN-curve method is a very good approach for comparative and global assessments, while the loss model is also applicable for local regions. We used Haiti earthquake

data, both past events data, and gridded data of the 2010 event, to illustrate the comparison of these two methods. In both methodologies, the results show Haiti, 2010 has the lowest resistance among the other earthquakes in Iran (2003), and Japan (1995). We also estimated the total number of fatalities in the commune of Port au Prince, between 26,778 and 65,851, based on three exposed population scenarios. Although this range is only for one of the 11 affected communes of Haiti, since the most affected commune was Port au Prince, we could conclude that the total fatalities will not exceed 100,000. This estimate is much smaller than the estimate of the Haitian government, 230,000.

Discussion:

The event specific resistance of Port au Prince, based on the numbers listed in Table 3.5 and P(PGA)=0.0035, DDR=0.009 would be **R_e=5.3, log(R_e)=0.72**. Since the number of exposed population affect the number of fatalities, their proportion would be the same for calculation of resistance. R_e of 0.72 is much closer to the resistance calculated for 230,000 scenario of Haiti 2010 (Table 3.7). This similarity suggests that the estimation of 230,000 fatalities is an upscale of the fatalities in the commune of Port au Prince which includes almost 50% of the total population of Haiti. This is a wrong estimation, because destruction of other communes are much smaller than Port au Prince.

Supplementary Data

List of 75 global earthquake disasters with fatalities greater than 1000 (1950-2012). Data is a combination of the USGS table of earthquakes with 1000 or more deaths since 1900, http://earthquake.usgs.gov/earthquakes/world/world_deaths.php, significant earthquakes database, NGDC-NOAA, http://www.ngdc.noaa.gov/nndc/struts/form?t=101650&s=1&d=1, and the list of deadly earthquakes in the world (Utsu, 2002), using our judgment.

Year	Lat	Long	Country	M	death	Source
1950	28.5	96.5	China	8.6	4000	Utsu/USGS
1951	-88.4	6.5	Nicaragua	6.5	1100	Utsu/USGS
1953	40.0	27.5	Turkey	7.4	1103	Utsu/USGS
1954	36.3	1.5	Algeria	6.7	1409	Utsu/USGS
1957	36.2	52.7	Iran	7.1	1200	Utsu/USGS
1957	34.5	48.0	Iran	7.2	2000	Utsu/USGS
1960	30.5	-9.6	Morocco	5.7	15000	USGS/Utsu
1960	-39.5	-74.5	Chile	8.5	5700	Utsu/USGS
1962	35.6	49.9	Iran	7.2	12225	Utsu/USGS
1963	35.6	49.9	Skopje	6.0	1100	USGS/Utsu
1966	37.4	114.9	China	7.0	1000	USGS
1966	37.5	115.1	China	7.2	8064	Utsu/USGS
1966	39.1	41.48	Turkey	6.8	2529	USGS/Utsu
1968	34.0	59.0	Iran	7.3	15000	Utsu/USGS
1969	21.61	111.83	China	5.9	3000	USGS
1970	24.2	102.7	China	7.8	15621	Utsu/USGS
1970	39.2	29.5	Turkey	7.1	1086	Utsu/USGS
1970	-9.4	-78.9	Peru	7.9	70000	USGS/Utsu
1971	38.83	40.52	Turkey	6.9	1000	USGS/Utsu
1972	28.4	52.8	Iran	7.1	5054	USGS/Utsu
1972	12.3	-86.1	Nicaragua	6.2	6000	Utsu/USGS
1973	31.3	100.7	China	7.6	2175	Utsu
1974	28.2	104.0	China	6.8	20000	USGS/Utsu
1974	72.8	6.2	Pakistan	6.2	5300	Utsu/USGS
1975	40.6	122.5	China	7	2000	USGS/Utsu
1975	38.5	40.7	Turkey	6.7	2300	USGS/Utsu
1976	15.3	-89.1	Guatemala	7.5	23000	Utsu/USGS
1976	46.4	13.3	Italy	6.5	1000	USGS/Utsu
1976	-4.6	140.0	Indonesia	7.1	6000	Utsu
1976	39.4	118.0	China	7.5	242800	Utsu/USGS
1976	6.2	124.0	Philippines	7.9	8000	Utsu/USGS
1976	-4.5	139.9	Indonesia	7.2	6000	Utsu
1976	39.1	44.0	Iran	7.3	5000	USGS/Utsu
1977	45.8	26.8	Romania	7.2	1581	Utsu/USGS
1978	33.4	57.4	Iran	7.4	18220	Utsu/USGS
1980	36.1	1.4	Algeria	7.7	5000	USGS/Utsu
1980	40.9	15.3	Italy	6.5	2735	USGS/Utsu
1981	29.9	57.7	Iran	6.9	3000	Utsu/USGS
1981	30.0	57.8	Iran	7.3	1500	Utsu/USGS
1981	-4.6	139.2	Indonesia	6.7	1300	Utsu
1982	14.7	44.4	Yemen	6.0	2800	Utsu/USGS
1983	40.3	42.2	Turkey	6.9	1400	Utsu/USGS
1985	18.2	-102.5	Mexico	8.1	9500	Utsu/USGS
1986	13.8	-89.1	El Salvador	5.4	1500	Utsu/USGS

Year	Lat	Long	Country	M	death	Source
1987	0.2	-77.8	Colombia	7	5000	Utsu/USGS
1988	26.8	86.6	Nepal	6.6	1450	Utsu/USGS
1988	41.0	44.2	Armenia	6.8	25000	Utsu/USGS
1990	37.0	49.4	Iran	7.4	50000	USGS/Utsu
1990	15.7	121.2	Philippine Islands	7.8	2430	Utsu/USGS
1991	30.8	78.8	India	7.0	2000	Utsu/USGS
1992	-8.5	121.9	Indonesia	7.5	2500	USGS/Utsu
1993	18.1	76.5	India	6.2	9748	Utsu/USGS
1995	34.6	135.0	Japan	7.2	6435	Utsu/USGS
1995	52.6	142.8	Russia	7.5	1989	Utsu/USGS
1997	33.8	59.8	Iran	7.3	1572	Utsu/USGS
1997	38.1	48.1	Iran	6.1	1100	Utsu
1998	37.1	70.1	Afghanistan	6.1	2323	Utsu/USGS
1998	37.1	70.1	Afghanistan	6.9	4000	Utsu/USGS
1998	03.0	141.9	Papua New Guinea	7.1	2700	Utsu/USGS
1999	4.5	-75.7	Colombia	5.7	1900	Utsu/USGS
1999	40.8	29.9	Turkey	7.8	17118	Utsu/USGS
1999	23.8	121.0	Taiwan	7.7	2413	Utsu/USGS
2001	23.3	70.3	India	7.6	20085	USGS
2002	35.9	69.2	Afghanistan	6.1	1000	USGS
2003	36.9	3.7	Algeria	6.8	2266	USGS
2003	28.9	58.3	Iran	6.6	31000	USGS
2004	3.3	95.9	Indonesia	9.1	227898	USGS
2005	2.1	97.0	Indonesia	8.6	1313	USGS
2005	34.5	73.6	Pakistan	7.6	86000	USGS
2006	-7.9	110.4	Indonesia	6.3	5749	USGS
2008	31.0	103.3	China	7.9	87652	USGS
2009	-0.7	99.9	Indonesia	7.5	1117	USGS
2010	33.2	96.5	China	6.9	2200	USGS
2010	18.4	-72.6	Haiti	7.0	65000	*
2011	38.3	142.4	Japan	9	20896	USGS

* Record of earthquake fatalities in Haiti varies between literatures. We choose 65,000 as an accurate estimation of life loss in Haiti based on Doocy et al. (2013) and Scwartz et al. (2011).

List of 12 largest earthquakes in Haiti from 1500 to 2010

Date	latitude	longitude	Mw	Reference
1564	19.38141	-70.5913	7	Schere, 1912
1692	17.8	-76.7	7.5	Utsu
1751	18.45966	-72.2439	7.5	Schere, 1912
1770	18.34708	-72.8683	7.3	Schere, 1912
1842	19.84992	-72.837	8	Schere, 1912
1860	18.38	-73	7	Schere, 1912
1887	19.7	-73.1	7	Schere, 1912
1899	18	-77	7.5	Utsu
1916	18.5	-68	7.8	Pager
1946	19.25	-69	7.9	Pager
1948	19.25	-69.25	7.1	Pager
2010	18.447	-72.55	7	USGS

List of earthquakes with more than 1 fatalities in Haiti (8 events), Chile (42 events), Japan (53 events), and Iran (117 events) between 1900-2009, based on Pager Catalogue (*http://earthquake.usgs.gov/research/data/pager/*), EM_DAT (*http://www.emdat.be/*), and Utsu (2002).

HAITI				CHILE				JAPAN				IRAN			
year	**M**	**death**	**Source**	**Year**	**M**	**Death**	**Source**	**Year**	**M**	**Death**	**Source**	**Year**	**M**	**Death**	**Source**
1907		1000	UTSU	**1906**	8.4	20000	EM-DAT	**1901**		18	EMDAT	**1903**	6.4	200	UTSU
1932		8		**1922**	8.5	1100	EM-DAT	**1905**		41	EMDAT	**1909**	7.3	5500	UTSU
1946		100	UTSU	**1928**	8	220	EM-DAT	**1907**		41	EMDAT	**1911**	6.2	700	UTSU
1952	5.9	6	UTSU	**1939**	7.8	30000	EM-DAT	**1909**	6.8	41	UTSU	**1913**	5.8	11	UTSU
1953	5.7	2	UTSU	**1942**	-	5	EM-DAT	**1914**	7.1	94	UTSU	**1923**	5.5	2219	UTSU
1962		1		**1943**	7.9	18	UTSU	**1914**	7.1	35	UTSU	**1923**	6.7	290	UTSU
1994	5.4	4	PAGER	**1945**	7.1	4	UTSU	**1922**	6.9	26	UTSU	**1923**	6.4	157	UTSU
2010	7.3	200000	UTSU	**1946**	7.5	2	UTSU	**1923**	7.9	142807	UTSU	**1925**	5.5	500	UTSU
				1949	7.3	57	UTSU	**1925**	6.8	428	UTSU	**1925**	5.5	2	UTSU
				1949	7.8	3	UTSU	**1927**	7.3	2925	UTSU	**1928**	5.4	10	UTSU
				1949	7.8	1	UTSU	**1930**	7	272	UTSU	**1928**	5	10	UTSU
				1950	8	4	UTSU	**1931**	7	16	UTSU	**1928**	5.5	4	UTSU
				1953	7.6	15	EM-DAT	**1933**	8.1	3064	UTSU	**1929**	7.2	3300	EMDAT
				1960	9	5700	UTSU	**1939**	6.8	27	UTSU	**1930**	7.3	2500	EMDAT
				1960	9.5	142	UTSU	**1943**	7.2	1083	EMDAT	**1932**	5.4	1070	UTSU
				1963	-	280	EM-DAT	**1944**	7.9	1251	UTSU	**1933**	6.2	4	UTSU
				1965	7.3	400	EM-DAT	**1945**	6.8	2306	UTSU	**1935**	6.4	500	UTSU
				1966	7.8	4	EM-DAT	**1946**	8	2000	EMDAT	**1935**	6	60	UTSU
				1971	7.5	83	UTSU	**1948**	7.1	5131	EMDAT	**1941**	6.4	680	UTSU
				1971	7	1	UTSU	**1952**	8.2	33	UTSU	**1944**	4.8	20	UTSU
				1975	6.9	2	PAGER	**1960**		138	EMDAT	**1945**	8	300	UTSU
				1976	7.5	1	PAGER	**1964**	7.5	26	UTSU	**1947**	6.9	500	UTSU
				1981	5.7	10	PAGER	**1968**	7.9	52	UTSU	**1948**	NA	200	EMDAT
				1981	7.1	1	PAGER	**1974**	6.7	30	PAGER	**1950**	5.8	20	UTSU
				1983	7.6	5	PAGER	**1974**	5.6	2	PAGER	**1953**	6.3	1000	EMDAT
				1985	7.9	200	PAGER	**1978**	7.6	28	UTSU	**1954**	5	1	UTSU
				1985	7.9	177	PAGER	**1978**	6.6	25	PAGER	**1956**	5.9	410	UTSU
				1985	7.1	2	PAGER	**1979**		27	EMDAT	**1957**	7.2	2000	UTSU

HAITI				CHILE				JAPAN				IRAN			
year	**M**	**death**	**Source**	**year**	**M**	**death**	**Source**	**year**	**M**	**death**	**Source**	**year**	**M**	**death**	**Source**
				1985	6.5	1	PAGER	**1980**	6	2	PAGER	**1957**	7.1	1200	UTSU
				1987	7.2	5	PAGER	**1980**	5.3	1	PAGER	**1957**	5	1	UTSU
				1987	7.5	1	PAGER	**1983**	7.7	108	UTSU	**1958**	6.7	191	EMDAT
				1995	8	3	PAGER	**1983**	5.4	1	PAGER	**1960**	6	480	EMDAT
				1997	7.1	8	PAGER	**1983**	5.6	1	PAGER	**1961**	7.2	60	EMDAT
				1998	6.4	2	PAGER	**1984**	6.2	29	PAGER	**1962**	7.2	12225	UTSU
				1998	7	1	PAGER	**1984**	7.4	1	PAGER	**1962**	5	6	UTSU
				2000	6	1	UTSU	**1987**	6.5	2	PAGER	**1962**	5.5	2	UTSU
				2001	8.2	130	UTSU	**1987**	6.6	1	PAGER	**1963**	5.2	5	UTSU
				2001	6.3	1	PAGER	**1989**	5.5	1	PAGER	**1963**	4.5	4	UTSU
				2005	7.8	11	PAGER	**1993**	7.7	230	PAGER	**1963**	7	4	UTSU
				2007	6.2	10	PAGER	**1993**	7.6	2	PAGER	**1965**	5.1	20	UTSU
				2007	7.7	2	PAGER	**1993**	7.6	2	PAGER	**1968**	7.3	15000	UTSU
				2010	8.5	547	UTSU	**1993**	6.9	1	PAGER	**1968**	6.4	900	UTSU
								1994	7.7	3	PAGER	**1968**	5.6	61	UTSU
								1995	7.2	6432	PAGER	**1969**	5.4	50	EMDAT
								2000	6.1	1	PAGER	**1970**	6.7	220	UTSU
								2001	6.8	2	PAGER	**1971**	5.9	1	UTSU
								2003		2	EMDAT	**1971**	6	1	UTSU
								2004	6.6	48	PAGER	**1971**	5.3	1	UTSU
								2005	6.6	1	PAGER	**1972**	6.8	5057	EMDAT
								2007	6.6	9	PAGER	**1973**	5.5	1	PAGER
								2007	6.7	1	PAGER	**1975**	6.1	7	PAGER
								2008	6.6	13	PAGER	**1975**	5.2	2	UTSU
								2009		1	EMDAT	**1976**	7.3	3900	UTSU
												1976	6	17	PAGER
												1976	5	3	UTSU
												1977	5.9	665	PAGER
												1977	6	366	PAGER
												1977	6.7	167	PAGER
												1977	5.6	3	PAGER
												1977	5.6	3	PAGER
												1978	7.4	18220	PAGER
												1978	6.3	100	UTSU

HAITI				CHILE				JAPAN				IRAN			
year	**M**	**death**	**Source**	**year**	**M**	**death**	**Source**	**year**	**M**	**death**	**Source**	**year**	**M**	**death**	**Source**
												1978	6.1	76	PAGER
												1979	6.5	280	PAGER
												1979	6.5	200	PAGER
												1979	7	17	PAGER
												1980	6.2	26	PAGER
												1980	5.7	3	PAGER
												1980	5.5	1	PAGER
												1981	6.6	3000	PAGER
												1981	7.2	1500	PAGER
												1983	5.4	100	PAGER
												1983	5.6	3	PAGER
												1985	5.4	1	PAGER
												1986	5.7	1	PAGER
												1987	5.3	2	PAGER
												1988	5.8	1	PAGER
												1988	6	1	PAGER
												1989	5.9	3	PAGER
												1990	7.4	45000	PAGER
												1990	6.6	22	PAGER
												1990	5.7	20	PAGER
												1991	5.6	1	PAGER
												1992	5.1	6	PAGER
												1992	5.6	1	PAGER
												1994	6.1	6	PAGER
												1994	5.9	3	PAGER
												1994	6	2	PAGER
												1997	7.2	1572	PAGER
												1997	6.1	1100	PAGER
												1997	6.5	100	PAGER
												1997	4.5	1	PAGER
												1998	5.7	12	PAGER
												1998	5.4	5	PAGER
												1998	6.6	5	PAGER
												1999	6.2	26	PAGER

HAITI				CHILE				JAPAN				IRAN			
year	**M**	**death**	**Source**	**year**	**M**	**death**	**Source**	**year**	**M**	**death**	**Source**	**year**	**M**	**death**	**Source**
												1999	4.5	1	PAGER
												1999	4.5	1	PAGER
												2000	5.3	1	PAGER
												2002	6.5	227	PAGER
												2002	5.4	2	PAGER
												2002	5.3	1	PAGER
												2003	6.6	26271	PAGER
												2003	5.7	1	PAGER
												2003	4.6	1	PAGER
												2004	6.3	35	PAGER
												2005	6.4	612	PAGER
												2005	5.9	13	PAGER
												2005	4.9	4	PAGER
												2006	6.1	70	PAGER
												2006	5.1	2	PAGER
												2006	5.9	1	PAGER
												2008	6	7	UTSU
												2010	6.7	7	UTSU
												2010	5.5	3	UTSU
												2010	5.6	1	UTSU
												2010	5.6	1	UTSU

Chapter 4 The magnitude and frequency of natural disasters caused by geological hazards

4.1 *Introduction*

Geological hazards have threatened human life throughout the history. Some of these natural events caused huge destructions and fatalities. During the past 50 years there have been 7 geological hazards (earthquakes, tsunamis, volcanic activities and landslides) that caused more than 50,000 casualties and more than USD $10,000,000 damage to the human communities (Table 4.1). These events are either called black swans or dragon kings by Taleb (2007, 2010), Sornette (2009), and Pate-Cornell (2012) due to their rareness and unpredictability. Black swan is a term used for rare events that are extremely unlikely to happen. However, they are not unpredictable events (Sornette, 2009). Dragon king is another term used for extreme events that are different from the rest of their neighbors both from statistical point of view [they are not predictable] and from mechanistically point of view [they seem to have different cause and effect from the rest of the data, thus they don't follow the trend of rest of the data] (Paté-Cornel, 2012).

Among the most destructive and fatal geological hazards listed in Table 4.1, Sumatra earthquake (Indonesia) in 2004 which cause a huge tsunami with 227,898 fatalities, and USD $ 10,000 M is the most disastrous event in the past 50 years. However, an earthquake with magnitude 9.1 is a rare event (black swan) and it lead to an extreme result. However, the rest of the events in the list are not rare events while they caused extreme damages and fatalities (dragon kings). This suggests that extreme geological disasters are not necessarily resulting from extreme geological hazards. Other factors such as resistance (social and technical), exposed population (population density and daily death rate), and monetary condition (GDP and corruption) of the affected areas also determine the extent of the disaster.

One of the objectives of this study is to assemble a database of natural disasters caused by geological hazards, map the geography of loss, and analyze the magnitude and frequency characteristics of disaster events. We also would like to define a loss threshold for a disaster and identify the most destructive geological processes that impose more risk on the global population.

Table 4.1: List of 7 most destructive and fatal geological hazards (1960-2010). Data is from National Geophysical Data Center / World Data Service (NGDC/WDS), available at http://www.ngdc.noaa.gov/hazard/.

Yr	Mon	Day	Hr	Min	Sec	Type	F-depth	Mw	Country	Lat	Long	Death	Damage -M$
1970	5	31	20	23	27.3	Eq	43	7.9	PERU	-9.20	-78.80	66794	530
1976	7	27	19	42	54.6	Eq	23	7.5	CHINA	39.57	117.98	242769	5600
1990	6	20	21	0	9.9	Eq	19	7.7	IRAN	36.96	49.41	50000	8000
2004	12	26	0	58	53.4	Ts	30	9.1	INDONESIA	3.30	95.98	227898	10000
2005	10	8	3	50	40.8	Eq	26	7.6	PAKISTAN	34.54	73.59	80361	5200
2008	5	12	6	28	1.5	Eq	19	7.9	CHINA	31.00	103.32	87652	86000
2010	1	12	21	53	10	Eq	13	7	HAITI	18.46	-72.53	65000[1]	8000

1 The original number of fatalities in Haiti was reported as 316,000 that we changed to 65,000 based on our results from Chapter 3.

Neumayer and Barthel (2011) looked at the trend of the normalized monetary loss due to natural disasters and showed that there is no significant trend in the $USD loss due to natural disasters during 1980-2010. This suggests that our advancements in knowledge and technology over the last 50 years have not changed the impacts of these events on human being. Our last objective in this chapter is to analyze the trend of the frequency of geological disasters and also their effectiveness in fatality.

4.2 Geological Hazards-review of the disaster-generating process

Geological hazards that we consider here are earthquakes, tsunamis, volcanic activities, and landslides which are processes that have been studied in many literature. The physical process and the way that their occurrence and magnitude are estimated and recorded are the focus of many research papers, such as Gutenberg and Richter (1942, 1956) (E), Yokoyama (1965) (V), Schuster and Krizek (1978) (L), Kanamori (1977, 1983) (E), Kagan and Knopoff (1980, 1987) (E), Abe (1989) (T), Ho (1996) (V), Kagan (1997) (E), Tanguy et al (1998), Gerassimos (2001) (T), Guzzetti et al. (2002) (L), Glade (2003) (L), Bardet et al. (2003) (T), Kanamori and Brodsky (2004) (E), Mason et al. (2004) (V), Gutierrez et al. (2005) (E, D), Witham (2005) (V), Evans (2006, 2008) (L), Evans and Alcantara-Ayala (2007) (L), Boore and Atkinson (2008) (E), Guthrie et al. (2008) (L), Siebert et al. (2011) (V), Sachs et al. (2012), Lovholt et al. (2012) (T), Tang et al. (2012) (T). The letters E, V, L, and T are abbreviations for earthquakes, volcanic

activities, landslides, and tsunamis, respectively. Furthermore, in many books, such as Scheidegger (1975), Bolt et al. (1975), and Woo (1999, 2002) the physics, mathematics, and general process of all natural hazards are gathered and summarized. Here, we briefly review the measures of magnitude for each of geological hazards based on some of the abovementioned literature.

4.2.1 Earthquakes

Earthquakes are caused by the sudden release of slowly accumulated strain energy along a fault in the earth's crust which creates seismic waves. Seismic activity is the frequency, type, and size of earthquakes over a period of time.

Earthquakes, due to their irregular time intervals between their events and their lack of adequate forecasting, are sources of severe threat. Some of the hazards associated to earthquakes are listed here based on Bender (1991)[22]:

- *Ground shaking is a direct hazard to any structure located near the earthquake's center. Structural failure takes many human lives in densely populated areas.*

- *Faulting, or breaches of the surface material, occurs as the separation of bedrock along lines of weakness.*

- *Landslides occur because of ground shaking in areas having relatively steep topography and poor slope stability.*

- *Liquefaction of gently sloping unconsolidated material can be triggered by ground shaking. Rows and lateral spreads (liquefaction phenomena) are among the most destructive geologic hazards.*

- *Subsidence or surface depressions result from the settling of loose or unconsolidated sediment. Subsidence occurs in waterlogged soils, fill, alluvium, and other materials that are prone to settle.*

[22] These points are gathered from Bender (1991).

- *Tsunamis or seismic sea waves, usually generated by seismic activity under the ocean floor, cause flooding in coastal areas and can affect areas thousands of kilometers from the earthquake center.*

The main measures for the magnitude of earthquakes: 1) moment magnitude, M_w, which is the accurate quantified measure of earthquake size calculated based on the seismic moment, M_0, of the region [23], in logarithmic scale, $\boldsymbol{M_W = \frac{\log_{10} M_0}{1.5} - 6.07}$ (M_0 in *Nm*); *Nm* stands for Newton-meter. The frequency of the magnitude of earthquakes is presented as Gutenberg-Richter law (Gutenberg and Richter, 1956) which follows a power-law distribution. Due to the seismic activity of a region, the frequencies vary; however, in most parts of the world, the frequency of small earthquakes (magnitude 3-4) is around 10 per year, the frequency of moderate earthquakes (magnitude 5-6) is 1 in 10 years, and the frequency of large earthquakes (more than magnitude 7) is less than 1 in 100 years (Kagan, 1997).

4.2.2 Tsunamis

Tsunami is a Japanese word for "harbor wave" which is associated with a series of water waves caused by the displacement of a large volume of a body of water, generally an ocean or a large lake. Tsunamis waves can be triggered by disturbances such as earthquakes, landslides, and volcanic eruptions. The crests of these waves can exceed heights of 25 meters on reaching shallow water. The unique characteristics of tsunamis (wave lengths commonly exceeding 100 km, deep-ocean velocities of up to 700 km/hour, and small crest heights in deep water) make their detection and monitoring difficult. Tsunamis can cause coastal flooding similar to storm surges. Storm surges are an abnormal rise in sea water level.

Most often, destruction by a storm surge can be associated either by the passing of the wave front and causing physical shock on the objects, or the hydrostatic/dynamic forces which lift the water and carry the objects. The most significant damages often result from the direct impact of waves

[23] $M_0=\mu DS$, where μ is the rigidity (shear modulus) of the material surrounding the fault (in dyn/cm^2), D is the average displacement of the fault (in *cm*) and S is the area of the rupture along the fault (in cm^2). Since M_0 depends on the state of the fault before and after an earthquake, it does not depend on the actual time history of faulting; therefore, it is a static parameter (Kanamori and Brodsky, 2004).

on fixed structures. Indirect impacts include flooding and undermining of major infrastructure such as highways and railroads.

One magnitude scale used for tsunamis, M_t, is based on the amplitude of tsunami waves and the distance from the earthquake epicenter in logarithmic scale, $M_t = \log_{10} H + a \log_{10} \Delta + D$, where H is the maximum single amplitude of tsunami waves (in m) measured by tide gages, Δ is the distance (in km) from the earthquake epicenter to the tide station along the shortest oceanic path, and a and D are constants (Abe, 1989). The source strength and the amplification factors of the sea floor can also affect the tsunami wave height (Shuto, 2005).

4.2.3 Volcanoes

Volcanoes are cracks in the earth's crust through which hot lava, volcanic ash, molten rock, and gases escape from the magma chamber to the surface. There are two classes of eruptions for volcanic activities: 1) Explosive eruptions which originate in the rapid dissolution and expansion of gas from the molten rock as it nears the earth's surface. Explosions pose a risk by scattering rock blocks, tephra, and lava at varying distances from the source. 2) Effusive eruptions in which lava flows rather than any explosion. Lava flows are governed by gravity, surrounding topography, and material viscosity (Self, 2006). Both of these types can occur in the extent of a few thousand cubic meters of magma, up to a thousand cubic kilometers of magma in extreme cases.

Hazards associated with volcanic eruptions include lava flows, falling ash and projectiles, mudflows, and toxic gases. Volcanic activity may also trigger other natural hazardous events including local tsunamis, deformation of the landscape, floods when lakes are breached or when streams and rivers are dammed, and tremor-provoked landslides (Bender, 1991).

One of the measures of the magnitude of volcanic eruptions is called the Volcanic Explosivity Index (VEI) which is based on the volume of the magma (in km^3) plus other parameters; with the indices between 0 and 8. The scale is logarithmic; an increase of 1 index indicates an eruption that is 10 times as powerful. The known magnitude measure for volcanic eruptions is based on the mass of erupted magma (in kg). The scale is again logarithmic, M= $\log_{10}$(erupted mass, kg)-7.0 (Self, 2006). Frequencies associated with different magnitudes of volcanic eruptions are from around 1 eruption per year (magnitude of 4) to 1 eruption in 100,000 years (magnitude of 8)

(Self, 2006, Fig. 3). The frequency of volcanic eruptions follows the power-law distribution (Ho, 1996), similar to earthquakes and tsunamis.

4.2.4 Landslides

The term landslide includes topple, fall, slide, lateral spread, flow and complex movement of unconsolidated materials. Landslides can be triggered by earthquakes, volcanic eruptions, soils saturated by heavy rain or groundwater rise, and river undercutting. Earthquake shaking of saturated soils creates particularly dangerous conditions. Although landslides are highly localized, they can be particularly hazardous due to their frequency of occurrence. Classes of landslide based on summary of Bolt et al. (1975), and Bender (1991) include[24]:

- *Rockfalls, which are characterized by free-falling rocks from overlying hills. These often collect at the bottom of the hill in a cliff-shape form of slopes which may pose an additional risk.*

- *Slides and avalanches, which are chaotic movements of overburden due to the reduction of internal shearing strength of the soil material. Avalanches are much more rapid than slides. If the displacement occurs in surface material without total deformation it is called a slump.*

- *Flows and lateral spreads, which occur in recent unconsolidated material associated with a low pore pressure. Although they are associated with a gentle topography, these liquefaction phenomena can travel significant distances from their origin.*

The impact of these events depends on the specific nature of the landslide. Rockfalls are obvious dangers to life and property but, in general, they pose only a localized threat due to their limited areal influence. In contrast, slides, avalanches, flows, and lateral spreads, due to having great areal extents, can cause massive loss of lives and property. Mudflows that are associated with volcanic eruptions can travel at great speed from their point of origin and are one of the most destructive volcanic hazards.

Landslides are basically results of mass movement due to gravitational forces. Landslides can also trigger tsunamis if the slides occur into the water (e.g., Vajont Dam in 1963 and Lituya Bay in 1958). The magnitude of landslides is based on the volume of the displaced mass and the rate of movement (Glade et al., 2005). The frequency of small landslides is as often as 1 per year to

[24] These points are summarized and gathered from Bolt et al. (1975) and Bender (1991).

as rare as 1 in 800,000 years. The magnitude-frequency relation of landslides also follows the power-law trend (Guthrie et al., 2008).

4.3. Geological Disasters

The risk and the impact of the geological hazards, summarized in section 4.2, on human societies are studied for many years, particularly to analyze the underlying factors and to reduce the loss of life due to their occurrence. In literature such as Lomnitz (1970) (E), Schuster and Krizek (1978) (L) Bilham (1988, 1996, 2004, 2011) (E), Knopoff and Sornette (1995) (E), Tanguy et al (1998) (V), Evans and DeGraff (2002) (L), Guzzetti et al. (2002) (L), Glade et al. (2005) (L), Gutierrez et al. (2005) (E), Fell et al. (2005) (L), Anbarci et al. (2005) (E), Shuto (2005) (T), Witham (2005) (V), Self (2006), Jackson (2006) (E), Hungr and Wong (2007) (L), Porter et al. (2007) (E), Evans (2006, 2008, 2011) (L, L, T), Evans and Alcantara-Ayala (2007) (L) Dowrick (2009) (E), Jaiswal et al. (2009, 2011) (E), Jaiswal et al. (2011) (L), Bangash (2011) (E), Shearer and Phillip (2012) (E), Lovholt et al. (2012) (T), Porter (2012) (L), Petley (2012) (L), So and Spence (2013) (E), there are studies that look at the impact of geological disasters and the methods of their risk assessment.

Furthermore, there is a literature in which more than one of geological disasters are analyzed in terms of their risk or underlying effects, such as Bender (1991), Degg (1992), Nishenko and Barton (1995), Pelling (2003), Dilley et al. (2005), Smolka (2006), Birkmann (2006), Grünthal et al. (2006), Houtsonen and Peltonen (2007), Kim (2012), Mishra et al. (2012), Sachs et al. (2012), and Pisarenko and Rodkin (2014).

However, the word disaster is not well defined, quantitatively. Different experiences and backgrounds define different meaning for the word catastrophe or disaster. In order to have a common ground for studies related to global disasters, having a threshold of loss is essential. We use 1,000 fatalities as the threshold of life-loss for geological disasters, i.e., any of the geological hazards that caused more than 1,000 fatalities is considered as a disaster. Although, the life of every human-being worth being considered as a threshold of loss, the threshold of 1,000 deaths is chosen based on the better data accuracy in the high numbers of fatality events. For events occurred in the past, due to the lack of data collection and information spread, the numbers of fatalities in small events are not recorded as reliably as large events, because there are not enough resources to compare and validate the data with. However, in large events, due to their

larger extent and more attentions, there are more records of the numbers which make the data more reliable.

4.3.1 Database of geological disasters 1600-2012

Considering 1,000 fatalities as a threshold of life-loss in geological hazards, we have gathered all the geological hazards recorded in literature and catalogues as disasters for our database. However, in some of the recorded events, there have been discrepancies about the figures for which we used our judgment based on the credibility of the catalogue to decide on the number we picked.

Nevertheless, there are lack quality and consistency in some of the recorded data, since the sources of information may not have been reliable, or some cautions made by the governments that reported the data. For example, in the case of Haiti 2010, the government of Haiti reported 230,000 fatalities, while in some literature the fatalities are estimated as around 65,000. Also, in the case of Tangshan earthquake, 1976, the numbers are underestimated as suggested in some literature. In this study, we use the figures that are reported in the available trustworthy databases. However, there might be some over- or under- estimations in our data.

For earthquakes, the main data source that we used is Utsu (2002). We used NGDC-NOAA database (http://www.ngdc.noaa.gov/nndc/struts/form?t=101650&s=1&d=1) with limiting criteria of years between 1600 and 2013, and deaths greater than 1000 as our secondary source of data. We cross checked the data with John Hopkins Report of earthquakes affected human between 1980 and 2009 (http://www.jhsph.edu/research/centers-and-institutes/center-for-refugee-and-disaster-response/natural_disasters/_Event_Earthquakes.html). Furthermore, we used USGS list of earthquakes with more than 1,000 fatalities (http://earthquake.usgs.gov/earthquakes/world/world_deaths.php) to double check some of the fatality records.

For tsunamis, NGDC-NOAA database (http://www.ngdc.noaa.gov/nndc/struts/form?t=101650&s=70&d=7) is used as the main source of data. Our search criteria are: years between 1600 and 2013, deaths more than 1000. John Hopkins Report on earthquakes affected human (http://www.jhsph.edu/research/centers-and-institutes/center-for-refugee-and-disaster-response/natural_disasters/_Event_Tsunamis.html) is

used to compare the data in NGDC-NOAA**.** Furthermore, we cross-checked the tsunami disasters recorded in the Cred dataset on EM-DAT (http://www.emdat.be/advanced-search).

For volcanoes, NGDC-NOAA database (http://www.ngdc.noaa.gov/nndc/servlet/ShowDatasets?dataset=102557&search_look=50&display_look=50) is used as the main source of data. Our search criteria are: years between 1600 and 2013, deaths more than 1000. John Hopkins Report on volcanic activities affected humans (http://www.jhsph.edu/research/centers-and-institutes/center-for-refugee-and-disaster-response/natural_disasters/_Event_Volcanoes.html) is used to compare the data in NGDC-NOAA. To double-check the range of fatalities in our data, we used Witham (2005). Furthermore, Volcanoes of the world (Siebert et al., 2010) (Pg. 40) is used to double-check some of the fatality numbers. For landslides we used the database of Evans (2008). Lists of all of the geological disasters and their selection criteria are given in the supplementary information.

Based on our geological disasters data base, in the period of 1600-2012, there are 285 earthquake disasters, 59 tsunamis, 44 volcanic disasters and 35 landslide disasters (total of 423 events). Fig. 4.1 is a global map that shows the place of all of geological disasters. As shown in Fig. 4.1, green dots are earthquake disasters, purple triangles are volcanic disasters, black squares are tsunamis, and orange ovals are landslide disasters if the world since 1600. The concentration of earthquake disasters is in the Middle East, China, North Africa and south of Europe, while volcanic disasters mainly have affected the center and south of America, south east of Asia, and Indonesia. Disastrous tsunamis are spread between the South Pacific Ocean coasts of central and south of America, Indonesia, Philippines, and south of India. The affected regions by landslide disasters are mostly in the South East Asia, China, and central and south of America.

Among 424 geological disasters, there are 11 mega-disasters with over 100,000 fatalities among which there are 2 tsunamis (1737 in India and 2004 in Indonesia), 1 landslides (1786 in China), and 8 earthquakes (1662 in China, 1703 in Japan, 1731 in China, 1779 in Iran, 1876 in India, 1920 in Italy, 1923 in Japan, and 1976 in China). The return period of the mega-disasters is around 3 every 100 years which is not relatively rare.

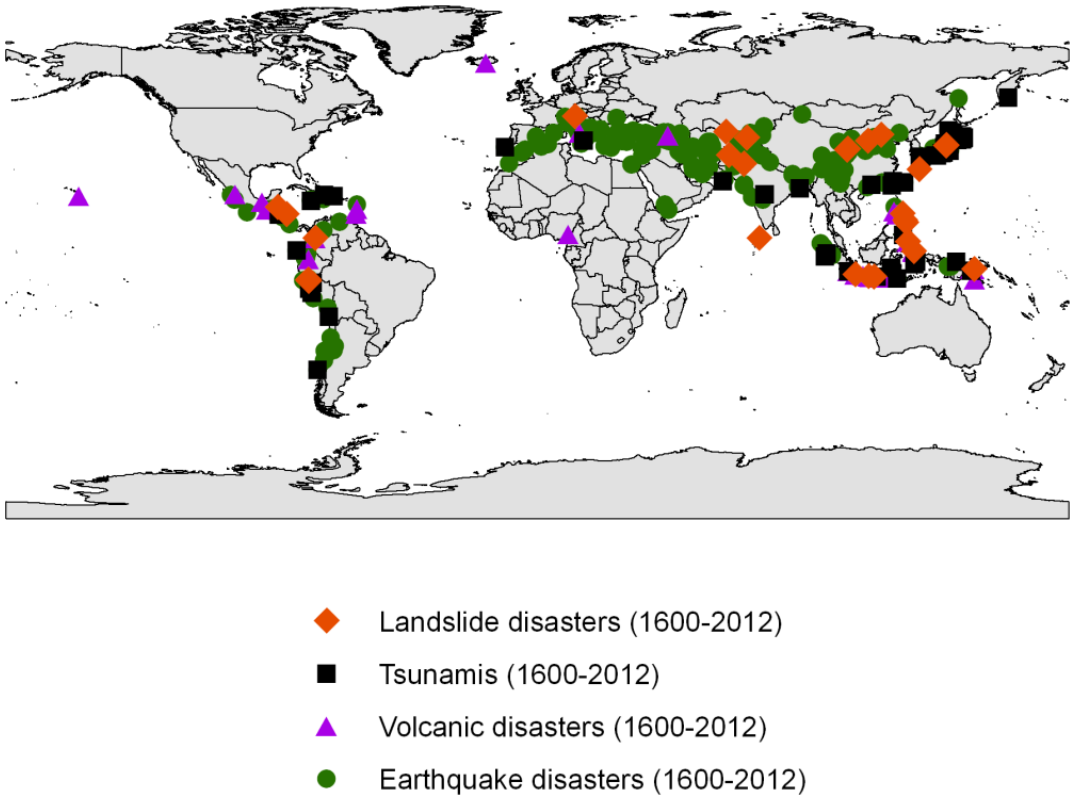

Figure 4.1: Spatial distribution of earthquake disasters (green dots, n=285), tsunamis (black squares, n=59), volcanic disasters (purple triangles, n=44), and landslide disasters (orange ovals, n=35) during 1600-2012. The main sources of data are Utsu (2002) for earthquakes, NGDC-NOAA for tsunamis and volcanic activities, and Evans (2008) for landslides. The detailed references of our database are given in the supplementary data.

4.3.2 Temporal analysis of cumulative fatalities

If we plot the cumulative trend of fatalities due to each geological disaster (Fig. 4.2) comparing to each other and to the overall trend of all geological disasters over the period of 1600 and 2012, we observe that earthquakes among earthquakes, tsunamis, volcanoes, and landslides, is on top of the graph with the highest record of disaster fatalities. The overall trend, the red line, is very close to the earthquake line; therefore, we can conclude that the contribution of other geological disasters is very small in the overall trend. Here, we also can compare the yearly trend of the geological disasters with themselves and with each other, e.g., in 1786 there is a jump in the landslide fatality trend which identifies a mega-disaster in that year (China). Furthermore, from Fig. 4.2, the total number of fatalities due to each disaster-generating process can be estimated as 4,320,722; 868,802; 171,091; and 221,475, respectively.

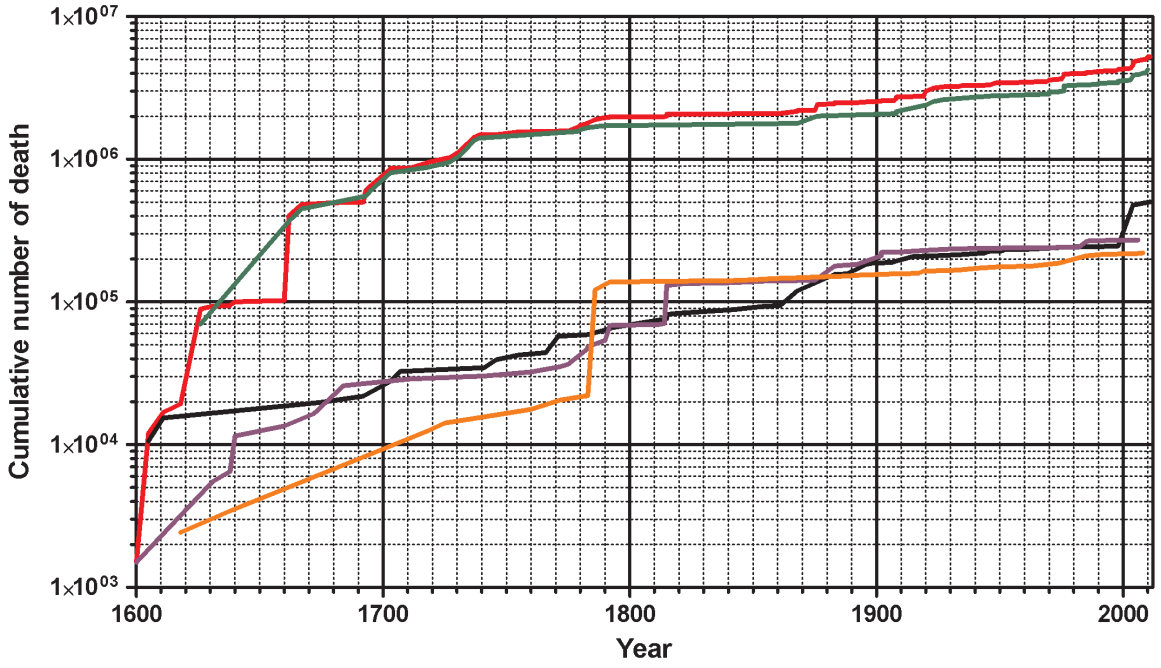

Figure 4.2: Cumulative number of fatalities due to geological disasters [earthquakes in green, tsunamis in black, volcanoes in purple and landslides in orange] compared to the cumulative number of fatalities in all geological disasters in red during the period of (1600-2012). Data is given in the supplementary information.

4.4 Geological Hazards II - a unifying energy scale of hazard magnitude

In section 4.1, we introduced the different magnitude scales that are used for each of the geological hazards. In order to be able to compare the extent of magnitudes and their potential strength for imposing any impact on human life, we need to unify the scale of these hazards. We introduce Log of energy (J) released at the source of geological hazards, to compare the extent of geological hazards with each other. For example, comparing Chilean earthquake with M_w of 9.5 in 1960 which released an energy of 1.12×10^{19} Joules (Kanamori, 1977); Tsunami in Japan (2011) with earthquake M_w of 9.1 that released tsunami energy of 3×10^{15} Joules (Tang et al., 2012); Tambora eruption with ejecta volume of 1×10^{17} m^3 in 1815 which released an energy of 8.4×10^{19} Joules (Yokoyama, 1965); and Frank slide in Alberta (1903) with volume of 3×10^{6} m^3 which released an energy of 3.2×10^{14} Joules (Lucchitta, 1978) are more comparable to each other than using only magnitudes of M_{eq}=9.5, M_t=9.1, Vol_v= 1×10^{17}, and Vol_l =3×10^{6}. This can be expanded to other hazard assessment that requires a unified magnitude scale.

Here, we summarize the methodologies suggested in literature for estimating the source energy of each of the geological hazards. However they are physically rigorous, there is room for improvement in these estimations. In this study, we used certain modifications needed for implementing the suggested methodologies. The methodologies explained in the following are used to calculate the source energy of the geological hazards generated disasters between 1600-2012. However, the information needed for these calculations were not available for all of the recorded hazards, especially for historical landslides; therefore, we only did the calculations for the ones where sufficient certain information was available to do so. List of these events and the estimated energies are provided in the supplementary information.

4.4.1 Earthquakes:

For earthquakes, we use Gutenberg's equation (Gutenberg and Richter, 1956) for radiated energy from earthquakes, $\log(E_{eq}) = 11.8 + 1.5\ M_s$ (ergs), where M_s is the surface magnitude of earthquakes. Kanamori (1983) compared the relationship between different magnitude scales and showed that for earthquakes $M_s \leq 8$, $M_s = M_w$ where M_w is a magnitude scale based on seismic moment of earthquakes and called moment magnitude. As Kanamori (1983) mention that Mw is a useful magnitude scale since it quantifies earthquakes based on the radiated energy; therefore, current earthquake catalogues record the moment magnitude as the main magnitude scale for earthquakes. However the magnitude scales are measured differently, their values do not vary significantly for the purpose of this paper. Therefore, we assume all the magnitudes recorded for the past events are also based on moment magnitude. We convert this energy, E_{eq}, to joules (energy (dyn)$\times 10^{-7}$) as an estimate of the source energy of earthquakes at the epicenter. The range of energies that radiated from earthquake-generated disasters between 1600-2012 were between 7.8×10^{12} -1.12×10^{19} (J). List of all the energies released by all geological disasters is provided in the supplementary tables.

4.4.2 Tsunamis:

For tsunamis that are caused by earthquakes which are 76% of 59 tsunamis disasters, we use an empirical relationship between moment-magnitude, M_w, and tsunami energy, E_t. Tang et al. (2012) compare the relationship between these two, E_t and M_w, in their paper (Table 3 in Tang et al., 2012). We used this table to plot E_t versus M_w and find their empirical relationship based on

the linear regression of the data for estimating the best fit. The best fit to the plot of E_t versus M_w is $E_T=0.029e^{4.37Mw}$ (J) (R^2=0.95, 95% confidence interval of slope: 4.28-4.45) (Fig. 4.3).

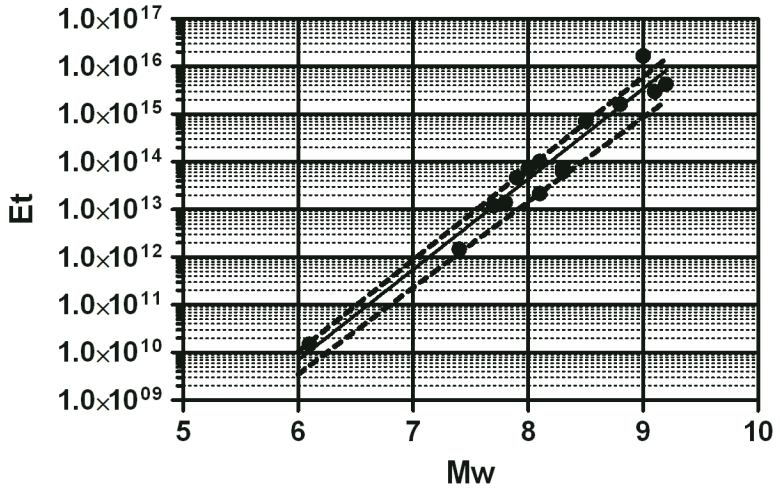

Figure 4.3: Tsunami energy (E_T) versus earthquake moment magnitude (M_W) based on Table 3 of tsunami energy of past events from Tang et al. (2011). Best fit to the data is $E_T=0.029e^{4.37Mw}$ (J) (R^2=0.95, 95% confidence interval of slope: 4.28-4.45). This equation is used to estimate the energy of tsunamis during 1600-2012.

The range of energy-released by tsunami disasters generated from earthquakes during 1600-2012 is between 4.6×10^9 and 3.1×10^{16} (J). The detailed list of tsunami disasters is provided in the supplementary information.

4.4.3 Volcanic activities:

The energy release from volcanic eruptions is calculated based on two main components; the kinetic energy of the ejecta, and thermal energy (Mason et al., 2004). Here, we use the potential energy from lava flow as the source energy of events using $E_v=\rho_v V_v g h_v$, where ρ_v is the density of lava (assumed to be 2669.9 (kg/m^3) from magma density estimation [Bottinga et al. (1982)]), V_v is the volume of the lava or tephra flow based on the recorded VEI (VEI=0 (V=1E+04), VEI=1 (V=1E+06), VEI=2 (V=1E+07), VEI=3 (V=1E+08), VEI=4 (V=1E+09), VEI=5 (V=1E+10), VEI=6 (V=1E+11), VEI=7 (V=1E+12), VEI=8 (V>1E+12) [Siebert et al. (2010)]), g is the gravity of the Earth (=9.8 m/s^2), and h_v is the height of the mountain. The estimated energy of volcanic eruptions during 1600-2012 is in the range of 6.13×10^{13} and 7.5×10^{19} (J). List of the energy of volcanic disasters that we could find their details of V_v and h_v are provided in the supplementary information.

4.4.4 Landslides:

For landslides, the energy release is calculated based on the potential energy of the displacement mass (McSaveney, 2002). Here, again we use the potential energy of slides based on $E_{ls}= \rho_{ls} V_{ls} g h_{ls}$, where ρ_{ls} is assumed to be ~2500 (kg/m^3) (rock) (Verruijt, 2010), V_{ls} is the volume of the slide that is reported, g is the gravity of the Earth (=9.8 m/s^2), and h_{ls} is the height at which the landslide occurred. However, the volume and height of past landslides are not recorded properly; therefore, we only calculated energy for the ones that data was available for the landslide disasters of 1600-2012. The list is provided in the supplementary data.

4.5 Energy magnitude-frequency graphs of geological disasters:

Similar to the magnitude-frequency graphs that are plotted for earthquakes which are log-log graphs that commonly hold a power-law equation, $y=ax^{-b}$, where a and b are parameters that vary by the characteristics of the region and the dataset, respectively. Here we plot the unified magnitude scale of geological disasters (Fig. 4.4). Fig. 4.4 compares the log(energy)-frequency graph of earthquakes (green dots), volcanic activities (purple triangles), tsunamis (black ovals), and landslides (orange squares) with each other and with the overall log(energy)-frequency curve of geological disasters (1600-2012). Fig. 4.4 illustrates a roll-over effect in the low energy-high frequency geological disasters, which is mainly caused by earthquakes. One of the interpretations of this roll-over on the frequency-energy graph is that even low energy events can cause more than 1,000 fatalities. Furthermore, using Fig. 4.4, we can compare the return period of a range of energy-releases by geological disasters. For example, the return period of energy of 10^{10} (J) is around 1 per year, while the return period of 10^{15} (J) is around 3 in 5 years, and 10^{17} (J) is around 1 in 100 years. Based on the energy released from geological disasters (listed in the supplementary data), the nominal energy threshold for geological disasters (that caused more than 1000 fatalities) is 4.6×10^9 (J) which is related to the tsunami in 1783 which was triggered by an earthquake of magnitude 5.9.

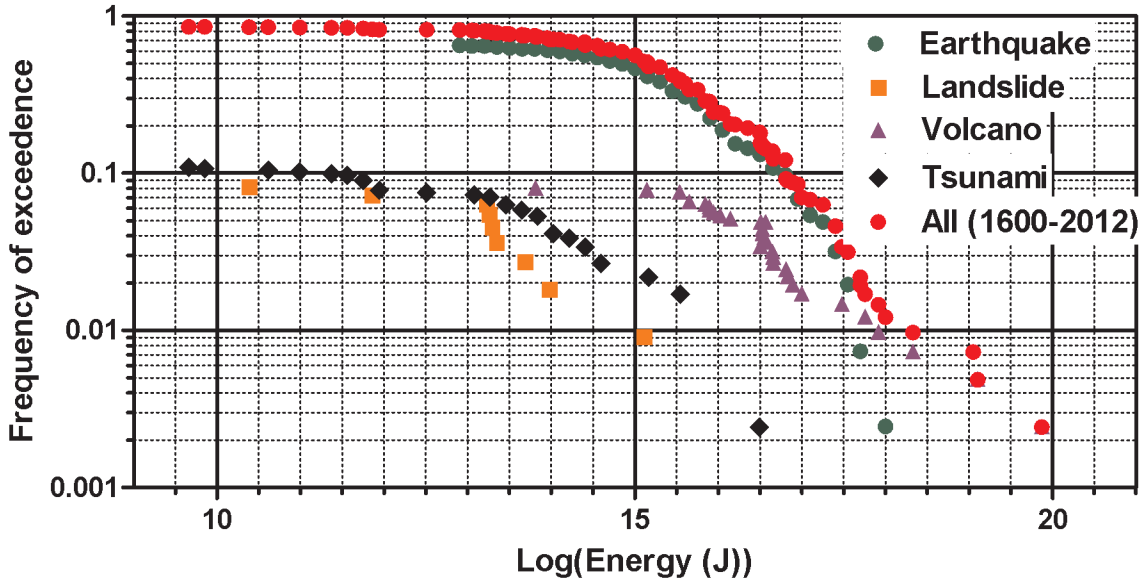

Figure 4.4: Frequency of energy-scale of geological disasters (fatalities≥1000), earthquakes (1600-2012), earthquakes (green circles), tsunamis (black ovals), volcanic activities (purple triangles), and landslides (orange squares) comparing with the overall frequency-energy of geological disasters. Earthquakes are dominant. Data used for energy are based on datasets developed from various databases given in supplementary data.

4.5.1 Energy efficiency of geological disasters:

Here, we introduce a new parameter that can be used to analyze the energy efficiency of geological disasters in causing life-loss. The total estimated energy release by geological disasters for the period of 1600-2013, for earthquakes is ~10^{19}, tsunamis ~10^{18}, volcanoes ~10^{20}, and landslides ~10^{16}. Total fatalities during this period are 4,320,722; 868,802; 171,091; and 221,475, respectively.

The ratio of number of deaths due to a geological disaster to the energy released by the disaster is considered as the energy efficiency of the geological disaster. This ratio allows comparing the deadliness of disasters with each other with units of death per joules (D/J). The average efficiency of earthquakes is ~10^{-11} (D/J), tsunamis ~10^{-8} (D/J), volcanoes ~ 10^{-13} (D/J), and landslides 10^{-9} (D/J). These average ratios suggest that tsunamis are the most efficient disasters among other geological disasters, i.e., the number of people killed by them with respect to the energy they release is the highest. Volcanoes have the lowest D/J efficiency which means that their energy release is less effective in life-loss.

4.6 Analysis: Risk of Geological Disasters

4.6.1 Introduction to FN-curves

Frequency-number (*FN*) curves are generally log-log plots that illustrate a frequency-number trend. These plots are traditionally generated from a set of data gathered over a period of time about a specific concept. In these plots, frequency of exceedance of the data is on the *y*-axis and value of the data is on the *x*-axis. A representative formula for a fitted line to a real-data *FN*-plot is power-law, $F(N)=a\times N^{-b}$, which is often plotted on a log-log scale, $log(y)=\log(a)-b\times log(x)$, where *log(a)* is the intercept and *b* is the slope. Since these curves are frequency-fatality plots, the slopes represent the ratio of low frequency fatalities to high frequency fatalities. More precisely, as Baek et al (2011) argued using Random Group Formation (RGF) theory, the slope is determined by the size of the largest group of fatalities here; i.e., the more frequent events (less number of fatalities) mainly influence on the trend of FN-curves.

However, there are other ways to construct frequency-number (*FN*) curves. Since first developed, these curves have also used for designing requirements (Lees (1996), Chapter 9). For the latter use, different countries impose different criteria for the shape of the *FN*-curve according to their desire for risk reduction. A summary of *FN*-curve-based criteria for societal risk reduction in industrial activities in certain countries has been gathered by Ball and Floyd (1998), and a complete overview of *FN*-curves is presented by Porske (2008) (Chapter 3.7). Table 4.2 is a summary of the criteria (on slope and intercept of *FN*-diagram) undertaken by certain countries. The values are based on Jonkman et al. (2003) and Trbojevic (2005).

Table 4.2 Summary of *FN*-curve based criteria for societal risk reduction used in some countries (based on Jonkman-et.al-2003)

Country	Slope	Intercept
UK	-1	1.00E-02
Hong Kong	-1	1.00E-03
The Netherlands	-2	1.00E-03
Denmark	-2	1.00E-02
Czech Republic	-2	1.00E-04
France	0	1.00E-07

4.6.2 FN-curve of all geological disasters

In literature that use real data on FN-curves for comparative risk assessment, such as from Ramussen (1975) and Mendes-Victor et al. (2009), the comparisons are based on the position of the plot, i.e., the disaster whose data on the *FN*-plot stands higher, is riskier. However, as showed in Table 4.2, the slope of the *FN*-curve is used for risk reduction purposed in some of the countries.

Here, using real historical geological disaster data (given in the supplementary information) on *FN*-diagrams, we compare the global risk of geological disasters to human life according to their fitted parameters (slope and intercept). Fig. 4.5 shows the *FN*-curve of global geological disasters with respect to each other. According to Fig. 4.5, the frequency of earthquake disasters is far above that of the other geological disasters causing the highest risk to the world.

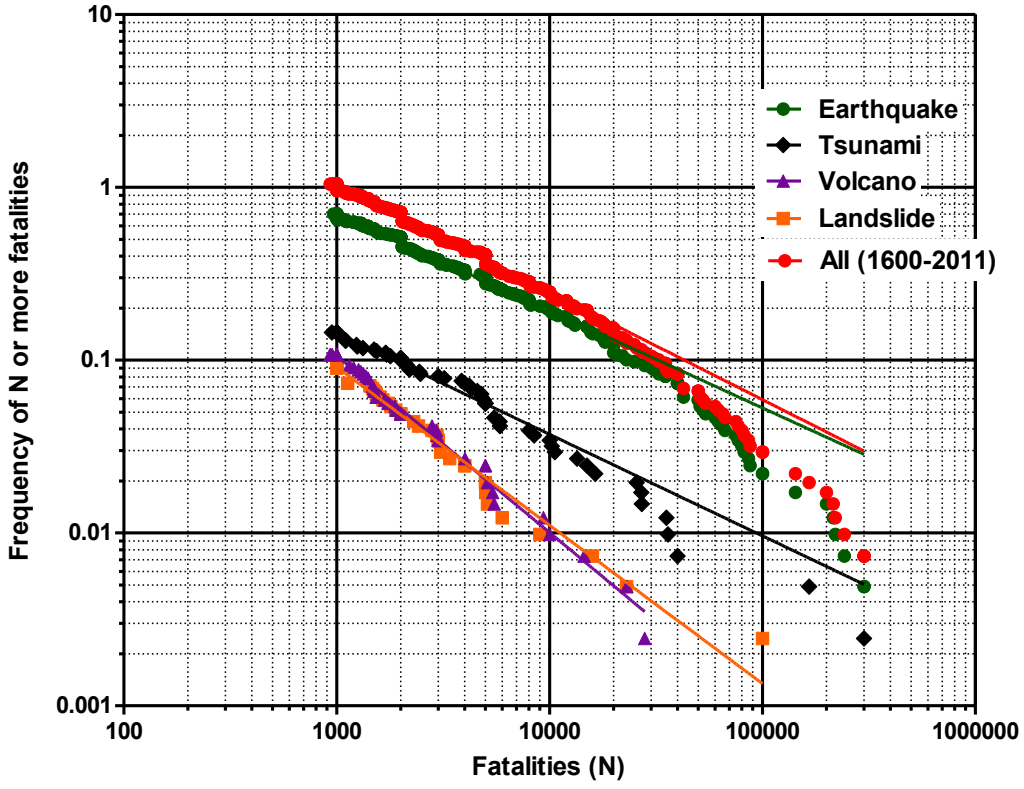

Figure 4.5: FN-curve of geological disasters (1600-2012), earthquakes (green circles), tsunamis (black ovals), volcanic activities (purple triangles), and landslides (orange squares) compared with the FN-curve of all geological disasters. Earthquakes are dominant.

Table 4.3 compares the power-law fits to the FN-curves of geological disasters. As can be seen, earthquakes and tsunamis have slopes that are closer to the overall FN-curve. Landslides and volcanic activities have similar slopes close to -1 which shows risk neutrality of the world to these disasters.

Table 4.3 Power-law fit of FN-curves plotted in Fig. 4.5; the R^2 values, and 95% confidence intervals of the slope of the curves.

Disaster	**Power-law fit**	**R^2**	**95% confidence interval of slope**
Earthquake	Log(*Y*)=1.54-0.56Log(*x*)	0.99 (n=286)	(-0.5713 to -0.5553)
Tsunami	Log(*Y*)=0.92-0.59Log(*x*)	0.98 (n=59)	(-0.6126 to -0.5622)
Volcano	Log(*Y*)=2.1-1.02Log(*x*)	0.99 (n=44)	(-1.069 to -0.9775)
Landslide	Log(*Y*)=1.77-0.94Log(*x*)	0.98 (n=35)	(-1.002 to -0.8820)
All	Log(*Y*)=1.89-0.62Log(*x*)	0.99 (n=426)	(-0.6287 to -0.6166)

Slopes of FN-curves (power-law fits to the frequenc-sfatality curves) of geological disasters are linearly related to their resistance (Khaleghy-Rad and Evans, 2014), i.e., the greater the slope, the higher the resistance). We use the slope and intercept of the power-law fit to the frequency-fatality curves to introduce a new factor that we call risk factor.

4.6.3 Risk factor of geological disasters:

In order to make a comparative quantitative risk assessment of individual disaster-generating geological processes, we propose a new parameter based on the slope and intercept of linear fits of real disaster data on *FN*-curves. We multiply the annual frequency of 1,000 or more fatalities, a_{1000}, by the inverse of the absolute value of the slope, $\frac{1}{b}$, to define the Risk Factor (RF) as in

$$RF = \alpha_{1000} \times \frac{1}{b} \qquad \text{(Eq. 4.1).}$$

Due to the linear relationship between slope and resistance (Khaleghy-Rad and Evans, 2014), we associate the term $\frac{1}{b}$ to the inverse of resistance to geological disaster, i.e., 1/*Resistance*", where *Resistance* is the risk-absorption level of a system (Aven (2011b), pg. 12). The values of RF for each group of geological disasters is summarized in Table 4.4.

Eq. 4.1 is similar to the standard risk equation, *Risk=Hazard×Vulnerability*(×*Exposure*) (e.g., Birkmann, 2006) with 1/*Resistance* replacing vulnerability. We note that the Exposure term is not considered in the Risk Factor (Eq. 4.1) and because in the context of global geological disasters, we assume that geological disasters affect the whole world (due to their extensive impact), therefore, Exposure is the world's population. Since world's population and its variations are the same for all of the geological disasters, its effect will be cancelled in comparison.

From Table 4.4 we could conclude that the world is more prone to earthquake disasters than any other geological disasters, because the frequency of 1,000 or more fatalities due to earthquakes is around 0.72 and the slope is -0.56, therefore, the risk factor is 1.29. The other disasters' parameters are much less than this (Table 4.4). This could suggest that the higher the risk factor, the more fatalities in the disasters. To evaluate this hypothesis, we compare the RFs listed in Table 4.4 for earthquakes, tsunamis, volcanic activities, and landslides with the total number of fatalities in the period of 1600-2012. This comparison reveals that if we exclude landslides, the sequence of RF and total number of fatalities due to the disasters are comparable. We justify this with the doubt that some of the volcanic disaster fatalities are counted in the landslide disasters. This can happen if flows, such as mudflow triggered by volcanic eruptions cause fatalities.

Table 4.4 List of F(N≥1000) and slope of the fitted power-law to the fatality-frequency (FN) curve of geological disasters, based on Table 4.3 and Fig. 4.5, and the associated risk factor (multiplication of the frequency of 1,000 fatalities and more by the inverse of the absolute value of the slope)

Disaster	**Annual frequency of 1,000 fatalities and more**	**Slope**	**Risk factor**
Earthquake	0.72	-0.56	1.29
Tsunami	0.14	-0.59	0.24
Volcano	0.11	-1.02	0.11
Landslide	0.09	-0.94	0.09
All	1.07	-0.62	1.73

As we introduced in section 4.6.1, FN-curves are used for risk reduction in some countries, such as UK, and Netherlands (Table 4.2), To compare the total risk of geological disasters (red circles on Fig. 4.6, with the acceptable level of risk in some countries such as the UK (blue dashed line on Fig. 4.6) and Netherlands (red dot-dashed line), the acceptable criteria in those countries are

plotted in comparison with the overall *FN*-curve of geological disasters. The acceptable criteria of the UK and the Netherlands are up-scaled for the world population to create a comparable scale. For that, we calculated the corresponding number of individuals in the world according to one individual in the UK and the Netherlands. The acceptable criteria for the Netherlands impose an intercept of 0.001 and slope of -2 (Jonkman et al., 2003). One individual in the Netherlands is equal to about 412 individuals in the world (with the population of the Netherlands assumed to be 16.6 Million (UNdata, http://data.un.org/Data.aspx?q=Population&d=PopDiv&f=variableID%3a12, 2012) and the population of the world to be 6.8 billion). This number for the UK is about 100 individuals in the world (with the population of the UK assumed to be 62 million (UNdata, http://data.un.org/Data.aspx?q=Population&d=PopDiv&f=variableID%3a12, 2012); the acceptable criteria for UK imposes an intercept of 0.01 and slope of -1 (Jonkman et al., 2003). Thus, the intercept associated with each acceptable level (of the UK and the Netherlands) shifted up.

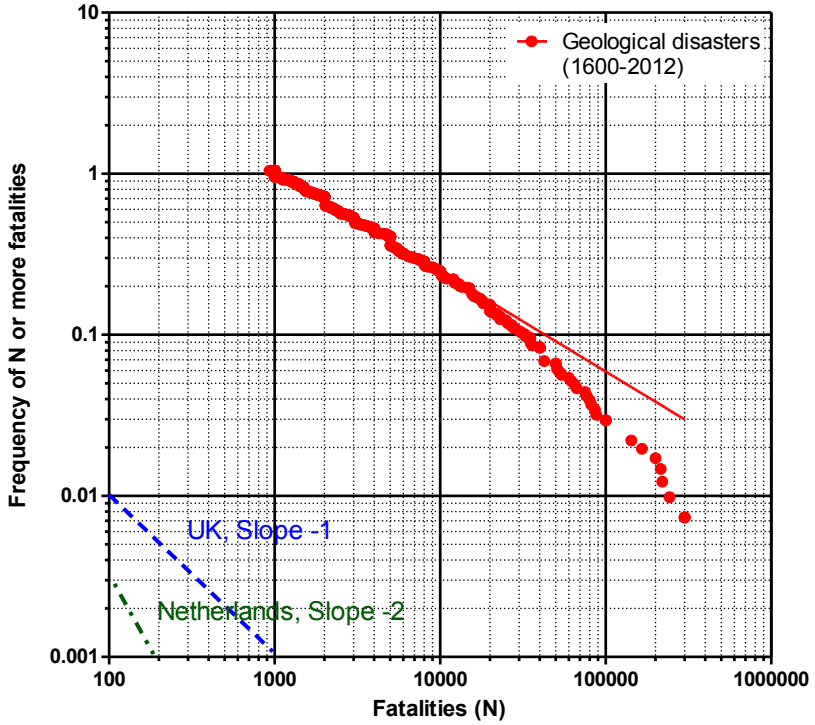

Figure 4.6: Overall frequency-fatality (FN) curve of global geological disasters (1600-2012) (red circles) in comparison with the acceptable criteria of UK (dashed blue line) and the Netherlands (dot-dashed green line) up-scaled for the world population

As shown on Fig. 4.6, the overall trend of geological disasters are far above the acceptable level of risk in the UK and the Netherlands. Quantitatively, the risk factor corresponding to the acceptable criteria in these two countries are 0.001 and 0.0000000015, respectively. The risk factor for the overall FN-curve of geological disasters is 0.5 which is 500 times greater than the acceptable risk factor in the UK and almost 3×10^8 times greater than the risk factor in the Netherlands. The huge difference between the Netherlands and the UK is due to the risk aversion criteria, slope of -2, in the Netherlands.

4.7 Statistical test on frequency and energy of events over time:

We examine the trend of frequency of geological disasters over time (1600-2012) using linear regression. We found that the P-value of linear regression for frequency of events versus time is significantly increasing ($P<0.01$) by factor of 0.004 over the last 412 years. Doocy et al. (2013, EQs, Fig. 3) compares the frequency of earthquake events that affected human life is increasing parallel to the growth of number of deaths due to earthquakes. Although the period of time that they considered is between 1900 and 2009, and their threshold of fatalities is 1, our result is in agreement with Doocy et al. (2013). The result of increasing frequency of geological disasters trend suggest that more geological hazards that cause over 1000 fatalities are expected. However, it must be noted that as the global population increased, the threshold that defines disasters also increased throughout 412 years. Considering this fact as a filter for gathering geological disasters might change our result dramatically, and possibly lead into a non-significant increase of frequency of disasters. The statistical method and results are given in Appendix II, and more elaboration on the effect of threshold is given the ***discussion*** session.

Furthermore, we analyze the temporal trend of energy released by geological disasters (1600-2012). The linear regression method (given in the Appendix II) show that the trend is not significantly increasing or decreasing over time either ($p=0.4$), i.e., there is no evidence that the energy released by geological disasters has been increasing or decreasing during the last 412 years. This confirms that the release of global geological disaster system has not significantly changed during the last 412 years. However, as we showed, the frequency of geological disasters has been increasing significantly. Putting these results together, we could conclude that the increase of the frequency of geological disasters is due to the increase of the global population,

which evidently causes an increase to the population, exposed to the geological disaster-prone areas.

4.7.1 Does the efficiency of geological disasters increase or decrease?

In the section 4.5.1, we introduced a new parameter, called geological disaster efficiency which holds the unit of death per joules (D/J). Here, we use a linear regression analysis to find the trend of D/J of geological disasters over time. The statistical method is provided in Appendix II. The result of our regression analysis shows that there is no evidence of significant (P=0.7) increase or decrease in the trend of D/J in the period of 1600-2012. Fig. 4.7 shows the plot of death per energy (D/J) values versus years of events. The median value of the data is at 1.804e-012 (D/J) (red line on Fig. 4.7) (median is used instead of average because the data is skewed).

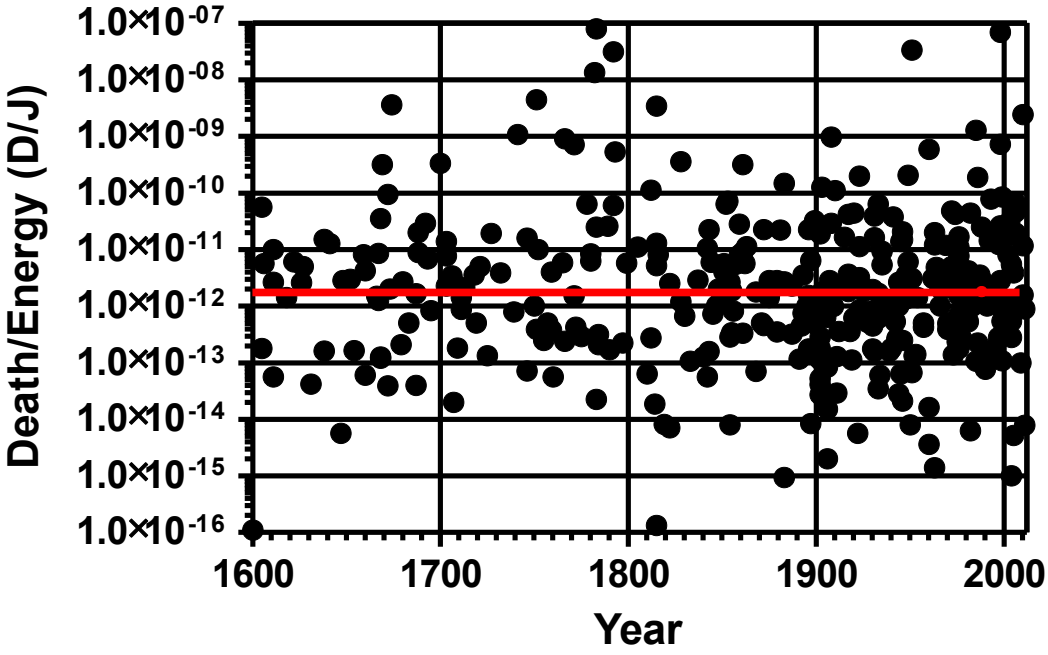

Figure 4.7: Trend of geological disasters' efficiency (death/energy, D/J) over time (black dots). The red line is at the median of 1.804e-012 (D/J).

4.8 Summary, Conclusion, and Discussion

Summary

In this study, we introduced several factors that help comparing both the extent and the impact of geological hazards. We first introduced a unified magnitude scale based on the source energy of hazards for a better comparison of geological hazards. Based on the total energy-release of hazards generated disasters (caused more than 1,000 fatalities) of geological events during 1600-2012, we found that volcanic disasters have had the highest total amount of energy-release that caused around 0.71 M fatalities. However, we also introduced another parameter which identifies the energy efficiency of the geological disasters (D/J). Our data shows that tsunami disasters have had the most efficient energy release in terms of life-loss, around 3.9×10^{-8}. The other factor that we introduced for comparison of risk of geological disasters is the risk factor (RF). Using the best fit to the FN-curve of geological disasters, we found that earthquakes have been the most disastrous geological disasters since 1600.

Furthermore, using statistical tests, we have shown that the frequency of geological disasters has been increasing over time. This result combined with the high risk factors of the geological disasters indicate that a serious global attempt is needed in order to reduce risk due to geological disasters in general and earthquakes, because of their highest risk factor, in particular.

Conclusion

Kagan (1997) claims that if an exponent value of a power-law is less than 1.0 for a set of fatalities, it means that the fatalities are mainly controlled by large events. The slopes gained from the datasets of geological disasters of 1600-2012 are all less than 1.0. This suggests that the fatalities due to geological disasters are mainly controlled by large events, and unless some risk-reverse strategies are applied, maximum possible losses will occur (Kagan, 1997). From the power-law relation in the geological disasters' *FN*-plots shown in Fig. 4.5 and using Kagan's theory regarding risk-averse strategies, we conclude that, in order to increase the slope of the *FN*-curves, and therefore, increase the global resistance toward geological disasters, or to reduce the frequency of events with over 1000 fatalities to lower the risk factor, we need to apply better risk reduction and mitigation strategies.

Discussion

In a statistical analysis, section 4.7, we showed that the frequency of geological disasters has been increasing since 1600 (with the factor of 0.004). We believe that this result is highly influenced by the threshold of 1000 fatalities for geological disasters, i.e., 1000 fatalities among 7 billion people exposed is 1000 times less effective as 1000 fatalities among 7 million exposures. If we consider the 1000 fatality threshold for the population of the world today (WP_{today}), the disaster threshold at year 1600 is $(1000 \times WP_{1600})/WP_{today}$. To have a better analysis for frequency of disasters, it is better to consider normalized death and therefore, a scaled threshold. Here, since we don't have that complete set of data for smaller thresholds, we will just keep in mind that this result (increasing temporal trend for the frequency of geological disasters) will be different and may become balanced over time if we consider a scaled threshold for disasters.

Appendix II- Statistical analysis of temporal trends

Frequency per year:

The testing Equation is: Fr=aYr+b, where Fr is frequency of events (here geological disasters) per year, and Yr is year of events. a and b are constant, a with the unit of $1/yr^2$, and b with the unit of 1/yr. Our hypotheses are: H0: a=0; H1: a≠0. We use linear model in R:

```
Call:
lm(formula = FrYr ~ Yr)
Residuals:
    Min      1Q  Median      3Q     Max
-2.2166 -1.0077 -0.1446  0.9554  4.9154
Coefficients:
             Estimate Std. Error t value Pr(>|t|)
(Intercept) -4.8184367  1.1152210  -4.321 1.94e-05 ***
Yr           0.0039995  0.0005989   6.678 7.63e-11 ***
---
Signif. codes:  0 ‘***’ 0.001 ‘**’ 0.01 ‘*’ 0.05 ‘.’ 0.1 ‘ ’ 1
Residual standard error: 1.397 on 424 degrees of freedom
Multiple R-squared: 0.09516,    Adjusted R-squared: 0.09303
F-statistic: 44.59 on 1 and 424 DF,  p-value: 7.629e-11
```

As the P-value is P<0.01, therefore, we can reject the null hypothesis and since the coefficient of Yr is positive (0.004) we could conclude that the frequency of geological disasters has been increasing by factor of 0.004 over the last 412 years significantly.

Energy release per year:

We use linear regression. The testing Equation is: E=aYr+b, where E is the source energy of events, and Yr is year of events. a and b are constant, a with the unit of joules/yr, and b with the unit of joules. Our hypotheses are: H0: a=0; H1: a≠0. We use linear model in R:

```
Call:
lm(formula = Energy ~ Yr)
Residuals:
       Min         1Q     Median         3Q        Max
-7.029e+17 -3.784e+17 -2.107e+17 -1.120e+17  7.420e+19
Coefficients:
             Estimate Std. Error t value Pr(>|t|)
(Intercept)  3.243e+18  3.555e+18   0.912    0.362
Yr          -1.582e+15  1.900e+15  -0.833    0.406
Residual standard error: 4.026e+18 on 351 degrees of freedom
Multiple R-squared: 0.001972,   Adjusted R-squared: -0.0008712
F-statistic: 0.6936 on 1 and 351 DF,  p-value: 0.4055
```

The P-value of linear regression between energy and time is not significant (0.4), therefore, we cannot reject the null hypothesis, i.e., there is no evidence that the energy released by geological disasters has been increasing or decreasing over time.

Supplementary Information

Table1: Earthquake disasters (1600-2012)

Yr	Lat	Long	location	Country	M	death	Source	Other death reports	Energy (J)
1605	19.9	110.5		China	7.5	2000	NOAA		1.12202E+16
1606	23.6	102.8		China	6.5	2000	NOAA		3.54813E+14
1611	37.6	139.8		Japan	6.9	3700	Utsu		1.41254E+15
1611	39	144		Japan	8.1	5000	Utsu		8.91251E+16
1618	18.9	72.9		India	6.9	2000	Utsu		1.41254E+15
1618	46.3	9.5		Italy	NA	1200	Utsu		NA
1622	36.5	106.3		CHINA	7	12000	NOAA		1.99526E+15
1626	39.4	114.2		China	7	5200	NOAA		1.99526E+15
1627	41.733	15.35	Italy: Naples	Italy	6.8	5000	Utsu		1E+15
1638	39.033	16.283		Italy	7	30000	NOAA/Utsu		1.99526E+15
1640	38.2	46.3		Ecuador	NA	5000	Utsu		NA
1641	37.9	46.1		Iran	6.8	12613	Utsi		1E+15
1647	-33.4	-70.6		Chile	8.5	2000	NOAA/Utsu		3.54813E+17
1648	38.3	43.5		Turkey	6.7	2000	Utsu		7.07946E+14
1652	25.4	100.5		China	6.8	3000	NOAA		1E+15
1653	38.2	28.2		TURKEY		15000	NOAA/Utsu		63095.73445
1654	34.3	105.5		CHINA	8	10400	NOAA		6.30957E+16
1659	38.7	16.3		Italy	6.4	2035	Utsu		2.51189E+14
1660	40	41.3		Turkey	6.5	1500	Utsu		3.54813E+14
1662	35.1	38.9	China			300000			63095.73445
1666	37.1	138.2		Japan	6.8	1500	Utsu		1E+15
1667	42.6	18.1		CROATIA	7.2	5000	NOAA		3.98107E+15
1667	37.2	57.5		Iran	6.9	12000	Utsu		1.41254E+15
1667	40.6	48.6	Azerbaijan:Caucasus (Shemakha)			80000			63095.73445
1668	38.4	27.1		TURKEY	6.6	17500	NOAA		5.01187E+14
1668	35.3	118.6		CHINA	8.5	42578	NOAA		3.54813E+17
1668	40.5	35		Turkey	8	8000	Utsu		6.30957E+16
1669	40.6	48.6		AZERBAIJAN	5.7	7000	NOAA/Utsu		2.23872E+13
1672	43.933	12.583		ITALY	5.6	1500	NOAA/Utsu	200	1.58489E+13
1673	36.3	59.3		IRAN	7.1	5600	NOAA/Utsu		2.81838E+15
1674	-3.5	128.2		Indonesia	NA	2342	Utsu		NA
1679	40.1	44.7		TURKEY		7600	NOAA		63095.73445
1679	40	117		CHINA	8	13162	NOAA		6.30957E+16
1680	25	101.5		CHINA	6.8	2700	NOAA		1E+15
1683	38.7	112.7		CHINA	7	1001	NOAA		1.99526E+15
1687	-15.2	-75.9		PERU	8.2	5000	NOAA/Utsu		1.25893E+17
1688	41.3	14.6		Italy	6.6	10000	Utsu		5.01187E+14
1688	38.4	26.9		TURKEY	7	17500	NOAA/Utsu		1.99526E+15
1692	17.8	-76.7		Jamaica	NA	3000	Utsu		NA
1693	37.1	15	Italy: Sicily	Italy	7.4	54000	Utsu		7.94328E+15
1964	40.9	15.4		Italy	6.8	4820	Utsu		1E+15
1695	39.6	116.2	China: Shanxi	China	8	52600	NOAA	20000	6.30957E+16
1703	42.467	13.2		Italy	6.7	9761	NOAA/Utsu		7.07946E+14
1703	35	140	Japan:Edo	Japan	8.1	200000	NOAA	5233	8.91251E+16

Supplementary Information

Yr	Lat	Long	location	Country	M	death	Source	Other death reports	Energy (J)
1706	42.1	14.1		Italy	6.7	2400	Utsu		7.07946E+14
1707	33.2	134.8		JAPAN	8.4	5000	NOAA		2.51189E+17
1709	37.4	105.3		CHINA	7.5	2032	NOAA		1.12202E+16
1711	34.3	134		JAPAN	6.7	1000	NOAA		7.07946E+14
1713	25.4	103.2		CHINA	6.8	2100	NOAA		1E+15
1716	36.9	2.9		Algeria	NA	20000	Utsu		NA
1718	35	105.2	China: Gansu	China	7.5	40000	Utsu		1.12202E+16
1719	40.8	29.5		Turkey	7	1000	Utsu		1.99526E+15
1721	37.9	46.7		Iran	7.4	40000	Utsu		7.94328E+15
1725	-9.2	-79.3		Peru	7.5	1500	Utsu		1.12202E+16
1727	38	46.2	Iran: Tabriz	Iran	7.2	77000	Utsu		3.98107E+15
1731	36.7	104.9	China:Peking			100000			63095.73445
1732	40.9	14.8		Italy	NA	2000	Utsu		NA
1732	41.1	15.1		Italy	6.6	1942	Utsu		5.01187E+14
1739	38.8	106.5	China:Ningxia	China	8	50000	Utsu		6.30957E+16
1741	41.6	139.4		Japan	NA	2000	Utsu		NA
1746	-12	-77.2		Peru	8.4	18000	Utsu		2.51189E+17
1749	39.5	-0.4		Spain	NA	5000	Utsu		NA
1750	36.3	22.8		Greece	7	2000	Utsu		1.99526E+15
1751	37.1	138.2		Japan	7.2	1541	Utsu		3.98107E+15
1752	35.5	35.5		Syria	7	20000	Utsu		1.99526E+15
1754	30	32		Egypt	NA	40000	Utsu		NA
1755	36	-11	Portugal: Lisbon	Portugal	NA	62000	Utsu		NA
1755	34.1	-5.3		Morocco	NA	3000	Utsu		NA
1757	-0.9	-78.6		ECUADOR	7	1000	NOAA/Utsu		1.99526E+15
1759	33.1	35.6		Syria	6.6	2000	Utsu		5.01187E+14
1759	33.7	35.9		Lebanon	7.4	3000	Utsu		7.94328E+15
1765	34.8	105		China	6.5	2068	Utsu		3.54813E+14
1766	40.7	140.6		Japan	7.3	1335	Utsu		5.62341E+15
1771	24	124.3		Japan	7.4	12000	Utsu		7.94328E+15
1778	34	51.4		Iran	6.2	8000	Utsu		1.25893E+14
1779	36	111.5	Iran:Tabriz		NA	100000			NA
1780	34	58		Iran	6.5	3000	Utsu		3.54813E+14
1780	38.1	46.3	Iran:Tabriz	Iran	7.4	50000	Utsu		7.94328E+15
1783	38.4	16	Italy: Calabria	Italy	6.9	35000	Utsu		1.41254E+15
1784	39.7	39.5		Turkey	7.6	5000	Utsu		1.58489E+16
1789	39	40	Turkey:Palu	Turkey	7	51000	Utsu		1.99526E+15
1792	32.8	130.3		Japan	6.4	15000	Utsu		2.51189E+14
1797	-1.7	-78.6		Ecuador	8.3	40000	Utsu		1.77828E+17
1799	23.8	102.4		China	6.5	2030	Utsu		3.54813E+14
1805	41.5	14.5		Italy	6.6	5573	Utsu		5.01187E+14
1810	35.7	25		Greece	7.8	2000	Utsu		3.16228E+16
1812	10.6	-66.9		Venezuela	6.3	20000	Utsu		1.77828E+14
1815	34.8	111.2		China	6.8	13000	Utsu		1E+15
1815	-8	115		INDONESIA	7	10253	NOAA		1.99526E+15
1816	31.4	100.7		CHINA	6.5	2854	NOAA		3.54813E+14

Supplementary Information

Yr	Lat	Long	location	Country	M	death	Source	Other death reports	Energy (J)
1819	23	70		India	8.3	1440	Utsu		1.77828E+17
1822	36.7	36.9		Syria	7.4	20000	Utsu		7.94328E+15
1828	40.7	5.7		Azerbaijan	5.7	8000	Utsu		2.23872E+13
1828	37.6	138.9		Japan	6.9	1681	Utsu		1.41254E+15
1830	36.4	114.2		CHINA	7.5	7477	NOAA		1.12202E+16
1833	25.2	103		CHINA	8	6700	NOAA		6.30957E+16
1837	33	35.5		Israel	7	5700	Utsu		1.99526E+15
1840	39.5	43.9		Turkey	7.4	1000	Utsu		7.94328E+15
1842	19.75	-72.2		HAITI	8.1	5000	NOAA		8.91251E+16
1843	16.5	-61		Guadaloupe	7.8	5000	Utsu		3.16228E+16
1843	38.6	44.8		Iran	5.9	1000	Utsu		4.46684E+13
1844	33.6	51.4		Iran	6.4	1500	Utsu		2.51189E+14
1847	36.7	138.2		Japan	7.4	8174	Utsu		7.94328E+15
1848	24.1	120.5		China	6.8	2000	Utsu		1E+15
1850	27.8	102.3		China	7.5	20650	Utsu		1.12202E+16
1851	36.8	58.5		Iran	6.9	2000	Utsu		1.41254E+15
1851	41	15.7		Italy	6.3	1000	Utsu		1.77828E+14
1851	40.7	19.7		Albania	6.6	2000	Utsu		5.01187E+14
1852	37.1	58.4		Iran	5.8	2000	Utsu		3.16228E+13
1853	10.5	-64.2		Venezuela	6.7	1000	NOAA		7.07946E+14
1853	29.6	52.5		Iran	6.2	9000	Utsu		1.25893E+14
1854	13.8	-98.2		El Salvador	6.6	1000	Utsu		5.01187E+14
1854	34.8	136		Japan	7.3	1600	Utsu		5.62341E+15
1854	34	137.8		Japan	8.4	2000	Utsu		2.51189E+17
1855	40.2	29.1		Turkey	7.3	1900	Utsu		5.62341E+15
1855	40.2	29.1		Turkey	6.7	1300	Utsu		7.07946E+14
1855	35.7	139.8		JAPAN	6.9	7444	Utsu		1.41254E+15
1857	40.4	15.9		Italy	7	10939	Utsu		1.99526E+15
1859	-0.3	-78.5		Ecuador	6.3	5000	Utsu		1.77828E+14
1859	40	41.5		Turkey	6.4	2000	Utsu		2.51189E+14
1861	-32.9	-68.9		Argentina	7	18000	Utsu		1.99526E+15
1862	23.4	120		TAIWAN	6.5	2000	NOAA		3.54813E+14
1863	38.1	48.5		Iran	6.1	1000	Utsu		8.91251E+13
1868	-18.5	-71		Chile	8.5	25000	Utsu		3.54813E+17
1868	0.3	-78.2	Ecuador/Colombia	Ecuador	7.7	40000	Utsu		2.23872E+16
1871	37.4	58.4		Iran	7.2	2000	Utsu		3.98107E+15
1872	37.1	58.4		Iran	6.3	4000	Utsu		1.77828E+14
1872	36.4	36.5		Turkey	7.2	1800	Utsu		3.98107E+15
1875	38.1	30		Turkey	6.7	2000	Utsu		7.07946E+14
1875	7.9	-72.5		Venezuela	7.5	16000	NOAA/Utsu		1.12202E+16
1876	38.12	46.29	India:Calcutta		NA	215000			NA
1879	37.8	47.9		Iran	6.7	2000	Utsu		7.07946E+14
1879	33.2	104.7		China	8	22000	NOAA/Utsu		6.30957E+16
1881	38.3	26.2		Greece	6.5	7866	Utsu		3.54813E+14
1883	40.8	13.9		Italy	5.6	2333	Utsu		1.58489E+13
1883	38.3	26.2		TURKEY	7.3	15000	NOAA		5.62341E+15

Supplementary Information

Yr	Lat	Long	location	Country	M	death	Source	Other death reports	Energy (J)
1887	43.1	76.8		Kyrgyzstan	7.3	1800	Utsu		5.62341E+15
1891	35.6	136.6		Japan	8	7272	Utsu		6.30957E+16
1893	38.3	38.5		Turkey	7	1500	Utsu		1.99526E+15
1893	37.1	58.4		Iran	7.1	10000	NOAA/Utsu	18000	2.81838E+15
1895	37.1	58.4		Iran	6.8	1000	NOAA/Utsu	11000	1E+15
1896	37.7	48.3		Iran	6.7	1100	Utsu		7.07946E+14
1896	39.5	144		Japan	8.2	22000	NOAA/Utsu	27122	1.25893E+17
1897	26.9	56		Iran	6.4	1600	Utsu		2.51189E+14
1897	26	91		India	8.3	1500	Utsu		1.77828E+17
1899	37.9	28.8		Turkey	6.9	1117	Utsu		1.41254E+15
1899	-3	128.5		Indonesia	7.4	3864	Utsu		7.94328E+15
1902	14.9	-91.5		Guatemala	7.5	2000	Utsu		1.12202E+16
1902	39.9	76.2		China	7.7	2500	NOAA		2.23872E+16
1902	40.8	72.3		Uzbakistan	6.4	4725	Utsu		2.51189E+14
1903	39.1	42.7		Turkey	7	3560	Utsu		1.99526E+15
1903	40.9	42.8		Turkey	5.4	1000	Utsu		7.94328E+12
1905	33	76		India	7.8	20000	Utsu		3.16228E+16
1906	1	-81.5		Ecuador	8.6	1000	Utsu		5.01187E+17
1906	23.6	120.5		China	6.8	1258	Utsu		1E+15
1906	-33	-72		Chile	8.4	3760	Utsu		2.51189E+17
1907	18.2	-76.7		Jamaica	6.5	1000	Utsu		3.54813E+14
1907	38.5	67.9		Uzbakistan	7.4	15000	Utsu		7.94328E+15
1908	39.3	16.2	Italy: Messina	Italy	7.1	82000	Utsu		2.81838E+15
1908	39	40	Sicily; Italy			75000			63095.73445
1909	33.4	49.1		Iran	7.3	5500	Utsu		5.62341E+15
1910	9.8	-83.9		Costa Rica	5.6	1750	Utsu		1.58489E+13
1911	19.7	-103.7		Mexico	7.9	1300	Utsu		4.46684E+16
1912	40.8	27.2		Turkey	7.4	2836	Utsu		7.94328E+15
1914	37.8	30.3		Turkey	7	4000	Utsu		1.99526E+15
1915	42	13.7		Italy	7	32610	Utsu		1.99526E+15
1917	-8.3	115		Indonesia	6.5	1300	Utsu		3.54813E+14
1917	28	104		China	6.8	1800	Utsu		1E+15
1917	14.6	-90.6		Guatemala	6	2650	NOAA		6.30957E+13
1918	24	117		China	7.3	2000	NOAA		5.62341E+15
1920	44.3	10.3		Italy	5.8	1400	NOAA		3.16228E+13
1920	36.7	104.9	China: Haiyuan	China	8.5	220000	Utsu		3.54813E+17
1922	-28.5	-70		Chile	8.3	1000	Utsu		1.77828E+17
1923	31.5	101		China	7.3	4800	Utsu		5.62341E+15
1923	35.3	59.2		Iran	5.5	2219	Utsu		1.12202E+13
1923	35.4	139.2	Japan: Kanto	Japan	7.9	142807	Utsu		4.46684E+16
1925	25.7	100.4		China	7	3600	Utsu		1.99526E+15
1927	35.6	134.9		Japan	7.3	2925	Utsu		5.62341E+15
1927	37.7	102.2	China:Nan-Shan	China	8	35000	Utsu		6.30957E+16
1929	37.8	57.8		Iran	7.2	3257	Utsu		3.98107E+15
1930	38	44.7		Iran	7.3	2514	Utsu		5.62341E+15
1930	41.1	15.4		Italy	6.7	1404	Utsu		7.07946E+14

Supplementary Information

Yr	Lat	Long	location	Country	M	death	Source	Other death reports	Energy (J)
1931	12.2	-86.3		Nicaragua	6	2450			6.30957E+13
1931	39.4	46		Armenia	6.3	2890	NOAA/Utsu	390	1.77828E+14
1931	47.1	89.8		China	8	10000	Utsu		6.30957E+16
1933	39.2	144.5		Japan	8.1	3064	Utsu		8.91251E+16
1933	31.9	103.4		China	7.5	6800	Utsu		1.12202E+16
1934	26.5	86.5		India	8.3	10700	Utsu		1.77828E+17
1935	24.3	120.8		China	7.1	3276	Utsu		2.81838E+15
1935	29.5	66.8	Pakistan	Pakistan	7.5	60000	Utsu		1.12202E+16
1935	24.3	120.8		Taiwan	6.5	3276	NOAA/Utsu	44	3.54813E+14
1939	-36.3	-72.3		Chile	8.3	28000	NOAA/Utsu		1.77828E+17
1939	40.1	38.2		Turkey	7.8	32700	Utsu		3.16228E+16
1940	45.8	26.8		Romania	7.3	1000	Utsu		5.62341E+15
1941	16.6	43.3		Yemen	5.8	1200	Utsu		3.16228E+13
1942	40.7	36.8		Turkey	7.3	3000	Utsu		5.62341E+15
1943	35.5	134.2		Japan	7.2	1083	Utsu		3.98107E+15
1943	41	34		Turkey	7.6	4020	Utsu		1.58489E+16
1944	-31.5	-68.6		Argentina	7.4	8000	Utsu		7.94328E+15
1944	41.5	32.5		Turkey	7.6	4000	Utsu		1.58489E+16
1944	33.6	136.2		Japan	7.9	1251	Utsu		4.46684E+16
1945	34.7	137.1		Japan	6.8	2306	Utsu		1E+15
1945	25	63.5		Pakistan	8	4000	NOAA/Utsu	300	6.30957E+16
1946	40	41.5		Turkey	6	1300	NOAA/Utsu	840	6.30957E+13
1946	-8.5	-77.5		Peru	7.3	1400	NOAA/Utsu	800	5.62341E+15
1946	33	135.6		Japan	8	1330	Utsu		6.30957E+16
1948	36.2	136.3		Japan	7.1	3769	Utsu		2.81838E+15
1948	37.7	58.7	Turkmenistan: Ashkhabad	Turkmenistan	7.3	19800	NOAA/Utsu	110000	5.62341E+15
1949	39.2	70.8		Tajikistan	7.4	12000	NOAA/Utsu	3500	7.94328E+15
1949	-1.5	-78.3		Ecuador	6.8	6000	Utsu		1E+15
1950	28.5	96.5	Near Zhamo (Rima), Xizang (Tibet), China, "Assam-Tibet" Earthquake	China	8.6	4000	NOAA/Utsu	1530	5.01187E+17
1951	13.5	-88.4	Cosiguina, Nicaragua	Nicaragua	6.5	1100	Utsu		3.54813E+14
1953	40	27.5	Yenice-Gonen, Turkey	Turkey	7.4	1103	Utsu		7.94328E+15
1954	36.3	1.5	Chlef (Orleansville, El Asnam), Algeria	Algeria	6.8	1409	Utsu		1E+15
1957	36.14	52.7	Near Sang Chai, Mazandaran, Iran	Iran	7.1	1200	Utsu		2.81838E+15
1957	34.5	48	Sahneh, Iran	Iran	7.2	2000	Utsu		3.98107E+15
1960	30.5	-9.6	Agadir, Morocco	Morocco	5.7	13100	Utsu		2.23872E+13
1960	-39.5	-74.5	Temuco-Valdivia, Chile	Chile	8.5	5700	Utsu		3.54813E+17
1962	35.6	49.9	Bu'in Zahra, Qazvin, Iran	Iran	7.2	12225	Utsu		3.98107E+15
1963	42	21.4	Skopje, Former Yugoslav Rep. of Macedonia(Makedonija, Yugoslavia)	Skopje	6.1	1070	Utsu		8.91251E+13
1966	37.3	114.9	East of Longyao, Hebei (Hopeh), China	China	6.8	1000			1E+15
1966	37.5	115.1	Southeast of Ningjin, Hebei (Hopeh), China	China	7.2	8064	Utsu		3.98107E+15
1966	39.2	41.6	Varto, Turkey	Turkey	6.8	2517	Utsu		1E+15
1968	34	59	Dasht-e Bayaz, Iran	Iran	7.3	15000	NOAA/Utsu	10488	5.62341E+15
1969	22.3	111.8	Yangjiang, Guangdong, China	China	6.4	3000	NOAA/Utsu	33	2.51189E+14
1970	24.2	102.7	Tonghai, Yunnan Province, China	China	7.8	15621	NOAA/Utsu	10000	3.16228E+16

Supplementary Information

Yr	Lat	Long	location	Country	M	death	Source	Other death reports	Energy (J)
1970	39.2	29.5	Gediz, Turkey	Turkey	7.1	1086			2.81838E+15
1970	-9.4	-78.9	Chimbote, Peru	Peru	7.8	66794			3.16228E+16
1971	38.8	40.5	Turkey	Turkey	7	1000	NOAA/Utsu	995	1.99526E+15
1972	28.4	52.8	southern Iran	Iran	6.8	5010	NOAA/Utsu	30000	1E+15
1972	12.3	-86.1	Nicaragua, Managua	Nicaragua	6.2	6000	NOAA/Utsu	10000	1.25893E+14
1973	31.3	100.7	China: Sichuan P.[Mangua E]	China	7.6	2175	Utsu		1.58489E+16
1974	28.2	104.1	China	China	7.1	1423	NOAA/Utsu	20000	2.81838E+15
1974	35	72.8	Pakistan	Pakistan	6.2	5300	Utsu		1.25893E+14
1975	40.7	122.8	Haicheng, China	China	7.3	1328	Utsu		5.62341E+15
1975	38.5	40.7	Turkey	Turkey	6.7	2370	Utsu		7.07946E+14
1976	15.3	-89.1	Guatemala	Guatemala	7.5	23000	Utsu		1.12202E+16
1976	46.4	13.3	northeastern Italy	Italy	6.1	965	Utsu		8.91251E+13
1976	-4.6	140.1	Papua, Indonesia	Indonesia	7.1	6000	Utsu		2.81838E+15
1976	39.4	118	Tangshan, China	China	7.8	242800	Utsu		3.16228E+16
1976	6.2	124	Mindanao, Philippines	Philippines	7.9	8000	Utsu		4.46684E+16
1976	-4.5	139.9	Indonesia (Irain Jaya)	Indonesia	7.2	6000	Utsu		3.98107E+15
1976	39.1	44	Turkey-Iran border region	Iran	7.3	3900	Utsu		5.62341E+15
1977	45.8	26.8	Romania	Romania	7.3	1581	Utsu		5.62341E+15
1978	33.4	57.4	Iran	Iran	7.4	18220	Utsu		7.94328E+15
1980	36.2	1.4	El Asnam, Algeria(formerly Orleansville)	Algeria	7.3	3500	NOAA/Utsu	5000	5.62341E+15
1980	40.9	15.3	southern Italy	Italy	6.7	2483	NOAA/Utsu	4689	7.07946E+14
1981	29.9	57.7	southern Iran	Iran	6.7	3000	Utsu		7.07946E+14
1981	30	57.8	southern Iran	Iran	7.1	1500	Utsu		2.81838E+15
1981	-4.6	139.2	Indonesia(Irian Jaya)	Indonesia	6.7	1300	Utsu		7.07946E+14
1982	14.7	44.4	Yemen	Yemen	6	2800	Utsu		6.30957E+13
1983	40.3	42.2	Turkey	Turkey	6.9	1400	NOAA/Utsu	1342	1.41254E+15
1985	18.2	-102.5	Mexico, Michoacan	Mexico	8.1	9500	Utsu		8.91251E+16
1986	13.8	-89.1	El Salvador	El Salvador	5.4	1500	NOAA/Utsu	1100	7.94328E+12
1987	0.2	-77.8	Colombia-Ecuador	Colombia	6.9	5000	Utsu		1.41254E+15
1988	26.8	86.6	Nepal-India border region	Nepal	6.6	1450	NOAA/Utsu	1091	5.01187E+14
1988	41	44.2	Spitak, Armenia	Armenia	6.8	25000	Utsu		1E+15
1990	37	49.4	Western Iran	Iran	7.7	35000	NOAA/Utsu	50000	2.23872E+16
1990	15.7	121.2	Luzon, Philippine Islands	Philippine Islands	7.8	2430	Utsu		3.16228E+16
1991	30.8	78.8	Northern India	India	7	2000	Utsu		1.99526E+15
1992	-8.5	121.9	Flores Region, Indonesia	Indonesia	7.5	1740	Utsu		1.12202E+16
1993	18.1	76.5	Latur-Killari, India	India	6.2	9748	NOAA/Utsu	11000	1.25893E+14
1995	34.6	135	Kobe, Japan	Japan	7.2	6435	Utsu		3.98107E+15
1995	52.6	142.8	Sakhalin Island, Russia	Russia	7.5	1989	Utsu		1.12202E+16
1997	33.9	59.8	Northern Iran	Iran	7.3	1572	NOAA/Utsu	1728	5.62341E+15
1997	38.1	48.1	Iran: Ardebil	Iran	6.1	1100	Utsu		8.91251E+13
1998	37.1	70.1	Hindu Kush region, Afghanistan	Afghanistan	6.1	2323	Utsu		8.91251E+13
1998	37.1	70.1	Afghanistan-Tajikistan Border Region	Afghanistan	6.9	4000	Utsu		1.41254E+15
1998	-3	141.9	Papua New Guinea	Papua New Guinea	7.1	2700	Utsu		2.81838E+15
1998					NA	80000			NA
1999	4.5	-75.7	Colombia	Colombia	5.7	1900	NOAA/Utsu	1185	2.23872E+13
1999	40.7	29.9	Turkey	Turkey	7.8	17118	Utsu		3.16228E+16

Supplementary Information

Yr	Lat	Long	location	Country	M	death	Source	Other death reports	Energy (J)
1999	23.8	121	Taiwan(Eastern Asia)	Taiwan	7.7	2413	Utsu		2.23872E+16
2001	23.4	70.2	Gujarat, India	India	7.8	20005	NOAA		3.16228E+16
2002	36	69.3	Hindu Kush Region, Afghanistan	Afghanistan	6.2	1000	NOAA		1.25893E+14
2003	36.9	3.6	Northern Algeria	Algeria	6.2	2266	NOAA		1.25893E+14
2003	28.99	58.31	Southeastern Iran	Iran	6.8	31000	NOAA		1E+15
2004	3.3	95.87	Sumatra, Indonesia	Indonesia	9.1	227898	USGS		2.81838E+18
2004	35.142	-3.997		MOROCCO	6.4	628	NOAA		2.51189E+14
2004	3.295	95.982		INDONESIA	8.8	1001	NOAA		1E+18
2005	2.08	97.1	Northern Sumatra, Indonesia	Indonesia	8.4	1303	NOAA USGS	1313	2.51189E+17
2005	34.53	73.58	Pakistan	Pakistan	7.7	86000	NOAA		2.23872E+16
2006	-7.961	110.446	Flores Region, Indonesia	Indonesia	6.2	5749	NOAA		1.25893E+14
2008	31	103.3	Eastern Sichuan, China	China	8.1	87652	NOAA		8.91251E+16
2009	-0.72	99.867	Southern Sumatra, Indonesia	Indonesia	7.5	1117	NOAA		1.12202E+16
2010	33.165	96.548	Southern China	China	6.9	2220	NOAA		1.41254E+15
2010	18.4	-72.5	Haiti region	Haiti	7.3	65000	NOAA/Doocy et al. (2013)		5.62341E+15
2011	38.297	142.373	Japan	Japan	8.3	1400	NOAA		1.77828E+17
	BLUE	Reported in EM-DAT or John Hopkins' report of EM-DAT							
	RED	Reported in NOAA							
	Orange	Reported in USGS earthquakes with more than 1000 fatalities list							
		Excluded because of no information							
		Excluded because of redundancy							
		Excluded because D<1000							
		Included because 965 deaths is considered as 1000							
		Caused Tsunami based on NGDC-NOAA							

Supplementary Information

Table 2: Tsunami disasters (1600-2012)

Year	Lat	Long	Country	Region	Death	Cause	Source	Notes	Other Death reports	Tsunami characteristics (Wave height (m), and Distance from Source (km))	Energy(J)-Tang et al (2012) $E_t=0.029e^{4.37Mw}$
1605	33	134.9	JAPAN	KEICHO (Shishikui,Boso, Enshunada Sea)	10600	7.9	NOAA			5000 D	2.85461E+13
1611	39	144.5	JAPAN	Urukawa (Hokkaido) SANRIKU	4783	8.1	NOAA			5000 D	6.841E+13
1640	42.07	140.68	JAPAN	UCHIURA BAY	700	6.5	NOAA	Kamagatake Volcano,			62882928134
1674	-3.75	127.75	INDONESIA	AMBON ISLAND, Malaku Islands	4300	6.8	NOAA			2244 D	2.33288E+11
1687	-13.5	-76.5	PERU	CALLAO	5000	8.5	NOAA				3.92886E+14
1692	17.8	-76.7	JAMAICA	PORT ROYAL	2200	7.7	NOAA	Landslide?		2000 D	1.19117E+13
1696			JAPAN		2450		NOAA				
1700	32.7	129.7	JAPAN	HIZEN, NAGASAKI PREFECTURE	1001	7	NOAA				5.5907E+11
1703	34.7	139.8	JAPAN	GENROKU: Kamakura	5833	8.2	NOAA				1.05903E+14
1707	34.1	137.8	JAPAN	HOEI: Tosa Bay,Owase, Osaka	4910	8.4	NOAA			5000&2000 D	2.53793E+14
1721	23	120.2	TAIWAN		2000		NOAA				
1737	20	77	INDIA	HOOGLY RIVER/infamous Bilham event	300000		NOAA				
1741	41.5	139.37	JAPAN	HOKKAIDO (Oshima Oshima Volcano)	2033	6.9	NOAA	VOLCANO		1475 D	3.61143E+11
1746	-11.996	-77.198	PERU	CALLAO	4800	8	NOAA				4.41909E+13
1751	37.2	138.1	JAPAN	NAOETSUKO, NW HONSHU	2100	6.6	NOAA				97346299041
1755	36	-11	PORTUGAL	LISBON EQ	3000	8.8	NOAA			50000 D	1.45756E+15
1765	23.12	113.25	CHINA	SOUTH CHINA SEA	10000		NOAA				
1766	40.9	140.7	JAPAN	AOMORI, SANRIKU	1700	6.9	NOAA				3.61143E+11
1771	24	124.3	JAPAN/Okinawa	MIYARA, ISHIGAKI ISL., Yaeyama tsunami	13486	7.4	NOAA	Boulders moved			3.2108E+12
1782	24.5	120.5	TAIWAN	TAIWAN STRAIT	40000	7	NOAA				5.5907E+11
1783	38.217	15.633	ITALY	SCILLA, CALABRIA/Rockfall into OCEAN	1500	5.9	NOAA	ROCKFALL			4568910227
1792	32.75	130.3	JAPAN	UTO, Ashikita [UNZEN] LANDSLIDE	5843	6.4	NOAA	LANDSLIDE		14524 D	40620575098
1793	38.5	144	JAPAN	Fukushima to Hachinhoe [SANRIKU]	1000	6.9	NOAA			720 D	3.61143E+11
1812	8	-66	VENEZUELA		NA						
1815	-8	115	INDONESIA	BALI ISLAND/LANDSLIDE	10253	7	NOAA	SUBMARINE LANDSLIDE		1200 D	5.5907E+11
1815	-5	120	INDONESIA	TAMBORA	5500	VOLCANO (4600)					
1819	20	77	INDIA	SINDREE	1543	Rann of Kutch Q/Bilham					
1820	-7	119	INDONESIA	BULUKUMBA, SULAWESI	500	7.5	NOAA				4.9705E+12

Supplementary Information

Year	Lat	Long	Country	Region	Death	Cause	Source	Notes	Other Death reports	Tsunami characteristics (Wave height (m), and Distance from Source (km))	Energy(J)-Tang et al (2012) $E_t=0.029e^{4.37Mw}$
1842	19.75	-72.2	HAITI	CAP-HAITIAN	5000	8.1	NOAA			300 D	6.841E+13
1853	8	-66	VENEZUELA		NA	Cumana destroyed					
1854	33.1	135	JAPAN	ANSEI [Nankaido]	5000	8.4	NOAA			3000 D	2.53793E+14
1856	-5	120	INDONESIA	Awu	NA	VOLCANO					
1861	-1	97.5	INDONESIA	SIMUK ISLAND, SUMATRA	1000	8.5	NOAA			1105 D	3.92886E+14
1861	0.009	98	INDONESIA	PALAU TELO, SUMATRA	950	7	NOAA				5.5907E+11
1868	-10	-76	PERU	TAMBO, ARICA destroyed	25674						
1874	22	89	BANGLADESH	SUNDERBANS	2000		NOAA				
1877	-21.5	-70.5	CHILE	FIJI ISLANDS (Chile?)	2477	8.3	NOAA				1.63943E+14
1883	-6.102	105.423	INDONESIA	SUNDA STRAIT/KRAKATOA	36000		NOAA	VOLCANO			
1888	-6	147	PAPUA NEW GUINEA	RITTER ISLAND	1100	VOLCANO					
1892	-5	120	INDONESIA	Awu	NA	VOLCANO					
1896	39.5	144	JAPAN	MEIJI SANRUKI	27122	8.3	NOAA				1.63943E+14
1899	-3	128.5	INDONESIA	PAULOHI, Tehoru, Banda Sea	3864	7.8	NOAA			2460 D	1.84399E+13
1906	1	-81.5	COLOMBIA/ECUADOR	Tumaco overwhelmed	1000	8.8	NOAA				1.45756E+15
1908	38.183	15.683	ITALY	MESSINA	4578	7.1	NOAA				8.65472E+11
1915	-5	120	INDONESIA	BALI ISLAND	15000						
1923	36	138	JAPAN	TAISHO KANTO: Sagami bay	2144	7.9	EM-DAT/JHSPH				2.85461E+13
1927			Japan	South-West Kyoto	1100		EM-DAT/JHSPH			2925 D/EM-DAT	
1930	17.3	96.5	MYANMAR (BURMA)	PEGU, SITTANG RIVER	500	7.2	NOAA				1.3398E+12
1933	39.1	144.7	JAPAN	N. RIKUCHU, Miyako	3200	8.4	NOAA			3022 D/6064 D/EM-DAT	2.53793E+14
1941	20	77	INDIA	Andaman Sea and E Coast India	5000						
1944	34	137.1	JAPAN	TONANKAI	1251	8.1	NOAA			1223 D	6.841E+13
1945	24.5	63	Pakistan	MAKRAN COAST	4200	8	NOAA			4000 D	4.41909E+13
1946	19.3	-68.9	DOMINICAN REPUBLIC	MATANZAS	1790	7.8	NOAA				1.84399E+13
1946	33	135.6	JAPAN	Nankaido	1330	8.1	NOAA			1362 D	6.841E+13
1946			Unimak			8.5	Tang et al	3.58E+17 Es	7.21E+14 Et		3.92886E+14
1951	13	-87.5	NICARAGUA	POTOSI, GULF OF FONSECA	1000	6	NOAA	LAHAR VOLCANO			7072929242
1952	52.75	159.5	USSR	KURIL	4000	9	NOAA			2300 D/EM-Dat/JHSPH	3.49301E+15
1960	-39.5	-74.5	CHILE	CHILE AS A WHOLE	1100	9.5	NOAA			1222 D	3.10551E+16
1964			Alaska			9.2	Tang et al	4.02E+18 Es	4.24E+15 Et		8.37092E+15
1976	6.262	124.023	PHILIPPINES	MAGUINDANAO PROVINCE	8000	8.1	NOAA			4376 D	6.841E+13
1979	-5	120	INDONESIA	LOMBLEN ISLAND/Submarine landslide	1239	SUBMARINE LANDSLIDE				539 D/EM-DAT/JHSPH	
1979	1.598	-79.358	COLOMBIA	Tumaco	600	7.7	NOAA				1.19117E+13

Supplementary Information

Year	Lat	Long	Country	Region	Death	Cause	Source	Notes	Other Death reports	Tsunami characteristics (Wave height (m), and Distance from Source (km))	Energy(J)-Tang et al (2012) $E_t=0.029e^{4.37Mw}$
1992	-8.48	121.896	INDONESIA	Flores	1713	7.8	NOAA			1169 D/1825 D/EM-DAT/JHSPH	1.84399E+13
1994			Kuril			8.3	Tang et al	1.79E+17 Es	7.53E+13Et		1.63943E+14
1996			Andreanof			7.9	Tang et al	4.51E+16 Es	4.69E+13 Et		2.85461E+13
1998	-2.961	141.926	PAPUA NEW GUINEA	WARAPU/Arop	2182	7	NOAA	SUBMARINE LANDSLIDE		2205 D/2182 D/EM-DAT	5.5907E+11
2003			Rat Island			7.7	Tang et al	2.26E+16 Es	1.21E+13 Et		1.19117E+13
2004			INDIAN OCEAN	Indonesia, India, Sri Lanka, Thailand	230000			2.01 E+18 Es	1.60E+16 Et		5.40738E+15
2004			India		16389	9	EM-DAT/JHSPH				3.49301E+15
2004			Indonesia		165708	9	EM-DAT/JHSPH				3.49301E+15
2004			Sri Lanka		35399	9	EM-DAT/JHSPH				3.49301E+15
2004			Thailand		8457	9	EM-DAT/JHSPH				3.49301E+15
2006	-9.254	107.411	INDONESIA	SOUTH OF JAVA	600	7.7	NOAA			802 D/EM-DAT/JHSPH	1.19117E+13
2006			Tonga			8	Tang et al	6.37E+16 Es	7.29E+13 Et		4.41909E+13
2006			Kuril			8.3	Tang et al	1.79E+17 Es	6.18E+13 Et		1.63943E+14
2007			Nicobar			6.1	Tang et al	8.99E+13 Es	1.5E+10 Et		10949291096
2007			Kuril			8.1	Tang et al	8.99E+16 Es	2.17E+13 Et		6.841E+13
2009			New Zealand			7.8	Tang et al	3.19E+16 Es	1.42E+13 Et		1.84399E+13
2009			Samoa			8.1	Tang et al	8.99E+16 Es	1.02E+14 Et		6.841E+13
2010			Chile			8.8	Tang et al	1.01E+18 Es	1.63E+15 Et		1.45756E+15
2010			Bonin			7.4	Tang et al	8.02E+15 Es	1.49E+12 Et		3.2108E+12
2011	38.297	142.373	JAPAN	SENDAI, SANRUKI	27000	9	NOAA	2.84E+18 Es	3.00E+15 Et	17150 D/19846 D/EM-DAT	3.49301E+15
	Excluded because of redundancy										
	Excluded because Death<1000										
	Excluded because no infor on death										
	Included because 950 deaths is considered as 1000										
	Included because of NOAA reported deaths (not included before because of NA)										
RED	Reported in NOAA										
BLUE	Reported in EM-DAT or John Hopkins' report of EM-DAT										
Purple	Reported by Tang et al (2012) for energy estimates										
Black	Gathered by Evans and Khaleghy										

Supplementary Information

Table 3: Volcanic disasters (1600-2012)

Yr	Volcano	Country	Region	Lat	Long	Killed	Note	VEI	Source	Elevation	Other death	Lava volume	Tephta Volume	VEI->Volume	Ek=(density (2669.9)* (VEI->Vol)*g*h
1600	Huaynaputina	Peru	South Am.	-16.608	-70.85	1400		6	NOAA	4850				1.00E+11	4.19E+18
1631	Vesuvius	Italy	Europe	40.821	14.426	1400	Tsu	4	NOAA	1281				1.00E+09	4.27E+16
1638	Raung	Indonesia		-8.125	114.042	1400		3	NOAA	3332				1.00E+08	4.29E+15
1640	Tungurahua	Ecuador	South Am.	-2	-77.5	5000									
1660	Long Island	Australia	Melanesia	-5.358	147.1199	2000	Tsu	4	NOAA	1280				1.00E+09	4.34E+16
1672	Merapi	Indonesia		-7.542	110.442	3000		4	NOAA	2947				1.00E+09	4.37E+16
1684	Grimsvotn	Iceland		65	-18	9350									
1711	Awu	Indonesia		3.67	125.5	3000		3	NOAA	1320				1.00E+08	4.48E+15
1741	Oshima-Oshima	Japan		36	138	1475									
1760	Makian	Indonesia		0.32	127.4	2000		4	NOAA	1357				1.00E+09	4.61E+16
1772	Papandayan	Indonesia		-7.32	107.73	2957		3	NOAA	2665				1.00E+08	4.64E+15
1775	Gamalama	Indonesia		0.8	127.325	1300		3	NOAA	1715				1.00E+08	4.64E+15
1783	Asama	Japan		36.4	138.53	1491	Siebert	4	NOAA	2560				1.00E+09	4.67E+16
1783	Laki	Iceland		65	-18	10521	Thorarinsson								0.00E+00
1784	Grimsvton	Iceland	NE	64.42	-17.33	9350		4	NOAA	1725				1.00E+09	4.67E+16
1790	Kilauea	U.S.A	Hawai	19.425	-155.292	5405	Douglas	4	NOAA	1222				1.00E+09	4.68E+16
1792	Unzen	Japan		36	138	14524	Siebert								
1812	Awu	Indonesia	S-E Asia	3.67	125.5	953	Siebert	3	NOAA	1320				1.00E+08	4.74E+15
1814	Mayon	Philippines	S-E Asia	13.257	123.685	1200		4	NOAA	2462				1.00E+09	4.75E+16
1815	Awu	Indonesia	S-E Asia	-8.25	118	60000	Tsu	7	NOAA	2850	10000			1.00E+12	4.75E+19
1822	Galunggung	Indonesia	S-E Asia	-7.25	108.05	4011		5	NOAA	2168				1.00E+10	4.77E+17
1840	Ararat		Europe	39.7	44.3	1900									
1845	Ruiz	Columbia		4.89	-75.32	1000		2	NOAA	5321				1.00E+07	4.83E+14
1856	Awu	Indonesia	S-E Asia	3.67	125.5	2806	Tsu	3	NOAa	1320				1.00E+08	4.86E+15
1875	Mayon	Philippines		13	122	1500									
1883	Kralatau	Indonesia	S-E Asia	-6.102	105.423	36417	Tsu	6	NOAA	813	2000			1.00E+11	4.93E+18
1888	Ritter Island		Melanesia	-5.5	148.11	3000									
1892	Awu	Indonesia	S-E Asia	3.67	125.5	1532	Tsu	3	NOAA	1320				1.00E+08	4.95E+15
1902	Santa Maria	Guatmala	Central Am.	14.756	-91.552	1500		4	NOAA	3772	6000/EM-DAT		2.00E+10	1.00E+09	4.98E+16
1902	Soufriere	St.Vincent	Caribbean	13.33	-61.18	1680	Tsu	4	NOAA	1220	1565/EM-DAT		3.80E+08	1.00E+09	4.98E+16
1902	Pelee	Martinique	Caribbean	14.82	-61.17	28000	Tsu	4	NOAA	1397	30000/EM-DAT	1.40E+08	2.00E+08	1.00E+09	4.98E+16
1902	Pelee	Martinique	West Indies.	14.82	-61.17	1000	Tsu	4	NOAA	1397	1500		2.00E+10	1.00E+09	4.98E+16
1909	Semeru	Indonasia		-8.108	112.92	5500		2	Em-Dat		221/NOAA			1.00E+07	4.99E+14
1911	Taal	Philippines	S-E Asia	14.002	120.993	1335	Tsu	4	NOAA	400			80000000	1.00E+09	5.00E+16
1919	Kelut	Indonasia	S-E Asia	-7.93	112.308	5110		4	NOAA	1731	5000		190000000	1.00E+09	5.02E+16
1929	Santa Maria	Guatmala	Central Am.	14.756	-91.552	5000		3	EM-Dat		200/NOAA	1100000000	100000000	1.00E+08	5.05E+15

Supplementary Information

Yr	Volcano	Country	Region	Lat	Long	Killed	Note	VEI	Source	Elevation	Other death	Lava volume	Tephta Volume	VEI->Volume	Ek=(density (2669.9)* (VEI->Vol)*g*h
1930	Merapi	**Indonasia**	S-E Asia	**-7.542**	**110.442**	**1369**		3	NOAA	2974		1500000	1700000	1.00E+08	5.05E+15
1931	Merapi	**Indonasia**		-7.542	110.442	**1300**		3	Em-Dat			1500000	1700000	1.00E+08	5.05E+15
1949	Paricutin	**Mexico**	AMRO	19.85	-102.25	**1000**		4	EM-Dat			700000000	130000000	1.00E+09	5.10E+16
1951	Lamington	**Papua New Guinea**	oceania	**-8.95**	**148.15**	**2942**		4	NOAA	1680	3000/EM-Dat	1000000000		1.00E+09	5.10E+16
1951	Kelut	**Indonasia**	SEARO	-7.93	112.308	**1300**		3	EM-Dat		7/NOAA			1.00E+08	5.10E+15
1963	Agung	**Indonasia**	S-E Asia	**-8.342**	**115.508**	**1148**	Tsu	5	NOAA	3142	**1584/EM-Dat**	100000000	1000000000	1.00E+10	5.14E+17
1966	Kelut	**Indonasia**		-7.93	112.308	**1000**		4	Em-Dat		**215/NOAA**		89000000	1.00E+09	5.14E+16
1982	El Chichon	**Mexico**	Central Am.	**17.36**	**-93.228**	**1879**		5	NOAA	1150	100/Em-Dat		2500000000	1.00E+10	5.19E+17
1985	Nevado del Ruiz	**Colombia**	South Am.	**4.89**	**-75.32**	**23080**		3	NOAA	5321	21800/Em-Dat		48000000	1.00E+08	5.19E+15
1986	Lake Nyos	**Cameroon**	Central Af.	**6**	**12**	**1746**								1.00E+05	5.20E+12
1986	Oku Volc Field		Africa/MidEast	**6.5**	**10.5**	**1746**		3	EM-DAT	3011	1700/NOAA			1.00E+08	5.20E+15
1991	Pinatubo	**Philippines**	S-E Asia	**13**	**122**	**932**		6			640/EM-DAT/JHSPH		1.10E+10	1.00E+11	5.21E+18
1998	San Cristobal		Central Am.	**16.75**	**-92.63**	**1620**									
2006	Mayon	**Philippines**		**13.257**	**123.685**	**1266**		1	NOAA	2462				1.00E+06	5.25E+13

	Excluded because of redundancy
	Excluded because of no confirmed information in Witham (2005)
IN RED	Reported in NOAA
IN BLUE	Reported in EM-DAT or John Hopkins' report of EM-DAT
In Green	**Witham (2005)**
In Purple	**Siebert et al (2010)**

Supplementary Information

Table 4: Landslide disasters (1600-2012)

Year	Lat	Long	Country	Area/ Locality	Event Process	Deaths	WP	Volume	Height	E(J)=rho(2500kg/m2)*Vol*h (130m assumed if no height info)	Source
1618	46.33	9.42	Italy	Piuro (Plurs)	Rock avalanche (est volume ~ 3-4 M m3)	2430	5.97E+08				Evans (unpublished data)
1638	-8.125	114.04	Indonesia	Raung	Lahar and flood	1000	6.17E+08				Evans (unpublished data)
1718	35.17	105.16	China	Tongwei	Loess landslide	9000	7.37E+08				Evans (unpublished data)
1725	-9.16	-77.58	Peru	Cordillera Blanca	Outburst flood/debris flow from moraine-dammed lake.	1750	7.59E+08				Evans (unpublished data)
1741	41.28	139.36	Japan	Oshima-Oshima	Landslide tsunami generated by partial flank collapse of volcano	1475	8.11E+08				Evans (unpublished data)
1760	0.533	127.66	Indonesia	Makian	Lahar	2000	8.72E+08				Evans (unpublished data)
1772	-7.32	107.73	Indonesia	Papandayan	Debris avalanche resulting from flank collapse	2957	9.1E+08				Evans (unpublished data)
1783	36.4	138.516	Japan	Asama	Lahar formed by transformation of huge pyroclastic flow	1433	9.74E+08				Evans (unpublished data)
1783	38.4	16	Italy	Scilla		1500					Evans (unpublished data)
1786	35	105	China	Sichuan	Outburt flood due to landslide dam failure	100000	9.55E+08				Evans (unpublished data)
1792	36.4	138.516	Japan	Mayuyama and Ariake Sea	Debris avalanche resulting from flank collapse and tsunami	15900	9.74E+08				Evans (unpublished data)
1841	30	70	Pakistan	Indus	Outburst flood due to landslide dam failure	3000	1.24E+09				Evans (unpublished data)
1845	4.89	-75.32	Colombia	Nevado del Ruiz	Lahar	1000	1.26E+09				Evans (unpublished data)
1856	3.67	125.5	Indonesia	Awu	Lahars	2806	1.32E+09				Evans (unpublished data)
1856	32.5	103.06	China	Sichuan	Rockslide	1000	1.32E+09				Evans (unpublished data)
1870	30	96.11	China	Sichuan	Rockslide	2000	1.58E+09				Evans (unpublished data)
1875	13.25	123.68	Philippines	Mayon	Lahars	1500	1.43E+09				Evans (unpublished data)
1888	-5.5	148.117	Papua New Guinea	Ritter Island	Landslide tsunami generated by collapse of volcano into sea.	3000	1.52E+09				Evans (unpublished data)
	39.9	116.4	China	Beijing		1000	1.52E+09				Evans (unpublished data)
	35	105	China	Sichuan		1000	1.52E+09				Evans (unpublished data)
1892	3.67	125.5	Indonesia	Awu	Lahars	1532	1.56E+09				Evans (unpublished data)
	41	64	Uzbekistan	Karatagh	Rock avalanche	3400	1.71E+09				Evans (unpublished data)
1917	35	105	China	Yunnan	Rock avalanche	1800	1.85E+09				Evans (unpublished data)
1919	-7.93	112.308	Indonesia	Kelud, Java	Lahars generated by crater lake ejection	5110	1.88E+09				Evans (unpublished data)
1933	35	105	China	Sichuan	Landslide and subsequent outburst flood due to landslide dam failure	3076	2.08E+09	150000000		4.875E+13	Evans (unpublished data)
1941	-9.53	-77.53	Peru	Huaraz	Outburst flood/debris flow from moraine-dammed lake.	5879	2.2E+09				Evans (unpublished data)
1949	39	71	Tajikistan	Khait	Rock avalanche	4000	2.43E+09	60000000		1.95E+13	Evans (unpublished data)

Supplementary Information

Year	Lat	Long	Country	Area/ Locality	Event Process	Deaths	WP	Volume	Height	E(J)=rho(2500kg/m2)*Vol*h (130m assumed if no height info)	Source
	-9.12	-77.6	Peru	Huascarán	Rock avalanche	4000	3.08E+09				Evans (unpublished data)
1963	46.15	12.7	Italy	Vajont	Landslide-generated wave	1896	3.08E+09	292000000		9.49E+13	Evans (unpublished data)
1970	-9.12	-77.6	Peru	Huascarán	Rock avalanche	6000	3.55E+09				Evans (unpublished data)
1971	33	65	Afghanistan	Khinjan Pass	Outburst flood due to landslide dam failure	1000	3.62E+09				Evans (unpublished data)
1974	15.6	-88	Honduras	Choloma	Outburst debris flood/debris flow due to landslide dam failure	2300	3.85E+09				Evans (unpublished data)
1985	4.89	75.32	Colombia	Nevado del Ruiz	Lahar	23000	4.69E+09	180000000	40	1.8E+13	Voight (1990)
1991	11	124.6	Philippines	Ormoc	Debris flow	5012	5.2E+09				Evans (unpublished data)
1998	13	-85	Nicaragua	Casita	Rock avalanche and subsequent debris flow	1650	5.84E+09	1600000	6	2.40E+10	Kerle(2002)
2005	30	70	Pakistan	Hattian Bala	Rock avalanche	1000	6.47E+09	68000000	130	2.21E+13	Dunning et al (2007)
2006	10.33	125.083	Philippines	Southern Leyte	Rock avalanche	1125	6.55E+09	15000000	450	1.6875E+13	Evans et al (2007)
2008	38	112	China	Shanxi		1600	6.71E+09	750000000	690	1.29375E+15	Tianbin (2008)
2010	36.06	103.83	China	Zhouqu		1744		2200000		7.15E+11	Tang et al (2011)
	Excluded because of redundancy										

Chapter 5 Has global societal earthquake resistance improved since 1973?

5.1 Introduction

Natural disaster is, as defined by Center for Research on the Epidemiology of Disasters (CRED) (http://www.emdat.be/glossary/9), *"a situation or event which overwhelms local capacity, necessitating a request to a national or international level for external assistance; an unforeseen and often sudden event that causes great damage, destruction and human suffering"*[25]. By this definition, the 2010 Haiti earthquake is a natural disaster, which highlighted several issues including the impact of a comparatively modest seismic event, the response of a vulnerable urban centre to seismic shaking (Ambraseys and Bilham, 2011) and the aetiology of earthquake-generated urban disasters. In the aftermath of the Haiti event, we introduce the global societal earthquake resistance and review casualties of deadly earthquakes in the period 1973 to 2013 in which a total of around 800,000 people died. In this chapter we attempt to establish whether global societal earthquake resistance has improved as a result of such factors as a greater understanding of global and regional seismology, advances in building design and construction, development of sophisticated warning system technologies, implementation of building codes and increased societal awareness of earthquake hazards and their effects.

To investigate possible changes in global societal earthquake resistance we examined a record of earthquake disasters, which we define as a seismic event that results in the loss of 1,000 or more lives. For the purposes of the present argument we do not distinguish direct (e.g., in building collapse) and indirect (e.g., in tsunami) deaths in earthquakes. Underlying the analysis is the assumption that the characteristics of these disasters are a close indicator of global societal earthquake resistance. We compiled a database of 54 events that fulfill this criterion in the period 1973-2013 in Table 5.S.1 and their global distribution is shown in Fig. 5.1. Data initially collected from United States Geological Survey (USGS) table of earthquakes with more than 1,000 fatalities (http://earthquake.usgs.gov/earthquakes/world/world_deaths.php). These data have been complemented by data from Utsu's (2002) table of deadly earthquakes since 1500. The list of these disasters, 54 events in the period 1973 to 2013, has also been cross-checked

[25] This definition is borrowed from the website of the CRED.

with the data of the National Geophysical Data Center (NGDC) (http://www.ngdc.noaa.gov/nndc/struts/form?t=101650&s=1&d=1). 779,676 deaths occurred in the 54 events of which 22% occurred in West and South West Asia, 20 % in East Asia, 17% in Central and South Asia, 17% in South East Asia, 13% in North Africa and Europe, and 11% in Central and South America. Countries affected by earthquake disasters during 1973-2013 in each of these categories (based on continental locations), number of events in each country, the percentages of the total number of events in each category, and corresponding number of deaths are given in Table 5.1. According to Table 5.1, East Asia has the highest percentage of deaths among all categories (46%). Central and South Asia is the second highest (17%), and West and South West Asia is the third highest (15%) percentage of deaths. This suggests that the number of earthquake disasters is not linearly related to the number of fatalities due to them. Thus, we understand that underlying factors, such as resistance of the region towards earthquake disasters, or population density, play roles in this process.

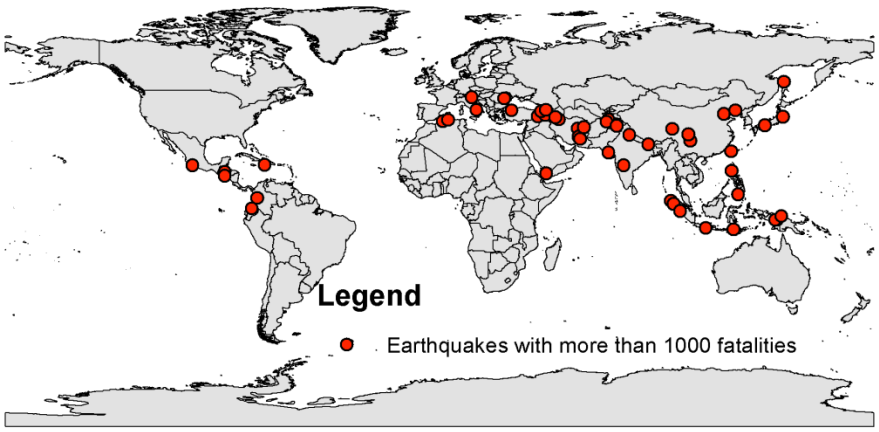

Figure 5.1: Global distribution of 54 earthquake disasters (1973-2013). Red dots are the location of earthquake disasters in which fatalities equaled or exceeded 1,000 deaths in the period 1973-2013 (listing of 54 events is given in Supplementary Table 5.S.1).

Table 5.1: List of countries affected by earthquake disasters (1973-2013), number of events in each countries, percentage of the total number of events in each category of countries (based on continental locations), number of deaths due to earthquake disasters in each country and percentage of the total number of deaths in each category.

Country	**N of events**	**%N**	**Deaths**	**%D**
China	6	0.1111	337598	0.4330
Taiwan	1	0.0185	2413	0.0031
Japan	2	0.0370	7835	0.0100
Philippines	2	0.0370	10430	0.0134
tot	**11**	**0.2037**	**358276**	**0.4595**
Turkey	3	0.0556	20888	0.0268
Iran	8	0.1481	95292	0.1222
Yemen	1	0.0185	2800	0.0036
tot	**12**	**0.2222**	**118980**	**0.1526**
Afghanistan	3	0.0556	7323	0.0094
Nepal	1	0.0185	1450	0.0019
India	3	0.0556	31753	0.0407
Pakistan	2	0.0370	91300	0.1171
tot	**9**	**0.1667**	**131826**	**0.1691**
El Salvador	1	0.0185	1500	0.0019
Mexico	1	0.0185	9500	0.0122
Colombia	2	0.0370	6900	0.0088
Haiti	1	0.0185	65000	0.0834
Guatemala	1	0.0185	23000	0.0295
tot	**6**	**0.1111**	**105900**	**0.1358**
Russia	1	0.0185	1989	0.0026
Italy	2	0.0370	3448	0.0044
Romania	1	0.0185	1581	0.0020
Armenia	1	0.0185	25000	0.0321
Algeria	2	0.0370	5766	0.0074
tot	**7**	**0.1296**	**37784**	**0.0485**
Indonesia	8	0.1481	24210	0.0311
Papua New Guinea	1	0.0185	2700	0.0035
tot	**9**	**0.1667**	**26910**	**0.0345**
Sum(tot)	**54**		**779676**	

From Table 5.1, we are also able to compare the percentage of the number of disastrous events to the total number of events in the countries in which the events occurred. Furthermore, the

percentage of deaths in earthquake disasters to the total deaths during this period is compared among countries. China has the highest number of earthquake-disaster fatalities (43%); Iran and Pakistan with around 12% of the fatalities, are next. However, the percentages of number of disastrous earthquakes are highest in Indonesia and Iran (14%), while China has 11% of the events. Although the percentage value of number of events in China is still among the highest, it is not as high as its rank for fatalities.

Doocy et al (2013) reported global earthquake fatalities in events with fatalities greater than 10, between 1980 and 2009. According to Doocy et al (2013), the total of 372,634 fatalities occurred during this period and fatalities are dominated in China (21%), Pakistan, and Iran (~20%). Although the estimated number of fatalities in their report is different from ours, the ranking of these percentages are the same. While local assessment of risk and life-loss on the most affected areas is valuable, in this study, we consider earthquake disasters as threats to the global population and analyze the global risk and the trend of global societal resistance towards earthquake disasters during 1973-2013.

In this study, we use a risk-based approach to develop a conceptual model for societal earthquake resistance wherein risk is a measure of the probability of harmful consequences. Here, these consequences are earthquake fatalities resulting from interactions between earthquake occurrence and vulnerable conditions (HSE (2001); UNDP (2004)). This conceptual model includes three effective components for human life-loss: hazard, vulnerability, and consequences which we express as Eq. 5.1, consists of life-loss (*Loss*), hazard (*H*), vulnerability of the region (*V*), and elements at risk (*EaR*). Eq. 5.1 is similar to the risk equation used by UNDP(2004), Baecher and Christian (2003), and Porske (2008).

$$Loss = H \times [V \times EaR] \qquad (5.1)$$

In Eq. 5.1, *Loss* is the estimated life-loss due to earthquake disasters with the unit of nbr/year (nbr stands for number), and *H* is the probability of the occurrence of earthquakes that can cause fatalities greater than 1,000 with the unit of 1/time (1/year), and *EaR* is the number of elements at risk (here fatalities). From our 54-event database we have established that the minimum magnitude associated with an earthquake disaster is *M*5.5. Many earthquake disaster databases do not specify the type of magnitude scale used to express earthquake magnitude. For the sake of simplicity, we do not specify the type of magnitude scale reported for a specific earthquake; we

suggest that this approximation has little effect on the results of a global investigation. Studies by Kanamori (1977; 1983) show that the values of various magnitude types are more or less coincident, except for very high magnitudes (Kanamori, 1983). Thus, the type of the magnitude used here is considered as a generic magnitude *M*, without subscripts, rounded to one decimal place USGS (http://earthquake.usgs.gov/aboutus/docs/020204mag_policy.php). Furthermore, in Eq. 5.1, *V* is the vulnerability of the region affected by earthquake disasters. In this study, the effects of earthquake disasters are considered global, therefore, global population at the time of earthquake disaster is considered as a rough proxy of *EaR*, elements at risk.

In general, earthquake vulnerability (*V*) is the characteristic condition of the region that determines the response to the seismic event and thus the losses from earthquake occurrence and effects (Fussel, 2007). With further reference to Eq.5.1, since we focus on life loss due to an earthquake disaster, *EaR*, is defined as the number of people exposed to earthquake disasters, therefore, we change *EaR* to *ExP* in Eq. 5.2. Since *H* has the unit of 1/time, the unit of *Loss* is annual earthquake-disaster life loss.

Additionally, to quantify the effects of earthquakes on global societies, we replace earthquake vulnerability (*V*) by the inverse of what we term the societal earthquake resistance (*R*), which is the immediate capacity of the society to withstand the hazard occurrence, i.e., $V=1/R$. Substituting *V* with $1/R$ and *EaR* with *ExP* in Eq. 5.1 gives us the earthquake-disaster Life Loss Equation, Eq. 5.2:

$$\boldsymbol{LifeLoss} = H\times[\frac{1}{R}\times ExP] \qquad (5.2)$$

In the next sections, we first analyze the probability of hazard, here earthquake disasters. Then, we compare the global earthquake-disaster fatality-rate with the global crude death-rate, and finally, we estimate the global societal resistance towards earthquake disasters and its trend during 1973-2013.

5.2 Hazard

Based on ISO31000 documents (Leitch, 2010), hazard is defined as the source of potential harm. A quantitative definition of hazard is the probability of occurrence of events that may cause harm. Here, as we introduced in the introduction, based on our earthquake disaster dataset, we

consider earthquakes with M5.5 and greater as the source of fatalities greater than 1,000 in an earthquake disaster. Therefore, hazard, here is the probability of the occurrence of earthquakes with magnitude M5.5 and greater. Since the occurrence of earthquakes over time [excluding aftershocks] is considered as a Poisson process (Scheidegger, 1975), the probability of hazard would follow the Poisson probability distribution, $P(x=k)=\lambda e^{-\lambda}/k!$, where x is a discrete random variable, k is the number of occurring at the unit time, and λ is the mean and variance of the number of events per unit time. In case of earthquake hazard, probability of occurrence of ***one*** event, k=1, is $P= \lambda e^{-\lambda}$, and probability of exceeding that magnitude, here M≥5.5, is $1-P$. Probability of exceeding magnitude 5.5 is one minus Poisson distribution function with parameter λ, which can be estimated in R using ppois model[26].

The λ is calculated over a certain period of time, based on the earthquake catalogues and the data available. For this study, we calculated the value of λ per day in a certain year for earthquake hazards, with M≥5.5, during 1973 to 2013. The reason that we use the daily value of λ (instead of yearly) is that we would like to estimate the probability of occurrence of an earthquake with M≥5.5 everyday. However, if we were to calculate the yearly probability, it would be 1, since the occurrence of these events is very often throughout the year. Hence, in order to calculate the yearly value of λ, based on the daily value, we use the total number of earthquakes in one specific year, and then average over the 365 days of the year.

We used the ANSS earthquake catalogue (http://www.ncedc.org/anss/catalog-search.html) for gathering the earthquake data. The selection criteria for the date was, start: 1973/01/01,00:00:00, end: 2013/01/01,00:00:00. The total number of earthquakes was 17,305 in 40 years. We also gathered the earthquake data from NEIC earthquake catalogue, which is accessible through the USGS website (http://earthquake.usgs.gov/earthquakes/search/), in order to compare the results. However, the total number of recorded earthquakes in NEIC was 19,513 in 40 years. The difference between the numbers of recorded earthquakes of M≥5.5 suggests that the NEIC catalogue include a more complete database. Table 5.2 summarizes the total number of earthquakes per year from both of the earthquake catalogues and their corresponding yearly probability of hazard, based on the Poisson distribution function.

[26] `ppois(1, lambda, lower.tail = FALSE, log.p = FALSE)`

Table 5.2 Total number of earthquakes with M≥5.5, and probability of earthquakes with M≥5.5, P(M≥5.5), during 1973 and 2013 based on ANSS and NEIC compared. We choose NEIC as a more complete catalogue due to the differences shown.

Year	M≥5.5 (ANSS)	P(M≥5.5)_ANSS	M≥5.5(NEIC)	P(M≥5.5)_NEIC
1973	396	0.296	414	0.313
1974	358	0.258	384	0.286
1975	410	0.310	439	0.337
1976	446	0.346	493	0.393
1977	419	0.319	469	0.368
1978	400	0.300	389	0.352
1979	343	0.243	389	0.289
1980	338	0.238	376	0.277
1981	291	0.191	350	0.251
1982	315	0.215	379	0.278
1983	413	0.313	478	0.379
1984	328	0.228	489	0.387
1985	336	0.236	487	0.385
1986	343	0.243	492	0.390
1987	362	0.262	509	0.405
1988	342	0.242	494	0.393
1989	318	0.218	494	0.394
1990	386	0.286	538	0.435
1991	322	0.222	435	0.338
1992	406	0.306	539	0.439
1993	379	0.279	471	0.374
1994	441	0.341	520	0.417
1995	521	0.419	607	0.495
1996	501	0.400	566	0.464
1997	437	0.337	470	0.373
1998	367	0.267	390	0.293
1999	432	0.332	443	0.343
2000	547	0.443	554	0.449
2001	441	0.341	445	0.347
2002	442	0.342	446	0.345
2003	481	0.380	485	0.382
2004	568	0.462	570	0.465
2005	534	0.431	533	0.431
2006	508	0.406	509	0.408
2007	609	0.498	611	0.499
2008	506	0.404	509	0.406
2009	507	0.415	517	0.414
2010	561	0.455	559	0.453
2011	718	0.586	705	0.575
2012	483	0.382	446	0.345

To analyze the temporal trend of hazard during the period of 1973-2013, we use linear regression method, given in appendix III. The temporal trend shows an average yearly increase of 0.003 ± 0.00078 per year over the 40 years of data (95% confidence interval: (0.0016, 0.0048); p-value<0.01). Fig. 5.2a illustrates the linear regression fit and the 95% confidence interval of the temporal trend of probability of hazard in this period. The yearly increase in the probability of occurrence of earthquakes suggests that the magnitude of earthquake disasters have also increased. In order to investigate this suggestion, we look at the temporal trend the energy released by earthquake disasters over the period of 1973-2013 in Fig. 5.2b.

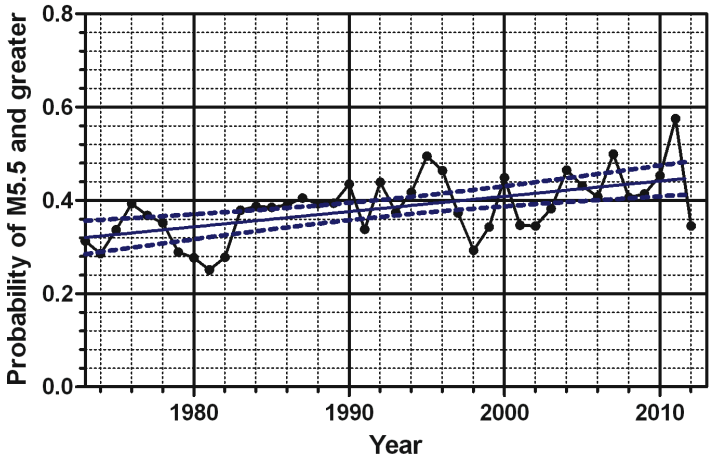

a) Temporal trend of probability of hazard, probability of occurrence of M≥5.5, linear regression fit, and its 95% confidence interval.

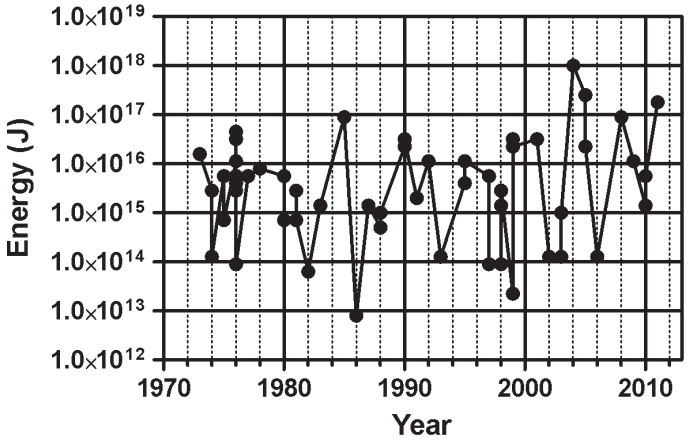

b) Temporal trend (1973-2013) in energy release of earthquake disasters (54 events). The mean energy release is 3.67×10^{16} J.

Figure 5.2: Temporal trend of hazard in the record of earthquake disasters (1973-2013). Data is given in Table 5.S.1.

The energies released by earthquake disasters are calculated by converting the earthquake magnitude (M) to energy (E) using Gutenberg's (Gutenberg and Richter, 1956) energy-magnitude relation, log E= 1.5M+11.8. We applied this to the record of 54 earthquake disasters given in Table 5.S.1. Fig. 5.2b shows the trend of energy, in log scale, over the period of 1973-2013 is not significantly increasing or decreasing over time. We applied linear regression at logarithmic scale (Appendix III) and found the 95% confidence interval: (-0.028, 0.086), and p-value: not significant. Constant trend of earthquake energy release, confirms the hazard exposure of the global population to earthquake disasters has not been changed since 1973, although the probability of earthquake hazard (with M≥5.5) has been increasing.

Shearer and Phillip (2012) also showed that there is no statistically significant proof in any clustering or in other words any increase trend in the dataset of large earthquakes, M≥7 since 1900. Their result is very much in line with our result. However, it has to be mentioned that, they have used the term *risk* instead of hazard, but since they have only looked at the earthquake magnitudes, without considering any of their effects on the human societies, we believe that using the term *risk* is not precise in this context.

Using Eq. 5.2 in the list of events of earthquake disaster database, we examine the role of ExP in loss of life due to earthquake disasters. In contrast to the increase of earthquake hazard, the world has experienced massive population growth in the period of 1973-2013. Indeed, the qualitative correlation between cumulative earthquake fatalities and world population has been previously noted in Bilham's work (1988, 2004, 2009) and in Fig. 5.3a where the estimate global population is plotted in comparison with cumulative earthquake fatalities. However, due to the autocorrelation that any cumulative plot indicates, analyzing the cumulative fatality plot is not possible. Instead, the effect of world population on the number of fatalities can be quantitatively illustrated by the temporal record of the ratio of number of fatalities to the population exposed to the event (Nishenko and Barton, 1995). We call this ratio as the earthquake fatality ratio. The exposed population in this study is estimated by considering the global population in the year of the event. The data of world population is gathered from World Bank database (http://data.worldbank.org/indicator/SP.POP.TOTL). Fig. 5.3b is the temporal record for the period under study, of the ratio of number of fatalities due to earthquake disasters to the exposed population. We applied a linear regression model to analyze the statistics of the temporal trend of

this ratio, and no significant trend is observed. The 95% confidence interval of linear regression fit to the data is also plotted in Fig. 5.3b.

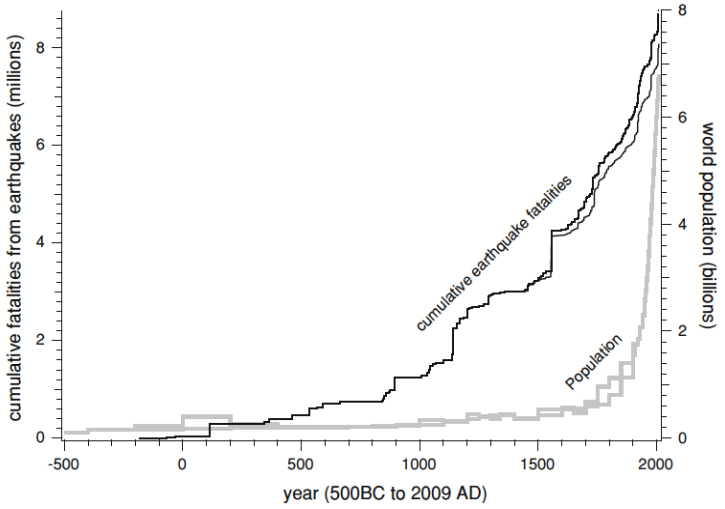

a) Earthquake fatalities in comparison with estimated global population. (Reproduced from Bilham, 2009, Fig.1)

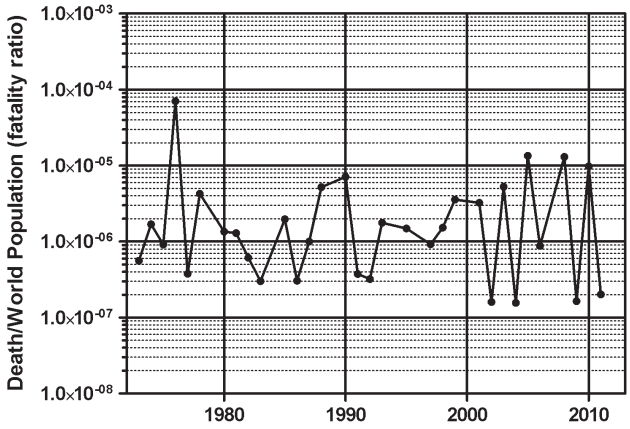

b) Temporal trend of fatality ratio (death/exposed population). Data for 54 earthquake disasters, given in Table 5.S.1, is cumulated for each year.

Figure 5.3: Global population growth and earthquake fatalities (a) in comparison with the annual ratio of earthquake fatalities to exposed population (b)

Due to large variations in the data of the death/exp.pop, linear regression is not applicable here. Furthermore, we checked Poisson regression as a non-linear model on this data and because of overdispersion situation, i.e., variance>mean (Berk and MacDonald, 2007), we modified the non-linear model and applied negative binomial distribution for our regression analysis. The results of negative binomial model indicated that there was a small (1-fold) insignificant increase

of D/P per year (95% confidence interval: ($e^{-0.023}$, $e^{0.018}$); p-value: not significant). Therefore, we do not have any evidence of change in the earthquake fatality ratio over the 40 year period.

5.3 Earthquake fatality rate and crude death rate

To assess the effectiveness of global attempts towards reducing fatalities in major earthquakes, we compare the earthquake disaster fatality ratio with the global annual United Nations Crude Death Rate (Fig. 5.4). The Crude Death Rate is defined as number of deaths caused by any event per 1,000 people per year (http://data.un.org/Glossary.aspx?q=Crude+death+rate) which reflects the health of the global population and the magnitude of disease-related fatalities. We take this metric as the background global death rate. In Fig. 5.4, the Crude Death Rate (blue curve) is seen to decrease over the period 1973 to 2013 in contrast to the ratio of earthquake fatalities per world population which, as we shown in section 5.2, does not have any evidence of increase or decrease over time.

To compare the crude death rate of the world during the same period of time with the trend of the death/exp.pop, since the crude rate data gathered from UNdata (http://data.un.org/Data.aspx?d=PopDiv&f=variableID%3A65) is at 5-year pentade level and it is per 1000 population exposed, calculating the 5-year average of the fatality ratio (black curve on Fig. 5.4), we call it earthquake fatality rate, over the 40 year period was required. On Fig. 5.4, for fatality rate of 1973-1974, and 2010-2012, we used 2-year and 3-year average respectively since we are comparing based on 5-year intervals recorded for crude death rate.

Fig. 5.4 illustrates the difference between crude death rate and earthquake disaster fatality rate. Using regression analysis of the fatality rate, since linear regression is not applicable, here, due to large variations of the data we used negative binomial model, we found that there is no significant increase or decrease in the data (p-value: not significant). This result shows that there was not a reduction in the earthquake fatality rate in the world despite scientific and engineering efforts to the contrary. However, the temporal trend of crude death rate can be modeled by linear regression. The result indicates that crude death rate has significantly decreased by factor of -0.000081 (95% confidence interval: (-0.00009, -0.00007); p-value<0.01; R-squared=0.93) per year. We suggest that this is mainly because of the increase in the life-expectancy. The decreasing trend of the Crude Death Rate is thought to reflect the successes of fighting disease and resulting better global health. The details of statistical models are reported in Appendix III.

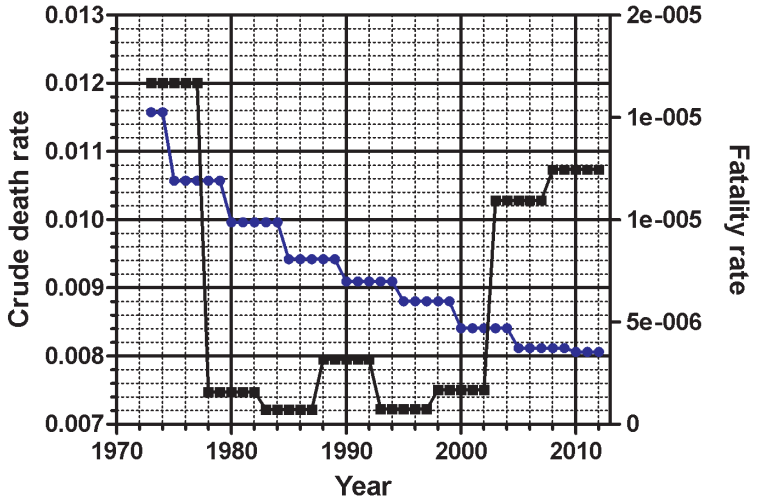

Figure 5.4: Temporal record of death per exposed population of earthquake disasters averaged for 5-year intervals (fatality rate) (black squares) based on 54 record of earthquake disasters in comparison with the Crude Death Rate (per individual) of the world (blue circles) based on UNdata(http://data.un.org/Data.aspx?d=PopDiv&f=variableID%3A65) during 1973-2013. The Crude Death Rate data are recorded in 5-year intervals. For fatality rate of 1973-1974, and 2010-2012, we used 2-year and 3-year average respectively.

5.4 Global societal earthquake resistance

As introduced in the introduction, societal resistance is a parameter that reflects the ability of a society to resist a possible disaster. Here, we aim to estimate the global societal resistance towards earthquake disasters. Based on Eq. 5.2, by re-arranging the earthquake-disaster Life Loss Equation, we obtain a formula for resistance (R), in Eq. 5.3:

$$R = H \times ExP / (LifeLoss) \qquad (5.3)$$

We have shown the temporal trend of earthquake hazard in Fig. 5.2b, and the temporal trend of earthquake disaster fatality ratio in Fig. 5.3b. The increasing trend of hazard, and no evidence of difference in the trend of earthquake disaster fatality with the trend of population growth, summarized in the fatality ratio, Eq. 5.3 suggests that the resistance of the world towards earthquake disasters has either increased or stayed constant over the 40 years period. In order to investigate this presumption, we use statistical methods. However, before that, we need to calculate the societal earthquake resistance (R) for the period under study, using Eq. 5.3.

The list of world population (World Bank, http://data.worldbank.org/indicator/SP.POP.TOTL), cumulated number of fatalities due to earthquake disasters, probability of occurrence of

earthquakes with magnitude greater than M5.5 per year (calculated in section 5.2), earthquake-disaster societal resistance, logarithm of resistance, crude death rate, and global earthquake fatality ratio for the period of 1973-2014 are given in Table 5.3.

As shown in Table 5.3, in some years, there is no earthquake disaster; therefore, the number of fatalities due to earthquake disasters is zero. We exclude those years, from our trend analysis of fatality ratio, and global societal resistance.

Applying linear regression method, we examined the temporal trend of global societal earthquake resistance for the period of 1973-2013. The trend does not show any decrease or increase over time (95% confidence interval: (-0.015, 0.025); p-value: not significant), Fig. 5.5. This result confirms our presumption about the constant global resistance towards earthquake disasters. In other words, the growth of earthquake-disaster fatalities has been so strong that the effect of increase in the trend of earthquake hazard has not been significant in the trend of resistance.

The average logarithm of societal earthquake resistance of the world is about 5.43. The highest societal earthquake resistance of the dataset is 6.47, associated with the year 2002, and the minimum value of log (Res) is about 3.75, associated with the year 1976. The very high number of fatalities as well as a high probability of hazard in 1976 explains the low societal earthquake resistance value for that year. There were 6 earthquake disasters in 1976 among the total of 54 events in the database, including the Tangshan (China) disaster with 255,000 fatalities (Table 5.S.1).

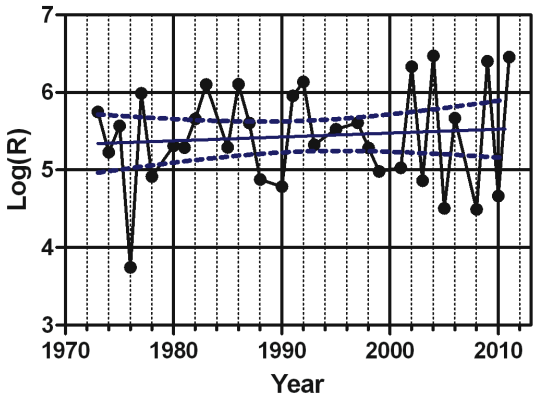

Figure 5.5: Temporal trend of the societal earthquake-disaster resistance, calculated from Eq. 5.3 based on data in Table 5.3. Linear regression fit, and its 95% confidence interval. No significant trend is observed in the trend.

Table 5.3 List of yearly earthquake disaster fatalities (Death), probability of hazard, probability of occurrence of magnitude M5.5 and greater based on the NEIC database (P(H)_NEIC), fatality ratio (DP), ratio of death to the world population (WP_worldBank), global societal resistance towards earthquake disasters (Res) calculated from Eq. 5.3, logarithm of societal resistance (Log(Res), and crude death rate (Crude-Rate) based on UNdata.

Year	WP_worldBank	P(M≥5.5)_NEIC	Death	DP	Res	Log(Res)	Crude-Rate
1973	3893163134	0.313	2175	5.58672E-07	561133	5.74907	0.011574
1974	3968980964	0.286	6723	1.69389E-06	169080	5.22809	0.011574
1975	4043384540	0.337	3698	9.1458E-07	368883	5.56689	0.010572
1976	4115916175	0.393	290665	7.06198E-05	5564.18	3.7454	0.010572
1977	4188436970	0.368	1581	3.77468E-07	974465	5.98877	0.010572
1978	4262342206	0.352	18220	4.27465E-06	82386.4	4.91586	0.010572
1979	4337808194	0.289	0	0			0.010572
1980	4413664738	0.277	5983	1.35556E-06	204595	5.31089	0.009961
1981	4490933561	0.251	5800	1.29149E-06	194459	5.28883	0.009961
1982	4570949029	0.278	2800	6.12564E-07	454398	5.65744	0.009961
1983	4651402233	0.379	1400	3.00985E-07	1260773	6.10064	0.009961
1984	4731579393	0.387	0	0			0.009961
1985	4813681852	0.385	9500	1.97354E-06	195213	5.29051	0.00942
1986	4898637867	0.390	1500	3.06208E-07	1273862	6.10512	0.00942
1987	4985891997	0.405	5000	1.00283E-06	404183	5.60658	0.00942
1988	5074052131	0.393	26450	5.2128E-06	75380.1	4.87726	0.00942
1989	5162050406	0.394	0	0			0.00942
1990	5258687153	0.435	37430	7.11775E-06	61153.3	4.78642	0.009095
1991	5345005256	0.338	2000	3.74181E-07	904275	5.9563	0.009095
1992	5427583250	0.439	1740	3.20585E-07	1369249	6.13648	0.009095
1993	5510964650	0.374	9748	1.76884E-06	211247	5.32479	0.009095
1994	5593291911	0.417	0	0			0.009095
1995	5676856597	0.495	8424	1.48392E-06	333698	5.52335	0.008803
1996	5758273395	0.464	0	0			0.008803
1997	5839859682	0.373	5372	9.19885E-07	405150	5.60762	0.008803
1998	5920583500	0.293	9023	1.52401E-06	192545	5.28453	0.008803
1999	6000290750	0.343	21431	3.57166E-06	96119.4	4.98281	0.008803
2000	6079865645	0.449	0	0			0.008408
2001	6157776977	0.347	20005	3.24874E-06	106888	5.02893	0.008408
2002	6235176063	0.345	1000	1.6038E-07	2152880	6.33302	0.008408
2003	6312628782	0.382	33266	5.26975E-06	72559.3	4.86069	0.008408
2004	6390268174	0.465	1001	1.56644E-07	2970288	6.4728	0.008408
2005	6468011305	0.431	87303	1.34977E-05	31905.4	4.50386	0.008116
2006	6545818799	0.408	5749	8.78271E-07	464740	5.66721	0.008116
2007	6623991685	0.499	0	0			0.008116
2008	6703056019	0.406	87652	1.30764E-05	31069.2	4.49233	0.008116
2009	6782172832	0.414	1117	1.64696E-07	2512677	6.40014	0.008116
2010	6862079727	0.453	67220	9.79586E-06	46209.7	4.66473	0.008061
2011	6942764512	0.575	1400	2.01649E-07	2852175	6.45518	0.008061
2012	7023106813	0.345	0	0			0.008061

5.3 Discussion

In this chapter, we showed that there is no evidence that the global societal resistance has been changed over time. Based on this result, we conclude that, although individual countries have improved their seismic engineering resistance through such measures as the implementation of building codes and increased construction quality, global societal earthquake resistance has not improved since 1973 and has effectively remained constant. Further, earthquake hazard (energy release by earthquake disasters, and probability of occurrence of earthquakes with magnitude M≥5.5 per year) is also effectively constant (Fig. 5.3), shows that any effort to build seismic resistance into the global earthquake disaster system has been offset by the increase in global population and thus the number of people exposed to earthquake hazard. One of the discussions remained is the actual effect of population growth on earthquake disaster life-loss. One of the first questions that can be asked, here, is that what is the expected number of life-loss in case that an earthquake disaster occurs somewhere in the world.

Equation 8.2 in Woo (1999) is a practical equation used for estimating expected economic loss in a factory site in case of a seismic shaking.

$$L = \sum_I F(I) \sum_K P(D_K|I) R(K) \times V \qquad \text{(eq. 8.2, Woo (1999), pg. 199)}$$

where L is expected annual economic loss in a factory site due to a seismic activity, F(I) is the frequency of seismic shaking with intensity I, $P(D_K|I)$ is the relative likelihood that in case of a seismic shaking with intensity I, damage D from category K occurs, R(K) is the mean loss ratio to the factory, if it suffers damage in category K, and V is the value of factory site at risk.

We could convert this equation to an equation that is compatible for earthquake disaster life-loss by renaming the components of the equation, F(I) to probability of occurrence of a specific magnitude, P(M); P(D|I) to the likelihood of fatalities greater than 1,000 happens in case of an earthquake with magnitude M, P(D≥1000|M); R(K) to the mean life-loss ratio if fatalities are greater than 1,000, R(D≥1000); and V to the number of people exposed to earthquake disasters, ExP. Eq. 5.4 is an equation that, hypothetically, can be used for prediction of life-loss in case of various disaster scenarios in future.

$$L = P(M) \times P(D \geq 1000|M) \times R(D \geq 1000) \times ExP \qquad (5.4)$$

We used the data for earthquake disasters (1973-2010) to estimate the P(M), P(D≥1000|M), and R(D≥1000), for M≥5.5, to estimate the life-loss we expect in the year 2013 in case of an

earthquake with magnitude M≥5.5. Likelihood of D≥1000 in case of M≥5.5 can be estimated from the ratio of the number of events with D≥1000 to the number of events with M≥5.5 with any fatality or none. If we calculate the average of the yearly values of each component and assume that the current global population as 7,181,580,000, then the expected life-loss from Eq. 5.4 would be around 52 person. Table 5.4 summarizes the result of this estimation of risk of life-loss based on the earthquake-disaster data given in Table 5.2, Table 5.3, and Table 5.S.1.

Table 5.4 List of components needed to calculate expected life-loss based on Eq. 5.4, and risk of life-loss (exp.life.loss × average resistance).

Avg-P(H)	0.652
Avg-R (D≥1000/WP/yr)	3.85065E-06
Avg-likelihood (#events with D≥1000/# events with M≥5.5)	0.0028
World Pop-2013	7,181,158,000
Exp-Loss (Eq. 5.4, based on eq.8.2, Woo, 1999)	**51.36**

The next step of this study would be to estimate the societal resistance and risk of life-loss in the most vulnerable cities and countries to earthquake disasters. According to Sundermann et al. (2013) (figure 5, pg 16), among 616 metropolitans Tokyo-Yokohama (Japan), Jakarta (India), Los Angeles (USA), Osaka-Kobe (Japan), Tehran (Iran), and Tashkent (Uzbekistan) are the cities that are at risk of earthquake disasters the most. Assuming global population as a proxy of exposure will not be beneficial in case of a city-based approach. In this study it is shown that the ratio of earthquake disaster fatalities to the global population at the time of fatalities has insignificantly increased/decreased over the last 40 years. However, since most of the life-losses due to disasters occurred in metropolitan areas (Sundermann et al., 2013), it is essential to consider the growth of population-at-risk, rather than population growth for risk assessment of natural disasters.

Supplimentary Table:

Table 5.S.1: List of 54 earthquake disasters (with more than 1,000 deaths) in the period of 1973-2013

Year	Lat	Long	location	M	death	Source	Other death reports	Energy (J)
1973	31.3	100.7	China: Sichuan P.[Mangua E]	7.6	2175	Utsu		5.62341E+51
1974	28.2	104.1	China	7.1	1423	NOAA/Utsu	20000	1.25893E+47
1974	35	72.8	Pakistan	6.2	5300	Utsu		1.99526E+57
1975	40.7	122.8	Haicheng, China	7.3	1328	Utsu		7.07946E+65
1975	38.5	40.7	Turkey	6.7	2370	Utsu		3.54813E+62
1976	15.3	-89.1	Guatemala	7.5	23000	Utsu		5.62341E+27
1976	-4.6	140.1	Papua, Indonesia	7.1	6000	Utsu		0.007943282
1976	39.4	118	Tangshan, China	7.8	242800	Utsu		7.94328E+63
1976	6.2	124	Mindanao, Philippines	7.9	8000	Utsu		1.25893E+14
1976	-4.5	139.9	Indonesia (Irain Jaya)	7.2	6000	Utsu		0.011220185
1976	39.1	44	Turkey-Iran border region	7.3	3900	Utsu		2.81838E+63
1976	46.4	13.3	northeastern Italy	6.1	965	Utsu		8.91251E+13
1977	45.8	26.8	Romania	7.3	1581	Utsu		3.16228E+73
1978	33.4	57.4	Iran	7.4	18220	Utsu		7.94328E+54
1980	36.2	1.4	El Asnam, Algeria (formerly Orleansville)	7.3	3500	NOAA/Utsu	5000	1.25893E+59
1980	40.9	15.3	southern Italy	6.7	2483	NOAA/Utsu	4689	1.41254E+66
1981	29.9	57.7	southern Iran	6.7	3000	Utsu		4.46684E+49
1981	30	57.8	southern Iran	7.1	1500	Utsu		6.30957E+49
1981	-4.6	139.2	Indonesia(Irian Jaya)	6.7	1300	Utsu		0.007943282
1982	14.7	44.4	Yemen	6	2800	Utsu		7.07946E+26
1983	40.3	42.2	Turkey	6.9	1400	NOAA/Utsu	1342	1.77828E+65
1985	18.2	-102.5	Mexico, Michoacan	8.1	9500	Utsu		1.25893E+32
1986	13.8	-89.1	El Salvador	5.4	1500	NOAA/Utsu	1100	3.16228E+25
1987	0.2	-77.8	Colombia-Ecuador	6.9	5000	Utsu		125892.5412
1988	26.8	86.6	Nepal-India border region	6.6	1450	NOAA/Utsu	1091	1E+45
1988	41	44.2	Spitak, Armenia	6.8	25000	Utsu		1.99526E+66
1990	37	49.4	Western Iran	7.7	35000	NOAA/Utsu	50000	1.99526E+60
1990	15.7	121.2	Luzon, Philippine Islands	7.8	2430	Utsu		2.23872E+28
1991	30.8	78.8	Northern India	7	2000	Utsu		1E+51
1992	-8.5	121.9	Flores Region, Indonesia	7.5	1740	Utsu		1.12202E-08
1993	18.1	76.5	Latur-Killari, India	6.2	9748	NOAA/Utsu	11000	8.91251E+31
1995	34.6	135	Kobe, Japan	7.2	6435	Utsu		5.01187E+56
1995	52.6	142.8	Sakhalin Island, Russia	7.5	1989	Utsu		5.01187E+83
1997	33.9	59.8	Northern Iran	7.3	1572	NOAA/Utsu	1728	4.46684E+55
1997	38.1	48.1	Iran: Ardebil	6.1	1100	Utsu		8.91251E+61
1998	37.1	70.1	Hindu Kush region, Afghanistan	6.1	2323	Utsu		2.81838E+60
1998	37.1	70.1	Afghanistan-Tajikistan Border Region	6.9	4000	Utsu		2.81838E+60

Year	Lat	Long	location	M	death	Source	Other death reports	Energy (J)
1998	-3	141.9	Papua New Guinea	7.1	2700	Utsu		1.995262315
1999	4.5	-75.7	Colombia	5.7	1900	NOAA/Utsu	1185	3.54813E+11
1999	40.7	29.9	Turkey	7.8	17118	Utsu		7.07946E+65
1999	23.8	121	Taiwan(Eastern Asia)	7.7	2413	Utsu		3.16228E+40
2001	23.4	70.2	Gujarat, India	7.8	20005	NOAA		7.94328E+39
2002	36	69.3	Hindu Kush Region, Afghanistan	6.2	1000	NOAA		6.30957E+58
2003	36.9	3.6	Northern Algeria	6.2	2266	NOAA		1.41254E+60
2003	28.99	58.31	Southeastern Iran	6.8	31000	NOAA		1.92752E+48
2004	3.295	95.982		8.8	1001	NOAA		5527134079
2005	2.08	97.1	Northern Sumatra, Indonesia	8.4	1303	NOAA/USGS	1313	83176377.11
2005	34.53	73.58	Pakistan	7.7	86000	NOAA		3.9355E+56
2006	-7.961	110.446	Flores Region, Indonesia	6.2	5749	NOAA		7.21938E-08
2008	31	103.3	Eastern Sichuan, China	8.1	87652	NOAA		1.99526E+51
2009	-0.72	99.867	Southern Sumatra, Indonesia	7.5	1117	NOAA		5248.074602
2010	33.165	96.548	Southern China	6.9	2220	NOAA		3.52777E+54
2010	18.4	-72.5	Haiti region	7.3	65000	NOAA/Doocy et al. (2013)		2.51189E+32
2011	38.297	142.373	Japan	8.3	1400	NOAA		1.75995E+62

Appendix III

Negative binomial regression for death/population

Negative Binomial: Applying Poisson regression, results in p-values and standard errors are too small it means that the data is overdispersed. Overdispersion happens when the variance is greater than the mean (Berk et al., 2007). To check the overdispersion: 1) examine the mean and standard deviation, 2) examine the ratio of the deviance to the degrees of freedom (it should be close to 1.0). There are two ways to correct overdispersion: 1) Pearson adjustment (which is only available in SAS) and 2) negative binomial distribution (it carries an error term which always corrects overdispersion. Here, I choose negative binomial distribution which is a modification of glm() in R; glm.nb() in the MASS package (Chambers and Hastie, 1991).

Hypothesis testing: Assuming Y=a+bX, where Y is the ratio of the death (D) to the world population (WP), X is the year and a, b are constants.

Null hypothesis (H_0) : b=0 (i.e., there is no X-trend for Y), Alternative hypothesis (H_1): b≠0 (i.e., there is a positive or negative trend)

```
Call:
glm.nb(formula = death ~ offset(log(WP)) + Yr, init.theta = 0.5161683824,
    link = log)
Deviance Residuals:
    Min       1Q   Median       3Q      Max
-1.3578  -1.1815  -0.9708  -0.3951   3.7861
Coefficients:
            Estimate Std. Error z value Pr(>|z|)
(Intercept) 10.96553   31.82452   0.345    0.730
Yr          -0.01193    0.01599  -0.746    0.455
(Dispersion parameter for Negative Binomial(0.5162) family taken to be 1)
    Null deviance: 69.022  on 53  degrees of freedom
Residual deviance: 68.257  on 52  degrees of freedom
AIC: 1128
Number of Fisher Scoring iterations: 1
              Theta:  0.5162
          Std. Err.:  0.0822
 2 x log-likelihood:  -1122.0350
```

Since the p-value is not significant, the null hypothesis cannot be rejected (i.e., there is no evidence of any increase or decrease of D/WP over time).

Linear regression for probability of hazard

Hypothesis testing: Assuming Y=a+bX, where Y is the probability of hazard (occuring M≥5.5) per year, X is the year and a, b are constants.

Null hypothesis (H_0) : b=0 (i.e., there is no X-trend for Y), Alternative hypothesis (H_1): b≠0 (i.e., there is a positive or negative trend)

```
Call:
lm(formula = PH ~ Year)
Residuals:
     Min       1Q   Median       3Q      Max

-0.10917 -0.03855  0.01082  0.03561  0.13030
Coefficients:
              Estimate Std. Error t value Pr(>|t|)

(Intercept) -6.1348140  1.5516376  -3.954 0.000324 ***
Year         0.0032718  0.0007787   4.201 0.000155 ***
---
Signif. codes:  0 ‘***’ 0.001 ‘**’ 0.01 ‘*’ 0.05 ‘.’ 0.1 ‘ ’ 1
Residual standard error: 0.05685 on 38 degrees of freedom
Multiple R-squared: 0.3172,     Adjusted R-squared: 0.2992
F-statistic: 17.65 on 1 and 38 DF,  p-value: 0.0001546
```

P-value is not significant here, therefore, we do not reject the null hypothesis, i.e., there is no significant trend in the probability of hazard.

Linear regression at logarithmic scale for overal Energy release

Hypothesis testing: Assuming Y=a+bX, where Y is the enegy release due to earthquake disasters per year, X is the year and a, b are constants.

Null hypothesis (H_0) : b=0 (i.e., there is no X-trend for Y), Alternative hypothesis (H_1): b≠0 (i.e., there is a positive or negative trend)

```
Call:
lm(formula = log(Energy) ~ Year)
Residuals:
    Min      1Q  Median      3Q     Max
-5.7577 -1.2368  0.3327  1.7472  5.4633
Coefficients:
             Estimate Std. Error t value Pr(>|t|)
(Intercept) -22.20501   56.63885  -0.392    0.697
Year          0.02904    0.02846   1.020    0.312
Residual standard error: 2.477 on 52 degrees of freedom
Multiple R-squared: 0.01963,    Adjusted R-squared: 0.0007722
F-statistic: 1.041 on 1 and 52 DF,  p-value: 0.3123
```

P-value is not significant here, therefore, we cannot reject the null hypothesis. This means that there is no significant trend of increase or decrease in the energy released by earthquake disasters per year.

Linear regression for crude death rate

Hypothesis testing: Assuming Y=a+bX, where Y is the ratio of the crude death rate (Crude5) to , X is the year and a, b are constants.

Null hypothesis (H_0) : b=0 (i.e., there is no X-trend for Y), Alternative hypothesis (H_1): b≠0 (i.e., there is a positive or negative trend)

```
Call:
lm(formula = Crude5 ~ Year)
Residuals:
       Min         1Q     Median         3Q        Max
-4.161e-04 -1.742e-04 -4.565e-05  1.003e-04  8.491e-04
Coefficients:
              Estimate Std. Error t value Pr(>|t|)
(Intercept)  1.702e-01  7.326e-03   23.23   <2e-16 ***
Year        -8.080e-05  3.677e-06  -21.98   <2e-16 ***
---
Signif. codes:  0 ‘***’ 0.001 ‘**’ 0.01 ‘*’ 0.05 ‘.’ 0.1 ‘ ’ 1
Residual standard error: 0.0002684 on 38 degrees of freedom
Multiple R-squared: 0.927,      Adjusted R-squared: 0.9251
F-statistic: 482.9 on 1 and 38 DF,  p-value: < 2.2e-16
```

The p-value is significant, therefore, we reject the null hypothesis and since the coefficient (-0.0000808) is negative, we conclude that the crude death rate has a negative trend over time.

Negative binomial for 5-year average earthquake disaster fatality ratio (fatality rate)

Since the variation of the data in our 5-year average fatality rate is huge, we cannot use linear regression model here. We use negative binomial generalized linear model instead.

Hypothesis testing: Assuming Y=a+bX, where Y is the ratio of the 5-year average death (D5) to the 5-year average world population (WP5), X is the year and a, b are constants.

Null hypothesis (H_0) : b=0 (i.e., there is no X-trend for Y), Alternative hypothesis (H_1): b≠0 (i.e., there is a positive or negative trend)

```
Call:
glm.nb(formula = D5 ~ offset(log(WP5)) + Year, init.theta = 1.080786527,
    link = log)
Deviance Residuals:
    Min       1Q   Median       3Q      Max
-1.4989  -0.9453  -0.8160   0.2731   1.5151
Coefficients:
             Estimate Std. Error z value Pr(>|z|)
(Intercept) -7.319338  26.253194  -0.279    0.780
Year        -0.002508   0.013176  -0.190    0.849
(Dispersion parameter for Negative Binomial(1.0808) family taken to be 1)
    Null deviance: 45.825  on 39  degrees of freedom
Residual deviance: 45.766  on 38  degrees of freedom
AIC: 892.79
Number of Fisher Scoring iterations: 1
              Theta:  1.081
          Std. Err.:  0.214
 2 x log-likelihood:  -886.792
```

Since p-value is not significant here, we cannot reject the null hypothesis, meaning that there is no significant evidence that shows an increase or decrease in the 5-year earthquake disaster fatality rate.

Linear Regression for Trend of Resistance

Hypothesis testing: Assuming Y=a+bX, where Y is the resistance value of each year, X is the year and a, b are constants.

Null hypothesis (H_0) : b=0 (i.e., there is no X-trend for Y), Alternative hypothesis (H_1): b≠0 (i.e., there is a positive or negative trend)

```
Call:
lm(formula = LogRes ~ Year)
Residuals:
     Min       1Q   Median       3Q      Max
-1.61018 -0.46063  0.00407  0.55136  0.97728
Coefficients:
             Estimate Std. Error t value Pr(>|t|)
(Intercept) -4.520133  19.820132  -0.228    0.821
Year         0.004998   0.009950   0.502    0.619
Residual standard error: 0.6592 on 30 degrees of freedom
Multiple R-squared: 0.008339,   Adjusted R-squared: -0.02472
F-statistic: 0.2523 on 1 and 30 DF,  p-value: 0.6191
```

Since p-value is not significant here, we cannot reject the null hypothesis, meaning that there is no significant evidence that shows an increase or decrease in the trend of the resistance of earthquake disasters over years.

Chapter 6 Risk and reliability in a natural disaster system

6.1 Introduction

Natural hazard is a natural process or phenomenon that may cause loss of life, injury or other health impacts, property damage, loss of livelihoods and services, social and economic disruption, or environmental damage (UNISDR, 2009). Natural hazards become natural disasters when they severely and adversely affect human life/environments. Natural disasters resulting from the occurrence of natural hazard processes such as hurricanes, earthquakes and landslides have had devastating effects on human life (Degg (1992); Du et al. (2009); GAR (2011)). Here, we define a "Natural Disaster System" as a system in which human life, environment or belongings are affected by a natural disaster due to the interaction between the natural disasters and the affected societies' resistance. The diverse effect of this interaction is considered to be fatalities more than a certain threshold (here, 1,000 fatalities). This is a serious disruption of the functioning of a society, which exceeds the ability of the affected community or society to cope using its own resources (UNISDR, 2009).

In this study we have three main objectives: 1) review the conceptual framework of risk (specially societal risk) assessment methods for application to natural disasters, 2) compare engineering risk assessment criteria and acceptable levels of engineering risk with natural disasters behavior and occurrence, and 3) propose a modification to reliability assessment for natural disasters as a complement to other societal risk assessment measures.

In general, two view points are associated with risk: individual risk (IR) and societal risk (SR). According to the Center for Chemical Process Safety, IR expresses the risk to an individual in the potential effect zone of an incident or set of incidents and SR measures the potential for impacts to a group of people located in the effect zone of an incident or set of incidents (CCPS, 2009). Here we consider societal risk, since frequently in the context of natural disasters, the effects are extensive in scale and multiple deaths occur. Societal risk measures are commonly illustrated in a graphical representation, Frequency-Number, *FN*-curve (CCPS, 2009).

We review the use of *FN*-curve, where F is the cumulative frequency of all events leading to N or more consequences which in our case is fatalities (e.g., used in dam or slope failure assessment in Hong Kong (1994). *FN*-curves are typically plotted on a log-log scale since the frequency and number of fatalities often range over several orders of magnitude (CCPS, 2009).

FN-curves are then compared to P_f–N curves (a probability-consequence curve on a log-log plot) (Baecher and Christian, 2003), where P_f is the annual probability of failure and N is either the number of fatalities or amount of financial loss (e.g., used in the Usoi dam risk assessment, Juang et al. (2011), pg.101). As stated above we focus on life loss.

Approaches to societal risk assessment can be complemented by the concept of reliability which is extensively used in the characterization of engineering systems such as factories, power-plants and dams (e.g. reliability in dams and hydraulic structures (Wunderlich, 2005). Reliability is the ability of a system or a component to perform its required functions under stated conditions for a specified period of time (Andrews and Moss, 2002). Thus, the value of reliability determines how effective the system is under any defined condition. A system is fully reliable if its reliability value is 1 and it is totally unreliable if its reliability is 0 (Andrews and Moss, 2002). In the context of natural disasters, we define a reliable system to be a natural disaster system with fatalities less than 1,000. Pisarenko and Rodkin (2014) utilize a statistical method to estimate the threshold of a set of disaster data based on the Limit Theorem of the Extreme Value Theory **(**EVT**)**. In this approach, a threshold that is high enough that the data will tend to Generalized Pareto Distribution (GPD) is picked based on the minimum Kolmogorov-Smirnov distance between the GPD fit and the real data. In Appendix IV using NGDC significant earthquake database (http://www.ngdc.noaa.gov/nndc/struts/form?t=101650&s=1&d=1) for the period of 1950-2013 with criteria of minimum 1 fatality due to earthquakes, we applied the Pisarenko and Rodkin (2014) approach (summarized in appendix IV) to investigate the best statistical threshold for risk assessment of earthquake disasters. Although the smallest kolmogorov-smirnov distance between the GPD fit and the real values of the data are for 10 and 3,000 fatalities, we pick 1,000 fatalities as our threshold since the highest 0.95% quantile value in 10 years occurs at 1,000 threshold after the 0.95% quantile of 10-fatalities threshold which is almost infinity.

In other words, we consider a natural disaster system as a system in which failure results in more than 1,000 fatalities. 1,000 fatalities due to a natural disaster event is interpreted as a reliable system and in the case of fatalities, the reliability decreases as the number of fatalities increases. Below, we explore the use of the reliability concept as a complement to conventional risk assessment methods for natural hazards based on the probability distribution of fatalities associated with natural hazard systems.

6.2 Conceptual model of natural disaster risk

Risk is the effect of uncertainty on objectives (Aven, 2011a) and includes two main components: 1) in-determination (probability of events) and 2) consequences (damages or deaths) (Porske, 2008). The conceptual definition of risk is conventionally stated, *Risk=Hazard×Consequences* (CCPS (2009), pg. 3). Here *Hazard* is a replacement word for "likelihood" and it expresses the frequency (or probability) of an incident occurrence (CCPS, 2009). *Consequences* are defined as harmful consequences or expected losses (in our case deaths) resulting from interactions between natural disasters and vulnerable conditions associated with human activity (UNISDR, 2009).

A further definition of risk, i.e., *Risk=Hazard×Vulnerability*(×*Exposure*) (e.g. Birkmann, 2006), consequences defined by the product of two parameters, *Vulnerability* and *Exposure*, defined respectively as the effect of uncertainty on the results at the occurrence of a disaster event, and the presence of an object subject to an event or risk source (Aven, 2011a).

In the context of natural disaster, we introduce a new parameter, Resistance, the inverse of which is a replacement for Vulnerability in the risk equation as follows, Risk=Hazard×(1/Resistance)×Exposure. Resistance defines the societal resilience (risk-absorption level of a system) (Aven (2011b), pg. 12) of a society to the occurrence of a natural disaster. In other words, a resistant society can withstand or tolerate even surprises. With this redefinition, we consider a natural disaster system as posing potential societal harm to a population, harm that can be resisted by human effort (engineering, rescues, warning, mitigation, preparedness). The value of 1/Resistance depends on a number of factors, including the financial capability of an affected region for adopting and development of technology for damage prevention. In this study, we consider data from historical disasters and we aim to analyze the consequences of natural disasters based on FN-curves.

6.3 FN-curves and risk assessment

FN-curves are introduced in Chapter 1. Here I briefly summarized some of their characteristics. FN-curves are log-log plots with F, the cumulative annual frequency of N or more consequences versus the value of these consequences. The visual characteristics of the *FN*-plot is a line that starts on a certain intercept (on y-axis) and possesses an inclination with a certain slope. The history of *FN*-curves goes back to the evaluation of nuclear power plant operations in the 1960s

(Farmer, 1967). As nuclear power plants and chemical-processing factories became important for human safety, researchers (e.g., Farmer, 1967, and Beattie, 1967) began to suggest acceptable risk criteria for these activities. *FN*-curves are also used for comparative risk assessment of various hazards (e.g., Gunthal et al. (2006)). Therefore, *FN*-curves are used for two main purposes: 1) analysis of real data for risk assessment (e.g., flood risk assessment, Jonkman (2007)) and 2) development of acceptable risk criteria (e.g., Skjong and Eknes (2002); Debesse (2007)).

The visual realization of the first approach indicates a line that connects a set of points and can be fitted to a straight line with an intercept and a slope associated with the data. The second approach, on the other hand, is originally generated based on an (power-law) equation containing an (imposed) intercept and a (imposed) slope that can create a line on a log-log plot to be used for engineering practice (e.g., Trbojevic (2005); Ale (2005)).

As introduced in previous sections, we associated the value of 1/*Resistance* with the slope of the *FN*-curves. Slopes vary due to the relation between frequency and magnitude of losses (fatalities). As the slope becomes steeper, the frequency of large fatality events becomes less frequent, which means that in general, societal resistance to the considered disaster decreases. Slopes of *FN*-curves of real data can be <1 (i.e., high fatalities are more frequent), =1 (i.e., equal frequency of all fatalities) or >1 (i.e., high fatalities are less frequent) depending on the risk proneness, neutrality or aversion of the region. We borrow the concepts of proneness, neutrality or aversion from the acceptable risk criteria used in the industrial practice (Slovic et al., 1984). We translate the slope of <1 (for the real data; not imposed criteria) as an indicator of low-resistance circumstances, and the slopes of >1, as an indicator of high-resistance circumstances.

In some countries where *FN*-curves are used for societal risk assessment, the acceptable levels of risk are determined based on the intercepts and the slopes that are justified by judgments of the authorities. Details of this method can be found in several studies by Vrijling and van Gelder (1997); Ball and Floyd (1998); Skjong and Eknes (2002); Jonkman et al. (2003); Trbojevic (2005).

The problem of this practice is that these criteria are developed for industrial activities and are used to define acceptable risk criteria for natural hazards. This is despite the fact that natural events have fewer controllable factors, i.e., natural procedures are mainly dominant in nature and mostly not controllable. To illustrate the problem, Fig. 6.1 shows the difference between the acceptable societal risk criteria of the United Kingdom and the Netherlands (as examples of the

European countries) and the *FN*-curves of the European countries' natural disasters real data. In Fig. 6.1, we use the EM-DAT database to gather the data on fatalities due to natural disasters (Note: due to the lack of data on over 1,000-fatality events, we use over 1-fatality events) between 1950 and 2012 in 32 European countries (shown by blue dots). Table 6.1 shows the list of European countries and number of fatalities due to each natural disaster. First important message from Fig. 6.1 is that the natural disaster data reveals an average slope of -0.5 which is less than 1 (risk prone; low resistance). Second, comparing the European countries' data to the acceptable risk criteria defined by the United Kingdom Health and Safety Executive, HSE (2001) R2P2 (Reducing Risk, Protecting People, which limits 50 or more fatalities with a frequency of 1 in 5000 per annum and imposes a slope of -1, risk neutral) criterion shown by a red dot; As Low As Reasonably Practicable (ALARP) criteria (HSE, 1989) that limits the minimum and maximum frequencies of fatalities with two lines of slope -1 (risk neutral) shown by black lines; and the Netherlands (with slopes of -2, risk averse) (Jonkman et al. (2003); Ale (2005); Trbojevic (2005)) shown by a purple line on Fig. 6.1, suggests that for 1,000 fatalities, the European countries' natural disaster frequency is about 3, 4 and 7 times greater than the UK, the ALARP and the Netherlands criteria, respectively. Thus, these criteria are far too conservative to be used for natural disaster risk assessment.

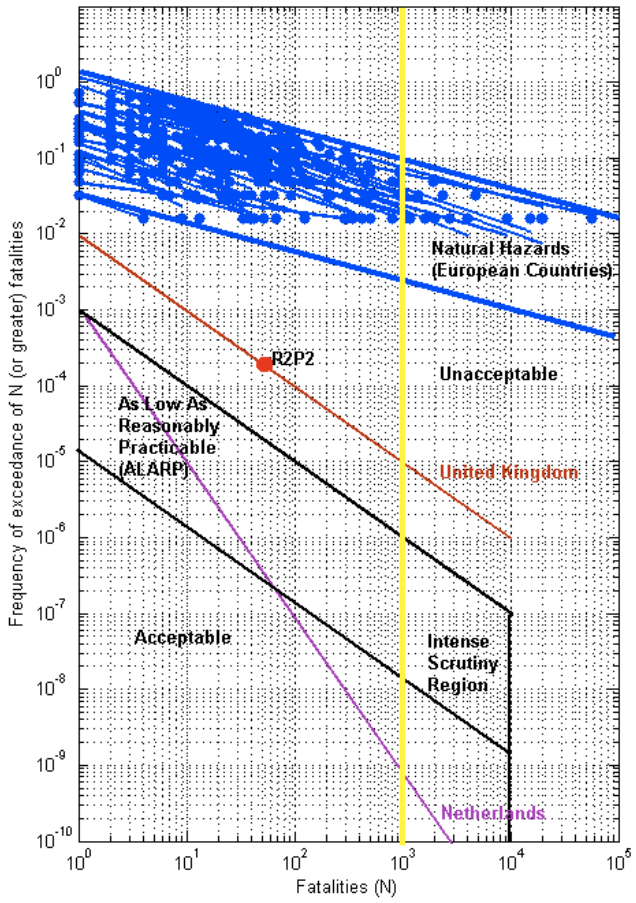

Figure 6.1: FN-curve of fatality (greater than 1) caused by natural hazards (earthquakes, landslides, volcanic activities, floods, wind storms, wild fires, extreme temperatures, drought and epidemics) in 32 European countries (thick blue lines) with respect to acceptable risk criteria in some of them. Red dot is the Health and Safety Executive criterion (HSE-2001) plotted on the red line with slope of -1 (Trbojevic-2005) and the purple line is the Netherlands upper criteria (Jonkman-et.al-2003; Trbojevic-2005; Ale-2005). Thin black lines are based on the ALARP criteria (HSE1989). The European fatality data is obtained from EM_DAT database.

Table 6.1: List of European countries and fatalities due to natural hazards (1950-2012), source: EM_DAT.

	Drought	Earthquake (seismic activity)	Epidemic	Extreme temperature	Flood	Mass movement dry	Mass movement wet	Storm	Volcano	Wildfire	Total
Albania	0	47	7	71	19	0	0	8	0	0	152
Armenia	0	0	0	0	5	0	0	0	0	0	5
Austria	0	0	0	357	39	0	358	22	0	0	776
Azerbaijan	0	33	0	5	19	0	11	0	0	0	68
Belgium	0	2	0	2133	21	0	0	37	0	0	2193
Bulgaria	0	24	0	73	57	0	11	2	0	10	177
Cyprus	0	42	0	61	0	0	0	3	0	0	106
Czech Rep	0	0	0	470	85	0	0	10	0	0	565
Denmark	0	0	0	0	0	0	0	24	0	0	24
France	0	11	21	20956	253	64	114	414	0	32	21865
Georgia	0	15	0	0	16	0	0	0	0	0	31
Germany	0	1	0	9418	50	0	5	196	0	0	9670
Greece	0	848	0	1129	84	0	0	99	48	108	2316
Hungary	0	0	0	662	310	0	0	60	0	0	1032
Iceland	0	1	0	0	0	0	50	0	0	0	51
Ireland	0	0	2	0	5	0	0	36	0	0	43
Italy	0	6258	3	20169	1053	0	2463	190	9	21	30166
Latvia	0	0	0	86	0	0	0	6	0	0	92
Lithuania	0	0	0	81	4	0	0	8	0	0	93
Netherlands	0	0	13	1966	2001	0	0	34	0	0	4014
Norway	0	0	0	0	1	0	0	4	0	0	5
Poland	0	0	0	1684	113	0	0	42	0	35	1874
Portugal	0	0	0	2737	596	0	0	47	0	60	3440
Romania	0	1650	0	516	694	0	0	44	0	0	2904
Russia	0	2019	33	57744	566	60	414	212	0	137	61185
Slovakia	0	0	0	128	64	0	0	2	0	6	200
Slovenia	0	1	0	289	0	0	0	6	0	0	296
Spain	0	21	2	15616	1287	0	84	151	0	66	17227
Sweden	0	0	0	0	11	0	13	11	0	0	35
Switzerland	0	0	0	1039	10	0	295	22	0	0	1366
Ukraine	0	0	275	968	82	0	0	21	0	0	1346
United Kingdom	0	0	71	319	83	0	140	4338	0	0	4951
Total	0	10973	427	138677	7528	124	3958	6049	57	475	168268

Created on: Jun-8-2012. - Data version: v12.07
Source: "EM-DAT: The OFDA/CRED International Disaster Database
www.emdat.be - Université Catholique de Louvain - Brussels - Belgium"

6.4 Comparison of P_f–N curves and FN-curves

In engineering practice, the P_f-N curve involves a log-log plot of annual probability of failure, P_f, versus the value of consequences, the probability-consequence curve) (Baecher and Christian, 2003). In these curves, P_f is not a function of consequences but it is the probability of failure of a system (based on the history of the malfunctioning of the concerned system). In contrast, *FN*-

curves are generated based on the annual frequency of exceedance of the consequences of a failure. Fig. 6.2 compares both types of plots.

Fig. 6.2a illustrates the annual probability of failure of various technological systems versus the consequences of their failure (Baecher (1982); Baecher and Christian (2003)). The annual probability of failure of the systems (y-axis of the graph) are calculated based on the history of the failures of a system (e.g., annual probability of oil spill, Baecher and Christian (2003), pg. 550). The consequences of these failures (x-axis) are either in monetary cost, lives lost, or both (Baecher and Christian (2003), pg. 553). The "marginally accepted" line on Fig. 6.2a imposes the acceptable level of risk line on engineering activities to demarcate safe practices from ones with unacceptable levels of risk (Baecher, 1982). However, on Fig. 6.2b, we have the acceptable societal risk criteria from risk assessment criteria for Hong Kong (1994), which are based on the annual frequency of N or more fatalities versus the number of fatalities to be imposed for natural and technological risk assessment (such as dam or slope failure) in Hong Kong (1994) and for landslide risk assessment by Fell et al. (2005). There are distinctive differences between the bases of these two graphs (such as different methods of calculation for P_f, based on failure rate of a system, and F, based on the frequency of exceedance of consequences), despite their being assumed to be interchangeable in some literature, including Christian (2004).

In order to be able to compare the two plots on Fig. 6.2, the same units are needed for the y-axis on both graphs, which means we need to convert the frequency of exceedance on the FN-curve (Fig. 6.2b) to the annual probability of failure (Fig. 6.2a). Since the concept of failure probability in Fig. 6.2a is based on the failure rate of a system (and failure here is defined in terms of life loss due to natural disasters) we can convert the frequency of exceedance of fatalities (Fig. 6.2b) to the annual probability of fatality due to failure of a system (Fig. 6.2a). Thus, we divide the annual frequency of events with more than 1000 of fatalities by the frequency of any (fatal and nonfatal) event of magnitude M≥5.5. In this way, the number of fatal events is normalized by the total number of events of similar magnitude. In the next section, we illustrate this method using life loss data from earthquake disasters.

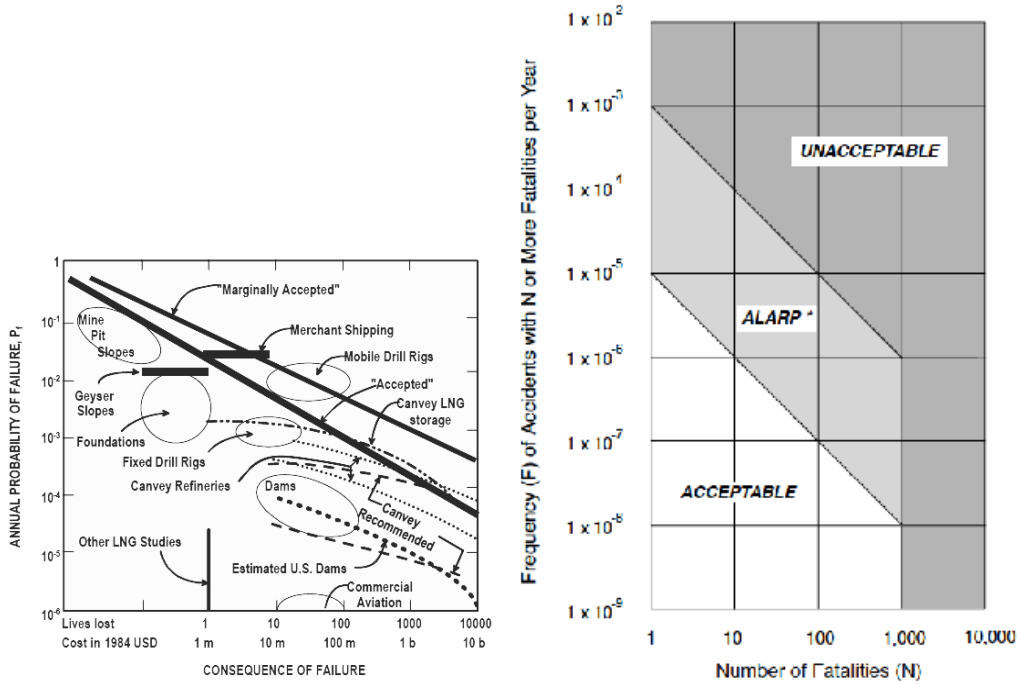

Chapter 1 (b)

Figure 6.2: Comparison of P_f-N (a, reproduced from Baecher (1982); Baecher and Christian (2003)) and FN (b, reproduced from Hong-Kong, 1994) curves. The P_f-N curve includes the approximate probability of failure of man-caused events versus both financial and life loss. The FN−curve shows the *Acceptable*, *As Low As Reasonably Practicable* and *Unacceptable* levels of risk in terms of fatalities (Hong-Kong, 1994).

6.5 Analysis of life loss in earthquake disasters

We use life loss data from earthquake disasters to compare the engineering P_f-N curve with the P_f-N of earthquake disasters. Earthquake disasters are defined here as earthquake events that cause more than 1,000 fatalities during the period 1950-2012; the earthquake disaster database was initially collected from the United States Geological Survey (USGS) table of earthquakes with more than 1,000 fatalities (http://earthquake.usgs.gov/earthquakes/eqarchives/epic/epic_global.php, 1000). These data have been complemented by data from Utsu's database (2002). The list of these disasters has also been cross-checked with the data of the National Geophysical Data Center (NGDC) (http://ngdc.noaa.gov/nndc/struts/form?t=101650&s=1&d=1, 2010). Our database consists of 75 earthquake disasters that occurred between 1950 and 2012 (62 years). We assume that 1,000 fatalities represent the failure of an earthquake disaster system due to lack of resistance.

Fig. 6.3 shows the *FN*-curve for the earthquake disasters in our database. The acceptable risk criterion proposed by the United Kingdom Health and Safety Executive (HSE, 2001), R2P2, which is 50 fatalities with a frequency of 1 in 5,000 for the United Kingdom (UK), is estimated for the global population (5,566 fatalities based on 6.2×10^7 UK population and 6.9×10^9 population of the world) with frequency of 1 in 500,000 (based on $F=0.01\times(N)^{-1}$, which is the acceptable line for the UK on the FN-curve based on the R2P2 point, red line on Fig. 6.3). We put this point, R2P2, which is the HSE's acceptable criterion for engineering operations as a reference point (from Fig. 6.1, R2P2 is on the upper limit of all acceptable lines) to show that the earthquake disaster data is 5 orders of magnitude above the acceptable level of risk.

To construct a probability-consequence curve, the first step is to find the probability of failure of an earthquake disaster system. Probability of failure here is defined as the probability of exceeding 1,000 fatalities when earthquakes of magnitude greater than 5.5 occurs. First, we need to find the probability of failure of the earthquake disaster system, number of events with ≥1000 fatalities normalized by the total number of earthquakes worldwide with magnitude 5.5 and greater in the year of the events. We used ANSS earthquake catalogue (http://www.ncedc.org/anss/catalog-search.html) to gather the data for years between 1950 to 2013. The selection criteria for start time and date of the data was, start: 1950/01/01,00:00:00, end: 2013/01/01,00:00:00. Since the recorded number of earthquakes in ANSS between 1950 and 1963 is 10 times less than the average number of recorded earthquakes in the following years, assuming the same distribution function for the number of events per year, we estimated and simulated the number of earthquakes (of magnitude 5.5 and greater) before this time (1950-1973), based on the mean and standard deviation of the following years[27].

Fig. 6.4 shows the cumulative annual probability of failure of earthquake disasters (P_f) versus the number of fatalities due to earthquake disasters during the period 1950-2012. The marginally accepted line on Fig. 6.2a (from Baecher (1982)) is reproduced on Fig. 6.4 (blue line) to compare the cumulative P_f-N curve of earthquake disasters and the acceptable level of risk on the P_f-N curve of the industrial events. As shown, the difference between the overall probability of system failure in the earthquake disaster system (the black line) and the blue line is still more than 2

[27] The average number of events (M≥5.5) from 1973-2011 is 392 events per year and the standard deviation is 36.38. The number of events for 1950-1973 are randomly generated based on the Normal Distribution with these two parameters (mean and standard deviation).

orders of magnitude. Comparing the difference between the R2P2 criteria and the earthquake disaster data on Fig. 6.3 (around 5 orders of magnitude) with the 2 orders of magnitude difference on Fig. 6.4, we can conclude that the cumulative P_f-N curve shows a more compatible risk for earthquake disasters based on engineering risk acceptability.

In general, to decrease the probability of failure of earthquake disaster systems, according to Fig. 6.4, the frequency of events with more than 1000 fatalities has to be decreased. Furthermore, to decrease the probability of failure of large events, the slope of the curve has to be increased (>1, risk averse) which means increasing resistance of the system and decreasing the frequency of large events. In section 6.6, we propose reliability assessment as a new measure for societal risk assessment of natural disasters.

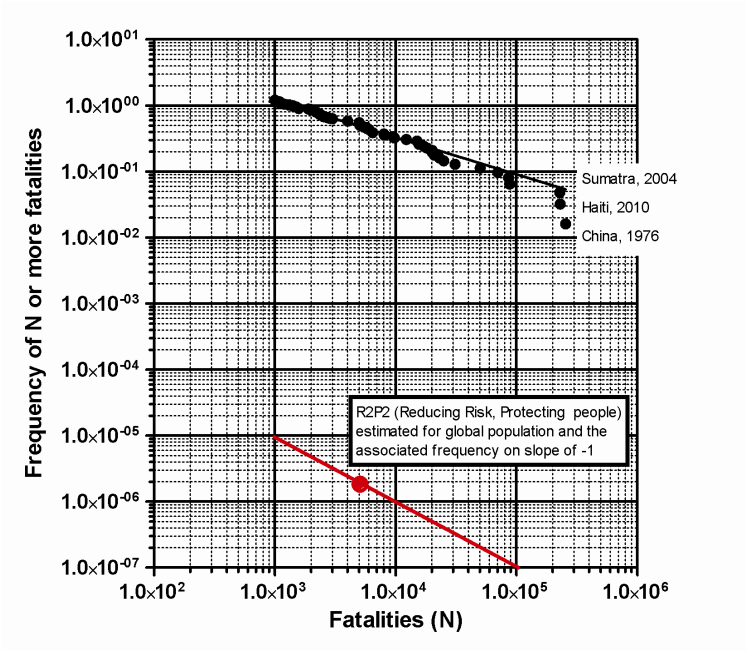

Figure 6.3: FN-curve of fatalities in earthquake disasters ($N \geq 1000$) black circles with fitted line of $F(N)=1.76 \times N^{-0.56}$. Note location of the Reducing Risk, Protecting People (R2P2) criterion (red dot) by Health and Safety Executive (HSE-2001) on the slope of -1 (red line), which is estimated for the current population of the world (~7 billion). Sumatra, 2004, Haiti, 2010 and China, 1976 are labeled as the three most fatal earthquake disasters in the period 1950-2012.

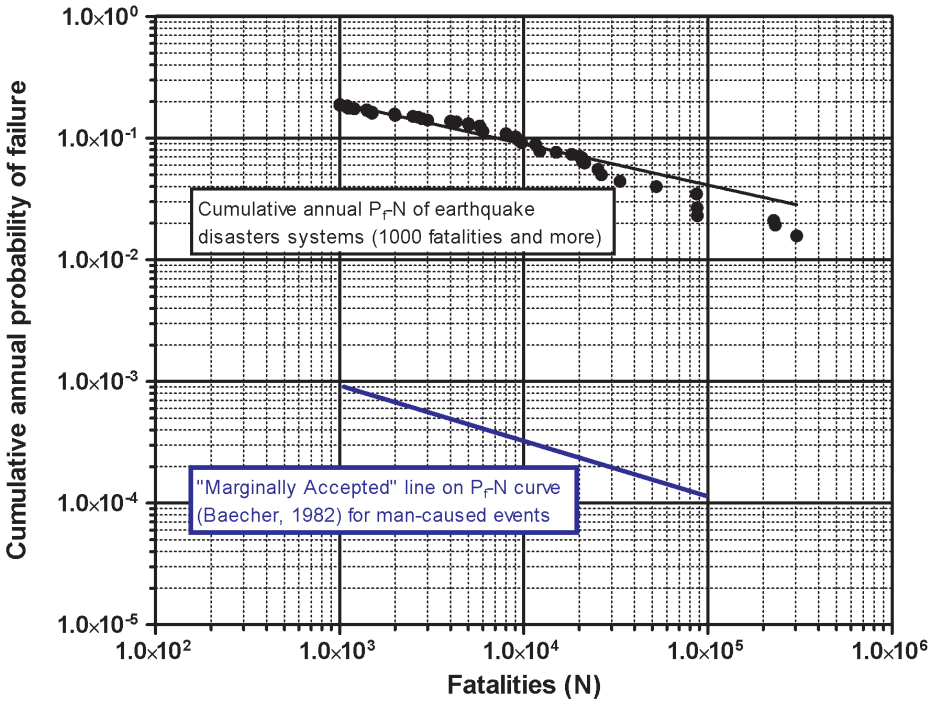

Figure 6.4: Cumulative P_f-N -curve of earthquake disasters (1950-2012), black dots, in comparison with the "Marginally Accepted" line on Fig. 6.2 from Baecher1982 (blue). The black line shows the trend of the annual probability of system failure in the earthquake disaster system ($P_f = 0.29\ N^{-0.34}$, R^2=0.96

6.6 Reliability of a natural disaster system

In the previous section, we compared the acceptable levels of risk according to the industrial-based methodologies and showed that on *FN*-curves, the risk of earthquake disasters systems is far above acceptable (Fig. 6.3). Using P_f instead of *FN* curve (dividing the annual frequency of exceedance of 1000 fatalities by the total number of earthquakes of magnitude 5.5 and greater at each year), we produced the annual probability of failure of earthquake disaster systems, decreases the difference between the marginally acceptable risk for man-caused events and the probability of failure of earthquake disaster systems (Fig. 6.4). This suggests that, the other risk assessment aspects in engineering related to probability of failure, such as reliability can be applied to the earthquake disaster system. Reliability is defined as the probability of success (or survival) (Wunderlich (2005), pg. 386). To evaluate the reliability of an earthquake disaster system, we define a reliability function. Here, we define a reliable earthquake disaster system as a system with no failure (fatalities greater than 1,000).

In order to estimate the reliability of earthquake disaster systems, first, we analyze the statistics of yearly earthquakes, disasters and consequences. Statistics of yearly number of earthquakes with magnitude 5.5 and greater shows that the number of recorded earthquakes has been stabilized at 393 between 1950 and 1991, a sharp increase between 1991 and 1996, and an increased trend since 1998 (Fig. 6.5). The significant increase of the number of earthquakes with magnitude M≥5.5 can be because of two reasons: 1) the threshold of fatalities for disasters as 1,000 fatalities might need to vary from years to years, or 2) the advancement of instruments for detecting the earthquakes.

Considering 1000 fatalities and greater as failure of earthquake disaster systems, the statistics of the frequency of the percentage of failure (Fig. 6.6) shows that the average percentage of failure is 0.003 per year[28] and the maximum percentage of failure is less than 0.015 per year. The percentage of failure is less than 0.006 in more than 90% of years, i.e., in most years the ratio of failure to the total number of events is less than 0.006.

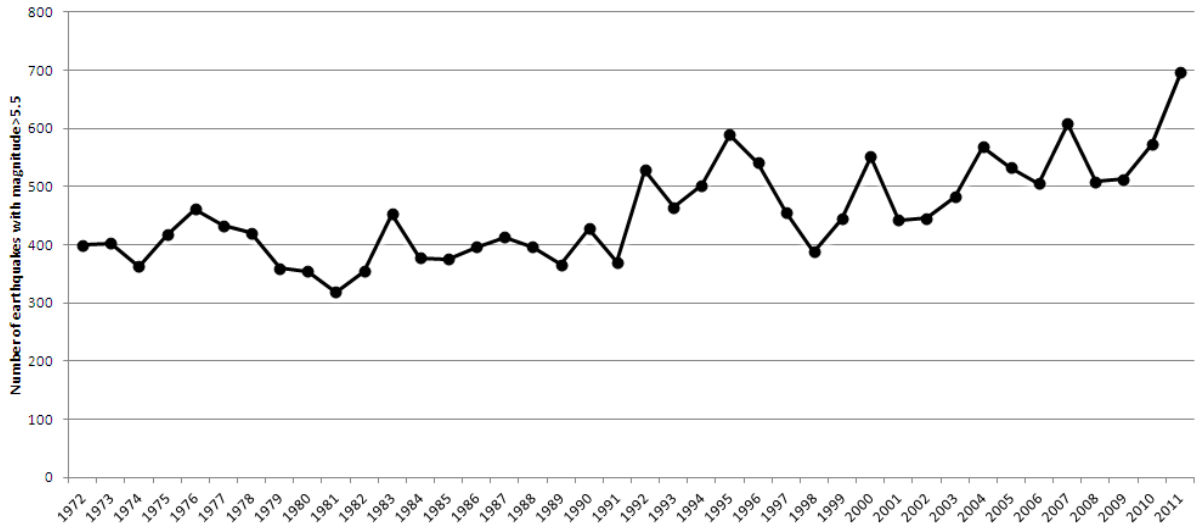

Figure 6.5: Yearly trend of earthquakes with magnitude 5.5 and greater occurrence (1950-2012).

[28] The average of 0.0027 is rounded to 0.003.

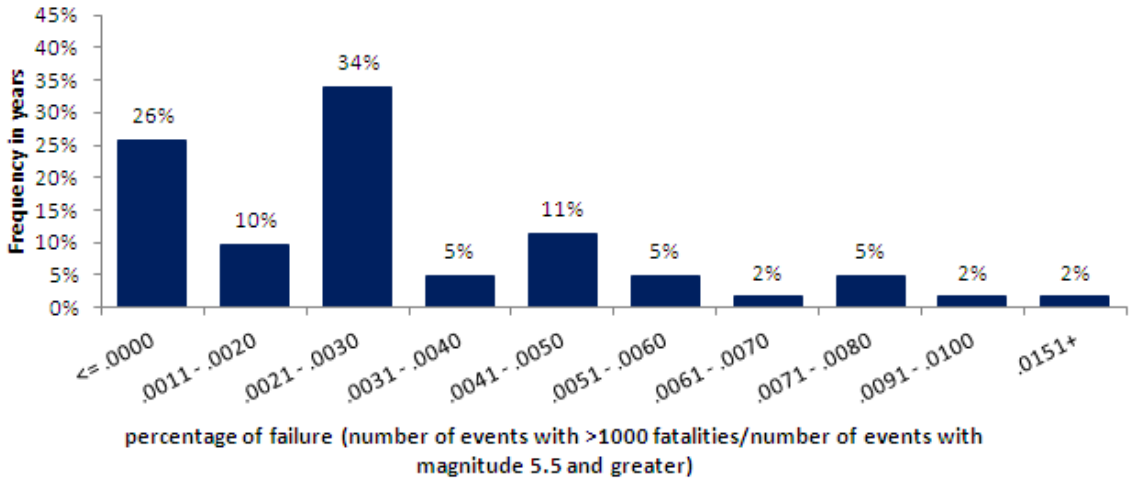

Figure 6.6: Frequency (in years under consideration) of the percentage of failure (number of earthquakes with more than 1000 fatalities/ number of earthquakes with magnitude 5.5 and greater).

The annual probability of failure can be modeled as a discrete random variable using the statistics of failure frequency. We first assume that each event with more than 1,000 fatalities (considered as failure here) represents an independent event in time and space, therefore, we could use a negative binomial distribution for the yearly failure of the system. This is similar to the analysis of the annual probability of levee failures in the Bay Delta done by Moss and Eller (2007). Woo (1999) (pg. 87) also states that negative binomial distribution has been used for describing loss distributions, epidemic spreading and contagious processes. Since all of these events' losses are categorized as discrete failures, the binomial distribution also can be used for our model. If F has a negative binomial distribution, Eq. 6.1 (Woo (1999), pg. 87) shows the general formula of the distribution:

$$Pr(F=k) \quad = \quad \binom{k+x-1}{k-1} p^k (1-p)^x \qquad (6.1)$$

Here, we consider the first event with more than 1000 fatalities in each year as the first failure in the row, therefore, the parameter k and consequently x are 1 (which is also equivalent to geometric distribution). We estimated the p parameter (overall probability of failure over 62 years of earthquake disaster data) as 0.00277 (same as black line on Fig. 6.4). Using the reliability function of the system defined as the probability of survival of the system, $R(t)$, over t times operation, Eq. 6.2 (Andrews and Moss, 2002),

$$R(t) = 1 - F(t) \quad (6.2)$$

where $F(t)$ is the cumulative annual failure probability distribution function (here, negative binomial), we could calculate the reliability of the earthquake disaster system (using parameter p) as a function of the number of earthquakes to occur till an earthquake kill more than 1,000 people. The reliability of the system at the current age is the probability that an earthquake will not kill 1,000 fatalities or greater till the end of the year given no deadly earthquake occurred so far.

The reliability of earthquake disaster system at the beginning of each year (at time 0 of each mission) is calculated based on the number of earthquakes (M≥5.5) at each year. The trend of the yearly reliability of earthquake disaster system illustrated in Fig. 6.5 shows an average of 0.3 which suggests unreliability of the system and a significant decreasing trend by factor of -0.007 per year (95% confidence interval: (-0.098, -0.005); p-value< 0.001). In order to increase the reliability of the system and to reduce the chance of deadly earthquakes, we need to reduce the probability of deadly earthquakes by increasing resistance of societies.

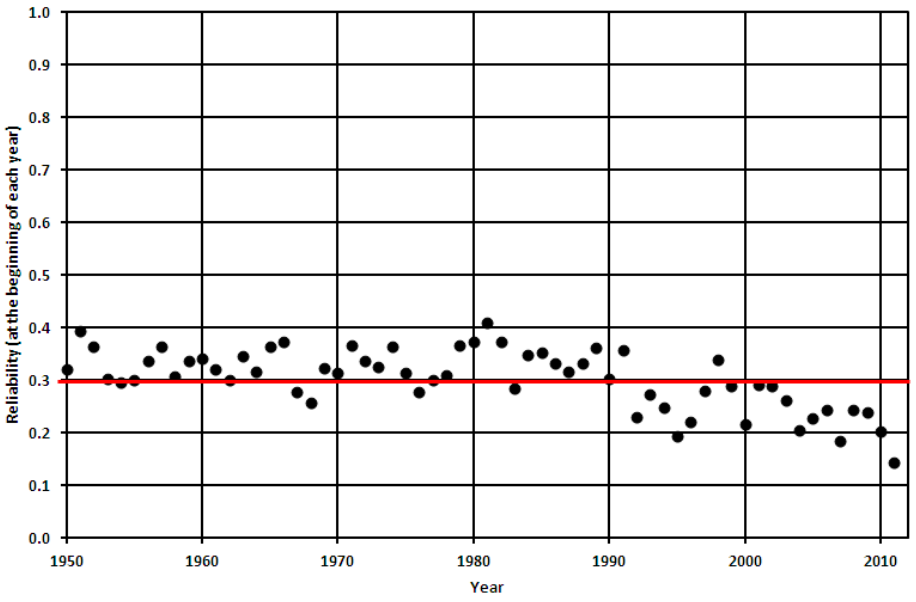

Figure 6.7: Yearly trend of reliability (1950-2012) at the beginning of each year based on overall failure rate of the system.

6.7 Summary and Discussion

In this paper, natural disasters are considered as systems that can cause harm to human life or environments. We compared natural disaster systems with industrial systems. As demonstrated in Fig. 6.1, the *FN*- criteria of two European countries appear far too conservative for natural disaster risk assessment. Considering the fact that the annual frequency of fatalities due to natural disaster events has been the basis of developing these criteria on *FN*-curves, it is not reasonable to use the same criteria for natural disaster risk assessment.

To reduce the risk of natural hazards, the only controllable parameters in the risk equation, *Risk*=*Hazard*×(1/*Resistance*)×*Exposure*, are *Exposure* and *Resistance*. In terms of *Exposure*, the controls can be applied in the form of mitigation. On the other hand, societal *Resistance* of the region, which is defined as the societal resilience of a society to the occurrence of a natural disaster, can be improved by technology, awareness and preparedness.

We also compared the P_f-N curve of earthquake disaster systems (N≥1000) to the acceptable level of risk in industry (marginally accepted line) in Fig. 6.4. We show that although the difference between the marginally accepted line and the annual probability of failure of global earthquake disasters is much smaller than on *FN*-curves, the earthquake disaster system is still not acceptable. Moreover, there is no significant correlation between the number of fatalities and the P_f. This is contrary to the assumption that is considered in industry.

Furthermore, we suggested a complementary method for global risk assessment of natural disasters. This method proposes that natural disasters are systems whose reliability can be analyzed similar to industrial set-ups. The essential component of this method is the record of failures of the system. We used the cumulative annual failure probability distribution function to estimate the reliability of the earthquake disaster system as a function of the number of earthquakes to occur till an earthquake kill more than 1,000 people. Our yearly trend of reliability (calculated at beginning of each year or at the 0 time of each mission) of earthquake disaster system illustrated in Fig. 6.5 is decreasing and shows an average of 0.3 which is a very unreliable system. Global reliability assessment can be a quantitative measure for natural hazard risk assessment as a complement to other societal risk measures.

In Chapter 5 of this thesis, we have shown that there is no evidence that the global societal resistance of earthquake disasters has been increasing or decreasing over the last 40 years. The decreasing trend of reliability in the earthquake disaster system suggests that the advancements in technologies for reducing consequences of earthquake disasters could only keep up with their pace of killing. However, since the ratio of the number of fatalities to the number of exposed population is also increasing or decreasing over this period, the main killing factor in the equation would be the number of exposed population. Therefore, either the pace of the increase in population needs to become slower, or more improvements in the technologies are required for staying ahead of the pace of population increase, in order to improve the reliability of the system.

*6.8 **Acknowledgements***

We would like to thank Dr. Yasaman H. Kashi (PhD. in Statistics, University of Waterloo, yasamankashi@alumni.uwaterloo.ca) for her helpful discussions on the statistical aspects of this work

Appendix IV (Generalized Pareto Distribution (GPD) fit to earthquake fatalities)

Methodology (based on Pisarenko and Rodkin, 2014):

Using Extreme Value Theory (EVT), and Generalized Pareto Distribution (GPD), Pisarenko and Rodkin (2014) illustrated how to estimate the probability of exceeding a certain threshold given the parameters of a GPD fit to a set of data of damages or losses of disasters whose distribution can be described by power-like laws with a heavy tail.

They also, based on some examples of natural hazards, suggest that the maximum possible (or observed) event is not a realistic estimation of loss for risk assessment, due to the instability of the M_{max} parameter which is a parameter used frequently in seismic risk assessment. Instead, the high level (e.g., 95%) q-value quantile of the GPD in the next τ years is a better estimation of risk since quantiles are more stable, robust characteristics.

Distributions of many natural processes, such as earthquake energy, and casualties from natural disasters, are often modeled by power-like laws, such as the Pareto distribution. The Pareto distribution function is as follows (Eq. 1.1 of Pisarenko and Rodkin, 2014):

$$F(x) = 1 - (\frac{h}{x})^{\beta}, x \geq h \qquad \text{(A.IX.1)}$$

where β is the exponent of the distribution. According to Pisarenko and Rodkin (2014), if $\beta \leq 1$, then the mathematical expectation of the corresponding random variable is infinite. Therefore, the mean and standard deviation of the distribution will be highly instable. These distributions are often called heavy tailed distributions. Losses of natural disasters follow these distributions.

If a sample is characterized by the Pareto distribution with index β, the maximum observed event parameter, $M^{(n)}_{max}=\max(x_1,\ldots,x_n)$, grows with the size of the sample as $n^{1/\beta}$. Pisarenko and Rodkin (2014) emphasize that:

"this tendency of a non-linear growth of $M^{(n)}_{max}$ with the sample size n or, equivalently, with the observation time span τ can be incorrectly interpreted as an evidence of a non-stationarity in time (Pisarenko and Rodkin, 2010). In many cases, the widespread belief that the rate of losses from natural disasters has a clear tendency of increasing with time is precisely connected with

the misinterpretation of this apparent non stationarity effect" (pg. 4, Pisarenko and Rodkin, 2014).

Pisarenko and Rodkin (2014) summarized some of the treatments of heavy-tailed data as:

1) **Using logarithms of original values**. Switching to logarithms (which can be done only when the original numerical values are positive) ensures almost always that all the statistical moments exist, and hence the Law of Large Numbers and the Central Limit Theorem are applicable to the sums of logarithms. It should be remarked that if X has the Pareto distribution, then log(X) has exactly exponential distribution.
2) **Using order statistics**: sample median, sample quantiles, interquartile range, etc. The main statistical tool suggested by Pisarenko and Rodkin (2014) for description of distribution tail—the family of quantiles $Q_q(\tau)$—is a continuous analog of the sample ordered statistics. This explains its robustness and stability.

Pisarenko and Rodskin (2014) model the sequence of disaster occurrences by Poisson point process. The effects of the disasters are different, such as fatalities and economic losses due to natural catastrophes, earthquake seismic moments and ground acceleration at a fixed point. These effects are called "marks" which are assigned to the occurrence times of the point Poisson process; marked point process. In our applications we shall model our catalog usually by a stationary Poisson process with intensity of λ events per year. The random number of events in stationary process for T years is a random Poisson variable with the mean λT.

Pisarenko and Rodskin (2014) use the total sum of events, $\Sigma_T \cong \lambda T.b + \xi.\sigma.(\lambda T)^{1/2}$, where ξ is some standard normal random variable, b is the expectation of a single event(>0), and σ is the standard deviation of a single event, to consider the ratio, R(T), of the total sum to the maximum event for T time period, $M_T \cong c.\log(\lambda T)$, where c is some constant, $R(T) = \frac{\Sigma_T}{M_T} \cong \left(\frac{b}{c}\right).\left(\frac{T}{\log(\lambda T)}\right)$.

This ratio for heavy-tailed distributions will grow slower than for light-tailed distributions. This means that the total sum is determined in a large extent by the single maximum event in heavy-tailed distributions. This result is important since in heavy-tailed distributions, the effect of large events is commonly downgraded due to their low frequency. However, their contribution, in long run is very effective, as this analogy shows.

In the statistics of natural hazards which are in the form of annual data, the conditional probability of x above h is:

$$GPD_h(x|\xi,s) = 1 - [1 + \left(\frac{\xi}{s}\right).(x-h)]^{-1/\xi}, x \geq h \quad \text{(A.IX.2)}$$

The distribution of $X_1>h$ (with probability of p with) which is distributed as GPD. Considering future maximum events, $M_\tau=\max(X_1,\ldots,X_\tau)$, for $x \geq h$, the distribution of X_1 is $(1-p)+p.GPD_h(x|\xi,s)$, and consequently, using $F_M(x)=q$, the q-level quantile $Q_q(\tau)$ of M_τ is as follows (eq. 2.44 in Pisarenko and Rodskin (2014)):

$$Q_q(\tau) = h + \left(\frac{s}{\xi}\right)\left[\left(\frac{1-q^{\frac{1}{\tau}}}{p}\right)^{-\xi} - 1\right], q > (1-p)^\tau \quad \text{(A.IX.3)}$$

where h is the threshold, s and ξ are parameters of GPD, p is the probability ($p \cong m/N$, where m is the number of events over a certain threshold (h), and N is the number of sequential years), q is the quantile value, τ is the time in future, and Q is the quantile of GPD.

Threshold of the data set can be picked based on the least kolmogrov-smirnov distance (KD) at which the GPD is the best fit to the data (Pisarenko and Rodskin, 2014). Pisarenko and Rodskin (2014) used earthquake fatalities in Japan to illustrate this method. They found the threshold of 2-fatalities is a reasonable threshold of life-loss in their study. They also estimated that the 95% quantile of expected life-loss in 10 years is 460,000 fatalities which is a reasonable estimation for the risk assessment purposes. We would apply this method to the earthquake disasters between 1950-2013 to estimate the best threshold for earthquake disasters.

Earthquakes disasters (1950-2013):

Here, we use NGDC significant earthquake database (http://www.ngdc.noaa.gov/nndc/struts/form?t=101650&s=1&d=1) for the period of 1950-2013 with criteria of minimum 1 fatality in earthquakes (n=947), to first, find the minimum threshold of earthquake losses that the data is best fitted to GPD. Then, using Eq. A.IX.3, we find the 95% quantile of fatalities in 10 years using the parameters of the best GPD fit in R. Fig. A.1 shows that the Kolmogorov-Smirnov distance (KD) versus various thresholds (10, 100, 150, 300, 500, 800, 1000, 1200, 1500, 1700, 2000, 2200, 2500, 2700, 3000, 3200, 3500, 3700, 4000, 5000). As

shown in Fig. A.1, the minimum KD after threshold of 1 is for 3,000 fatalities. However, since the other minimums of Fig. A.IX.1 include 300, 1,200, 2,000, and, 5000, and also we would like to minimize the threshold for life-loss risk assessment and every person's life counts, we also compare the 95% estimated quantile of these thresholds to see which one of these thresholds lead into the highest expected loss in 10 years.

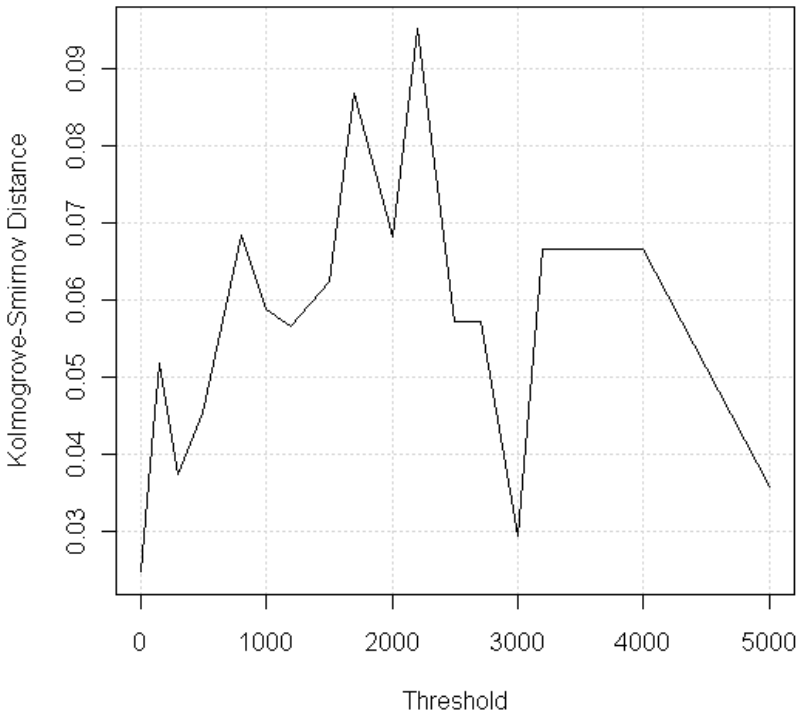

Figure A.IX.1 Kolmogorov-Smirnov distance versus thresholds of fatalities (10,100,150,300,500,800,1000,1200,1500,1700,2000,2200,2500,2700,3000,3200,3500,3700,4000,5000) in the 947 data of with fatalities greater than 1 (data source: NGDC).

Fig. A.IX.2 illustrates the comparison between the 95% quantile values of GPD in 10 years for various thresholds. This shows that after threshold of 1, the highest 95% quantile is for 1,000 fatalities. Therefore, we pick the threshold of 1,000 in our further risk assessment analysis and as the threshold of failure in a natural disaster system.

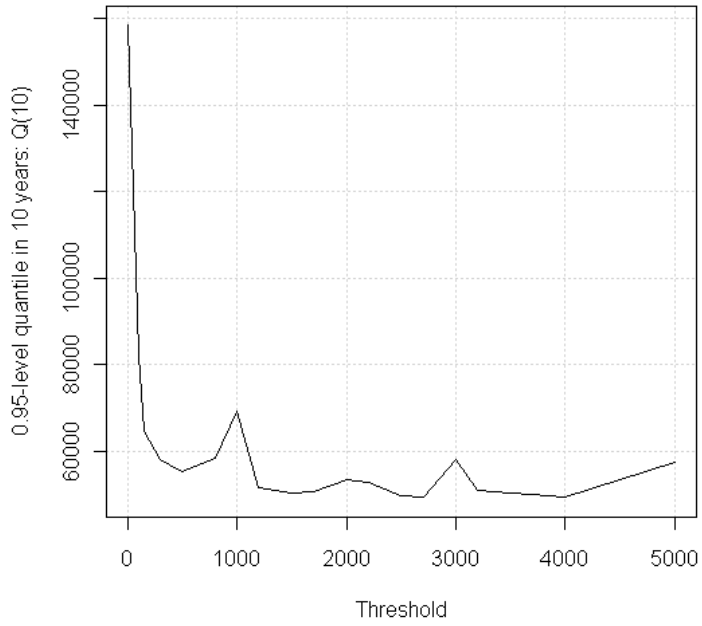

Figure A.IX.2 0.95% quantile value of GPD in 10 years considering thresholds thresholds of fatalities (10,100,150,300,500,800,1000,1200,1500,1700,2000,2200,2500,2700,3000,3200,3500,3700,4000,5000) in the 947 data of with fatalities greater than 1 (data source: NGDC)

Chapter 7 Synthesis

7.1 Introduction

This thesis is intended to provide a better understanding of effective parameters for the assessment of risk in natural disasters. Risk assessment strategies available in engineering are considered. In particular, the focus is on geological disasters, especially earthquakes. Possible quantified modifications to the current risk assessment methods and criteria are analyzed and applied for natural disaster risk assessment. Driving each chapter is the rationale that by better understanding the underlying concept of risk, statistical, spatial and temporal distribution of losses, and the available risk measures, we can improve the risk assessment strategies for natural hazards. To this end, the main conclusions from each chapter are summarized below.

7.2 Review of FN-curves for natural hazard risk assessment

Chapter 2 reviewed the background of FN-curves, their underlying concepts and mathematics, in literature. We show that FN-criteria are adequate, mathematically, and provide a useful basis for (comparative) risk assessment. However, to have a frame-independent approach, normalization of FN-curves based on exposed population is a reasonable option. We used real natural hazard data on European countries as an example to compare risk of natural hazards with acceptable levels of risk in Europe. We used the population of certain countries to normalize the FN-curves and suggested that the normalized FN-curves can be more informative in terms of the preparedness of the underlying societies. We found that the available European acceptable levels of the risk are far too conservative for risk assessment of natural hazards.

Furthermore, the slopes of FN-curves generated from real-data of natural hazards all are in the same range of around 0.5. This suggests that, first, natural hazards cause risk-prone situations (slope<1), and second, aside from their origins, a certain slope on their frequency-fatality graphs universally imposes the background effect of natural hazards.

7.3 Concept of Resistance and Haiti 2010

Chapter 3 introduced the concept of resistance from two perspectives: 1) from modification of risk equation (*Risk=Hazard*×(1/*Resistance*)×*Exp.Pop*) and 2) from the slope of the FN-curves. By equating these two definitions, we derived the main resistance equation, R, which increases by the increase of the slope of the FN-curve.

We defined two types of resistance, country-specific resistance, R_c, and event-specific resistance, R_e, both derived from the main resistance equation, R. For the country-specific resistance, we have to find the best fit to the FN-curve of the past events of the country. Furthermore, we need to estimate the probability of hazard, here probability of exceeding a certain magnitude. We compared the R_c of Iran, Japan, and Haiti which shoed that Haiti has the lowest resistance.

For the event-specific resistance, we need to consider the daily death rate of the country at the time of the event. The probability of hazard at the location of the most important city of the affected region is also required; here probability of exceeding a certain peak ground acceleration. We compared the R_e of Kobe (1995), and Bam (2003) with the Haiti (2010) which showed that Bam had the lowest resistance among the three events. The difference between R_c and R_e and particularly $R_e<R_c$ shows that the studied event has been an anomaly to the country that occurred in. For the case of Haiti 2010, the difference is very small, especially when we consider the 65,000-fatalities scenario, instead of 230,000-fatalities. This suggests that, the event of Haiti 2010 was not an anomaly with respect to the country's background and preparedness.

In this chapter, we also used the equation of resistance to calculate the actual gridded resistance of the commune of Port au Prince after the 2010 Haiti earthquake as a case study for resistance calculation on a local level. We also estimated the total fatalities in the commune of Port au Prince based on the destruction maps and estimation of 1.5 deaths/buildings destructed. We showed that the total of 230,000 fatalities is not a reasonable estimate for Haiti, since the range of fatalities that we estimated for the commune of Port au Prince, which is the most destructed commune at the occurrence of the 2010 earthquake, is between 26,778 and 65,851.

7.4 Magnitude and frequency of geological disasters

Chapter 4 summarizes the magnitude-frequency relationships in all geological disasters, earthquakes, tsunamis, landslides and volcanic activities. We, first, introduced a unified scale for comparison of geological hazards based on the source energy of the events. We found that the total energy that volcanic eruptions that cause more than 1,000 fatalities (disasters) release is the highest among the other geological hazards. Furthermore, we calculated the energy-efficiency of geological hazards in causing disasters. Based on our data, we found that tsunamis have the highest energy-efficiency.

To compare the risk that these hazards impose on human life with each other, we used FN-curves and showed that geological disasters are dominated by earthquake disasters. Furthermore, the slopes of FN-curves in geological disasters are all less than 1.0, which suggests that they are mainly controlled by large events.

We also introduced a new parameter, called risk factor (RF) which is conducted based on the inverse of the slope of the FN-curves and the frequency of exceedance of 1,000 fatalities of the geological disasters. RF of earthquake disasters is the highest; the next most risky geological disasters are tsunamis, volcanic activities and landslides, in descending order.

Furthermore, we showed that frequency of events with more than 1000 fatalities has increased significantly by factor of 0.004 since 1600 while we could not find any significant proof that the total energy-release by geological disasters and the energy-efficiency of the geological disasters have been decreasing or increasing during this period.

7.5 Global societal earthquake resistance

Chapter 6 is devoted to investigating the global trend of earthquake resistance since 1973. We developed a simple risk-based conceptual model. In order to develop this model, we carried out a survey of global earthquake events, and introduced the concept of “global societal earthquake resistance". In our proposed approach, there are three main determinants of global societal earthquake resistance: the hazard (overall energy release by earthquakes with $M \geq 5.5$ per year), the number of fatalities and the exposed

population. We statistically tested the temporal trend of all three components. Furthermore, we showed that, according to our data, the annual ratio of earthquake casualties to exposed populations did not increase or decrease during the relevant period. This is in contrast to the decreased total number of deaths per year per 1000 people (crude death rate)which has decreased during the same period of time. Although the energy release by earthquakes increased since 1973, the temporal trend of the societal resistance of earthquake disasters did not increase or decrease significantly.

7.6 Risk and reliability in a natural disaster system

In Chapter 7, we first compared the engineering P_f-N curves with the similar curve of earthquake disasters. We showed that there is no correlation between the number of fatalities and probability of failure in earthquake disaster system. We also suggested improvements in the risk assessment methodologies used for natural hazard systems by borrowing a relevant idea (reliability) from engineering studies. Reliability of a system is defined as the probability of survival of that system over a certain period of time. We examined the reliability of the world due to earthquake disasters over 1950-2012. We estimated the probability distribution function of failure of the system (negative binomial) to evaluate reliability as a function of earthquakes to occur till more than 1,000 fatalities killed by earthquakes. The temporal trend of yearly reliability (at the beginning of each year) of the earthquake disaster system has been significantly decreasing since 1950. The temporal trend shows an average of around 0.3, which is an unreliable system comparing to the reliability assessment criteria defined for industrial settings (0.9).

7.7 Future Work

In this thesis, we have illustrated a simple quantitative risk-based approach to natural hazards. We have shown that in the case of natural hazards, the response of societies to natural hazards can be summarized in the losses and resistance of the underlying society. In order to improve this method and to advance our ability to quantify risk, knowing detailed physical properties of each hazard is essential, and particularly, the effect of a specific hazard on a specified society (e.g., the effect of landslides (Fig. 7.1) in a village in Italy (Arattano et al., 2010)) and, the effect of human activity on the occurrence of a

specific hazard (e.g., the effect of deforestation (Fig. 7.2) on the occurrence of landslides in New Zealand (Glade, 2003))

Figure 7.1: landslide occurred in Villar Pellice, near Turin, Piemonte Region, Italy on 29 May 2008 (photo: EPA/Tonino Di Marco)

Figure 7.2: Deforestation in New Zealand (South Island- Tasman, Westcoast) (photo: Martin Wegmann)

Furthermore, the secondary effects of natural hazards that have not been considered in risk assessment before need to be added to the risk calculations. For example, one of the known effects of a tsunami on a society other than fatalities is considered to be water

damage to properties. However, in the recent tsunami in Japan (2012), the secondary effect of the tsunami was the destruction of nuclear power plants and consequent nuclear contamination of water. These are unpredicted effects that need to be considered in future risk assessments.

The effect of infrastructural characteristics of a society on a disaster is another component affecting risk that needs to be considered and quantified for risk assessment purposes. As Bilham (2010) said about the 2010 Haiti earthquake, “corruption kills”. For example, in the case of any huge future earthquake in Tehran, the secondary effects need to be analyzed since the infrastructure of the city is not well developed (Nateghi-A, 2001).The risk of life loss would be very high since Tehran is the capital of Iran and consequently the heart-holding hospitals, businesses and the government; it is also located at the base of mountain foothills, which makes escaping for people almost impossible.

One way to include more details in the risk calculations is using more accurate data for risk assessment. Dasymetric mapping method (based on land-cover data) that in a separate project I used for the spatial analysis of earthquake fatalities in the Middle East is an example illustrating the importance of this point. Further analysis on the controlling factors of risk is also essential.

We hope that this thesis could brought about some of the major issues for the risk assessment of natural hazards helpful for further investigations and could connect science with policy in a new perspective.

References

Abe, K. (1989). Quantification of tsunamigenic earthquakes by the mt scale. Tectonophysics, 166:27 – 34.

Abrahamsson, M. and Johansson, H. (2006). Risk preferences regarding mul-tiple fatalities and some implications for societal risk decision making—an empirical study. Journal of Risk Research, 9(7):703–715.

Adger, W. N. (2006). Vulnerability. Global Environmental Change, 16(3):268–281.

Ale, B. (2005). Tolerable or acceptable: A comparison of risk regulation in the United Kingdom and in the Netherlands. Risk Analysis, 25(2):231–241.

Ale, B., Laheij, G., and de Haag, P. U. (1996). Zoning instruments for major ac-cident prevention. In Cacciabue, C. and Papazoglou, I., editors, Probabilistic Safety Assessment and Management, ESREL 96, page 1911.

Ambraseys, N. and Bilham, R. (2011). Corruption kills. Nature, 469(7329):153– 155.

Anbarci, N., Escaleras, M., and Register, C. A. (2005). Earthquake fatalities: the interaction of nature and political economy. Journal of Public Economics, 89(9):1907–1933.

Andrews, J. and Moss, T. (2002). Reliability and Risk Assessment. American Society of Mechanical Engineering.

Arattano, M., Conte, R., Franzi, L., Giordan, D., Lazzari, A., and Luino, F. (2010). Risk management on an alluvial fan: a case study of the 2008 debris-flow event at villar pellice (piedmont, n-w italy). Natural Hazards and Earth System Science, 10(5):999–1008.

Aven, T. (2011a). On the new iso guide on risk management terminology. Reliab. Eng. Syst. Saf., 96(7):719 – 726.

Aven, T. (2011b). Quantitative Risk Assessment: The Scientific Platform. Cam-bridge University Press.

Aven, T. and Renn, O. (2009). The role of quantitative risk assessments for char-acterizing risk and uncertainty and delineating appropriate risk management options, with special emphasis on terrorism risk. Risk Analysis, 29(4):587– 600.

Baecher, G. B. (1982). Playing the odds in rock mechanics. In Proceedings 23rd Symposium on Rock Mechanics, pages 67–85, New York, NY, USA. Soc of Min Eng of AIME. CD: PSRMA; NU: 13454135.

Baecher, G. B. and Christian, J. T. (2003). Reliability and Statistics in Geotech-nical Engineering. John Wiley and Sons.

Baek, S. K., Bernhardsson, S., and Minnhagen, P. (2011). Zipf's law unzipped. New Journal of Physics, 13(4):043004.

Ball, D. and Floyd, P. (1998). Societal risks, final report. Available from Health and Safety Executive, Risk Assessment; Policy Unit, 2 Southwark Bridge, London SE1 9HS.

Ballard, G. (1993). Guest editorial: Societal risk–progress since farmer. Relia-bility Engineering & System Safety, 39(2):123 – 127.

Bangash, Y. (2011). Earthquake Resistant Buildings: Dynamic Analyses, Numerical Computations, Codified Methods, Case Studies and Examples. Springer.

Bardet, J.-P., Synolakis, C. E., Davies, H. L., Imamura, F., and Okal, E. A. (2003). Landslide tsunamis: Recent findings and research directions. Pure and Applied Geophysics, 160:1793–1809.

Beattie, J. (1967). Risks to the population and the individual from iodine releases. Nuclear Safety, 8(6):573.

Bender, S. (1991). Primer on natural hazard management in integrated regional development planning. Organization of American States. Dept. of Regional Development and Environment and United States. Agency for International Development. O*ffi*ce of U.S. Foreign Disaster Assistance.

Berk, R. and MacDonald, J. M. (2008). Overdispersion and poisson regression. Journal of Quantitative Criminology, 24(3):269–284.

Bernstein, P. (1998). Against the Gods: The Remarkable Story of Risk. Wiley.

Bilham, R. (1988). Earthquakes and urban growth. Nature, 336(6200):625–626.

Bilham, R. (1996). Global fatalities from earthquakes in the past 2000 years: prognosis for the next 30. In Rundle, J., Turcotte, D., and Klein, W., editors, Reduction and predictability of natural disasters: proceedings of the workshop of Reduction and Predictability of Natural Disasters held January 5-9, 1994 in Santa Fe, New Mexico, volume XXV of SANTA FE INSTITUTE STUD-IES IN THE SCIENCES OF COMPLEXITY PROCEEDINGS, pages 19–31. Addison-Wesley.

Bilham, R. (2004). Urban earthquake fatalities: A safer world, or worse to come? Seismological Research Letters, 75(6):706–712.

Bilham, R. (2009). The seismic future of cities. Bulletin of Earthquake Engi-neering, 7:839–887.

Bilham, R. (2010). Lessons from the haiti earthquake. Nature, 463(7283):878– 879.

Birkmann, J. (2006). Measuring vulnerability to natural hazards : towards dis-aster resilient societies. United Nations University.

Blong, R. (2009). Country natural hazard and vulnerability assessment proce-dure, consultant's report rsc-c80366 (aus). Technical report.

Bolt, H., MacDonald, G., and Scott, R. (1977). Geological Hazards; Revised, 2nd Edition. Springer-Verlag.

Boore, D. M. and Atkinson, G. M. (2008). Ground-motion prediction equations for the average horizontal component of pga, pgv, and 5%-damped psa at spectral periods between 0.01 s and 10.0 s. Earthquake Spectra, 24(1):99–138.

Bottelberghs, P. (2000). Risk analysis and safety policy developments in the netherlands. Journal of Hazardous Materials, 71(1–3):59 – 84.

Carter, D. (1995). The scaled risk integral- a simple numerical representation of case societal risk for land use planning in the vicinity of major accident hazards. Loss Prevention in the Process Industries, 2:219–224.

Cassidy, K. (1996). Risk criteria for the siting of hazardous installations and the development in their vicinity. In Proc. ESREL/PSIAM, Crete, page 1892.

Cavalcante, H. L. d. S., Oriá, M., Sornette, D., Ott, E., and Gauthier, D. J. (2013). Predictability and suppression of extreme events in a chaotic system. Physical Review Letters, 111(19):198701.

Cavallo, E., Galiani, S., Noy, I., and Pantano, J. (2010). Catastrophic natural disasters and economic growth.

CCPS (2000). Guidelines for chemical process quantitative risk analysis (2nd edition). CCPS Guidelines series. American Institute of Chemical Engineers (AIChE). Center for Chemical Process Safety (CCPS).

CCPS (2009). Guidelines for Developing Quantitative Safety Risk Criteria. American Institute of Chemical Engineers, Center for Chemical Process Safety (CCPS), John Wiley & Sons.

Chambers, J. and Hastie, T. (1992). Statistical models in S . Wadsworth &Brooks/Cole computer science series.

Christian, J. (2004). Geotechnical engineering reliability: How well do we know what we are doing? J. Geotech. Geoenviron. Eng., 130(10):985–1003.

Clauset, A., Shalizi, C. R., and Newman, M. E. J. (2009). Power-law distribu-tions in empirical data. SIAM Review, 51(4):661–703.

Corbane, C., Saito, K., DellÕOro, L., Gill, S., Piard, B., Huyck, C., Kemper, T., Lemoine, G., Spence, R., Krishnan, R., et al. (2011). A comprehensive analysis of building damage in the january 12, 2010 mw7 haiti earthquake us-ing high-resolution satellite and aerial imagery. Photogrammetric Engineering and Remote Sensing (PE&RS), 77(10).

Cox, D. C. and Baybutt, P. (1982). Limit lines for risk. Nuclear Technology, 57:320.

Cutter, S. L. (1996). Vulnerability to environmental hazards. Progress in Human Geography, 20(4):529–539.

Cutter, S. L., Boruff, B. J., and Shirley, W. L. (2003). Social vulnerability to environmental hazards. Social Science Quarterly, 84(2):242–261.

Debesse, L. (2007). The Use for Frequency-consequence Curves in Future Reac-tor Licensing. Massachusetts Institute of Technology, Department of Nuclear Science and Engineering; and, (S.M.)–Massachusetts Institute of Technology, Engineering Systems Division, Technology and Policy Program.

Degg, M. (1992). Natural disasters: recent trends and future prospects, vol-ume 77. National Emergency Training Center.

Delaney, K. (2011). Destruction of the city of port au prince from haiti 2010 earthquake. Technical report.

Dilley, M., Chen, R., Deichmann, U., Dilley, M., Lerner-Lam, A. L., and Arnold, M. (2005). Natural disaster hotspots: a global risk analysis. Number pt. 611 in Disaster risk management series. World Bank.

Doocy, S., Cherewick, M., and Kirsch, T. (2013a). Mortality following the haitian earthquake of 2010: a stratified cluster survey. Population health metrics, 11(1):5.

Doocy, S., Daniels, A., Packer, C., Dick, A., and Kirsch, T. D. (2013b). The human impact of earthquakes: a historical review of events 1980-2009 and systematic literature review. PLoS Currents, 5.

Dowrick, D. J. (2009). Earthquake resistant design and risk reduction. Wiley.

Du, B., Xi, X., Kang, Y., Weng, L., and (2009). Natural disaster. In Gullo, A., Lumb, P. D., Besso, J., and Williams, G. F., editors, Intensive and Critical Care Medicine, pages 379–390. Springer Milan.

Dunning, S., Mitchell, W. A., Rosser, N. J., and Petley, D. N. (2007). The hattian bala rock avalanche and associated landslides triggered by the kashmir earthquake of 8 october 2005. Engineering Geology, 93(3):130–144.

Eberhard, M. O., Baldridge, S., Marshall, J., Mooney, W., and Rix, G. J. (2010). The mw 7.0 haiti earthquake of january 12, 2010: Usgs/eeri advance recon-naissance team report. U.s. geological survey open-file report 2010Ð1048, U.S. Geological Survey.

Eijs, R. V., Mulders, F., Nepveu, M., Kenter, C., and Scheffers, B. (2006). Correlation between hydrocarbon reservoir properties and induced seismicity in the netherlands. Engineering Geology, 84(3–4):99 – 111.

Evans, A. and Verlander, N. Q. (1998). What is wrong with criterion fn-lines for judging the tolerability of risk? Risk Analysis, 17(2):157–168.

Evans, S. (2006). Single-event landslides resulting from massive rock slope fail-ure: characterising their frequency and impact on society. In Landslides from Massive Rock Slope Failure, pages 53–73. Springer.

Evans, S. and DeGraff, J. (2002). Catastrophic Landslides: Effects, Occurrence, and Mechanisms. Number v. 15 in Reviews in Engineering Geology. Geological Society of America.

Evans, S. G. (2008). Landslide disasters 1000-2008 a.d. Technical report.

Evans, S. G. (2011). Tsunami disasters 1600-2011 a.d. Technical report.

Evans, S. G. and Alcantara-Ayala, I. (2007). Disasters resulting from landslides, snow avalanches, and geotechnical failures in north america (canada, united states, and mexico) 1841-2006: a first assessment. In Turner, A. K. and Schuster, R. L., editors, Landslide and Society, pages 3–23. Association of Engineering Geologists Special Publication 22.

Farmer, F. (1967a). Reactor safety and siting: A proposed risk criterion. Nuclear Safety, 8(6):539.

Farmer, F. (1967b). Siting criteria-a new approach. Atom, 128:152–166.

Farmer, F. (1980). Safety and risk. The Journal of the Royal Society for the Promotion of Health, 100(4):133–137.

Farmer, F. R., K. D. J. and Andrews, D. (1981). Experience in the quantifica-tion of engineering risks [and discussion]. Proceedings of the Royal Society of London. A. Mathematical and Physical Sciences, 376(1764):103–119.

Fell, R., Ho, K., Lacasse, S., and Leroi, E. (2005). A framework for landslide risk assessment and management. In Hungr, O., Fell, R., and Couture, R., editors, Landslide Risk Management, pages 3–26. Taylor & Francis Group, London.

Ferreira, J. and Slesin, L. (1976). Observations on the social impact of large accidents. Technical report 122, Operations Research Center, Massachusetts Institute of Technology, Cambridge, Mass.

GAR (2011). Global assessment report on disaster risk reduction: Revealing risk, redefining development. Technical report, International Safety for Dis-aster Reduction, United Nations Global Assessment Report on Disaster Risk Reduction.

Ghahramani, N. (2011). Seismic hazard assessment for the city of port au prince. Technical report.

Glade, T. (2003). Landslide occurrence as a response to land use change: a review of evidence from new zealand. Catena, 51(3-4):297–314.

Glade, T., Anderson, M., and Crozier, M. (2005). Landslide hazard and risk. J. Wiley.

Griffths, R. and Fryer, L. (1979). World-wide data on the incidence of multiple-fatality accidents. UKAEA Report SRD R149. London.

Griffths, R. F. (1981). Dealing with RISK;The planning, management and acceptability of technological risk. Manchester University Press.

Groningen (May 1978). Criteria for risks related to dangerous goods. Technical report.

Grünthal, G., Thieken, A., Schwarz, J., Radtke, K., Smolka, A., and Merz, B. (2006). Comparative risk assessments for the city of cologne – storms, floods, earthquakes. Natural Hazards, 38:21–44.

Gutenberg, B. and Richter, C. F. (1942). Earthquake magnitude, intensity, energy, and acceleration. Bulletin of the Seismological Society of America, 32(3):163–191.

Gutenberg, B. and Richter, C. F. (1944). Frequency of earthquakes in california.

Bulletin of the Seismological Society of America, 34(4):185–188.

Gutenberg, B. and Richter, C. F. (1956). Earthquake magnitude, intensity, energy, and acceleration. Bulletin of the Seismological Society of America, 46(2):105–145.

Guthrie, R., Deadman, P., Cabrera, A. R., and Evans, S. (2008). Exploring the magnitude–frequency distribution: a cellular automata model for landslides. 5(1).

Gutierrez, E., Taucer, F., De Groeve, T., Al-Khudhairy, D. H. A., and Zaldivar, J. M. (15 June 2005). Analysis of worldwide earthquake mortality using mul-tivariate demographic and seismic data. American Journal of Epidemiology, 161(12):1151–1158.

Guzzetti, F., Malamud, B. D., Turcotte, D. L., and Reichenbach, P. (2002). Power-law correlations of landslide areas in central italy. Earth and Planetary Science Letters, 195(3):169–183.

Hagon, D. O. (1984). Use of frequency-consequence curves to examine the conclusions of published risk analyses and to define broad criteria for major hazard installations. Chemical Engineering Research and Design, 62(6):381– 386. Cited By (since 1996): 5.

Hayes, G., Briggs, R., Sladen, A., Fielding, E., Prentice, C., Hudnut, K., Mann, P., Taylor, F., Crone, A., Gold, R., et al. (2010). Complex rupture during the 12 january 2010 haiti earthquake. Nature Geoscience, 3(11):800–805.

Helbing, D. (2013). Globally networked risks and how to respond. Nature, 497(7447):51–59.

Hirst, I. (1998). Risk assessment a note on f–n curves, expected numbers of fatalities, and weighted indicators of risk. Journal of Hazardous Materials, 57(1-3):169 – 175.

Ho, C.-H. (1996). Volcanic time-trend analysis. Journal of Volcanology and Geothermal Research, 74(3–4):171 – 177.

Holling, C. S. (1973). Resilience and stability of ecological systems. Annual review of ecology and systematics, 4:1–23.

Holzer, T. L. and Savage, J. C. (2013). Global earthquake fatalities and popu-lation. Earthquake Spectra, 29(1):155–175.

Hong-Kong (1994). Practice note for professional persons, potentially hazardous installations, ProPECC, PN 2/94. Technical report.

Horn, M. E. T., Fulton, N., and Westcott, M. (2008). Measures of societal risk and their potential use in civil aviation. Risk Anal., 28(6):1711–1726.

Houtsonen, L. and Peltonen, A. (2007). Natural disasters in europe. In Lidstone, J., Dechano, L. M., and Stoltman, J. P., editors, International Perspectives on Natural Disasters: Occurrence, Mitigation, and Consequences, volume 21 of Advances in Natural and Technological Hazards Research, pages 263–280. Springer Netherlands.

HSE (1978). Canvey: an investigation of potential hazards from operations in the canvey island/thurrock area. Technical report, Health and Safety Execu-tive, London.

HSE (1989). Risk Criteria for Land-Use Planning in the Vicinity of Major Industrial Hazards. Great Britain. Health and Safety Executive and Health And Safety Executive Staff, H.M. Stationery Office.

HSE (1992). Risk: Analysis, Perception and Management. Royal Society (Great Britain).

HSE (2001). Reducing Risk, Protecting People. Health and Safety Executive Books.

Hungr, O. and Wong, H. N. (2007). Landslide risk acceptability criteria: Are f-n plots objective? Geotechnical News, 25(4):47–50.

IHSI (2009). Population totale, population de 18 ans et plus menages et densites estimes en 2009. Technical report.

IoCE (1985). Nomenclature for Hazard and Risk Assessment in the Process Industries. Engineering Practice Committee. Working Party and Institution of Chemical Engineers (Great Britain).

Jackson, J. (2006). Fatal attraction: living with earthquakes, the growth of villages into megacities, and earthquake vulnerability in the modern world.

Philosophical Transactions of the Royal Society A: Mathematical, Physical and Engineering Sciences, 364(1845):1911–1925.

Jaiswal, K., Wald, D. J., and Hearne, M. (2009). Estimating casualties for large earthquakes worldwide using an empirical approach [electronic resource]. U.S. Geological Survey.

Jaiswal, K. S., Wald, D. J., Earle, P. S., Porter, K. A., and Hearne, M. (2011a). Earthquake casualty models within the usgs prompt assessment of global earthquakes for response (pager) system. In Spence, R., So, E., and Scawthorn, C., editors, Human Casualties in Earthquakes, volume 29 of Ad-vances in Natural and Technological Hazards Research, pages 83–94. Springer Netherlands.

Jaiswal, P., Van Westen, C., and Jetten, V. (2011b). Quantitative estimation of landslide risk from rapid debris slides on natural slopes in the nilgiri hills, india. Natural Hazards and Earth System Sciences, 11:1723–1743.

Jonkman, S. (2007). Loss of life estimation in flood risk assessment theory and application. Doctoral Thesis. ISBN 978-90-9021950-9.

Jonkman, S., Lentz, A., and Vrijling, J. (2010). A general approach for the estimation of loss of life due to natural and technological disasters. Reliability Engineering & System Safety, 95(11):1123 – 1133.

Jonkman, S., van Gelder, P., and Vrijling, J. (2003). An overview of quantitative risk measures for loss of life and economic damage. J. Hazard. Mater., 99(1):1– 30.

Juang, C., Phoon, K., Puppala, A., Green, R., and Fenton, G. (2011). GeoRisk 2011: Geotechnical Risk Assessment & Management. Geotechnical Special Publication. American Society of Civil Engineers.

Kagan, Y. Y. (1997). Earthquake size distribution and earthquake insurance. Communications in Statistics. Stochastic Models, 13(4):775–797.

Kagan, Y. Y. and Knopoff, L. (1980). Spatial distribution of earthquakes: the two-point correlation function. Geophysical Journal of the Royal Astronomical Society, 62(2):303–320.

Kagan, Y. Y. and Knopoff, L. (1987). Random stress and earthquake statistics: time dependence. Geophysical Journal of the Royal Astronomical Society, 88(3):723–731.

Kahn, M. E. (2005). The death toll from natural disasters: the role of income, geography, and institutions. Review of Economics and Statistics, 87(2):271– 284.

Kanamori, H. (1977). The Energy Release in Great Earthquakes. Journal of Geophysical Research, 82(20):2981–2987.

Kanamori, H. (1983). Magnitude scale and quantification of earthquakes. Tectonophysics, 93(3–4):185 – 199.

Kanamori, H. and Brodsky, E. E. (2004). The physics of earthquakes. Reports on Progress in Physics, 67(8):1429.

Kaplan, S. and Garrick, B. J. (1981). On the quantitative definition of risk. Risk Analysis, 1(1):11–27.

Kemper, T., Lemoine, G., Corbane, C., Gill, S., Eguchi, R., Bjorgo, E., and DellOro, L. (2010). Building damage assessment report-haiti earthquake 12 january 2010 joint damage assessment. European Commission, JRC59706.

Kerle, N. (2002). Volume estimation of the 1998 flank collapse at casita volcano, nicaragua: a comparison of photogrammetric and conventional techniques. Earth surface processes and landforms, 27(7):759–772.

Khaleghy-Rad, M. and Evans, S. (2014). The magnitude and frequency of natural disasters caused by geological hazards.

Kim, N. (2012). How much more exposed are the poor to natural disasters? global and regional measurement. Disasters, 36(2):195–211.

Knopoff, L. and Sornette, D. (1995). Earthquake Death Tolls. Journal de Physique I, 5:1681–1668.

Kobe-Statistics (2009). The great hanshin-awaji earthquake statistics and restoration progress. Technical report.

Kuwata, Y., Takada, S., and Bastami, M. (2005). Building damage and human casualties during the bam-iran earthquake. Asian Journal of Civil Engineer-ing (Building and Housing), 6(1-2):1–19.

Ladyman, J., Lambert, J., and Wiesner, K. (2013). What is a complex system? 3(1).

Lees, F. P. (1996). Loss Prevention in the Process of Industries. Vol. 1-3, 2nd Edition.

Leitch, M. (2010). Iso 31000:2009 - the new international standard on risk management: Perspective. Risk Analysis , 30(6):887–892.

Li, L., Wang, J., Leung, H., and Zhao, S. (2012). A bayesian method to mine spatial data sets to evaluate the vulnerability of human beings to catastrophic risk. Risk Analysis, 32(6):1072–1092.

Lomnitz, C. (1970). Casualties and behavior of populations during earthquakes.

Bulletin of the Seismological Society of America, 60(4):1309–1313.

Løvholt, F., Glimsdal, S., Harbitz, C. B., Zamora, N., Nadim, F., Peduzzi, P., Dao, H., and Smebye, H. (2012). Tsunami hazard and exposure on the global scale. Earth-Science Reviews, 110(1–4):58–73.

Lucchitta, B. K. (November, 1978). A large landslide on mars. Geological Society of America Bulletin, 89(11):1601–1609.

Marfai, M. A. and Njagih, J. K. (2004). Vulnerability analysis and risk assess-ment for seismic and flood hazard in Turrialba city, Costa Rica. Enschede, International Institute for Geo-information Sciences and Earth Observation ITC , NL.

Marshall, V. (1987). Major chemical hazards. Ellis Horwood series in chemical engineering. E. Horwood.

Mason, B. G., Pyle, D. M., and Oppenheimer, C. (2004). The size and frequency of the largest explosive eruptions on earth. Bulletin of Volcanology, 66:735– 748.

McGuire, W. (2006). Global risk from extreme geophysical events: threat iden-tification and assessment. Philosophical Transactions of the Royal Society A: Mathematical, Physical and Engineering Sciences, 364(1845):1889–1909.

McSaveney, M. (2002). Recent rock falls and rock avalanches in Mount Cook National Park. Geological Society of America.

Mendes-Victor, L. A., Oliveira, C. S., Azevedo, J., Ribeiro, A., Wenzel, F., Bendimerad, F., and Merz, B. (2009). Risk estimates for germany. In Ansal, A., editor, The 1755 Lisbon Earthquake: Revisited, volume 7 of Geotechni-cal, Geological, and Earthquake Engineering, pages 187–196. Springer Nether-lands.

Meng, Q., Qu, X., Yong, K. T., and Wong, Y. H. (2011). Qra model-based risk impact analysis of traffic flow in urban road tunnels. Risk Analysis, 31(12):1872–1882.

Mishra, V., Fuloria, S., and Bisht, S. S. (2012). Enhancing disaster management by mapping disaster proneness and preparedness. Disasters, 36(3):382–397.

Moss, R. E. S. and Eller, J. M. (2007). Estimating the Probability of Failure and Associated Risk of the California Bay Delta Levee System, chapter 13.

Musson, R. (2012). The Million Death Quake: The Science of Predicting Earth's Deadliest Natural Disaster . MacSci. Palgrave Macmillan.

Mustafa, D., Ahmed, S., Saroch, E., and Bell, H. (2011). Pinning down vulner-ability: from narratives to numbers. Disasters, 35(1):62–86.

Nateghi-A, F. (2001). Earthquake scenario for the mega-city of tehran. Disaster Prevention and Management, 10(2):95–100.

Neumayer, E. and Barthel, F. (2011). Normalizing economic loss from natural disasters: a global analysis. Global Environmental Change, 21(1):13–24.

Newman, M. (2005). Power laws, pareto distributions and zipf's law. Contem-porary Physics, 46(5):323–351.

Nishenko, S. P. and Barton, C. C. (1995). Scaling laws for natural disaster fatalities. U.S. Dept. of the Interior, U.S. Geological Survey.

Nitsch, V. (2005). Zipf zipped. Journal of Urban Economics, 57:86–100.

Noy, I. (2009). The macroeconomic consequences of disasters. Journal of De-velopment Economics, 88(2):221–231.

Papadopoulos, G. A. and Imamura, F. (2001). A proposal for a new tsunami intensity scale. In Proceedings of the International Tsunami Symposium 2001 (ITS 2001), volume 5, pages 569 –577 No.5–1.

Paté-Cornell, E. (2012). On Òblack swansÓ and Òperfect stormsÓ: Risk analysis and management when statistics are not enough. Risk Analysis, 32(11):1823– 1833.

Pelling, M. (2003). The vulnerability of cities [electronic resource] : natural disasters and social resilience. Earthscan Publications London ; Sterling, VA.

Pelling, M., Maskrey, A., Ruiz, P., Hall, L., Peduzzi, P., Dao, Q.-H., Mouton, F., Herold, C., and Kluser, S. (2004). Reducing disaster risk: a challenge for development.

Petley, D. (2012). Global patterns of loss of life from landslides. Geology, 40(10):927–930.

PIELKE JR, R. A. (2006). Disasters, death, and destruction. Oceanography, 19(2):138.

Pikaar, M. and Seaman, M. (1995). A review of risk control. 27A. A report commissioned by the Distributiecentrum Ministry VROM, P.O. Box 351, 2700 AJ ZOETERMEER, The Netherlands, No. 11030/150.

Pinto, C. M., Lopes, A. M., and Machado, J. T. (2012). A review of power laws in real life phenomena. Communications in Nonlinear Science and Numerical Simulation, 17(9):3558 – 3578.

Pisarenko, V. and Rodkin, M. (2010). Distributions of characteristics of natural disasters: Data and classification. In Heavy-Tailed Distributions in Disaster Analysis, pages 1–22. Springer.

Pisarenko, V. F. and Rodkin, M. V. (2014). Statistical Analysis of Natural Disasters and Related Losses. Springer.

Porter, K., Wald, D., Allen, T., and Jaiswal, K. (2007). An empirical relation-ship between fatalities and instrumental mmi. In 1st International Workshop on Disaster Casualties, Kyoto University, Nov 28-29.

Porter, M. and Morgenstern, N. (2012). Landslide risk evaluation in canada. In Proc. Joint XI th International & 2 nd North America Symposium on Landslides, Banff (Alberta), pages 2–8.

Proske, D. (2008). Catalogue of Risks Natural, Technical, Social and Health Risks. Springer, Berlin.

Prugh, R. (1992). Improved f/n graph presentation and criteria. J. Loss Prev. Process Ind., 5(4):239–247.

Rasmussen, N. (1975). Reactor safety study: An assessment of accident risk in us commercial nuclear power plants. Technical report, US Nuclear Regulatory Commission, WASH-1400 NUREG 75/014, Washington, D.C.

Richardson, L. (1960). Statistics of deadly quarrels. Boxwood Press.

Richardson, L. F. (1948). Variation of the frequency of fatal quarrels with magnitude. Journal of the American Statistical Association, 43(244):523–546.

Rijnmond (1982). Risk analysis of six potentially hazardous industrial objects in the rijnmond area. Technical report, Rijnmond Public authority and Open-baar Lichaam Rijnmond and COVO Steering Committee (Netherlands).

Sachs, M., Yoder, M., Turcotte, D., Rundle, J., and Malamud, B. (2012). Black swans, power laws, and dragon-kings: Earthquakes, volcanic eruptions, land-slides, wildfires, floods, and soc models. The European Physical Journal Spe-cial Topics, 205(1):167–182.

Scheidegger, A. (1975). Physical aspects of natural catastrophes. Elsevier Scien-tific Publishing.

Scherer, J. (1912). Great earthquakes in the island of haiti. Bulletin of the Seismological Society of America, 2(3):161–180.

Schofield, S. L. (1993). A framework for offshore risk criteria. Journal of the Safety and Reliability Society, 13(2).

Scholz, R. W., Blumer, Y. B., and Brand, F. S. (2012). Risk, vulnerability, robustness, and resilience from a decision-theoretic perspective. Journal of Risk Research, 15(3):313–330.

Schumacher, I. and Strobl, E. (2011). Economic development and losses due to natural disasters: The role of hazard exposure. Ecological Economics, 72:97–105.

Schuster, R. L. and Krizek, R. (1978). Landslides: analysis and control. Un-known, 1.

Schwartz, T., Pierre, Y.-F., and Calpas, É. (2011). Building assessments and rubble removal in quake-affected neighborhoods in haiti. BARR Survey Final Report.

Self, S. (2006). The effects and consequences of very large explosive volcanic eruptions. Philosophical Transactions of the Royal Society A: Mathematical, Physical and Engineering Sciences, 364(1845):2073–2097.

Shearer, P. M. and Stark, P. B. (2012). Global risk of big earthquakes has not recently increased. Proceedings of the National Academy of Sciences, 109(3):717–721.

Shuto, N. (2005). Tsunamis: their coastal effects and defense works. In Pro-ceedings of Scientific forum on the tsunami, its impact and recovery, 6th ?– 7th June, Asian Institute of Technology, Thailand, pages 1–12.

Siebert, L., Simkin, T., and Kimberly, P. (2011). Volcanoes of the world. University of California Press. University of California Press.

Skjong, R. (2003). Criteria for establishing risk acceptance. In Bedford and van Gelder, editors, Safety and Reliability: Proceedings of ESREL 2003, European Safety and Reliability Conference 2003, 15-18 June 2003, Maastricht, The Netherlands.

Skjong, R. and Eknes, M. L. (2002). Societal risk and societal benefits. Risk, Decision and Policy, 7(01):57–67.

Slovic, P., Lichtenstein, S., and Fischhoff, B. (1984). Modelling the societal impact of fatal accidents. Management Science, 30(4):464–474.

Smolka, A. (2006). Natural disasters and the challenge of extreme events: risk management from an insurance perspective. Philosophical Transactions of the Royal Society A: Mathematical, Physical and Engineering Sciences, 364(1845):2147–2165.

So, E. and Spence, R. (2013). Estimating shaking-induced casualties and build-ing damage for global earthquake events: a proposed modelling approach.

Bulletin of Earthquake Engineering, 11(1):347–363.

Song, W., Wang, J., Satoh, K., and Fan, W. (2006). Three types of power-law distribution of forest fires in japan. Ecological Modelling, 196(3–4):527 – 532.

Sornette, D. Dragon-kings, black swans and the prediction of crises. Swiss Finance Institute Research Paper Series 09-36, Swiss Finance Institute.

Spence, R., Coburn, A., Pomonis, A., and Sakai, S. (1992). Correlation of ground motion with building damage: The definition of a new damage-based seismic intensity scale. In Proceedings of the Tenth World Conference on Earthquake Engineering, Madrid, Spain, volume 1, pages 551–56.

Stallen, P. J. M., Geerts, R., and Vrijling, H. K. (1996). Three conceptions of quantified societal risk. Risk Analysis, 16(5):635–644.

Stein, S., Geller, R. J., and Liu, M. (2012). Why earthquake hazard maps often fail and what to do about it. Tectonophysics, 562–563(0):1–25.

Stroud, P. D., Sydoriak, S. J., Riese, J. M., Smith, J. P., Mniszewski, S. M., and Romero, P. R. (2006). Semi-empirical power-law scaling of new infection rate to model epidemic dynamics with inhomogeneous mixing. Mathematical Biosciences, 203(2):301 – 318.

Sundermann, L., Schelske, O., and Hausmann, P. (2013). Mind the risk- a global ranking of cities under threat from natural disasters. Technical report, Swiss Reinsurance Company Ltd., Swiss Reinsurance Company Ltd., Zurich, Switzerland.

Taleb, N. N. (2007). Black swans and the domains of statistics. The American Statistician, 61(3):198–200.

Taleb, N. N. (2010). The black swan: The impact of the highly improbable. Random House Trade Paperbacks.

Tang, L., Titov, V. V., Bernard, E. N., Wei, Y., Chamberlin, C. D., Newman, J. C., Mofjeld, H. O., Arcas, D., Eble, M. C., Moore, C., Uslu, B., Pells, C., Spillane, M., Wright, L., and Gica, E. (2012). Direct energy estimation of the 2011 japan tsunami using deep-ocean pressure measurements. Journal of Geophysical Research, 117:1–28.

Tanguy, J.-C., Ribière, C., Scarth, A., and Tjetjep, W. S. (1998). Victims from volcanic eruptions: a revised database. Bulletin of Volcanology, 60:137–144.

Tianbin, H. R. P. X. L. (2008). Basic characteristics and formation mechanism of the largest scale landslide at dagungbao occurred during the wenchuan earthquake [j]. Journal of Engineering Geology, 6:002.

Trbojevic, V. (2005). Risk criteria in e.u. Presented at Conference on European Safety and Reliability(ESREL'05), Tri-city, Poland, 27-30 June.

UNDP (2004). Reducing disaster risk: a challenge for development. United Nations Development Programme, Bureau for Crisis Prevention and Recovery.

UNISDR (2009). United nations international strategy for disaster reduction (UNISDR) terminology on disaster risk reduction. http://www.unisdr.org/ eng/library/lib-terminology-eng\%20home.htm.

Utsu, T. (2002). 42 a list of deadly earthquakes in the world: 1500–2000. In William H.K. Lee, Hiroo Kanamori, P. C. J. and Kisslinger, C., editors, International Handbook of Earthquake and Engineering Seismology, volume 81, Part A of International Geophysics, pages 691 – XVII. Academic Press.

Verruijt, A. (2010). An Introduction to Soil Dynamics. Theory and Applications of Transport in Porous Media. Springer.

Voight, B. (1990). The 1985 nevado del ruiz volcano catastrophe: anatomy and retrospection. Journal of Volcanology and Geothermal Research, 42(1):151– 188.

Vranes, K. and Pielke Jr, R. (2009). Normalized earthquake damage and fatal-ities in the united states: 1900–2005. Natural Hazards Review, 10(3):84–101.

Vrijling, J. K. and van Gelder, P. (1997). Societal risk and the concept of risk aversion. In Soares, C. G., editor, Advances in Safety and Reliability, number 1 in ESREL Confrences, pages 45–52, Lisbon, Portigal. Elsevier Science.

Vrijling, J. K., van Hengel, W., and Houben, R. J. (1995). A framework for risk evaluation. J. Hazard. Mater., 43(3):245–261.

Wasowski, J., Keefer, D. K., and Lee, C.-T. (2011). Toward the next genera-tion of research on earthquake-induced landslides: current issues and future challenges. Engineering Geology, 122(1):1–8.

Watts, M. J. and Bohle, H. G. (1993). The space of vulnerability: the causal structure of hunger and famine. Progress in Human Geography, 17(1):43–67.

Wilson, R. (1975). The costs of safety. New Scientist, pages 274–275.

Wisner, B. and Luce, H. R. (1993). Disaster vulnerability: Scale, power and daily life. GeoJournal, 30(2):127–140.

Woo, G. (1999). The mathematics of natural catastrophes. Applied Mathemat-ics. Imperial College Press.

Woo, G. (2002). Natural catastrophe probable maximum loss. British Actuarial Journal, pages 943–959.

Wunderlich, W. (2005). Hydraulic Structures: Probabilistic Approaches To Maintenance. ASCE Press.

Yokoyama, I. (1956). Energetics in active volcanoes, 2nd paper. Bulletin of the Earthquake Research Institute, University of Tokyo, 34(185):75–97.

Zhou, H., Wan, J., Jia, H., et al. (2010). Resilience to natural hazards: a geographic perspective. Natural Hazards, 53(1):21–41.

Zio, E. and Aven, T. (2012). Industrial disasters: Extreme events, extremely rare. some reflections on the treatment of uncertainties in the assessment of the associated risks. Process Safety and Environmental Protection.